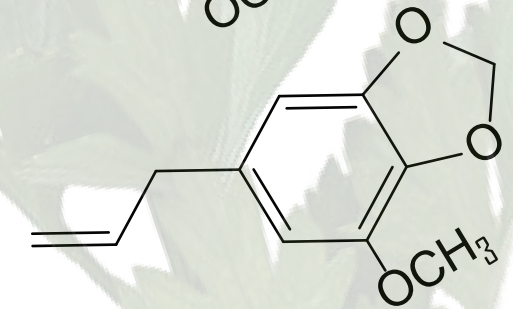
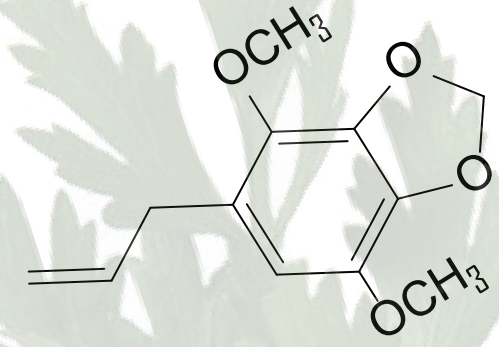


Mode of action based risk assessment of the botanical food-borne alkenylbenzenes apiol and myristicin

Abdalmajeed M. Alajlouni

Mode of action based risk assessment of the botanical food-borne alkenylbenzenes apiol and myristicin



Abdalmajeed M. Alajlouni

PROPOSITIONS

1. Physiologically based kinetic (PBK) modelling facilitates read-across from compounds for which in vivo toxicity studies on tumor formation are available to compounds for which these data are unavailable.
(this thesis)
2. Consumption of parsley and dill based teas or plant food supplements (PFS) is of concern if consumed for longer periods of time.
(this thesis)
3. The use of the retrospective data on specific disease outbreaks in addition to forecasting models will help preventing a new outbreak.
4. The use of wireless devices to collect the lost energy of surrounding waves and converting it into electricity will provide a novel alternative source of energy.
5. Smart phones affect the creativity of children.
6. When traveling the same roads, turtles acquire more knowledge about road quality than rabbits.

Propositions belonging to the PhD thesis, entitled:

Mode of action based risk assessment of the botanical food-borne alkenylbenzenes apiol and myristicin.

Abdalmajeed Alajlouni

Wageningen, 05 September 2017

Mode of action based risk assessment of the botanical food-borne alkenylbenzenes apiol and myristicin

Abdalmajeed M. Alajlouni

Thesis committee

Promotor

Prof. Dr I.M.C.M. Rietjens
Professor of Toxicology
Wageningen University & Research

Co-promotors

Dr J.J.M. Vervoort
Associate professor, Laboratory of Biochemistry
Wageningen University & Research

Dr S. Wesseling
Research assistant, Sub-department of Toxicology
Wageningen University & Research

Other members

Prof. Dr A.J. Murk, Wageningen University & Research
Prof. Dr E. Kampman, Wageningen University & Research
Dr T.F.H. Bovee, Wageningen University & Research
Dr J. van Benthem, National Institute for Public Health and the Environment (RIVM), Bilthoven

This research was conducted under the auspices of the Graduate School VLAG (Advanced studies in Food Technology, Agrobiotechnology, Nutrition and Health Sciences).

Mode of action based risk assessment of the botanical food-borne alkenylbenzenes apiol and myristicin

Abdalmajeed Mahmoud Alajlouni

Thesis

submitted in fulfillment of the requirements for the degree of doctor

at Wageningen University

by the authority of the Rector Magnificus

Prof. Dr A.P.J. Mol,

in the presence of the

Thesis Committee appointed by the Academic Board

to be defended in public

on Tuesday 5 September 2017

at 1:30 p.m. in the Aula.

Abdalmajeed Mahmoud Alajlouni

Mode of action based risk assessment of the botanical food-borne alkenylbenzenes apiol and myristicin,
212 pages

PhD thesis, Wageningen University, Wageningen, the Netherlands (2017)
With references, with summaries in English

ISBN: 978-94-6343-458-4

DOI: <http://dx.doi.org/10.18174/416931>

Table of Contents

Chapter 1	General Introduction	7
Chapter 2	Mode of action based risk assessment of the botanical food-borne alkenylbenzene apiol from parsley using physiologically based kinetic (PBK) modelling and read-across from safrole	25
Chapter 3	Physiologically based kinetic modelling of the bioactivation of myristicin	67
Chapter 4	Level of alkenylbenzenes in parsley and dill based teas and associated risk assessment using the Margin of Exposure approach	117
Chapter 5	Risk assessment of combined exposure to alkenylbenzenes through consumption of plant food supplements containing parsley and dill.	145
Chapter 6	General Discussion	173
Chapter 7	Summary	201
	Appendices	207

Chapter 1

General Introduction

Short description and aim of the thesis

Apiol and myristicin are two compounds that belong to the group of alkenylbenzenes found in several herbs and spices including for example parsley, dill, and nutmeg (Semenov et al., 2007). The presence of apiol in parsley gives this herb its characteristics odor (Shamina and Parthasarathy, 2008). Alkenylbenzenes also occur in the essential oils of these herbs and spices.

Alkenylbenzenes containing herbs and spices as well as their essential oils are used as food flavoring agents in many food types such as sauces, soups, stuffing, rissoles, minces, and many others. In addition, parsley derived preparations are also sprinkled over vegetables or salads. Apiol and myristicin are alkenylbenzenes with a molecular structure that resembles that of other alkenylbenzenes including safrole, methyleugenol and estragole (Figure 1).

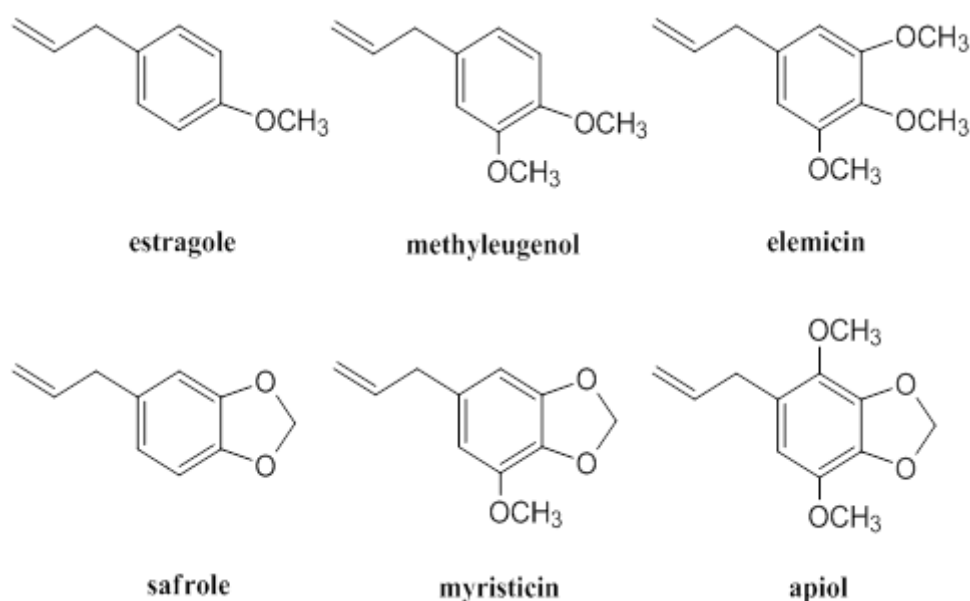


Figure 1: Structures of alkenylbenzenes.

Methyleugenol, estragole and safrole were shown to induce liver tumors at high dose levels in rodents via a mode of action that includes formation of DNA adducts (Boberg et al., 1986, Boberg et al., 1983, Phillips et al., 1984, Randerath et al., 1984, Wiseman et al.,

1985, Wislocki et al., 1976, Miller et al., 1983). For methyleugenol, formation of DNA adducts was also detected in 29 out of 30 human liver samples at levels that amounted for the median to maximum levels from 13 to 37 adducts per 10^8 nucleosides respectively (Herrmann et al., 2013), indicating that at current levels of intake DNA adducts in human liver can actually be detected. Given that DNA adducts are generally considered a marker of exposure rather than of risk the actual risk that the presence of these DNA adducts would pose to human health remains to be established. This also holds for exposure to other alkenylbenzenes including apiol and myristicin.

The currently preferred risk assessment approach used to assess the risk of exposure to compounds that are both genotoxic and carcinogenic is the so-called margin of exposure (MOE) approach (EFSA, 2005). The MOE is calculated as the ratio between a dose level derived from human epidemiological data or from in vivo carcinogenicity data obtained in experimental animals and the estimated daily intake (EDI). The preferred point of departure derived from the in vivo data to calculate the MOE is the lower confidence of the dose level that results in 10% extra cancer incidence above background levels the so-called $BMDL_{10}$ (O'Brien et al., 2006, EFSA, 2005). For some alkenylbenzenes, including estragole, methyleugenol and safrole, tumor data from rodent bioassays enabling definition of a $BMDL_{10}$ are available, while for the two related alkenylbenzenes of the present thesis, apiol and myristicin, such data do not exist.

The aim of the present PhD project was to perform a mode of action based risk assessment of exposure to low doses of apiol and myristicin by using physiologically based kinetic (PBK) modelling based read-across from other alkenylbenzenes and to use the results obtained for risk assessment of consumption of plant food supplements (PFS) and other botanical products containing parsley and dill.

Apiol and myristicin; chemical and physical properties.

Apiol (C₁₂H₁₄O₄) and myristicin (C₁₁H₁₂O₃) are alkenylbenzenes with a molecular weight of 222.23 g/mol and 192.21 g/mol respectively. They are soluble in most organic solvents like ethanol, ethyl ether, and chloroform and relatively insoluble in water. Apiol has a boiling point of 294 °C and myristicin has a boiling point of 173 °C (NTP, 2000), which indicates that these two molecules even though they are hydrophobic are not real volatiles.

Apiol, myristicin and structurally related alkenylbenzenes.

Alkenylbenzene compounds have common structural features consisting of an allylbenzene nucleus containing one or more alkoxy ring substituents. Safrole, myristicin and apiol contain a 3,4-methylenedioxy substituent with one additional methoxy substituent in case of myristicin and two in case of apiol (Figure 1). Estragole, methyleugenol and elemicin contain only methoxy substituents with estragole containing one, methyleugenol two and elemicin three of these moieties (Figure 1). Because these compounds have similar structures it can be foreseen that they may share similar metabolism, mode of action and biological effects (WHO, 2009, Van den Berg et al., 2012). This similarity provides the basis for the mode of action based read-across and risk assessments of the present thesis.

Human exposure to apiol and myristicin.

As already stated above, alkenylbenzenes can be found in many herbs and spices such as anise, basil, fennel, nutmeg, dill, parsley and tarragon (National Toxicology Program, 1999, WHO, 2009, Kreydiyyeh and Usta, 2002, Simon and Quinn, 1988, Stavri and Gibbons, 2005). Human exposure to apiol and myristicin mainly occurs through the consumption of different forms of parsley and dill preparations such as teas, spices and/or PFS. The EDI of safrole, estragole, methyleugenol, and myristicin (Gavin et al., 2007) due to daily

consumption of spice has been estimated to be within the range of 400-600 ug/person per day (Gavin et al., 2007). The maximum dietary intake for myristicin and safrole based on EU import data for nutmeg and mace in the USA is 684 and 879 $\mu\text{g}/\text{person}/\text{day}$ respectively (Gavin et al., 2007). For methyleugenol the average daily human intake from all sources, including use as a food flavor, has been estimated to be 217 $\mu\text{g}/\text{kg bw}/\text{day}$ for a 60 kg person (SCF, 2001a) and for estragole this daily human intake from all sources has been estimated to be 72 $\mu\text{g}/\text{kg bw}/\text{day}$ for a 60 kg person (SCF, 2001b). Since these estimates have been reported by the SCF, the use of methyleugenol and estragole as pure substance in foodstuff has been prohibited in the EU from September 2008 onwards (European Commission (EC), 2008) and as a consequence these EDIs from all sources will at present likely be lower.

In general, human exposure to apiol is considered as the lowest among the alkenylbenzenes. In the USA, the mean intake of apiol from spice and spice oils per capita is estimated to amount to 2.84 $\mu\text{g}/\text{person}/\text{day}$ while for other alkenylbenzenes, including myristicin, exposure may be at least 10 times higher (Gavin et al., 2007). Given that several of the related alkenylbenzenes cause liver carcinogenicity by a genotoxic mode of action, the possible risks associated with exposure may need further investigation in line with the WHO recommendation stating that: “Further research is needed to assess the potential risk to human health from low-level dietary exposure to alkoxy-substituted allylbenzenes present in foods and essential oils and used as flavoring agents”. (WHO, 2009).

Absorption, distribution, metabolism, and excretion of alkenylbenzenes.

Following exposure, alkenylbenzenes are rapidly absorbed, metabolized, and excreted (Lee et al., 1998, Benedetti et al., 1977, Kamienski and Casida, 1970, WHO, 2009). In human, safrole, estragole or methyleugenol, are completely absorbed, metabolized and eliminated within 24 h (WHO, 2009).

In general, in rodents the distribution and metabolism of alkenylbenzenes follow a dose-dependent trend in which increasing the dose level will lead to an increase in the plasma concentration of the alkenylbenzenes and their metabolites (Benedetti et al., 1977).

In a study performed by the National Toxicology Program (NTP, 2000), different groups of male and female mice were given 25, 50 or 75 mg/kg bw of methyleugenol by gavage. AUCs were 4.91–48.4 $\mu\text{g/ml}$ per minute for males and 3.27–60.5 $\mu\text{g/ml}$ per minute for females. In the same study groups of rat that were given 37, 75 or 150 mg/kg bw of methyleugenol by gavage showed AUC values amounting to 33.50–459.5 $\mu\text{g/ml}$ per minute for males and 27–307.9 $\mu\text{g/ml}$ per minute for females. Based on those results it was concluded that methyleugenol was eliminated more rapidly in mice than in rats (NTP, 2000).

The metabolic pathways of methoxy-substituted alkenylbenzenes and methylenedioxy-substituted alkenylbenzenes involve three processes (*O*-demethyl(en)ation, epoxidation and 1-hydroxylation of the alkene side chain) (Figure 2) (WHO, 2009). *O*-demethyl(en)ation is catalysed by liver cytochrome P450 enzymes and involves oxidation and cleavage of a methoxy substituent or of the methylenedioxy substituent in an *O*-dealkylation reaction. This is considered the predominant pathway, yielding polar hydroxy- or dihydroxyallylbenzene metabolites that are readily excreted either free or as sulfate or glucuronic acid conjugates. In rodents, at high dose levels *O*-demethyl(en)ation becomes saturated, and 1-hydroxylation and epoxidation of the allyl side-chain (Figure 2) compete to a larger extent. 1-Hydroxyalkenylbenzene metabolites can subsequently be conjugated with glucuronic acid or sulfate groups (Benedetti et al., 1977, Miller et al., 1983, Drinkwater et al., 1976). The sulfate conjugate of the 1-hydroxyalkenylbenzenes is unstable, leading to formation of a putative carbocation that reacts with cellular macromolecules including DNA (Drinkwater et al., 1976, Miller et al., 1983, Swanson et al., 1981, Gardner et al., 1996, Smith et al., 2002). The relative importance of the above three biotransformation processes is dose dependent, in which *O*-

demethyl(en)ation is dominant at all concentrations (Anthony et al., 1987, Sangster et al., 1987, Beyer et al., 2006), while the relative percentage of epoxide and 1-hydroxy formation increases at higher doses (Anthony et al., 1987, Zangouras et al., 1981). For example, in a study with mice and rats given doses of 0.05, 5, 50, 500, and 1000 mg/kg bw, the percentage of formation of the 1-hydroxy metabolite amounted to 1.3, 2.1, 5.2, 7.8, and 9.4%, respectively (Anthony et al., 1987, Zangouras et al., 1981). In line with this the results of estragole bioactivation and detoxification in male rat obtained using PBK models showed the same shifting (Punt et al., 2008). However, the dose levels at which this metabolic switch may occur may be higher than the dose levels causing carcinogenicity and are higher than estimated daily intake levels (Rietjens et al., 2014).

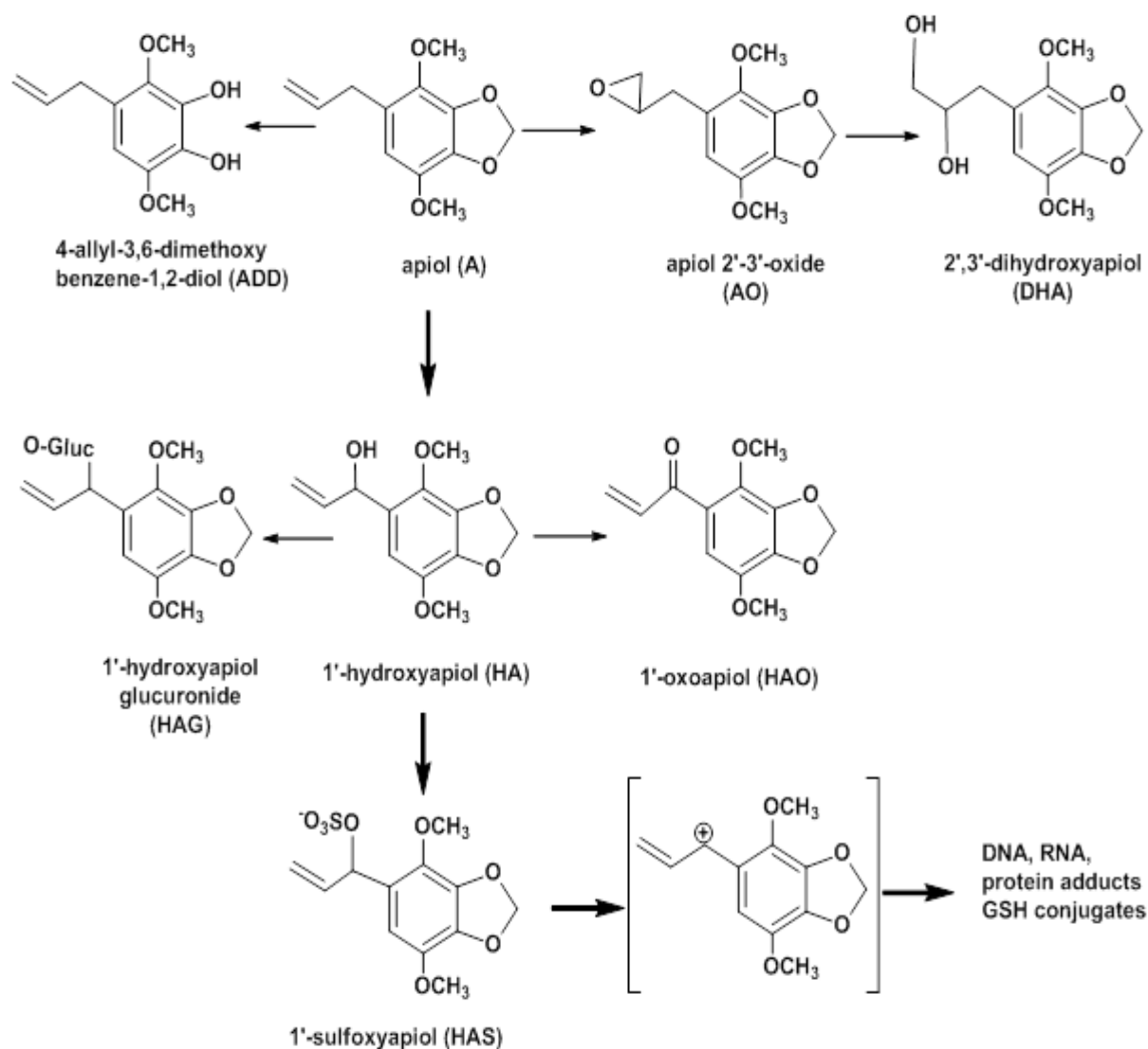


Figure 2: Metabolic pathways of apiol with the bioactivation route highlighted with solid arrows.

Alkenylbenzenes toxicity and carcinogenicity.

The metabolic pathways of the alkenylbenzenes described above reveal the ability of these compounds to form DNA adducts, and this has been confirmed in experimental studies and is considered an important part of the mode of action underlying the formation of liver tumors (Borchert et al., 1973, Drinkwater et al., 1976, Miller et al., 1983, Phillips et al., 1984, Wiseman et al., 1985, Wiseman et al., 1987). Randerath et al. 1984, using ^{32}P -postlabeling indicated that estragole, safrole, methyleugenol, myristicin, elemicin, and apiol can produce DNA adducts in adult mouse liver. Estragole, methyleugenol and safrole showed the highest

activity of the alkenylbenzenes tested (Randerath et al., 1984). Similar results were shown by Phillips et al. 1984, who reported that in neonatal mice the ability to form DNA adducts decreased as follows: methyleugenol > estragole > safrole > myristicin > apiol (Phillips et al., 1984). Zhou et al. used cultured human HepG2 cells to study the DNA adduct formation of alkenylbenzenes and concluded that at low concentration (50 $\mu\text{mol/l}$), high level of DNA adduct formation by estragole, methyleugenol and safrole can be detected while for myristicin at a concentration of 450 $\mu\text{mol/l}$ the level of adduct formation was increased and as high as that of safrole and methyleugenol (Zhou et al., 2007).

In addition to studies reporting DNA adduct formation several studies reported formation of liver tumors upon exposure to alkenylbenzenes.

Borchert et al. reported that, upon administration of safrole at a dose of 1265 mg/kg bw per day, liver tumors were induced in 65% of the males and 100% of the females (Borchert et al., 1973). Miller et al. reported a study in mice dosed with 370 mg safrole / kg bw twice a week by gavage up to 35 days, in which 62 % of the males and 12% of females developed hepatomas (Miller et al., 1983). Within the same study groups of 50 male and females' CD-1 mice were injected intraperitoneally with safrole, estragole, methyleugenol, elemicin, myristicin, and apiol. The results showed increased incidences of hepatocellular carcinoma especially with safrole, estragole and methyleugenol. Together these studies indicate that the related alkenylbenzenes are compounds that are genotoxic and carcinogenic, while they may differ in relative potency.

Approaches for risk assessment.

Since alkenylbenzenes are considered as compounds that are both genotoxic and carcinogenic (Borchert et al., 1973, Miller et al., 1983, Phillips et al., 1984, Wislocki et al., 1977), the

suitable approach for risk assessment of these compounds is the MOE approach (EFSA, 2005, O'Brien et al., 2006). As already indicated above, the MOE is the dimensionless ratio between a reference point based on epidemiologic data or experimental data on tumor incidence which is divided by the EDI in humans (Barlow et al., 2006, EFSA, 2005). The reference point used to calculate the MOE is the BMDL₁₀. When using an MOE value based on a BMDL₁₀ value obtained from animal data, a value of 10000 was suggested to be the value based on which to make the risk management decision (*i.e* an MOE value lower than 10000 would be of concern for human health and is considered as a priority for risk management) (EFSA, 2005). The value of 10000 was considered to include all possible uncertainties that may be involved and affect the risk assessment. The value of 10000 includes a factor of 100 for kinetic and dynamic differences between species and within humans, a factor of 10 that presents the variability in cell cycle control and DNA repair within humans, and a factor of 10 that takes into account that the BMDL₁₀ is not a no effect level but represents a 10% Bench Mark Response (BMR). Besides the BMDL₁₀, human exposure data reflected by the EDIs for the relevant population groups are needed to calculate the MOE value (EFSA, 2005). The MOE is a useful approach to compare the possible human risk from exposure to different carcinogenic compounds, but it requires that a BMDL₁₀ value and thus carcinogenicity data for the compound under consideration are available. However, this may not always be the case. For myristicin and apiol, the model compounds of the present thesis, such data that enable definition of a BMDL₁₀ and calculation of MOE values are not available. In the present thesis, we tested whether in such situations a mode of action based approach using physiologically based kinetic (PBK) modelling and read-across from compounds for which such data are available can be applied. In order to apply such a read-across approach for a group of compounds, the chemical and physical properties of these compounds should be defined and similar, enabling definition the structural-activity relationships (SARs) among these

compounds enabling to read-across from the compounds with available in vivo data to those with no data (EPA 2005). In the present thesis, the relevant relationships that enabled the read-across were defined using so-called PBK modelling. In the next section, some background information on this PBK modelling and how it could be used to define BMDL₁₀ values for compounds for which carcinogenicity data are lacking is presented.

PBK modelling

PBK models are models based on different parameters including physiological parameters, physico-chemical parameters, and metabolic parameters in order to build up mathematical equations that describe the kinetic processes of the compound of interest in the organ and species of interest. The models include absorption, distribution, metabolism and excretion (ADME) (Krewski et al., 1994, Chiu et al., 2007, Rietjens et al., 2011). The use of PBK models allows the study of possible time- and dose-dependent variations in metabolism, predicting the concentrations of the chemical and its metabolites within tissues and blood (Rietjens et al., 2011), and the study of interspecies differences through use of parameters of the species of interest (Andersen and Krishnan, 1994). Development of PBK models involves several steps including i) definition of the conceptual model, ii) translation into a mathematical model, iii) setting parameter values, iv) solving the model equations, v) model evaluation and vi) making predictions. Definition of the conceptual model means describing the structure of the model including organs and tissues that are of importance for the kinetic processes and the toxicity of the compound of interest. A conceptual model will include separate tissue compartments for the tissues that are relevant for the kinetics and toxicity of the compound and the remaining organs and tissues can be pooled in compartments representing slowly or richly perfused tissues. If the compound is lipophilic the fat tissue can be represented by a separate compartment. All compartments are mutually connected through

the systemic circulation. Following that, describing the kinetic processes of the compound of interest will be done through definition of the mathematical equations for each compartment. In a subsequent step the relevant parameters, including physiological, anatomical, physico-chemical and kinetic values need to be defined for each equation. This can be done based on available literature data, computer models, and/or using in vitro or in vivo experiments. Once the mathematical model is established and the relevant parameters have been defined, the equations can be solved using specific software in order to obtain concentrations of the compound of interest and its metabolite(s) in relevant compartments of the body, at certain dose levels and points in time. Then, the validity of the model needs to be evaluated through comparison of its output with available in vivo data. In addition, a sensitivity analysis can be performed to study how the input parameters of the model influence the model output. When evaluated and shown to be adequate, the model can be used to make predictions.

Objectives and outline of the thesis

The aim of the present PhD project was to perform a mode of action based risk assessment of exposure to low doses of apiol and myristicin by using PBK modelling based read-across to other alkenylbenzenes and to use the results obtained for risk assessment of consumption of PFS and other botanical products containing parsley and dill.

Chapter 1, the current chapter, starts with a short introduction and definition of the aim of the thesis, followed by a description of the chemical, ADME and toxicity characteristics of apiol and myristicin and other structurally related alkenylbenzenes, as well as a brief outline of the method used for their risk assessment and a short introduction to PBK modelling.

Chapter 2 defines PBK models for apiol in male rat and human, enabling prediction of dose-dependent effects in bioactivation and detoxification of apiol. In addition to that the outcomes of the rat and human model were compared to evaluate the occurrence of species differences in metabolic activation and detoxification of apiol. The PBK model based predictions were subsequently compared to those for safrole enabling estimation of a BMDL₁₀ for apiol from read-across from the BMDL₁₀ available for safrole, thereby enabling risk assessment of current dietary exposure to apiol.

Chapter 3 defines a PBK model for the related alkenylbenzene myristicin in male rat and human, enabling prediction of dose-dependent effects in bioactivation and detoxification of myristicin. In addition to that, the outcomes of the rat and human model were compared to evaluate the occurrence of species differences in metabolic activation and detoxification of myristicin. The PBK model based predictions were subsequently compared to those for safrole enabling estimation of a BMDL₁₀ for myristicin from read-across to the BMDL₁₀ available for safrole, thereby enabling risk assessment of current dietary exposure to myristicin.

Chapter 4 evaluates the risk of exposure to apiol and related alkenylbenzenes through drinking of parsley and dill based herbal teas. Chemical analyses of hot water extracts of the various teas were performed and the amount of alkenylbenzenes that would be consumed through consumption of a cup of tea were quantified. MOE values were calculated for the individual alkenylbenzenes as well as taking into account the presence of more than one alkenylbenzenes within selected herbal teas.

Chapter 5 describes the chemical analysis of parsley and dill based PFS and a subsequent risk assessment of exposure to alkenylbenzenes upon ingestion of recommended doses of these supplements.

Finally, **chapter 6** summarizes the results obtained in the thesis, compiles the overall discussion and presents the future perspectives that follow from the results obtained.

References:

1. Andersen, M. E. & Krishnan, K. 1994. Physiologically based pharmacokinetics and cancer risk assessment. *Environmental Health Perspectives*, 102 Suppl 1, 103-8.
2. Anthony, A., Caldwell, J., Hutt, A. J. & Smith, R. L. 1987. Metabolism of estragole in rat and mouse and influence of dose size on excretion of the proximate carcinogen 1'-hydroxyestragole. *Food and chemical toxicology : an international journal published for the British Industrial Biological Research Association*, 25, 799-806.
3. Barlow, S., Renwick, A. G., Kleiner, J., Bridges, J. W., Busk, L., Dybing, E., Edler, L., Eisenbrand, G., Fink-Gremmels, J., Knaap, A., Kroes, R., Liem, D., Muller, D. J., Page, S., Rolland, V., Schlatter, J., Tritscher, A., Tueting, W. & Wurtzen, G. 2006. Risk assessment of substances that are both genotoxic and carcinogenic report of an International Conference organized by EFSA and WHO with support of ILSI Europe. *Food and chemical toxicology : an international journal published for the British Industrial Biological Research Association*, 44, 1636-50.
4. Benedetti, M. S., Malnoe, A. & Broillet, A. L. 1977. Absorption, metabolism and excretion of safrole in the rat and man. *Toxicology*, 7, 69-83.
5. Beyer, J., Ehlers, D. & Maurer, H. 2006. Abuse of Nutmeg (*Myristica fragrans* Houtt.): Studies on the Metabolism and the Toxicologic Detection of its Ingredients Elemicin, Myristicin, and Safrole in Rat and Human Urine Using Gas Chromatography/Mass Spectrometry. *Therapeutic Drug Monitoring*, 28, 568-575.
6. Boberg, E. W., Miller, E. C. & Miller, J. A. 1986. The metabolic sulfonation and side-chain oxidation of 3'-hydroxyisosafrrole in the mouse and its inactivity as a hepatocarcinogen relative to 1'-hydroxysafrole. *Chemico-biological interactions*, 59, 73-97.
7. Boberg, E. W., Miller, E. C., Miller, J. A., Poland, A. & Liem, A. 1983. Strong evidence from studies with brachymorphic mice and pentachlorophenol that 1'-sulfoxysafrole is the major ultimate electrophilic and carcinogenic metabolite of 1'-hydroxysafrole in mouse liver. *Cancer research*, 43, 5163-73.
8. Borchert, P., Miller, J. A., Miller, E. C. & Shires, T. K. 1973. 1'-Hydroxysafrole, a proximate carcinogenic metabolite of safrole in the rat and mouse. *Cancer research*, 33, 590-600.
9. Chiu, W. A., Barton, H. A., DeWoskin, R. S., Schlosser, P., Thompson, C. M., Sonawane, B., Lipscomb, J. C. & Krishnan, K. 2007. Evaluation of physiologically based pharmacokinetic models for use in risk assessment. *Journal of applied toxicology : JAT*, 27, 218-37.
10. Drinkwater, N. R., Miller, E. C., Miller, J. A. & Pitot, H. C. 1976a. Hepatocarcinogenicity of estragole (1-allyl-4-methoxybenzene) and 1'-hydroxyestragole in the mouse and mutagenicity of 1'-acetoxyestragole in bacteria. *Journal of the National Cancer Institute*, 57, 1323-31.
11. EFSA 2005. Opinion of the Scientific Committee on a request from EFSA related to A Harmonised Approach for Risk Assessment of Substances Which are both Genotoxic and Carcinogenic. *The EFSA Journal*, 282, 1-31.
12. European Commission (EC) 2008. Regulation (EC) No 1334/2008 of the European Parliament and of the Council of 16 December 2008 on flavourings and certain food ingredients with flavouring properties for use in and on foods and amending Council Regulation (EEC) No 1601/91, Regulations (EC) No 2232/96 and (EC) No 110/2008 and Directive 2000/13/EC.
13. Gardner, I., Bergin, P., Stening, P., Kenna, J. G. & Caldwell, J. 1996. Immunochemical detection of covalently modified protein adducts in livers of rats treated with methyleugenol. *Chem Res Toxicol*, 9, 713-21.
14. Gavin, C. L., Williams, M. C. & Hallagan, J. B. 2007. 2005 FEMA poundage and technical effects update survey. . Washington, DC, USA,: Flavor and Extract Manufacturers Association.
15. Herrmann, K., Schumacher, F., Engst, W., Appel, K. E., Klein, K., Zanger, U. M. & Glatt, H. 2013. Abundance of DNA adducts of methyleugenol, a rodent hepatocarcinogen, in human liver samples. *Carcinogenesis*, 34, 1025-30.

16. Kamienski, F. X. & Casida, J. E. 1970. Importance of demethylenation in the metabolism in vivo and in vitro of methylenedioxyphenyl synergists and related compounds in mammals. *Biochem Pharmacol*, 19, 91-112.
17. Krewski, D., Withey, J. R., Ku, L. F. & Andersen, M. E. 1994. Applications of physiologic pharmacokinetic modeling in carcinogenic risk assessment. *Environmental Health Perspectives*, 102 Suppl 11, 37-50.
18. Kreydiyyeh, S. I. & Usta, J. 2002. Diuretic effect and mechanism of action of parsley. *Journal of Ethnopharmacology*, 79, 353-7.
19. Lee, H. S., Jeong, T. C. & Kim, J. H. 1998. In vitro and in vivo metabolism of myristicin in the rat. *J Chromatogr B Biomed Sci Appl*, 705, 367-72.
20. Miller, E. C., Swanson, A. B., Phillips, D. H., Fletcher, T. L., Liem, A. & Miller, J. A. 1983. Structure-activity studies of the carcinogenicities in the mouse and rat of some naturally occurring and synthetic alkenylbenzene derivatives related to safrole and estragole. *Cancer research*, 43, 1124-34.
21. National Toxicology Program 1999. Estragole (CASRN 140-67-0) review of toxicological literature. National Institute of Environmental Health Sciences.
22. NTP 2000. Toxicology and carcinogenesis studies of methyleugenol (CAS No. 93-15-12) in F344/N rats and B6C3F1 mice (gavage studies) United States Department of Health and Human Services, National Institutes of Health (Draft NTP-TR-491; NIH Publication) Park, NC, USA.
23. O'Brien, J., Renwick, A. G., Constable, A., Dybing, E., Muller, D. J., Schlatter, J., Slob, W., Tueting, W., van Benthem, J., Williams, G. M. & Wolfreys, A. 2006. Approaches to the risk assessment of genotoxic carcinogens in food: a critical appraisal. *Food and chemical toxicology : an international journal published for the British Industrial Biological Research Association*, 44, 1613-35.
24. Phillips, D. H., Reddy, M. V. & Randerath, K. 1984. 32P-post-labelling analysis of DNA adducts formed in the livers of animals treated with safrole, estragole and other naturally-occurring alkenylbenzenes. II. Newborn male B6C3F1 mice. *Carcinogenesis*, 5, 1623-8.
25. Punt, A., Freidig, A. P., Delatour, T., Scholz, G., Boersma, M. G., Schilter, B., van Bladeren, P. J. & Rietjens, I. M. 2008. A physiologically based biokinetic (PBBK) model for estragole bioactivation and detoxification in rat. *Toxicology and applied pharmacology*, 231, 248-59.
26. Randerath, K., Haglund, R. E., Phillips, D. H. & Reddy, M. V. 1984. 32P-post-labelling analysis of DNA adducts formed in the livers of animals treated with safrole, estragole and other naturally-occurring alkenylbenzenes. I. Adult female CD-1 mice. *Carcinogenesis*, 5, 1613-22.
27. Rietjens, I. M., Cohen, S. M., Fukushima, S., Gooderham, N. J., Hecht, S., Marnett, L. J., Smith, R. L., Adams, T. B., Bastaki, M., Harman, C. G. & Taylor, S. V. 2014. Impact of structural and metabolic variations on the toxicity and carcinogenicity of hydroxy- and alkoxy-substituted allyl- and propenylbenzenes. *Chemical research in toxicology*, 27, 1092-103.
28. Rietjens, I. M., Louisse, J. & Punt, A. 2011. Tutorial on physiologically based kinetic modeling in molecular nutrition and food research. *Molecular nutrition & food research*, 55, 941-56.
29. Sangster, S. A., Caldwell, J., Hutt, A. J., Anthony, A. & Smith, R. L. 1987. The metabolic disposition of [methoxy-14C]-labelled trans-anethole, estragole and p-propylanisole in human volunteers. *Xenobiotica; the fate of foreign compounds in biological systems*, 17, 1223-32.
30. SCF 2001a. Opinion of the Scientific Committee of Food on Methyleugenol (1-allyl-1,2-dimethoxybenzenen).
31. SCF 2001b. Opinion of the Scientific Committee on Food on Estragole (1-allyl-4-methoxybenzene). European Commission Health & Consumer Protection Directorate-General Brussel. http://ec.europa.eu/food/fs/sc/scf/out104_en.pdf.
32. Semenov, V. V., Rusak, V. V., Chartov, E. M., Zaretskii, M. I., Konyushkin, L. D., Firgang, S. I., Chizhov, A. O., Elkin, V. V., Latin, N. N., Bonashek, V. M. & Stas'eva, O. N. 2007.

- Polyalkoxybenzenes from plant raw materials 1. Isolation of polyalkoxybenzenes from CO₂ extracts of Umbelliferae plant seeds. *Russian Chemical Bulletin*, 56, 2448-2455.
33. Shamina, A. & Parthasarathy, V. 2008. Parsley. *chemistry of spices*. CABI International.
 34. Simon, J. E. & Quinn, J. 1988. Characterization of essential oil of parsley. *J Agric Food Chem*, 36,, 467-472.
 35. Smith, R. L., Adams, T. B., Doull, J., Feron, V. J., Goodman, J. I., Marnett, L. J., Portoghese, P. S., Waddell, W. J., Wagner, B. M., Rogers, A. E., Caldwell, J. & Sipes, I. G. 2002. Safety assessment of allylalkoxybenzene derivatives used as flavouring substances - methyl eugenol and estragole. *Food Chem Toxicol*, 40, 851-70.
 36. Stavri, M. & Gibbons, S. 2005. The antimycobacterial constituents of dill (*Anethum graveolens*). *Phytotherapy Research*, 19, 938-941.
 37. Swanson, A. B., Miller, E. C. & Miller, J. A. 1981. The side-chain epoxidation and hydroxylation of the hepatocarcinogens safrole and estragole and some related compounds by rat and mouse liver microsomes. *Biochim Biophys Acta*, 673, 504-16.
 38. Van den Berg, S. J., Punt, A., Soffers, A. E., Vervoort, J., Ngeleja, S., Spenkeliink, B. & Rietjens, I. M. C. M. 2012. Physiologically based kinetic models for the alkenylbenzene elemicin in rat and human and possible implications for risk assessment. *Chemical research in toxicology*, 25, 2352-67.
 39. WHO 2009. Safety evaluation of certain additives, prepared by the Sixty-ninth meeting of the Joint FAO/WHO Expert Committee on Food Additives. *World Health Organization*
 40. Wiseman, R. W., Fennell, T. R., Miller, J. A. & Miller, E. C. 1985. Further characterization of the DNA adducts formed by electrophilic esters of the hepatocarcinogens 1'-hydroxysafrole and 1'-hydroxyestragole in vitro and in mouse liver in vivo, including new adducts at C-8 and N-7 of guanine residues. *Cancer research*, 45, 3096-105.
 41. Wiseman, R. W., Miller, E. C., Miller, J. A. & Liem, A. 1987. Structure-activity studies of the hepatocarcinogenicities of alkenylbenzene derivatives related to estragole and safrole on
 42. administration to preweanling male C57BL/6J x C3H/HeJ F1 mice. *Cancer research*, 47, 2275-83.
 43. Wislocki, P. G., Borchert, P., Miller, J. A. & Miller, E. C. 1976. The metabolic activation of the carcinogen 1'-hydroxysafrole in vivo and in vitro and the electrophilic reactivities of possible ultimate carcinogens. *Cancer research*, 36, 1686-95.
 44. Wislocki, P. G., Miller, E. C., Miller, J. A., McCoy, E. C. & Rosenkranz, H. S. 1977. Carcinogenic and mutagenic activities of safrole, 1'-hydroxysafrole, and some known or possible metabolites. *Cancer research*, 37, 1883-91.
 45. Zangouras, A., Caldwell, J., Hutt, A. J. & Smith, R. L. 1981. Dose dependent conversion of estragole in the rat and mouse to the carcinogenic metabolite, 1'-hydroxyestragole. *Biochemical pharmacology*, 30, 1383-6.
 46. Zhou, G.-D., Moorthy, B., Bi, J., Donnelly, K. C. & Randerath, K. 2007. DNA adducts from alkoxyallylbenzene herb and spice constituents in cultured human (HepG2) cells. *Environmental and Molecular Mutagenesis*, 48, 715-721.

Chapter 2

Mode of action based risk assessment of the botanical food-borne alkenylbenzene apiol from parsley using physiologically based kinetic (PBK) modelling and read-across from safrole

Abdalmajeed M. Alajlouni , Amer J. Al_Malahmeh, Reiko Kiwamoto, Sebastiaan Wesseling, Ans E.M.F. Soffers, Ala A.A. Al-Subeihi, Jacques Vervoort, and Ivonne M.C.M. Rietjens.

Based on: Journal of Food and Chemical Toxicology (2016), 89: 138–150

Abstract

The present study developed physiologically-based kinetic (PBK) models for the alkenylbenzene apiol in order to facilitate risk assessment based on read-across from the related alkenylbenzene safrole. Model predictions indicate that in rat liver the formation of the 1-sulfoxy metabolite is about 3 times lower for apiol than for safrole. These data support that the lower confidence limit of the benchmark dose resulting in a 10% extra cancer incidence (BMDL₁₀) that would be obtained in a rodent carcinogenicity study with apiol may be 3-fold higher for apiol than for safrole. These results enable a preliminary risk assessment for apiol, for which tumor data are not available, using a BMDL₁₀ value of 3 times the BMDL₁₀ for safrole. Based on an estimated BMDL₁₀ for apiol of 5.7-15.3 mg/kg body wt per day and an estimated daily intake of 4×10^{-5} mg/kg body wt per day, the margin of exposure (MOE) would amount to 140000-385000. This indicates a low priority for risk management. The present study shows how PBK modelling can contribute to the development of alternatives for animal testing, facilitating read-across from compounds for which in vivo toxicity studies on tumor formation are available to compounds for which these data are unavailable.

Introduction

Apiol (1-allyl-2,5-dimethoxy-3,4-methylenedioxybenzene) is one of alkenylbenzene compounds found in herbs and other botanicals like parsley, fennel, nutmeg and elemi tree. High levels of apiol are especially present in parsley and apiol gives parsley its characteristics odor (Miller et al., 1983, Parthasarathy, 2008, Tunali et al., 1999). Parsley parts (leaves, stems, roots and seeds) are used as food flavoring agent in many food types such as sauces, soups, stuffing, rissoles, and minces, and are also sprinkled over vegetables or salads. Beside the use of parsley in food, medicinal uses of apiol extracted from the Triple Moss curled variety of parsley have been reported (Parthasarathy, 2008). The structure of apiol is closely related to that of safrole, myristicin, estragole, methyleugenol, and elemicin (Figure 1).

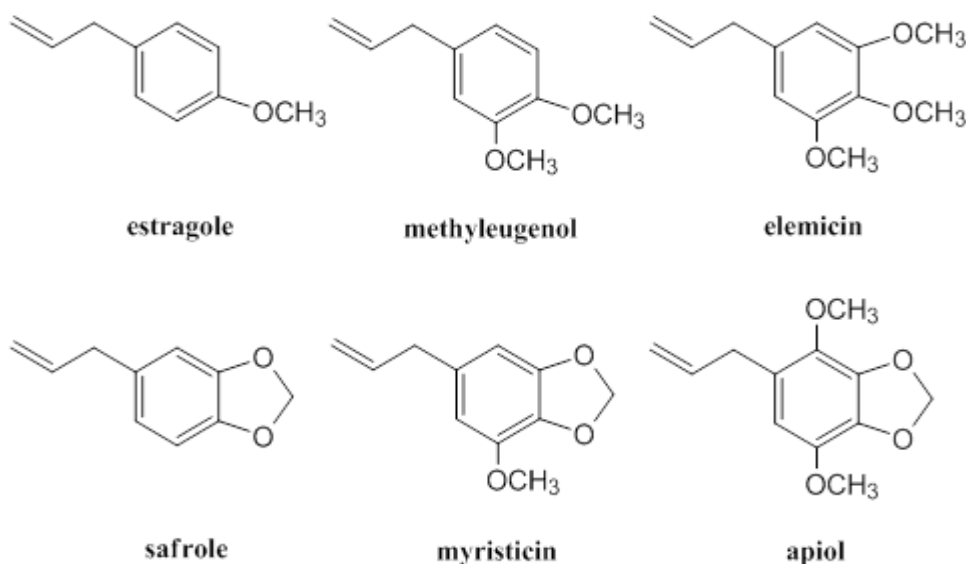


Figure 1: The structural formulas of the alkenylbenzenes estragole, methyleugenol, elemicin, safrole, myristicin and apiol.

These alkenylbenzenes are of concern because they can be converted to DNA reactive 1-sulfoxy metabolites that readily form DNA adducts that may contribute to the formation of hepatomas in rodent bioassays upon exposure to these alkenylbenzenes at high dose levels (Miller et al., 1983, Randerath et al., 1984, SCF, 2001b, SCF, 2001a, SCF, 2002, Wiseman et al., 1987). DNA adduct formation results from bioactivation of apiol following the metabolic pathways presented in figure 2 (WHO, 2009). Apiol however is less well studied than its

related alkenylbenzene safrole and rodent carcinogenicity studies on apiol are not available hampering its risk assessment.

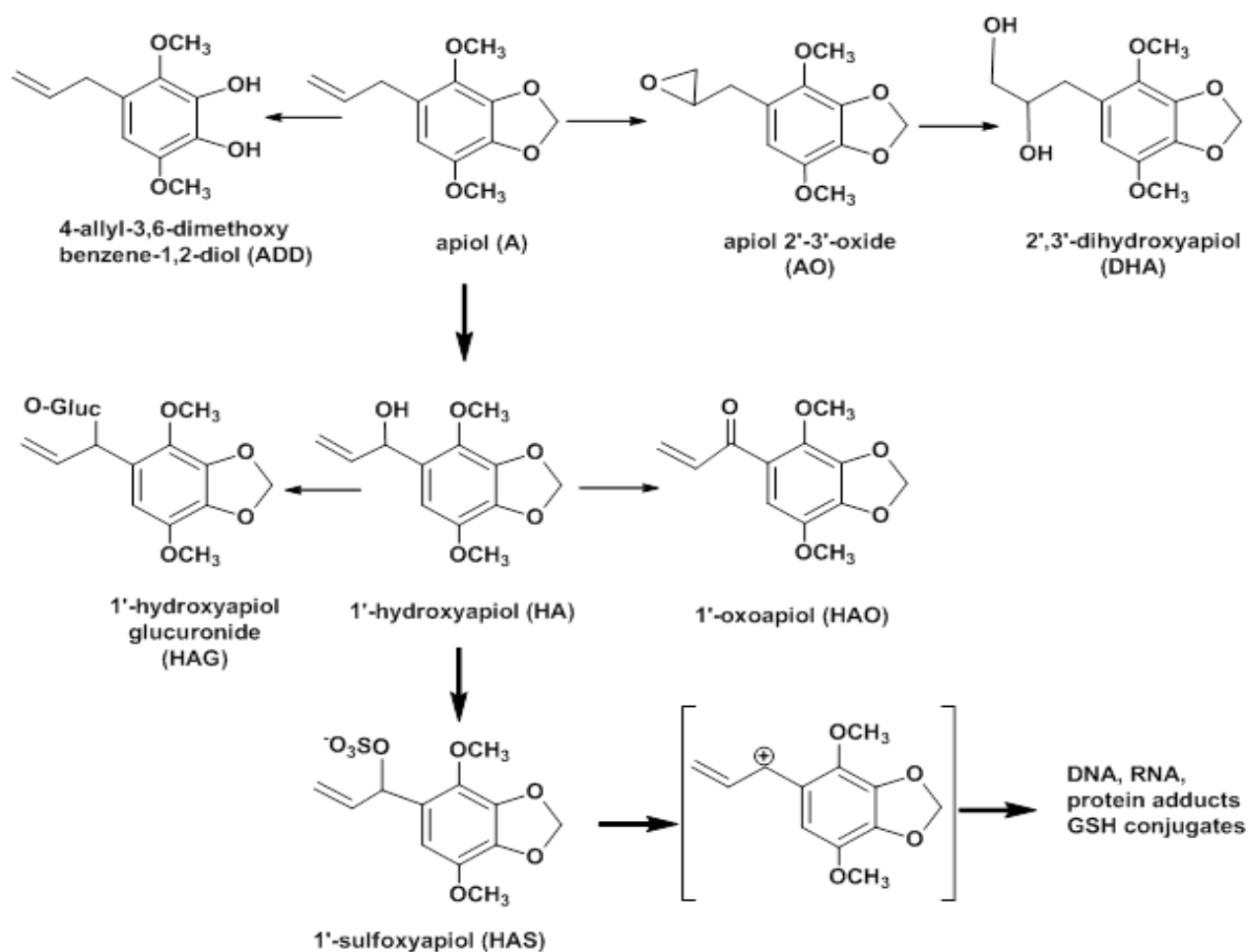


Figure 2: Suggested metabolic pathways of apiol.

The structural similarity of apiol to safrole raises a concern and provides a rationale for an updated risk assessment of exposure to apiol via food including food supplements. Several studies have reported on the DNA adduct formation by apiol in animal in vivo studies or in human in vitro models as compared to the related alkenylbenzenes and found apiol to be less potent than its structural analogues (Miller et al., 1983, Phillips et al., 1984, Randerath et al., 1984, Zhou et al., 2007).

The safety of human exposure to apiol has been assessed by the WHO in 2009 concluding that the structural similarities to safrole with available experimental data give evidence that apiol

may cause toxicity and carcinogenicity in rodents exposed to high dose levels (WHO, 2009). Because rodent bioassays characterizing the possible carcinogenicity of apiol are not available, the aim of the present study was to perform a risk assessment for apiol based on PBK-modelling based read-across from safrole for which rodent tumor data are available (Miller et al., 1983, Phillips et al., 1984, Randerath et al., 1984).

Materials and methods

Caution: Apiol and 1-hydroxyapiol are possible carcinogens and should be handled with care.

Chemicals and Reagents:

Apiol, uridine 5-diphosphoglucuronic acid trisodium salt (UDPGA), reduced L-glutathione (GSH), alamethicin (from *Trichoderma viride*), and 3-phosphoadenosine-5-phosphosulfate (PAPS) were obtained from Sigma Aldrich (Zwijndrecht, Netherlands). Reduced - nicotinamide adenine dinucleotide phosphate (NADPH) and nicotinamide adenine dinucleotide (NAD⁺) were from Roche Diagnostic (Mannheim, Germany), and dimethyl sulfoxide (DMSO) was obtained from Acros Organics (Geel, Belgium). Chromatographic grade trifluoroacetic acid (TFA) was obtained from Merck (Darmstadt, Germany). Potassium dihydrogen phosphate, dipotassium hydrogen phosphate trihydrate, acetic acid, and magnesium chloride were provided by VWR International (Darmstadt, Germany). Acetonitrile (ACN) (ULC/MS grade) was purchased from Biosolve BV (Valkenswaard, The Netherlands). Pooled male rat liver microsomes and S9 from Sprague–Dawley and mixed gender pooled human liver microsomes and S9 were from BD Gentest (Woburn, United States). Pooled male Sprague–Dawley rat lung, kidney, and small intestinal microsomes and pooled gender human lung, kidney, and intestinal microsomes were purchased from BioPredic International (Rennes, France).

Synthesis of 1 -hydroxyapiol and 1 -oxoapiol

The synthesis of 1 -hydroxyapiol from apiol was done as described previously for the synthesis of 1 -hydroxysafrole from safrole by Jeurissen et al., (2004) and 1 -oxoapiol was synthesized from 1 -hydroxyapiol according to the method used for synthesis of 1 -oxoestragole from 1 -hydroxyestragole (Wislocki et al., 1976).

In vitro incubations.

Microsomal metabolism of apiol by rat and human microsomes:

Liver, kidney, lung and small intestine microsomes from male Sprague Dawley rat and from human were used to determine tissue-specificity of the microsomal biotransformation of apiol in rat and human. Incubations were performed by adding 1 mg/ml of the microsomal protein preparation to an incubation mixture containing (final concentrations) 3 mM NADPH in 0.2 M Tris-HCl (pH 7.4). After a 1 minute pre-incubation at 37°C, apiol (final concentration 1000 µM) was added from a 100 times concentrated stock solution in DMSO so that the final DMSO content was 1% (v/v). After 120 minutes incubation at 37°C for rat and human microsomes the reactions were terminated by adding 25 µl ice-cold acetonitrile. All samples were centrifuged for 5 minutes at 16,000 g and the supernatant was stored at -20°C until Ultra Performance Liquid Chromatography (UPLC) analysis.

For both male rat and human, metabolism of apiol was only observed in incubations with liver microsomes (See the Results section) and hence kinetic constants for the formation of microsomal metabolites were determined only for liver microsomes. To determine the kinetic constants incubations following the conditions described above were done using final concentrations of apiol from 25 to 1000 µM for rat and human liver while keeping the DMSO

content at 1% (v/v). Blank incubations were performed in the absence of the cofactor NADPH. All incubations were performed in triplicate.

Glucuronidation of 1 -hydroxyapiol to 1 -hydroxyapiol glucuronide by rat and human liver S9

The kinetic constants for the metabolic conversion of 1 -hydroxyapiol to 1 -hydroxyapiol glucuronide in incubations with both male rat and human liver fractions were determined as described previously for related 1 -hydroxyalkenylbenzenes (Al-Subeihi et al., 2012, Al-Subeihi et al., 2011, Martati et al., 2011, Martati et al., 2012, Punt et al., 2008, Punt et al., 2009, Van den Berg et al., 2012). In short, incubations were performed using (final concentrations) 10 mM UDPGA and 0.5 mg/ml male Sprague–Dawley rat or pooled gender human S9 protein in 0.2 M Tris-HCl (pH 7.4) containing 10 mM MgCl₂. First the incubations were pre-treated on ice for 15 minutes with 0.025 mg/ml alamethicin added from a 200 times concentrated stock solution in methanol to overcome enzyme latency and to obtain maximal glucuronidation activity. After the pre-treatment on ice and pre-incubation at 37 °C for 1 minute, the reactions were subsequently started by adding 1 -hydroxyapiol in final concentrations of 10 to 2000 μM. 1 -Hydroxyapiol was added from 100 times concentrated stock solutions dissolved in DMSO. The reaction was incubated for 30 and 120 minutes for rat and human S9, respectively, and terminated by adding 25 μL of ice-cold acetonitrile. Blank incubations were carried out in the absence of the cofactor UDPGA. Experiments were performed in triplicate. All samples were centrifuged for 5 minutes at 16000g, and the supernatant was stored at –20 °C until UPLC analysis.

Oxidation of 1 -hydroxyapiol to 1 -oxoapiol by rat and human liver microsomes

The kinetic constants for the enzymatic conversion of 1 -hydroxyapiol to 1 -oxoapiol were determined using incubation mixtures containing (final concentrations) 3 mM NAD⁺, 2 mM GSH, and 1 mg/mL rat or human liver microsomes in 0.2 M Tris-HCl (pH 7.4). GSH was added to the incubation mixtures to trap the reactive 1 -oxometabolite formed after oxidation of 1 -hydroxyapiol. To determine the kinetic constants incubations following the conditions described above were done using final concentrations of 1 -hydroxyapiol from 50 to 2000 μM added to the incubation mixture from 100 times concentrated stock solutions in DMSO. After pre-incubation for 1 minute at 37 °C the reactions were started by adding the 1 -hydroxyapiol and were terminated after 60 minutes of incubation at 37°C by adding 25 μL of ice-cold acetonitrile. The formation of the GSH conjugate of 1 -oxoapiol, GS-1 -oxoapiol, was linear with time and microsomal protein under the experimental conditions used. Blank incubations were performed without the cofactor NAD⁺. Incubations were performed in triplicate. All samples were centrifuged for 5 minutes at 16000g, and the supernatant was stored at -20 °C until UPLC analysis.

Sulfonation of 1 -hydroxyapiol to 1 -sulfoxyapiol by rat and human liver S9

The kinetic constants for the enzymatic conversion of 1 -hydroxyapiol to 1 -sulfoxyapiol were determined using incubation mixtures containing (final concentrations) 10 mM GSH, 0.2 mM PAPS, and 3 mg/ml Sprague–Dawley rat or mixed gender pooled human liver S9 proteins in 0.1 M potassium phosphate buffer (pH 8.0). GSH was used as a scavenger of the reactive carbocation formed due to the unstable nature of the 1 -sulfoxy metabolite in an aqueous environment. After pre-incubation for 1 minute at 37 °C 1 - hydroxyapiol dissolved in DMSO was added in final concentrations ranging between 50 and 2000 μM, while keeping the final DMSO content at 1% (v/v). The reaction was terminated after 360 minutes

by adding 25 μ L of ice-cold acetonitrile. The formation of the GSH conjugate of 1-sulfoxyapiol was linear with time and S9 protein concentration under the experimental conditions used. The scavenging may either be chemically or catalysed by the glutathione S-transferases present in the S9 incubations in which the sulfonation of 1-hydroxyapiol was measured. Blank incubations were performed in the absence of PAPS. Incubations were performed in triplicate. All samples were centrifuged for 5 minutes at 16000g, and the supernatant was stored at -20 °C until UPLC analysis.

Identification and quantification of apiol metabolites

Apiol metabolites formed in microsomal incubations were identified using a photodiode array detection (UPLC-PDA) composed of a Waters (Waters, Milford, MA) Acquity solvent manager, sample manager, and diode array detector, equipped with a Water Acquity UPLC BEH C18 column. The gradient was made with a mixture of ACN and ultrapure water containing 0.1% (v/v) TFA. The flow rate was 0.6 ml/min. After equilibrating the column at the starting condition of 10% ACN, ACN increased to 50% over 4 minutes, was further increased to 80% over 0.5 minutes, decreased to 10% over 0.5 minutes and was finally kept at 10% for 1 minutes. Metabolites were identified as described in the Result section. Quantification of microsomal apiol metabolites was done by comparison of the peak areas obtained at a wavelength of 208 nm to the calibration curve of synthesized 1-hydroxyapiol because UV spectra of all metabolites were similar.

The concentration of 1-hydroxyapiol glucuronide was determined using the same UPLC-PDA system as described above. The gradient was made with acetonitrile and ultrapure water containing 0.1% (v/v) TFA. The flow rate was 0.6 ml/min. In a mixture of ACN and ultrapure water containing 0.1% (v/v) TFA, the gradient started at 10% ACN, increased to 60% ACN over 3.5 minutes, further increased to 80% over 0.5 minutes, kept at 80% ACN for 0.5 minutes

and then decreased to 10% ACN over 0.5 minutes. 1 -hydroxyapiol glucuronide was identified as described in the Result section. Quantification of 1 -hydroxyapiol glucuronide was done by comparison of the peak areas obtained at a wavelength of 208 nm to the calibration curve of synthesized 1 -hydroxyapiol.

The concentration of the glutathione conjugate of 1 -oxoapiol was determined using the same UPLC-PDA system as described above. The gradient was made with acetonitrile and ultrapure water containing 0.1% (v/v) TFA. The flow rate was 0.6 ml/min. In a mixture of ACN and ultrapure water containing 0.1% (v/v) TFA, the gradient started at 10% ACN, increased to 30% ACN over 2.5 minutes, was further increased to 80% ACN over 0.5 minutes, kept at 80% ACN for 0.5 minutes and finally decreased to 10% ACN over 0.5 minutes, and kept at 10% ACN for 0.5 minutes. Quantification of the GSH adduct of the metabolite was done by comparison of the peak areas obtained at a wavelength of 280 nm to the calibration curve of the GSH adduct of the synthesized 1 -oxoapiol.

The concentration of the glutathione conjugate of 1 -sulfoxyapiol was determined using the same UPLC-PDA system described above. The flow rate was 0.6 ml/min. In a mixture of ACN and ultrapure water containing 0.1% (v/v) TFA, the gradient started at 0% ACN, increased to 20% ACN over 0.2 minutes, further increased to 30% ACN over 4.3 minutes, and again increased to 100% ACN over 0.3 minutes, kept at 100% ACN for 0.2 minutes, and finally decreased to 0% ACN over 0.2 minutes and kept at 0% ACN for 0.8 minutes. The GSH adduct of 1 -sulfoxyapiol formed was identified by LC-MS using a microOTOF MS (Bruker) coupled to an Agilent LC (1200 Series) equipped with an Altima C18 column (150 x 4.6 mm, 3 μ m). The mobile phase used consisted of nanopure water with 0.1 % formic acid and ACN with 0.1 % formic acid. Elution was at a flow rate of 0.8 ml/min, starting at 22 % ACN with a linear increase to 100 % ACN in 30 minutes. Subsequently, the gradient returned linearly to the initial condition in 2 minutes and remained 13 minutes at this condition prior to the next injection.

Quantification of the GSH adduct of 1 -sulfoxyapiol was done by comparison of the peak areas obtained at a wavelength of 280 nm to the calibration curve of the GSH adduct of synthesized 1 -oxoapiol since their UV spectra are comparable. Mass spectrometric analysis was in the negative electrospray mode using a spray capillary voltage of 4500 V, a capillary temperature of 200°C and nitrogen as nebulizer gas at 8.0 L/min.

Determination of kinetic constants of apiol and 1 -hydroxyapiol metabolic conversions

Kinetic constants for the metabolic conversions of apiol and 1 -hydroxyapiol were calculated by two equations depending on the dose-dependency of the kinetics of the conversion. If the reaction reached saturation with increasing substrate concentration, the kinetic constants were derived by fitting the data to the standard Michaelis-Menten equation; $v = V_{\max} \times [S]/(K_m + [S])$, in which [S] represents the substrate concentration, V_{\max} the maximum velocity and K_m the Michaelis-Menten constant for the formation of the different metabolites of apiol or 1 -hydroxyapiol. Data analysis was accomplished using GraphPad Prism, version 5.04 (GraphPad Software, San Diego, California, USA). When the reaction did not reach saturation and rather displayed a linear increase in the rate of conversion with increasing substrate concentration, the kinetic rate constant for a first order reaction was derived by using the following equation; $v = k \cdot [S]$, with k being the first order rate constant and [S] representing the substrate concentration.

Apiol PBK models in rat and human

PBK models were developed describing the dose-dependent bioactivation and detoxification of apiol in respectively rat and human. The apiol models were based on the PBK models previously defined for the metabolism of estragole, methyleugenol, elemicin and safrole in rat (Al-Subeihi et al., 2011, Martati et al., 2011, Punt et al., 2008, Van den Berg et al., 2012) and

human (Al-Subeihi et al., 2012, Martati et al., 2012, Punt et al., 2009, Van den Berg et al., 2012). Figure 3 presents an overview of the developed PBK models for apiol metabolism in rat and human.

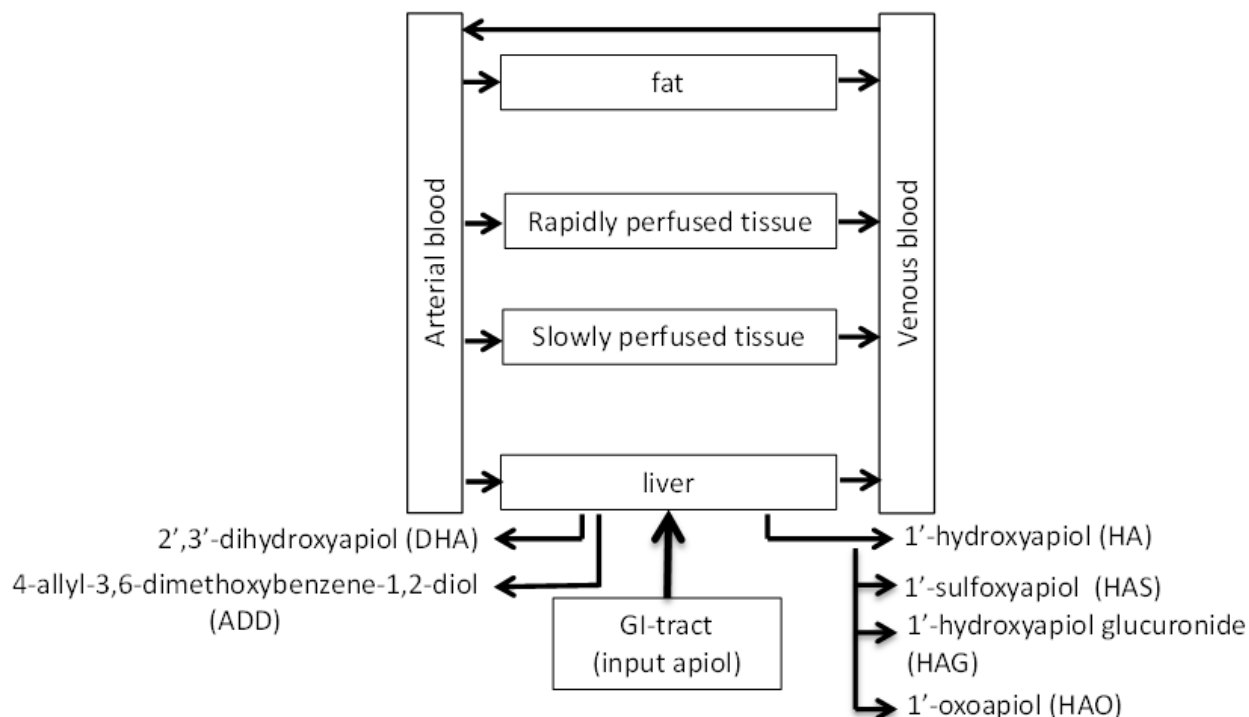


Figure 3: Overview of the PBK model for apiol.

The models consist of several compartments representing different organs and tissues (*i.e.* liver, fat tissue, rapidly perfused tissues and slowly perfused tissues) which are connected through the systemic circulation. First order kinetics was used to describe the uptake of apiol from the gastrointestinal tract assuming a direct and complete uptake by the liver with an absorption rate constant (k_a) of 1.0 h^{-1} which is based on the fast and complete absorption of the structurally related alkenylbenzene estragole from the gastrointestinal tract (WHO, 2009).

For both rat and human, only the liver microsomes were able to convert apiol to different microsomal metabolites (see Result section) and this is why no other tissue compartments were described as separate compartments in the model. In liver microsomal incubations 2,3-

Mode of action based risk assessment of the botanical food-borne alkenylbenzene apiol dihydroxyapiol (DHA), 1-hydroxyapiol (HA), and 4-allyl-3,6-dimethoxybenzene-1,2-diol (ADD) were formed and their formation was included. Since 2,3-dihydroxyapiol is formed after hydrolysis of apiol-2,3-oxide, data for both metabolites that result from epoxidation of apiol were combined and referred to as 2,3-dihydroxyapiol. Accordingly, a mass balance equation for apiol in rat and human liver is as follows:

$$\begin{aligned} \partial AL_A / \partial t &= \partial Uptake / \partial t + QL \times (CA_A - CL_A / PL_A) \\ &\quad - V_{max, HA} \times CL_A / PL_A / (K_m, HA + CL_A / PL_A) \\ &\quad - V_{max, DHA} \times CL_A / PL_A / (K_m, DHA + CL_A / PL_A) \\ &\quad - V_{max, ADD} \times CL_A / PL_A / (K_m, ADD + CL_A / PL_A) \\ \partial Uptake / \partial t &= -\partial AGI_A / \partial t = K_a \times AGI_A, \\ AGI_A(0) &= \text{oral dose} \\ CL_A &= AL_A / VL \end{aligned}$$

Where uptake_A (μmol) is the amount of apiol taken up from the gastrointestinal tract, AGI_A (μmol) is the amount of apiol remaining in the gastrointestinal tract, AL_A (μmol) is the amount of apiol in liver. CL_A is the apiol concentration in the liver (μmol/L). CA_A is the apiol concentrations in the arterial blood (in μmol/L), QL is the blood flow rate to liver (L/h), VL is the volume of the liver (L), PL_A is the liver/blood partition coefficient of apiol, and V_{max}, and K_m, are the values representing the maximum rate of formation and Michaelis-Menten constant, respectively, for the formation of 1-hydroxyapiol (HA), 2,3-dihydroxyapiol (DHA), and 4-allyl-3,6-dimethoxybenzene-1,2-diol (ADD).

In both models, the conversion of apiol to 2,3-dihydroxyapiol and 4-allyl-3,6-dimethoxybenzene-1,2-diol are described, but further reactions with these metabolites were not included in the model. It was assumed that these metabolites and/or their possible conjugates were completely excreted into the urine. Since the liver is the major target organ for

alkenylbenzene-induced carcinogenicity in rats and mice, the present study focused primarily on metabolic conversion of 1 -hydroxyapiol by glucuronidation, oxidation and sulfonation in the liver only. The mass balance equation for 1 -hydroxyapiol in rat and human liver is as follows:

$$\begin{aligned}
 \text{Rat:} \quad \partial AL_{HA}/\partial t &= V_{max, HA} \times CL_A/PL_A / (K_{m, HA} + CL_A/PL_A) \\
 &\quad - V_{max, HAG} \times CL_{HA}/PL_{HA} / (K_{m, HAG} + CL_{HA}/PL_{HA}) \\
 &\quad - k_{HAO} \times CL_{HA}/PL_{HA} \\
 &\quad - k_{HAS} \times CL_{HA}/PL_{HA} \\
 CL_{HA} &= AL_{HA}/VL
 \end{aligned}$$

$$\begin{aligned}
 \text{Human:} \quad \partial AL_{HA}/\partial t &= V_{max, HA} \times CL_A/PL_A / (K_{m, HA} + CL_A/PL_A) \\
 &\quad - V_{max, HAG} \times CL_{HA}/PL_{HA} / (K_{m, HAG} + CL_{HA}/PL_{HA}) \\
 &\quad - V_{max, HAO} \times CL_{HA}/PL_{HA} / (K_{m, HAO} + CL_{HA}/PL_{HA}) \\
 &\quad - k_{HAS} \times CL_{HA}/PL_{HA}
 \end{aligned}$$

where AL_{HA} is the amount of 1 -hydroxyapiol in the liver (μmol), CL_{HA} is the 1 -hydroxyapiol concentration in the liver ($\mu\text{mol/L}$), PL_{HA} is the liver/blood partition coefficient of 1 -hydroxyapiol, V_{max} , and K_m , are the maximum rate of formation and Michaelis-Menten constant, respectively, for the formation of the different apiol metabolites, including 1 -hydroxyapiol glucuronide (HAG) in the rat and human liver and 1 -oxoapiol (HAO) in human, and k is the first order rate constant for formation of 1 -oxoapiol in rat, and 1 -sulfoxyapiol (HAS) in rat and human liver.

V_{max} and K_m values and first order rate constants k in case of absence of saturation (for oxidation in rat and sulfonation of 1 -hydroxyapiol) for the different metabolic pathways of

apiol and 1-hydroxyapiol were derived *in vitro* in the present study. V_{\max} values that were derived *in vitro* expressed as $\text{nmol min}^{-1} (\text{mg liver microsomal or S9 protein})^{-1}$ were scaled to values representing the V_{\max} per $\mu\text{mol h}^{-1} (\text{g liver})^{-1}$ using microsomal yields of 35 mg/g liver in rat and 32 mg/g liver in human and S9 protein yields of 143 mg/g liver as defined by Punt *et al.* (Punt *et al.*, 2008, Punt *et al.*, 2009) based on Medinsky *et al.* (Medinsky *et al.*, 1994) First order rate constants k expressed in $\text{ml min}^{-1} (\text{mg liver microsomal or S9 protein})^{-1}$ were scaled to values expressed in ml h^{-1} per g liver using the same conversion factor for microsomal and S9 protein yield.

Tables 1 and 2 summarize the physiological parameters (*i.e.* tissue volumes, cardiac output and tissue blood flows) for rat and human respectively which were derived from literature (Brown *et al.*, 1997). Partition coefficients were derived *in silico* based on a method described by DeJongh *et al.* (DeJongh *et al.*, 1997) using the $\log K_{ow}$. $\log K_{ow}$ values for apiol (ClogP 3.12) and 1-hydroxyapiol (ClogP 1.56) were estimated using ChemBio3D 2010 (CambridgeSoft, USA). Mass balance equations were coded and numerically integrated in Berkeley Madonna 8.3.18 (Macey and Oster, UC Berkeley, CA, USA) using the Rosenbrock's algorithm for stiff systems. The PBK models were run during 720 hours after the dosing to allow full conversion of the parent compound.

Table 1: Parameters used in the physiologically based biokinetic model for apiol in male rat.

Physiological parameters		Tissue: blood partition	
Body wt (kg)	0.25	coefficients	
Percentage of body wt		apiol	
liver	3.4	liver	2.40
fat	7.0	fat	75.93
rapidly perfused	5.1	rapidly perfused	2.40
slowly perfused	60.2	slowly perfused	0.80
arterial blood	1.85		
venous blood	5.55		
Cardiac output (L/h)	5.4	1 -hydroxyapiol	
Percentage of cardiac output		liver	1.10
liver	25.0		
fat	7.0		
rapidly perfused	51.0		
slowly perfused	17.0		

Table 2: Parameters used in the physiologically based biokinetic model for apiol in human.

Physiological parameters		Tissue: blood partition	
Body wt (kg)	60	coefficients	
Percentage of body wt		apiol	
liver	2.6	liver	6.45
fat	21.4	fat	104.74
rapidly perfused	5.0	rapidly perfused	6.45
slowly perfused	51.7	slowly perfused	4.08
blood	7.9		
		1 -hydroxyapiol	
Cardiac output (L/h)	310	liver	1.55
Percentage of cardiac output			
liver	22.7		
fat	5.2		
rapidly perfused	47.3		
slowly perfused	24.8		

Model sensitivity analysis using normalized sensitivity coefficients

A sensitivity analysis was used to determine which parameters have the greatest influence on model predictions, and performed as described previously (Al-Subeihi et al., 2012, Al-Subeihi et al., 2011, Martati et al., 2011, Martati et al., 2012, Punt et al., 2008, Punt et al., 2009, Van den Berg et al., 2012). For this purpose, normalized sensitivity coefficients (SC) were determined using the following equation: $SC = (C - C)/(P - P) \cdot (P/C)$, with C being the initial

value of model output, C the modified value of the model output resulting from an increase in parameter value, P being the initial parameter value and P' representing the modified parameter value. An increase of 5% in parameter values was used to analyse the effect of a change in parameter on the formation of 1-hydroxyapiol and 1-sulfoxyapiol (expressed as a percentage of the dose over 720 hours). Each parameter was analysed individually while the other parameters were kept at their initial value.

Comparison of the newly developed apiol PBK models based predictions with PBK model predictions for the structurally related compound safrole.

The PBK model-based predictions for the formation of 1-hydroxyapiol and 1-sulfoxyapiol were compared to the PBK model-based predictions for the dose-dependent formation of the 1-hydroxy and 1-sulfoxy metabolites of the structurally related alkenylbenzene safrole. For this purpose, the previously defined PBK models for safrole in rat and human described by Martati *et al.* (Martati *et al.*, 2011b, Martati *et al.*, 2012b) were used. For comparison with apiol, the models describing the metabolism of safrole were also run for 720 hours.

Results

To identify the organs involved in the metabolism of apiol in both male rat and human, incubations were performed using microsomal protein preparations from liver, kidney, lung and small intestine. UPLC analysis of these incubations revealed that for both rat and human conversion of apiol was detected only in incubations with liver microsomes. An example of a chromatogram of an incubation of apiol with male rat liver microsomes and NADPH as the cofactor was shown in figure 4.

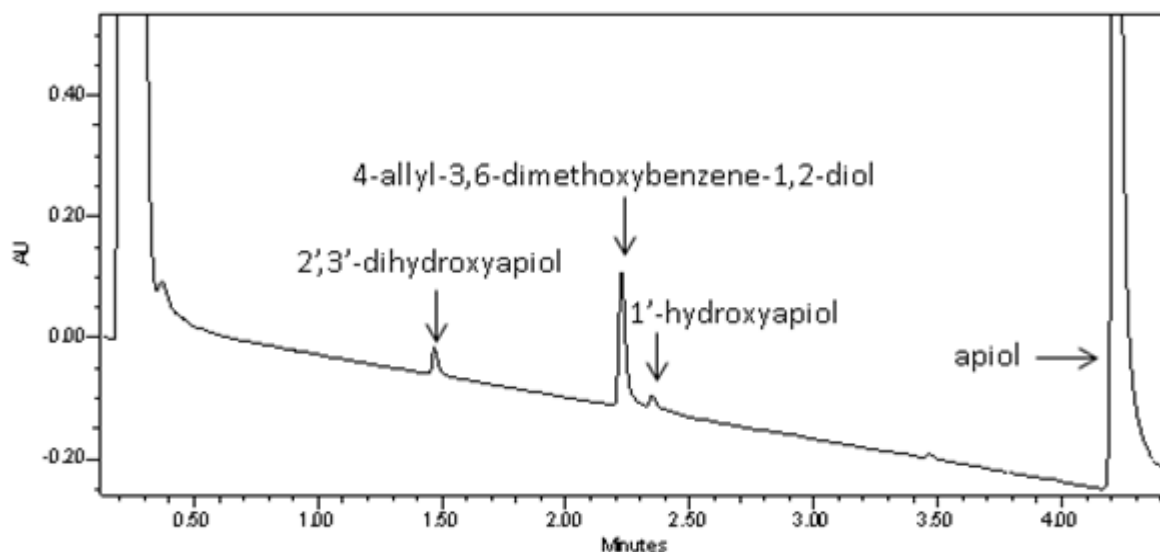


Figure 4: Chromatogram showing the different metabolites of apiol formed in incubations with male rat liver microsomes.

The metabolites formed in incubations with both rat and human liver microsomes were 2,3-dihydroxyapiol (RT 1.5 minutes), 1-hydroxyapiol (RT 2.4 minutes), and 4-allyl-3,6-dimethoxybenzene-1,2-diol (RT 2.2 minutes). Identification of 1-hydroxyapiol was done based on comparison of the UV-spectrum and retention time of the formed 1-hydroxyapiol with those of the specific synthesized reference compound. Tentative identification of 4-allyl-3,6-dimethoxybenzene-1,2-diol, resulting from the *O*-demethylenation of apiol (Benedetti et al., 1977, Beyer et al., 2006, Lee et al., 1998), and 2,3-dihydroxyapiol was based on analogy to UPLC chromatograms of metabolic conversions of safrole and the fact that apiol-2,3-oxide, formed following incubation of apiol with liver microsomes and NADPH, would be hydrolysed by epoxide hydrolase to 2,3-dihydroxyapiol as was previously demonstrated for the structurally related alkenylbenzenes (Al-Subeihi et al., 2011, Martati et al., 2011b, Punt et al., 2008, Luo et al., 1992, Luo and Guenther, 1996, Guenther and Luo, 2001). Furthermore, the formation of these three major metabolites is in line with the overview presented by JECFA of the three primary biotransformation pathways for methylenedioxy-substituted alkenylbenzenes including safrole, myristicin and apiol (WHO, 2009). Safrole, myristicin and apiol were

reported to be converted primarily by 1,2 ring-*O*-demethenylation yielding diphenolic derivatives(Benedetti et al., 1977, Beyer et al., 2006, Lee et al., 1998), by epoxidation of the double bond in the allyl side-chain yielding the 2,3-epoxide(Luo and Guenther, 1996, Luo et al., 1992), and by hydroxylation of the alkene side-chain to yield the 1-hydroxy metabolite(Benedetti et al., 1977, Miller et al., 1983, Zangouras et al., 1981).Apiol concentration-dependent formation of the various microsomal metabolites was also characterised and the kinetic constants derived from these data on the concentration-dependent microsomal metabolite formation of apiol in incubations with both male rat and human liver samples are presented in Table 3.

Table 3: Kinetic constants for metabolism of apiol and 1 -hydroxyapiol in incubations with Sprague–Dawley male rat liver microsomes or S9 fractions and mixed gender pooled human liver microsomes or S9 fractions (n=3)

Metabolite	Abbreviation	RAT				HUMAN			
		$K_m^{a,b} \pm SD$	$V_{max}^{a,c} \pm SD$	$k^d \pm SD$	in vitro catalytic efficiency ^e	$K_m^{a,b} \pm SD$	$V_{max}^{a,c} \pm SD$	$k^d \pm SD$	in vitro catalytic efficiency ^e
2,3-dihydroxyapiol	DHA	152 ± 18	0.15 ± 0.01		0.99		0.032 ± 0.026		0.48
	HA	95 ± 19	0.10 ± 0.02		1.05		0.035 ± 0.033		0.34
	ADD	37 ± 7.7	0.81 ± 0.07		21.89		0.58 ± 0.45		4.2
1 -hydroxyapiol									
1 -hydroxyapiol glucuronide	HAG	621 ± 459	5.1 ± 1.8		8.21		0.28 ± 0.19		0.74
	HAO			$13 \times 10^{-5} \pm 3 \times 10^{-5}$			1.13 ± 0.28		0.44
	HAS			$61 \times 10^{-7} \pm 15 \times 10^{-7}$				$45 \times 10^{-7} \pm 4 \times 10^{-7}$	

^a Mean values of three independent measurements ± SD

^b μM

^c nmol min⁻¹ (mg microsomal or S9 protein)⁻¹

^d First order rate constant for product formation (ml/min/mg protein)

^e μl min⁻¹ (mg microsomal or S9 protein)⁻¹, ($V_{max}/K_m \times 1000 \mu\text{l/ml}$)

Glucuronidation of 1 -hydroxyapiol to 1 -hydroxyapiol glucuronide by rat and human liver

S9

UPLC analysis of incubations with male rat liver S9 or mixed gender pooled human liver S9, UDPGA as cofactor and 1 -hydroxyapiol as substrate revealed a peak at 1.5 minutes, representing 1 -hydroxyapiol glucuronide since this peak was increased with increasing apiol concentration. Chromatographic analysis of blank incubations performed in the absence of the cofactor UDPGA did not show this peak at a retention time of 1.50 minutes, and the formation and elution behaviour of the metabolite was in analogous to results from similar incubations with safrole (Martati et al., 2011, Martati et al., 2012).

The 1 -hydroxyapiol concentration-dependent increase in glucuronidation of 1 -hydroxyapiol to 1 -hydroxyapiol glucuronide in incubations with both male rat and human liver fractions is presented in figures 5A and 5D respectively. The kinetic constants derived from these data are presented in Table 3.

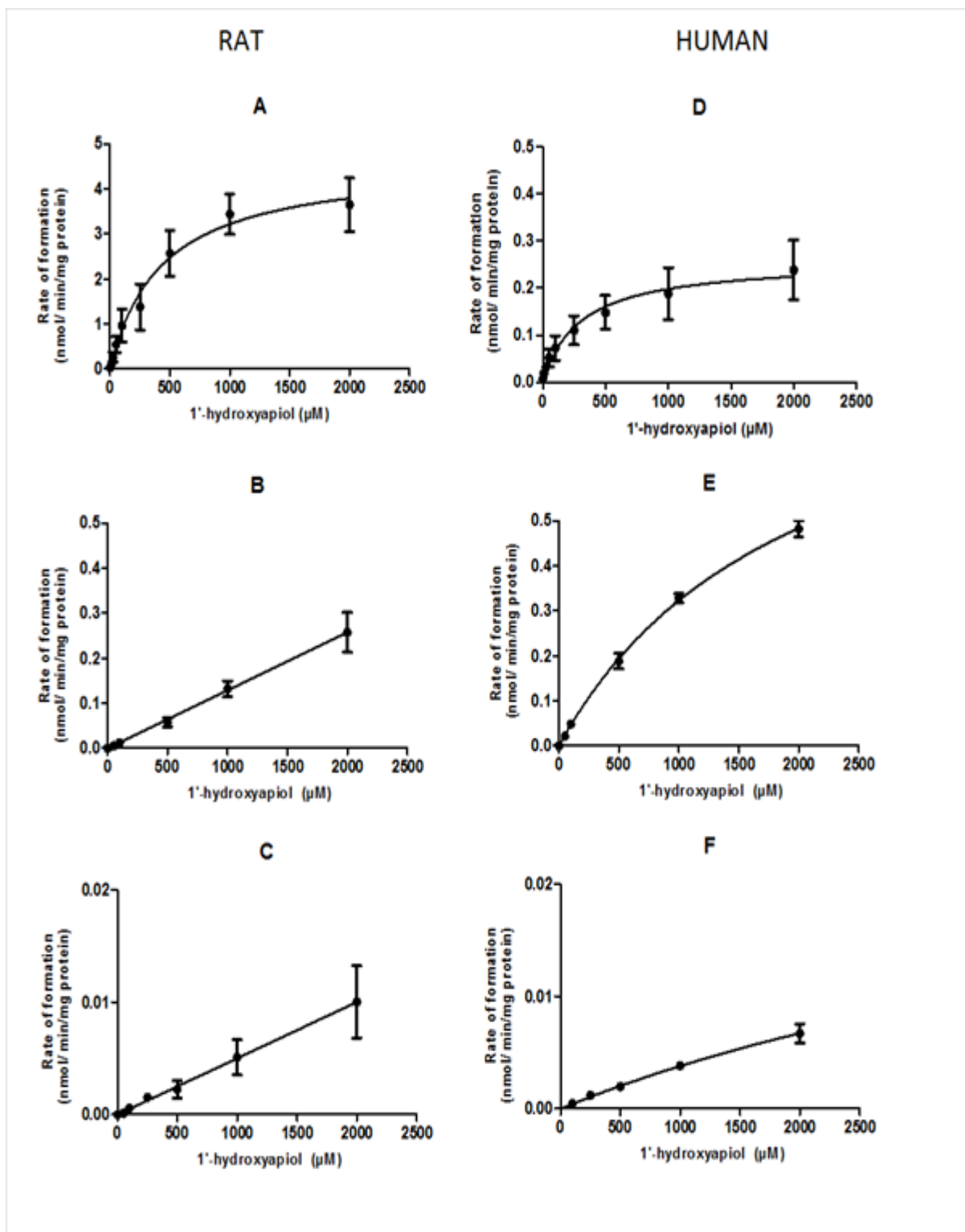


Figure 5: Concentration-dependent rate of (A) glucuronidation of 1-hydroxyapiol in incubations with pooled male rat liver S9 or (D) pooled human mixed gender liver S9, (B) oxidation of 1-hydroxyapiol in incubations with pooled male rat liver microsomes or (E) pooled human mixed gender liver S9, and (C) sulfonation of 1-hydroxyapiol in pooled male rat liver S9 or (F) pooled human mixed gender liver S9. Data points represent mean values +/- SD of three or four individual experiments.

Oxidation of 1-hydroxyapiol to 1-oxoapiol by rat and human liver microsomes

UPLC analysis of incubations with male rat liver microsomes or mixed gender pooled human liver microsomes, NAD⁺ as cofactor and 1-hydroxyapiol as substrate revealed a peak at 2.0 minutes. In this incubation GSH was also added to trap the reactive oxidation metabolite 1-oxoapiol. The peak at 2.0 minutes was identified as the GSH conjugate of 1-oxoapiol, GS-1-oxoapiol. Identification of GS-1-oxoapiol was done based on comparison of the UV-spectrum and retention time of the formed GS-1-oxoapiol with those of the synthesized reference compound.

The rate of oxidation of 1-hydroxyapiol in male rat liver microsomes and pooled human liver microsomes with increasing concentrations of 1-hydroxyapiol is presented in figures 5B and 5E respectively. Table 3 presents the kinetic constants derived from these data.

Sulfonation of 1-hydroxyapiol to 1-sulfoxyapiol by rat and human liver S9

The reactive 1-sulfoxyapiol formed upon sulfonation of the proximate carcinogenic metabolite 1-hydroxyapiol was trapped by using GSH. The scavenging may be either chemically or catalysed by the glutathione S-transferases present in the S9 incubations in which the sulfonation of 1-hydroxyapiol was measured.

UPLC analysis of incubations with male rat liver S9 or mixed gender pooled human liver S9, 1-hydroxyapiol, PAPS and GSH revealed a peak at 1.3 minutes. The LC-MS analysis showed increased signal of m/z 526 with negative ion mode. The ion at m/z 526 corresponds to the theoretically expected $[M-H]^-$ mass of a GSH adduct of 1-sulfoxyapiol. Figures 5C and 5F present the 1-hydroxyapiol concentration dependent rate of formation of 1-sulfoxyapiol in incubations with male rat liver S9 or mixed gender pooled human liver S9. The kinetic constants for the conversion of 1-hydroxyapiol to 1-sulfoxyapiol in rat and human liver derived from these data are presented in Table 3.

Comparison of the kinetic constants for conversion of apiol and 1-hydroxyapiol by male rat and mixed gender pooled human tissue fractions

In order to allow a comparison between the kinetic constants for metabolism of apiol and 1-hydroxyapiol by male rat and mixed gender pooled human tissue fractions, V_{\max} values that were derived in vitro expressed as $\text{nmol min}^{-1} (\text{mg microsomal or S9 protein})^{-1}$ were scaled to values representing the V_{\max} per $\mu\text{mol h}^{-1} (\text{g tissue})^{-1}$ using microsomal and S9 protein yields as described in literature (Medinsky et al., 1994) and previously used by Punt et al., (Punt et al., 2009, Punt et al., 2008) Al-Subeihi et al. (Al-Subeihi et al., 2012, Al-Subeihi et al., 2011) and Martati et al. (Martati et al., 2012b, Martati et al., 2011b). The in vivo V_{\max} values derived accordingly, were used to calculate a scaled catalytic efficiency (scaled V_{\max} in vivo/ K_m) for the formation of apiol metabolites (Table 4). These values revealed that the catalytic efficiency for formation of the proximate carcinogenic metabolite of apiol, 1-hydroxyapiol, is 3.3 times higher in male rat liver than in human liver. The difference in the formation rate is mainly due to the 3-fold difference in the maximum velocity (V_{\max}) for the conversion of apiol to 1-hydroxyapiol (see Table 3).

Table 4: Scaled kinetic constants for metabolic conversion of opiol and 1 -hydroxyapiol by male rat and human liver fractions.

species	Metabolite	K_m^a (μ M)	scaled V_{max} in vivo ^b (μ mol/h/g tissue)	in vivo catalytic efficiency ^c (ml/h/g tissue)	$k^d \pm SD$ (ml/min/mg protein)	Scaled k^e (ml/h/g tissue)
RAT	2,3 -dihydroxyapiol	152 \pm 18	0.32	2.07		
	1 -hydroxyapiol	95 \pm 19	0.21	2.21		
	4-allyl-3,6- dimethoxybenzene-1,2-diol	37 \pm 8	1.7	46.00		
	1 -hydroxyapiol glucuronide	621 \pm 459	43.76	70.75		
	1 -oxoapiol				13 \times 10 ⁻⁵ \pm 3 \times 10 ⁻⁵	0.27
	1 -sulfoxyapiol				61 \times 10 ⁻⁷ \pm 15 \times 10 ⁻⁷	0.052
HUMAN	2,3 -dihydroxyapiol	67 \pm 7	0.061	0.92		
	1 -hydroxyapiol	102 \pm 38	0.67	0.66		
	4-allyl-3,6- dimethoxybenzene-1,2-diol	138 \pm 18	1.11	8.13		
	1 -hydroxyapiol glucuronide	381 \pm 350	2.40	6.31		
	1 -oxoapiol	2592 \pm 755.7	2.17	0.85		
	1 -sulfoxyapiol				45 \times 10 ⁻⁷ \pm 4 \times 10 ⁻⁷	0.039

^a Mean values of three independent measurements \pm SD

^b Scaled V_{max} were converted from in vitro V_{max} based on microsomal protein yield of 35 mg/g liver in rat and 32 mg/g liver in human and S9 protein yield of 143 mg/g liver.

^c Catalytic efficiency (scaled $V_{max}(\text{app})/K_m$).

^d First order rate constant for product formation.

^e Scaled k were converted from k based on microsomal protein yield of 35 mg/g liver and S9 protein yield of 143 mg/g liver.

The formation of 1-hydroxyapiol glucuronide was found to represent the main metabolic reaction for detoxification of 1-hydroxyapiol in rat and human liver while in rat liver the catalytic efficiency for this conjugation was found to be 11.2-fold higher than in human.

For 1-hydroxyapiol oxidation, the scaled k for rat liver was found to be 3.1 times lower than the scaled in vivo catalytic efficiency for human liver. While for sulfonation the scaled k was 1.3-fold higher in rat liver than in human liver.

Altogether, the results revealed that glucuronidation of 1-hydroxyapiol, representing a detoxification pathway, is the most important pathway in rat and in human for conversion of 1-hydroxyapiol, and bioactivation of 1-hydroxyapiol by sulfonation was found to represent only a minor pathway in both rat and human.

Evaluation of apiol PBK model performance

Since there are no available quantitative experimental data on the excretion of the apiol metabolites formed after metabolism in both rat and human exposed to apiol, the performance of the newly developed PBK models for apiol could not be evaluated against in vivo data. Therefore, the evaluation of the PBK models for apiol was based on the evaluation of the similar PBK models for safrole and the other alkenylbenzenes, for which more in vivo data allowing evaluation of the models were available. The performance of the rat PBK model developed for safrole was evaluated by Martati et al. (Martati et al., 2011) where the predicted and observed levels of a variety of safrole metabolites in plasma or the urine of rats were compared. The predicted and observed safrole metabolite levels were found to be similar (Martati et al., 2011). Besides that, a comparison could be made between the predictions of the developed human PBK model for safrole (Martati et al., 2012) and the known in vivo data for human plasma concentrations or the urinary excretion of selected safrole metabolites. Furthermore, a comparison of the predictions of the developed PBK models for other alkenylbenzenes

(estragole and methyleugenol) (Al-Subeihi et al., 2012, Al-Subeihi et al., 2011, Punt et al., 2008, Punt et al., 2009) and the reported plasma and urine levels of their metabolites could be done to support the validity of developed PBK models for the alkenylbenzenes, thus indirectly supporting the validity of the apiol models. Based on the above considerations showing the validity of developed PBK models for all other alkenylbenzenes, it was concluded that it is a reasonable assumption that these models also adequately describe the metabolite levels formed in vivo in both rat and human after ingestion of different oral doses of apiol.

Apiol PBK model predictions for rat and human

Figure 6A shows the PBK model-based predictions for the dose-dependent formation of the different microsomal metabolites of apiol in rat liver. 4-Allyl-3,6-dimethoxybenzene-1,2-diol appears to be the major metabolite formed amounting to 91.5-85% of the dose with the percentage somewhat decreasing with increasing dose. The percentage of the dose converted to 1-hydroxyapiol was predicted to increase in a dose-dependent manner from 4% to about 7% of the dose at low and high dose levels respectively. Concurrent with the increase in the percentage of the dose that undergoes 1-hydroxylation of the alkene side chain, a dose-dependent increase from about 4% to 8% of the dose converted by epoxidation was observed. Figure 6B shows the PBK model-based predictions for the dose-dependent increase in the formation of the metabolites of 1-hydroxyapiol in rat liver. The percentage of the dose of apiol converted to 1-sulfoxyapiol varies with the dose amounting to 0.0032 % at a low dose of 0.05 mg/kg bw to 0.0050 % of the dose at a relatively high dose of 300 mg/kg bw, while these percentages amount to 0.017 % at low dose and 0.026 % at high dose for 1-oxoapiol. Glucuronidation appears to be the major metabolic route for 1-hydroxyapiol at all dose levels as 1-hydroxyapiol glucuronide amounts to about 4.38 % of the dose at low dose levels and to 6.80% of the dose at high dose levels.

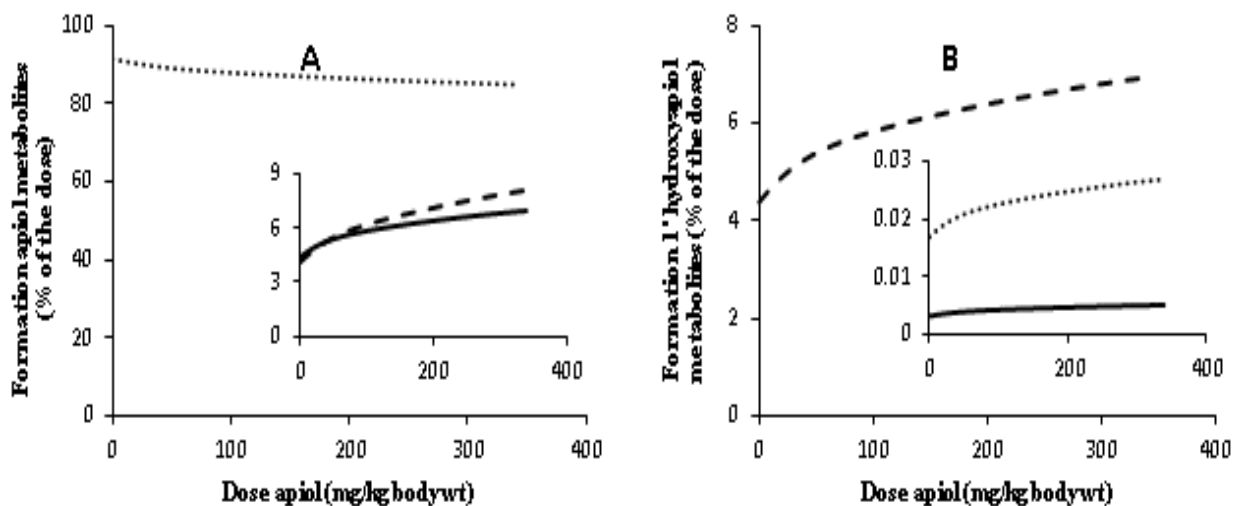


Figure 6: PBK-predicted dose-dependent changes in overall formation of (A) microsomal metabolites of apiol in rat liver and (B) metabolites of 1-hydroxyapiol in rat liver. The lines correspond to (A) 4-allyl-3,6-dimethoxybenzene-1,2-diol (), 1-hydroxyapiol (), and 2,3-dihydroxyapiol (), and (B) 1-hydroxyapiol glucuronide (), 1-sulfoxyapiol (), and 1-oxoapiol ().

Figure 7A shows the PBK model-based predictions for the dose-dependent formation of the different microsomal metabolites of apiol in human liver. In human liver 4-allyl-3,6-dimethoxybenzene-1,2-diol was predicted to be the major microsomal metabolite amounting to about 82.6-83.5% of the dose. In human liver, the percentage of the dose converted to 1-hydroxyapiol was only slightly decreased with the dose amounting to 6.7-6.3% of the dose. The decrease in the formation of 1-hydroxyapiol with increasing dose, is predicted to be accompanied by a decrease in the formation of apiol-2,3-oxide. Figure 7B shows the dose-dependent decrease in the relative formation of 1-hydroxyapiol glucuronide and 1-oxoapiol and the dose-dependent decrease of the relative formation of 1-sulfoxyapiol in human liver. There were only limited changes in the relative percentage of the different metabolites with the dose. 1-Hydroxyapiol glucuronide appears to be the major 1-hydroxyapiol metabolite amounting to about 5.9-5.5% of the dose, while 1-oxoapiol amounts to about 0.75% of the dose and 1-sulfoxyapiol to 0.035% of the dose.

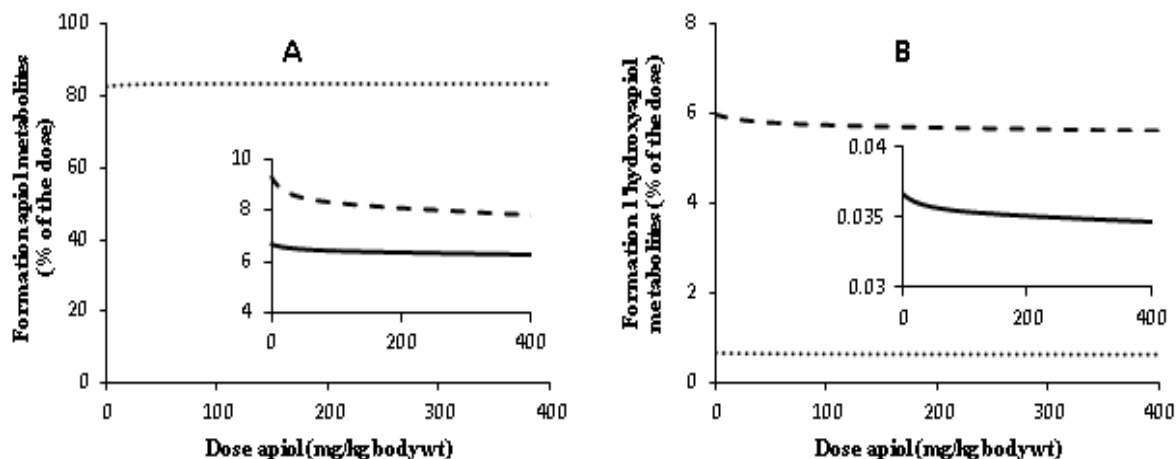


Figure 7: PBK-predicted dose-dependent changes in overall formation of (A) microsomal metabolites of apioI in human liver and (B) metabolites of 1-hydroxyapioI in human liver. The lines correspond to (A) 4-allyl-3,6-dimethoxybenzene-1,2diol (), 1-hydroxyapioI (), and 2,3-dihydroxyapioI (), and (B) 1-hydroxyapioI glucuronide (), 1-sulfoxyapioI (), and 1-oxoapioI ().

Figure 8 shows a comparison of the relative extent of bioactivation of apioI by rat and human liver. There are species differences in the formation of 1-hydroxyapioI (Figure 8A) and 1-sulfoxyapioI (Figure 8B) (expressed as nmol/g liver). In rat liver, the formation of 1-hydroxyapioI at low dose was almost 2 times lower than in human liver and gradually increased with increasing the dose to reach almost the same relative level as in human at high dose. Human liver was predicted to be more efficient in formation of 1-sulfoxyapioI being 15-fold higher at low dose and 8-fold higher at high dose than 1-sulfoxyapioI formation by rat liver (Figure 8B). This higher relative formation of 1-sulfoxyapioI in human than rat liver in spite of the almost equal rate of formation of its metabolic precursor 1-hydroxyapioI in rat and human liver is due to the fact that the glucuronidation of 1-hydroxyapioI in rat liver is around 10 times more efficient than that in human liver providing increased opportunity for the competing sulfonation. The difference in overall formation of the 1-sulfoxyapioI formation between rat and human is not due to a marked difference in the kinetics for sulfonation of the

1-hydroxyapiol since this difference appeared limited with an only 1.35-fold higher first order rate constant for sulfonation in rat than human liver (see Table 3).

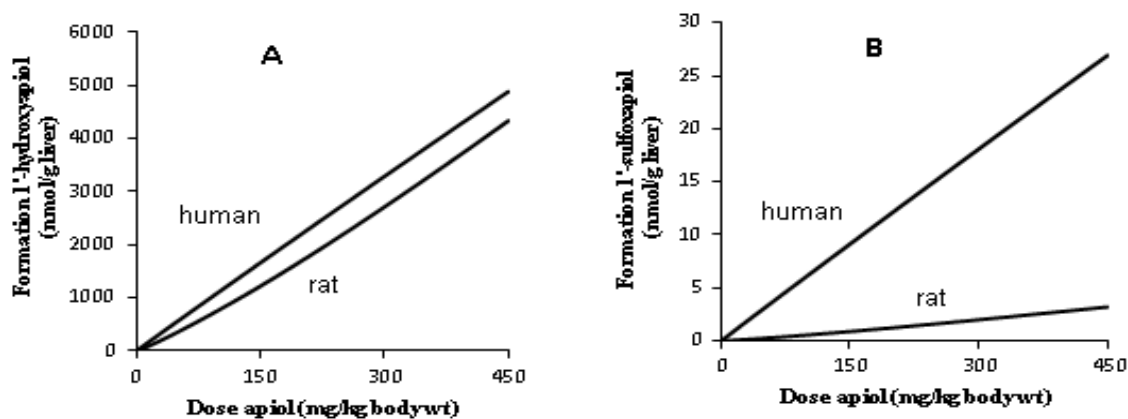


Figure 8: PBK-predicted dose-dependent formation of (A) 1-hydroxyapiol and (B) 1-sulfoxyapiol in rat and human liver.

Sensitivity analysis

In order to know the model parameters that have the highest impact on the formation of 1-hydroxyapiol and 1-sulfoxyapiol in rat and human liver, a sensitivity analysis was performed. The analysis was done at an apiol dose of 0.05 mg/kg body wt per day to calculate the normalized sensitivity coefficients for all model parameters. Normalized sensitivity coefficient values higher than 0.1, affecting the formation of 1-hydroxyapiol and 1-sulfoxyapiol in rat and human liver, are shown in figures 9A and 9B. Figure 9 shows that in both rat and human the parameters that influence the formation of both metabolites to the highest extent are the same. 1-Hydroxyapiol formation is mainly influenced by the kinetic constants for formation of 1-hydroxyapiol ($V_{\max,HA}$, $k_{m,HA}$) and the kinetic constants for formation of 4-allyl-3,6-dimethoxybenzene-1,2-diol ($V_{\max,ADD}$, $k_{m,ADD}$). Besides the above parameters, 1-sulfoxyapiol formation was influenced by kinetic constants for formation of 1-hydroxyapiol glucuronide ($V_{\max,HAG}$, $k_{m,HAG}$) and of 1-sulfoxyapiol (k_{HAS}).

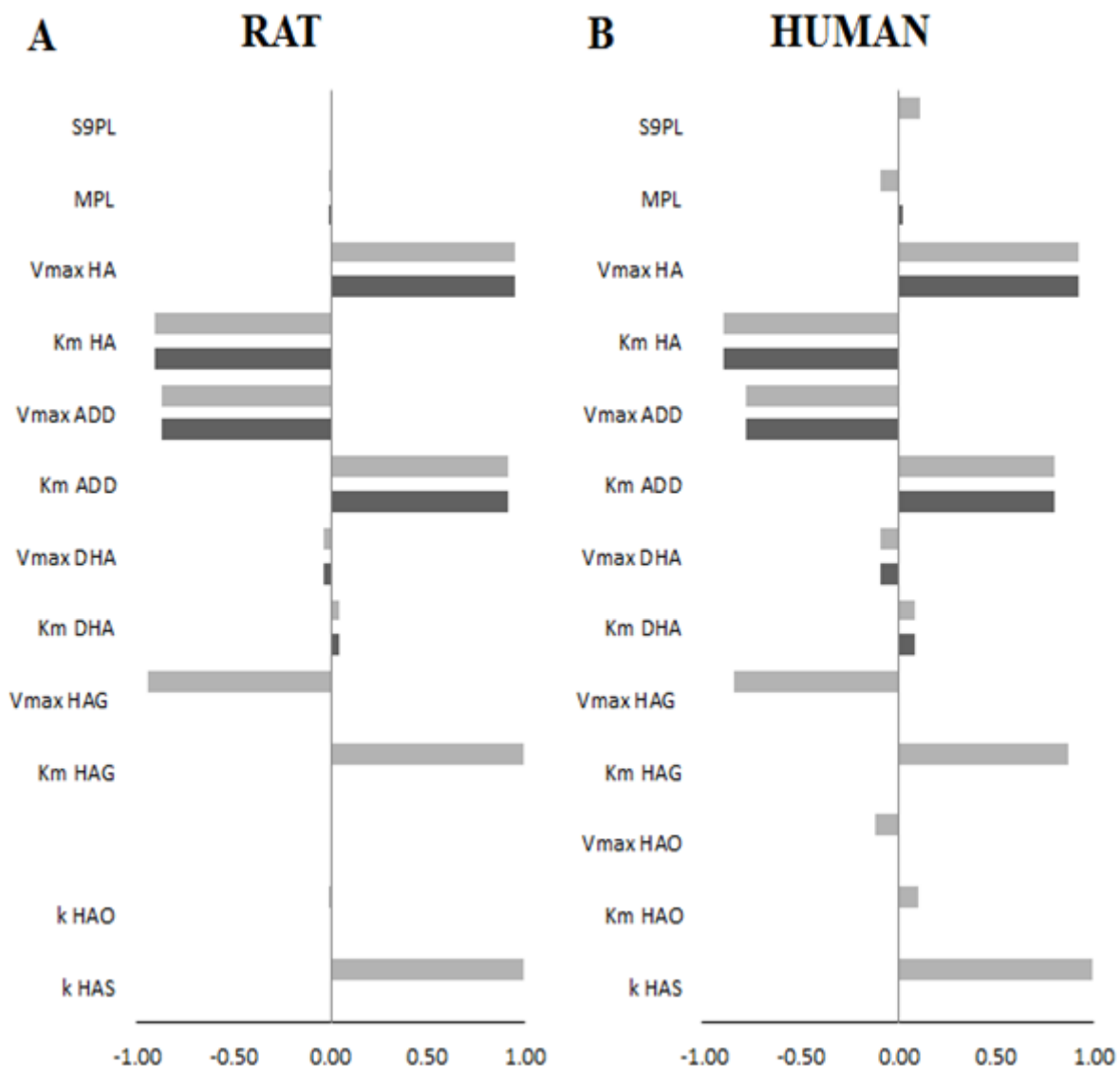


Figure 9: Normalized sensitivity coefficients for the formation of 1-hydroxyapiol (black)

and 1-sulfoxyapiol (grey) in the liver of rat and human. S9PL = S9 protein yield of the liver, MPL = microsomal protein yield of the liver, Vmax the maximum velocity and Km the Michaelis-Menten constant for the formation of the different metabolites, k = the kinetic rate constant for a first order reaction, ADD = 4-allyl-3,6-dimethoxybenzene-1,2-diol, DHA, = 2,3-di hydroxyapiol, HA = 1-hydroxyapiol, HAG = 1-hydroxyapiol glucuronide, HAO = 1-oxoapiol; HES = 1-sulfoxyapiol.

Comparison of the PBK model-based prediction of bioactivation of apiol by rat and human to the PBK model predictions for bioactivation of the structurally related compound safrole.

The PBK model-based predictions for bioactivation of apiol in rat and human, were compared to the PBK model-based predictions for bioactivation of safrole to facilitate a read-across-based risk assessment. Figure 10 shows the dose-dependent formation of the 1-hydroxy and 1-sulfoxy metabolites in rat liver as predicted by the respective PBK models from dose levels representing estimated human daily intakes up to dose levels causing liver tumors in rodent bioassays with safrole. In rat liver, the PBK model-based predicted formation of the proximate carcinogenic 1-hydroxy metabolite was found to be 2.8-fold lower for apiol than for safrole at low dose and 2.0-fold lower at the highest dose (Fig. 10A). Figure 10B shows the predicted model outcomes for the formation of the ultimate carcinogenic 1-sulfoxy metabolites of apiol and safrole. In rat liver, the formation of the 1-sulfoxy metabolite is predicted to be about 3-fold lower for apiol than for safrole. For both alkenylbenzenes the formation of their 1-sulfoxy metabolite increases linearly with increase of the dose.

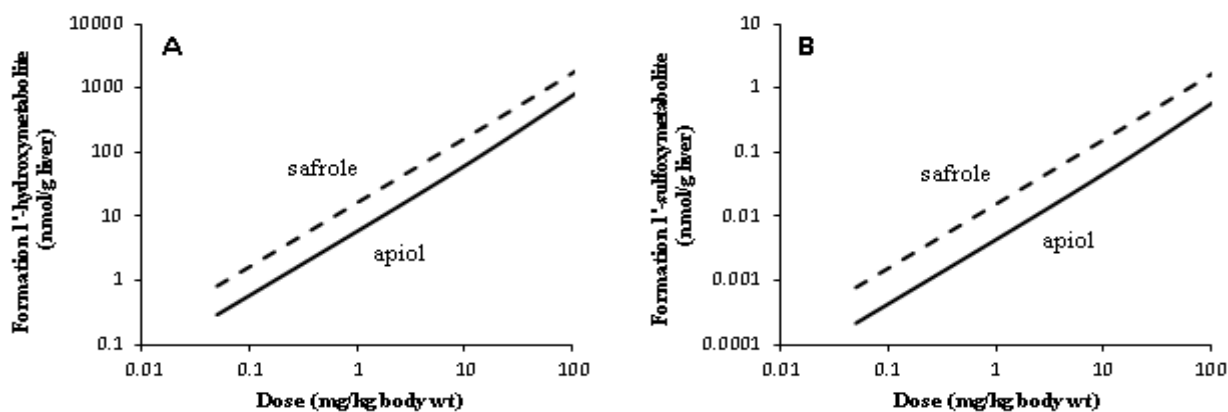


Figure 10: PBK-predicted dose-dependent formation (nmol / g liver) of (A) 1-hydroxy metabolites and (B) 1-sulfoxy metabolites of apiol () and safrole () in male rat liver.

Figure 11 shows the predicted dose-dependent formation of the 1-hydroxymetabolites and 1-sulfoxy metabolites of apiol and safrole in human liver. The predicted formation of the 1-hydroxy metabolite is predicted to be about 8-fold lower for apiol than for safrole at low dose and about 6-fold lower at high dose levels. In human liver, the formation of the 1-sulfoxy metabolites of apiol is predicted to be 2 times lower for apiol than for safrole.

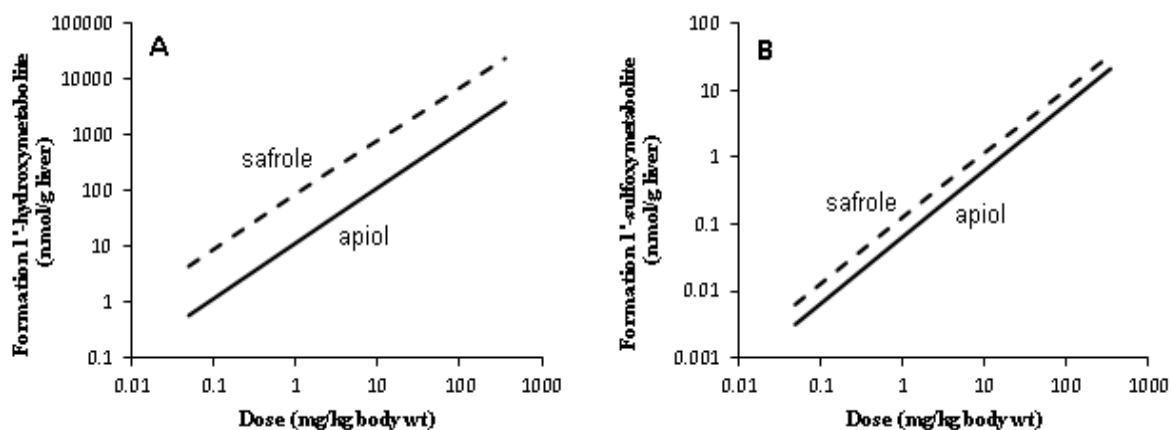


Figure 11: PBK-predicted dose-dependent formation (nmol / g liver) of (A) 1-hydroxymetabolites and (B) 1-sulfoxy metabolites of apiol () and safrole () in human liver.

Implications for risk assessment

In order to evaluate the possible human health hazards due to daily consumption of apiol, the margin of exposure (MOE) approach can be used. The MOE is the preferred approach to assess the safety of a compound that is carcinogenic and genotoxic (EFSA, 2005).

Carcinogenicity data for apiol from which a BMDL₁₀ can be derived are absent, hampering the application of the MOE approach in the risk assessment of apiol. On the other hand, the results of the PBK model predictions presented above indicate that at dose levels in the range at which safrole exposed rodents develop tumors (10-100 mg/kg body wt per day) (Long et al., 1963), the formation of 1-sulfoxy metabolites of apiol in rat liver is about 3-fold lower than that of safrole. Based on this result it can be assumed that the PBK modelling supports use of the BMDL₁₀ for tumor formation by safrole for risk assessment of the related compound apiol

making a correction for the expected 3-fold lower formation of the ultimate carcinogenic 1-sulfoxy metabolite assuming the same mode of action for these two analogues. Depending on the differences of formation of ultimate carcinogen of apiol and safrole in rat liver at dose levels that induce liver tumor formation in rodents exposed to safrole, the BMDL₁₀ of safrole which amounts to 1.9-5.1 mg/kg body wt per day (van den Berg et al., 2011) was multiplied by factor of 3 resulting in a BMDL₁₀ of 5.7-15.3 mg/kg body wt per day. The estimated mean daily intake of apiol from spice and spice oil in the USA was reported to amount to 4×10^{-5} mg/kg body wt per day (WHO, 2009). Using a BMDL₁₀ of 5.7-15.3 mg/kg body wt per day and an estimated daily intake of apiol of 4×10^{-5} mg/kg body wt per day the MOE for apiol would amount to 140000 -385000. This indicates that there would be a low concern and a low priority for risk management of the current levels of exposure to apiol. For comparison, the MOE values of safrole can be given, obtained at the estimated daily intake of safrole from spice and spice oil in USA that amounts to 1×10^{-3} mg/kg body wt per day (WHO, 2009), and using a BMDL₁₀ of safrole of 1.9-5.1 mg/kg body wt per day. These data result in an MOE for safrole of 1900-5100 indicating a priority for risk management that is higher than for apiol.

Discussion:

The present paper describes the definition of mode of action-based PBK models for detoxification and bioactivation of the alkenylbenzene apiol in rat and human and the use of predictions made by these models to facilitate a read-across-based risk assessment to the structurally related alkenylbenzene safrole (Martati et al., 2011, Martati et al., 2012), for which in vivo carcinogenicity data are available. Previously, using a similar approach and read-across to estragole and methyleugenol, the risks of exposure to elemicin for which also no in vivo rodent tumor data were available could be evaluated (Van den Berg et al., 2012). The approach enables a preliminary risk assessment of apiol for which in vivo toxicity data are limited

without the need for additional animal studies. The physiological parameters for rat and human and the biochemical and physiochemical parameters for apiol were defined to develop the apiol PBK models.

The newly developed PBK models for apiol provide insight into the species-differences in the relative extent of bioactivation and detoxification, and could also be used to compare the level of metabolic activation of apiol to that of safrole in male rat and human liver (Martati et al., 2011, Martati et al., 2012). Comparing the apiol and safrole model-based predictions showed that the formation of the proximate and ultimate carcinogenic metabolites of the two alkenylbenzenes in rat is predicted to be comparable within an order of magnitude. The PBK models predict the formation of the ultimate carcinogenic 1-sulfoxy metabolite at a dose level of 100 mg/kg body wt, at which safrole is causing liver tumors in rodent animal (Long et al., 1963, WHO, 2009), to be 3-fold lower for apiol than for safrole in rat liver. In line with these differences, Randerath et al. (Randerath et al., 1984), using ^{32}P -postlabeling reported that the number of DNA adducts formed by apiol in adult mouse liver was lower than for safrole. In a parallel study, Phillips et al. (Phillips et al., 1984) reported that in preweaning male mice the level of DNA adducts formed after neonatal apiol exposure was about 12-fold lower than after neonatal safrole exposure (Phillips et al., 1984). In addition, the ability of apiol to form DNA adducts in cultured human (HepG2) cells was reported to be 3-5 times lower than that of safrole (Zhou et al., 2007).

It is important to note that the PBK model-based predictions quantify the amount of the ultimate carcinogenic metabolite formed and not the ability of these compounds to bind to DNA or other macromolecules. One could argue that this reactivity may differ between the different alkenylbenzene compounds and that an increasing number of methoxy groups may reduce the electrophilicity of the 1-sulfoxy metabolite or its carbocation decreasing its ability to bind to DNA (Miller et al., 1983, Randerath et al., 1984). However, given that the PBK model-based

predicted differences are in line with the currently available data from in vivo and cellular in vitro studies on DNA adduct formation by apiol and safrole it is concluded that these possible differences in electrophilicity of the two 1-sulfoxy metabolites does not affect the predictions to an extent that it would modify the conclusions of the current MOE based preliminary risk assessment.

Based on the rat PBK model predictions for formation of the related 1-sulfoxy metabolite, being 3-fold lower for apiol than for safrole at dose levels that are known to induce tumors in safrole-exposed rodent models, it was concluded that the BMDL₁₀ that would be expected in a rodent animal bioassay for apiol could be 3-fold higher than that of safrole. Based on these considerations a preliminary risk assessment was performed for apiol using the MOE approach and an estimated BMDL₁₀ for apiol, of 3 times the BMDL₁₀ for safrole (1.9-5.1 mg/kg body wt per day) (van den Berg et al., 2011) and the MOE for apiol was calculated to amount to 140000-385000. It is of interest to note that the PBK model of the present study predicted that the formation of the ultimate carcinogenic 1-sulfoxy metabolite of apiol in human liver would be about 10 times higher than its formation in rat liver. This difference is included in the MOE of 10 000 which was defined to include a factor of 10 for interspecies differences (EFSA, 2005). Given that the MOE values actually obtained for apiole are 14-38-fold higher than 10 000 they could accommodate an even larger species difference than the 10-fold difference now included in the MOE of 10000 without leading to a different conclusion. Furthermore, comparison of the MOE values obtained in the present study for apiol and safrole, indicate a priority for risk management of safrole that is higher than for apiol, due to its 3 times lower BMDL₁₀ and its 25-fold higher estimated daily intake.

In conclusion, the present study reports the development of apiol PBK models for rat and human providing insight into the occurrence of species differences in the metabolic activation of this food-borne compound that is genotoxic and carcinogenic. In addition, the PBK model

predictions were applied to support read-across from safrole for which tumor data are available facilitating a preliminary risk assessment for apiol for which limited in vivo data are available. This example illustrates how PBK modelling can be used to contribute to risk assessment eliminating the need for animal bioassays thereby contributing to the 3Rs of animal testing in human safety assessments.

Acknowledgements

The authors would like to thank Dr. Yiannis Fiamegos for the synthesis of 1 -hydroxyapiol and Mr. Bert Spenkelink for the synthesis of 1 -oxoapiol. AMA and AJAM acknowledge financial support from the SOIT foundation (the Foundation for Stimulation Of Innovation in Toxicology). Part of this work has been supported by financial assistance of the European Union under the ENPI CBC Mediterranean Sea Basin Programme under project I.B/4.1/257, BRAMA (Botanicals Risk Assessment Training in the Mediterranean Area).

References

1. Al-Subeihi, A. A., Spenkelink, B., Punt, A., Boersma, M. G., van Bladeren, P. J. & Rietjens, I. M. C. M. 2012. Physiologically based kinetic modeling of bioactivation and detoxification of the alkenylbenzene methyleugenol in human as compared with rat. *Toxicology and applied pharmacology*, 260, 271-84.
2. Al-Subeihi, A. A., Spenkelink, B., Rachmawati, N., Boersma, M. G., Punt, A., Vervoort, J., van Bladeren, P. J. & Rietjens, I. M. C. M. 2011. Physiologically based biokinetic model of bioactivation and detoxification of the alkenylbenzene methyleugenol in rat. *Toxicology in vitro : an international journal published in association with BIBRA*, 25, 267-85.
3. Benedetti, M. S., Malnoe, A. & Broillet, A. L. 1977. Absorption, metabolism and excretion of safrole in the rat and man. *Toxicology*, 7, 69-83.
4. Beyer, J., Ehlers, D. & Maurer, H. H. 2006. Abuse of nutmeg (*Myristica fragrans* Houtt.): studies on the metabolism and the toxicologic detection of its ingredients elemicin, myristicin, and safrole in rat and human urine using gas chromatography/mass spectrometry. *Therapeutic drug monitoring*, 28, 568-75.
5. Brown, R. P., Delp, M. D., Lindstedt, S. L., Rhomberg, L. R. & Beliles, R. P. 1997. Physiological parameter values for physiologically based pharmacokinetic models. *Toxicol Ind Health*, 13, 407-84.
6. DeJongh, J., Verhaar, H. J. & Hermens, J. L. 1997. A quantitative property-property relationship (QPPR) approach to estimate in vitro tissue-blood partition coefficients of organic chemicals in rats and humans. *Arch Toxicol*, 72, 17-25.
7. EFSA 2005. Opinion of the Scientific Committee on a request from EFSA related to A Harmonised Approach for Risk Assessment of Substances Which are both Genotoxic and Carcinogenic. *EFSA J*, 282, 1-31.
8. Guenther, T. M. & Luo, G. 2001. Investigation of the role of the 2',3'-epoxidation pathway in the bioactivation and genotoxicity of dietary allylbenzene analogs. *Toxicology*, 160, 47-58.
9. Jeurissen, S. M., Bogaards, J. J., Awad, H. M., Boersma, M. G., Brand, W., Fiamegos, Y. C., van Beek, T. A., Alink, G. M., Sudholter, E. J., Cnubben, N. H. & Rietjens, I. M. 2004. Human cytochrome p450 enzyme specificity for bioactivation of safrole to the proximate carcinogen 1'-hydroxysafrole. *Chemical research in toxicology*, 17, 1245-50.
10. Lee, H. S., Jeong, T. C. & Kim, J. H. 1998. In vitro and in vivo metabolism of myristicin in the rat. *Journal of chromatography. B, Biomedical sciences and applications*, 705, 367-72.
11. Long, E. L., Nelson, A. A., Fitzhugh, O. G. & Hansen, W. H. 1963. Liver tumors produced in rats by feeding safrole. *Archives of Pathology*, 76, 595-604.
12. Luo, G. & Guenther, T. M. 1996. Covalent binding to DNA in vitro of 2',3'-oxides derived from allylbenzene analogs. *Drug metabolism and disposition: the biological fate of chemicals*, 24, 1020-7.
13. Luo, G., Qato, M. K. & Guenther, T. M. 1992. Hydrolysis of the 2',3'-allylic epoxides of allylbenzene, estragole, eugenol, and safrole by both microsomal and cytosolic epoxide hydrolases. *Drug metabolism and disposition: the biological fate of chemicals*, 20, 440-5.
14. Martati, E., Boersma, M. G., Spenkelink, A., Khadka, D. B., Punt, A., Vervoort, J., van Bladeren, P. J. & Rietjens, I. M. 2011. Physiologically based biokinetic (PBBK) model for safrole bioactivation and detoxification in rats. *Chem Res Toxicol*, 24, 818-34.
15. Martati, E., Boersma, M. G., Spenkelink, A., Khadka, D. B., van Bladeren, P. J., Rietjens, I. M. & Punt, A. 2012. Physiologically based biokinetic (PBBK) modeling of safrole bioactivation and detoxification in humans as compared with rats. *Toxicol Sci*, 128, 301-16.
16. Medinsky, M. A., Leavens, T. L., Csanady, G. A., Gargas, M. L. & Bond, J. A. 1994. In vivo metabolism of butadiene by mice and rats: a comparison of physiological model predictions and experimental data. *Carcinogenesis*, 15, 1329-40.

17. Miller, E. C., Swanson, A. B., Phillips, D. H., Fletcher, T. L., Liem, A. & Miller, J. A. 1983. Structure-activity studies of the carcinogenicities in the mouse and rat of some naturally occurring and synthetic alkenylbenzene derivatives related to safrole and estragole. *Cancer research*, 43, 1124-34.
18. Parthasarathy, V. A., chembackam, B.T., Zachariah, T. 2008. Chemistry of Spices. Kerala: CABI.
19. Phillips, D. H., Reddy, M. V. & Randerath, K. 1984. 32P-post-labelling analysis of DNA adducts formed in the livers of animals treated with safrole, estragole and other naturally-occurring alkenylbenzenes. II. Newborn male B6C3F1 mice. *Carcinogenesis*, 5, 1623-8.
20. Punt, A., Freidig, A. P., Delatour, T., Scholz, G., Boersma, M. G., Schilter, B., van Bladeren, P. J. & Rietjens, I. M. 2008. A physiologically based biokinetic (PBBK) model for estragole bioactivation and detoxification in rat. *Toxicology and applied pharmacology*, 231, 248-59.
21. Punt, A., Paini, A., Boersma, M. G., Freidig, A. P., Delatour, T., Scholz, G., Schilter, B., van Bladeren, P. J. & Rietjens, I. M. C. M. 2009. Use of physiologically based biokinetic (PBBK) modeling to study estragole bioactivation and detoxification in humans as compared with male rats. *Toxicological sciences : an official journal of the Society of Toxicology*, 110, 255-69.
22. Randerath, K., Haglund, R. E., Phillips, D. H. & Reddy, M. V. 1984. 32P-post-labelling analysis of DNA adducts formed in the livers of animals treated with safrole, estragole and other naturally-occurring alkenylbenzenes. I. Adult female CD-1 mice. *Carcinogenesis*, 5, 1613-22.
23. SCF 2001a. Opinion of the Scientific Committee of Food on Estragole (1-allyl-4-methoxybenzenen).
24. SCF 2001b. Opinion of the Scientific Committee of Food on Methyleugenol (1-allyl-1,2-dimethoxybenzenen).
25. SCF 2002. Opinion of the Scientific Committee of Food on Safrole (1-allyl-3,4-methylene dioxybenzenen)
26. Tunali, T., Yarat, A., Yanardag, R., Ozcelik, F., Ozsoy, O., Ergenekon, G. & Emekli, N. 1999. Effect of parsley (*Petroselinum crispum*) on the skin of STZ induced diabetic rats. *Phytotherapy research : PTR*, 13, 138-41.
27. Van den Berg, S. J., Patrizia Restani, Marelle G. Boersma, Luc Delmulle & Rietjens, I. M. C. M. 2011. Levels of Genotoxic and Carcinogenic Compounds in Plant Food Supplements and Associated Risk Assessment. *Food and Nutrition Sciences*, 989-1010.
28. Van den Berg, S. J., Punt, A., Soffers, A. E., Vervoort, J., Ngeleja, S., Spenkelink, B. & Rietjens, I. M. C. M. 2012. Physiologically based kinetic models for the alkenylbenzene elemicin in rat and human and possible implications for risk assessment. *Chemical research in toxicology*, 25, 2352-67.
29. WHO 2009. Safety evaluation of certain additives, prepared by the Sixty-ninth meeting of the Joint FAO/WHO Expert Committee on Food Additives. *World Health Organization* http://whqlibdoc.who.int/publications/2009/9789241660600_eng.pdf.
30. Wiseman, R. W., Miller, E. C., Miller, J. A. & Liem, A. 1987. Structure-activity studies of the hepatocarcinogenicities of alkenylbenzene derivatives related to estragole and safrole on administration to preweanling male C57BL/6J x C3H/HeJ F1 mice. *Cancer research*, 47, 2275-83.
31. Wislocki, P. G., Borchert, P., Miller, J. A. & Miller, E. C. 1976. The metabolic activation of the carcinogen 1'-hydroxysafrole in vivo and in vitro and the electrophilic reactivities of possible ultimate carcinogens. *Cancer research*, 36, 1686-95.
32. Zangouras, A., Caldwell, J., Hutt, A. J. & Smith, R. L. 1981. Dose dependent conversion of estragole in the rat and mouse to the carcinogenic metabolite, 1'-hydroxyestragole. *Biochemical pharmacology*, 30, 1383-6.
33. Zhou, G. D., Moorthy, B., Bi, J., Donnelly, K. C. & Randerath, K. 2007. DNA adducts from alkoxyallylbenzene herb and spice constituents in cultured human (HepG2) cells. *Environmental and molecular mutagenesis*, 48, 715-21.

Chapter 3

Physiologically based kinetic modelling of the bioactivation of myristicin

Amer J. Al_Malahmeh, Abdalmajeed M. Alajlouni , Reiko Kiwamoto, Sebastiaan Wesseling,
Ans E.M.F. Soffers, Ala A.A. Al-Subeihi, Jacques Vervoort, and Ivonne M.C.M. Rietjens.

Based on: Archives of Toxicology (2017), 91: 713–734

Abstract

The present study describes physiologically based kinetic (PBK) models for the alkenylbenzene myristicin that were developed by extension of the PBK models for the structurally related alkenylbenzene safrole in rat and human. The newly developed myristicin models revealed that the difference between rat and human in the formation of the proximate carcinogenic metabolite 1-hydroxymyristicin in liver is 1.8-fold higher in rat at most, and limited for the ultimate carcinogenic metabolite 1-sulfoxymyristicin to (2.8-4.0)-fold higher in human. In addition, a comparison was made between the relative importance of bioactivation for myristicin and safrole. Model predictions indicate that for these related compounds the formation of the 1-sulfoxy metabolites in rat and human liver are comparable with a difference of less than 2.2-fold over a wide dose range. The results from this PBK analysis support that risk assessment of myristicin may be based on the BMDL₁₀ derived for safrole of 1.9-5.1 mg/kg bw per day. Using an estimated daily intake of myristicin of 0.0019 mg/kg bw per day resulting from use of herbs and spices, this results in MOE values for myristicin that amount to 1000-2700 indicating a priority for risk management. The results obtained illustrate that PBK modelling provides insight in possible species differences in the metabolic activation of myristicin. Moreover, they provide an example of how PBK modelling can facilitate a read-across in risk assessment from a compound for which in vivo toxicity studies are available to a related compound for which tumor data are not reported, thus contributing to alternatives in animal testing.

Introduction

Myristicin (1-allyl-5-methoxy-3,4 methylene-dioxybenzene or methoxysafrole) is naturally occurring and present in several spices including nutmeg and mace of trees of *Myristica* species, principally *Myristica fragrans* Hout, and their essential oils (Forrest and Heacock, 1972, Matthews and Pickering, 1974, Sammy and W.W., 1968). There is a potential for human exposure to myristicin through foods, beverages, food supplements and traditional medicines. Myristicin belongs to the group of alkenylbenzenes, that contains structural analogues like methyleugenol, estragole, elemicin, safrole and apiol (Figure. 1), compounds that are all naturally occurring in herbs and spices like basil, nutmeg, and their essential oils (Barceloux, 2009). Safrole, estragole, and methyleugenol have been shown to induce hepatic tumors in rats or mice upon chronic oral exposure to high doses and upon administration to male CD-1 mice during the preweaning period (Borchert et al., 1973, Drinkwater et al., 1976, Ioannides et al., 1981, Wislocki et al., 1977, 1973, Innes, 1969, National Toxicology, 2000). Tumors were found especially in the liver at frequencies that amounted to for example 2/50, 3/50, 14/50 and 25/50 at 0, 37.5 and 150 mg methyleugenol/kg bw per day in male rats (NTP, 2000). A summary of further incidences of malignant tumor formation in mice and rats after administration of estragole, methyleugenol or safrole can be found in our previous paper (van den Berg SJPL, 2011). However, myristicin is less well studied than its structurally related analogues, and only limited toxicological data are available. While in vitro genotoxicity studies indicate that myristicin is mutagenic and capable of inducing the formation of DNA adducts (EFSA, 2009, Zhou et al., 2007b), no 2-year carcinogenicity studies of myristicin in experimental animals are available hampering its risk assessment.

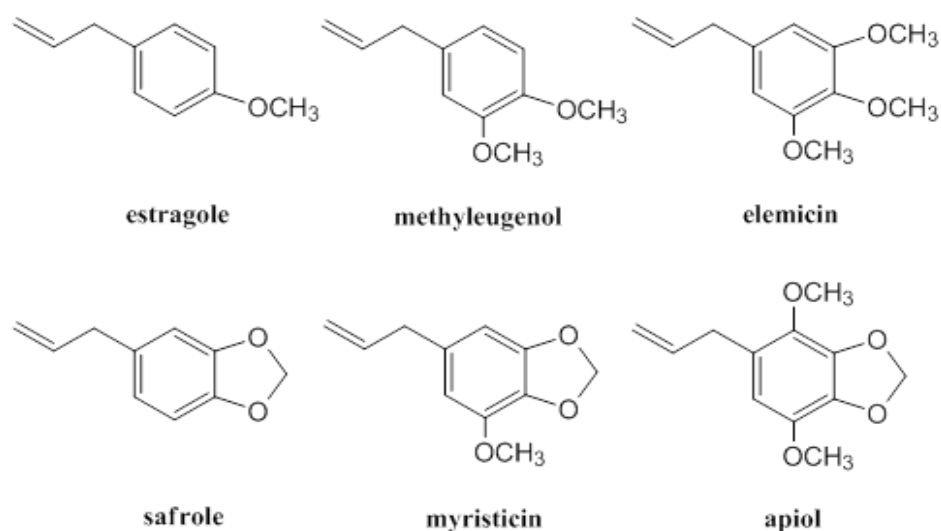


Figure 1: The structural formulas of the alkenylbenzenes estragole, methyleugenol, elemicin, safrole, myristicin and apiol.

Some short-term studies were conducted on the induction of hepatic tumors, in which male B6C3F1-mice were given myristicin during the preweaning period in 2 separate experiments. In the first experiment myristicin was injected at a total dose of 3.75 μ moles to 33 male B6C3F1-mice over a period of 22 days, and the total duration of the experiment was 12 months. In a second experiment 45 male B6C3F1-mice were each injected a total dose of 4.75 μ moles myristicin over a period of 22 days, and the total duration of the experiment was 18 months. In these short term exposure experiments, myristicin had no detectable activity for the initiation of hepatic tumours (Miller et al., 1983).

In agreement with hepatocarcinogenicity in mice (Miller et al., 1983), DNA adduct formation upon exposure to myristicin was generally lower and less persistent than DNA adduct formation upon exposure to methyleugenol, estragole and appeared to be about 2-fold lower than DNA adduct formation upon exposure to safrole, both in *in vitro* study (Zhou et al., 2007a) as well as in *in vivo* studies (Table. 1) (Phillips et al., 1984, Randerath et al., 1984).

Table 1: Comparison of data on DNA adduct formation from in vitro and rodent studies using safrole and myristicin

Model	Sex	Route of admin.	myristicin		safrole		DNA adducts identified	Duration of Exposure	DNA isolation and persistence study	Analysis technique of DNA adduct	Ref.
			Dose or conc.	pmol adduct/mg DNA	Dose or conc.	pmol adduct/mg DNA					
Cultured Human HepG2 cells			50 [#]	0.017	50 [#]		N2-(trans-propenylbenzene-3'-yl) deoxyguanosine (major) and N2-(allylbenzene-1'-yl) deoxyguanosine (minor).	The cells were treated with different doses, incubated, and then harvested after 24 h		³² P- Postlabeling, studying DNA binding ability in vitro	(Zhou et al., 2007b)
			150 [#]	0.049	150 [#]	0.083					
			450 [#]	0.165	450 [#]	0.102					
Mouse liver CD-1	Female	i.p	400*	49.5	400*	203.4	N2-(trans - propenylbenzene-3'-yl) deoxyguanosine and N2-(allylbenzene-1'-yl) deoxyguanosine (both major), N6--(trans - propenylbenzene-3'-yl) deoxyadenosine (minor)	livers were collected 24 h after treatment	after admin. Of dose 400 mg/Kg.bw safrole, livers were taken after 24 h, 28, 58, 98, & 140 days after each treatment, after 140 days adduct was 21 pmol/mg DNA	³² P- Postlabeling, studying DNA binding ability in vivo	(Randerath et al., 1984)
			80*	16.8	80*	45.9					
New born mice B6C3F1	Male	i.p	36.5*	7.8	30.8*	17.5	N2-(trans & cis-propenylbenzene-3'-yl) deoxyguanosine and N2-(allylbenzene-1'-yl) deoxyguanosine (both major) (both major). N6--(trans - propenylbenzene-3'-yl) deoxyadenosine (minor)	22 days after birth (1, 8, 15, & 22 days of injection)	days 23, 29, & 43. Adducts were still available after 43 days	³² P- Postlabeling, studying DNA binding ability in vivo	(Phillips et al., 1984)

*for dose in mg/kg bw, # for concentration in uM.

N²-(trans-isomyristicin-3-yl)-2-deoxyguanosine was found to be the major myristicin DNA adduct formed when mice were given cola drinks instead of water up to 8 weeks. In a parallel experiment, pregnant ICR mice were treated by gastric intubation with a single dose of 6 mg myristicin, level of myristicin adducts in maternal and fetal liver were 68% and 63% of the total adducts (Randerath K, 1993). In freshly isolated rat hepatocytes in primary culture, safrole, estragole, and methyleugenol, induced unscheduled DNA synthesis (UDS) and cytotoxicity at concentrations of 10⁻⁶-10⁻³M, (Howes et al., 1990) while myristicin showed cytotoxicity. In these studies concentrations inducing UDS were generally close to or already at concentrations detecting cytotoxicity, hampering interpretation of the data. The data supporting a genotoxic mode of action for the tumor induction by the alkenylbenzenes rather comes from studies reporting DNA adduct formation. In these studies, myristicin, as well as estragole, methyleugenol and safrole all showed positive results (Zhou et al., 2007a, Kobets et al., 2016, Phillips et al., 1984, Randerath et al., 1984). A schematic overview of the detoxification and bioactivation of myristicin that is similar to that of its structurally related compound safrole (Swanson et al., 1979, Borchert et al., 1973, Drinkwater et al., 1976) is shown in (Figure. 2). Epoxidation of the double bond in the allyl side-chain yields the 2,3-epoxide. In in vitro experiments, the epoxide readily forms DNA adducts, but rapid detoxification by epoxide hydrolase and glutathione *S*-transferases (GSTs) prevents it from forming detectable levels of DNA adducts in vivo (Luo et al., 1992, Luo and Guenther, 1996).

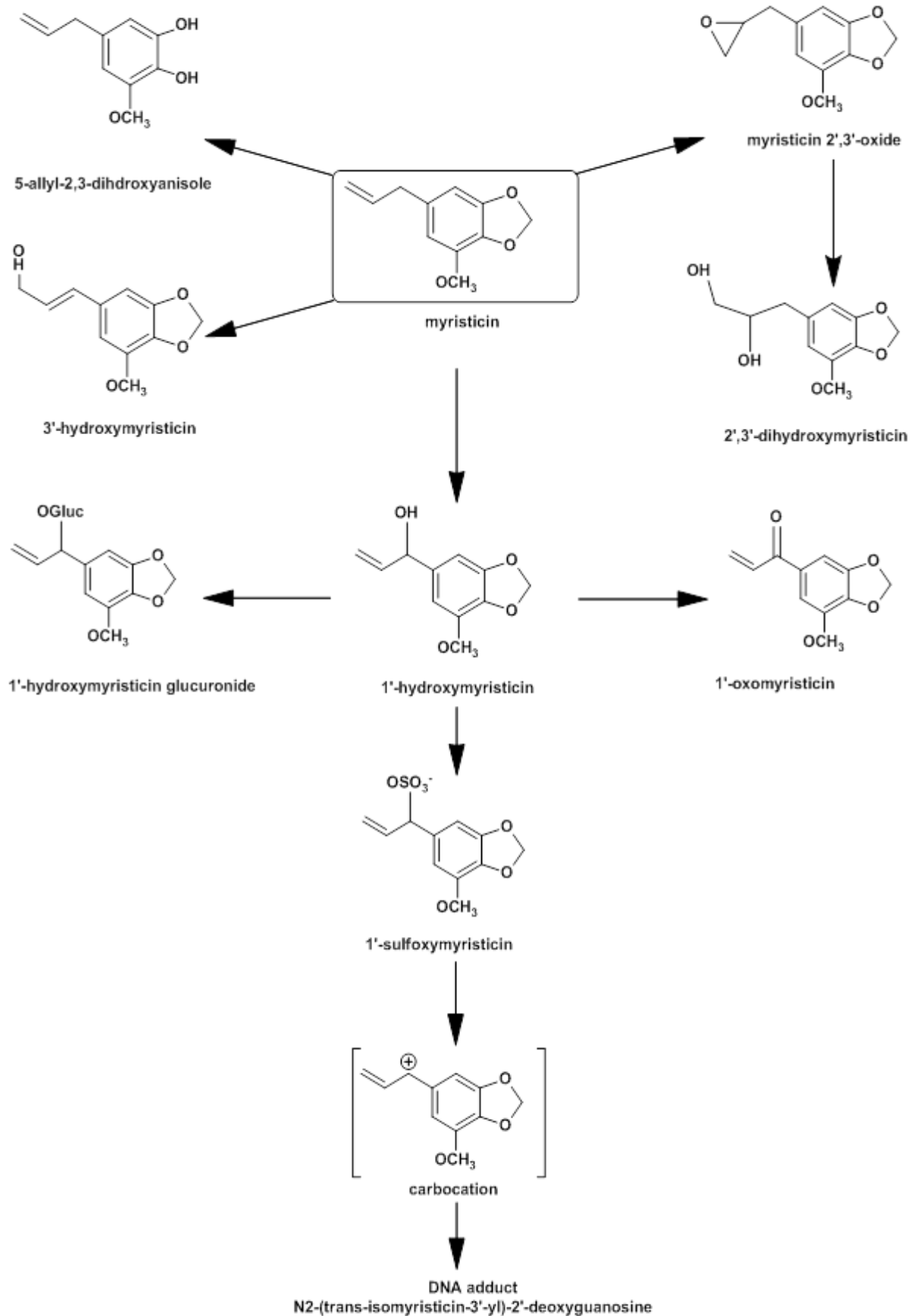


Figure 2: Proposed metabolic pathways of the alkenylbenzene myristicin.

The primary bioactivation pathway of myristicin is 1-hydroxylation of the alkene side-chain to yield the 1-hydroxy metabolite which can be conjugated with either glucuronic acid representing a detoxification reaction or sulfate representing the ultimate bioactivation to 1-sulfoxymyristicin (Drinkwater et al., 1976, Benedetti et al., 1977, Zangouras et al., 1981, Miller et al., 1983). The 1-sulfoxy metabolite represents the ultimate carcinogenic metabolite (Wiseman et al., 1987, Wiseman et al., 1985, Randerath et al., 1984, Phillips et al., 1984). 1-Sulfoxy metabolites of alkenylbenzenes may react readily with DNA, RNA, and proteins but can also be detoxified through reaction with H₂O or conjugation with glutathione (Phillips et al., 1984, Miller et al., 1983, Fennell, 1984, Ishii et al., 2011). Therefore, only a fraction of the 1-sulfoxy metabolite is expected to form DNA adducts (Rietjens et al., 2014).

Although myristicin is thus likely to also induce DNA adducts and liver tumors its risk assessment at low realistic dietary intake levels is hampered by the fact that carcinogenicity studies are lacking (Hallstrom and Thuvander, 1997). Therefore, the aim of the present study was to characterise the detoxification and bioactivation of myristicin and to develop a physiologically based kinetic (PBK) model to describe the ultimate formation of the 1-sulfoxy metabolite in the liver of both rat and human and subsequently perform a read-across-based risk assessment using a similar PBK model previously described for safrole for which tumor data from long term toxicity testing are available. Previously, using a similar approach and read-across from estragole and methyleugenol the risk of exposure to elemicin for which also only limited in vivo rodent tumor data were available could be evaluated (van den Berg et al., 2012). Such a PBK modelling based read-across illustrates a novel approach for animal-free risk assessment of a genotoxic carcinogen without the need for a long term carcinogenicity study.

Materials and methods

Chemicals

Myristicin, tris(hydroxymethyl)aminomethane, uridine 5'-diphosphoglucuronide acid (UDPGA), reduced L-glutathione (GSH), alamethicin (from Trichoderma viride), 3-phosphoadenosine-5-phosphosulfate (PAPS), -nicotinamide adenine dinucleotide (NAD⁺), reduced -nicotinamide adenine dinucleotide phosphate (NADPH), were obtained from Roche Diagnostics (Mannheim, Germany). Dimethyl sulfoxide (DMSO) was obtained from Acros Organics (Geel, Belgium). Potassium dihydrogen phosphate, dipotassium hydrogen phosphate trihydrate, acetic acid, and magnesium chloride were supplied by VWR International (Darmstadt, Germany). Acetonitrile (ACN) (UPLC/MS grade) was purchased from Biosolve BV (Valkenswaard, The Netherlands). Trifluoroacetic acid TFA was obtained from Merck (Darmstadt, Germany). Pooled male rat liver microsomes and S9 from Sprague–Dawley and mixed gender pooled human liver microsomes and S9 were obtained from BD Gentest (Woburn, United States). Pooled male Sprague–Dawley rat lung, kidney, and small intestinal microsomes and pooled gender human lung, kidney, and intestinal microsomes were purchased from BioPredic International (Rennes, France).

Synthesis of 1-hydroxymyristicin and 1-oxomyristicin

The synthesis of 1-hydroxymyristicin from myristicin was done as described previously by Jeurissen et al. (Jeurissen et al., 2004), and 1-oxomyristicin was synthesized from 1-hydroxymyristicin according to the method used for synthesis of 1-oxoestradiol from 1-hydroxyestradiol (Wislocki et al., 1976).

Microsomal metabolism of myristicin.

First it was determined which organs are involved in the biotransformation of myristicin in rat and human. For this purpose, liver, kidney, lung, and small intestine microsomes from male Sprague-Dawley rat and pooled gender human were used. Incubations were performed by adding myristicin to incubation mixtures containing 1 mg/ml of the microsomal protein preparations and 3mM NADPH in 0.2M Tris-HCl (PH 7.4). After 1 minutes pre-incubation at 37°C, myristicin (final concentration, 1000 µM) was added from a 100 times concentrated stock solution in DMSO so that the final DMSO content was 1% (v/v). Incubations were carried out for 30 minutes after which the reactions were terminated by adding 25µl (0.25 times the incubation volume) of ice-cold ACN. Samples were centrifuged for 5 minutes at 13000g, and the supernatant was stored at -20°C until ultra-performance liquid chromatography (UPLC) analysis. As metabolism of myristicin was observed only in incubations with liver microsomes for male rats and pooled gender human the determination of kinetic constants for the formation of microsomal metabolites were performed only for the liver fractions. Incubations to determine kinetic constants were performed following the conditions described above using final concentrations of myristicin from 25 to 1000 µM for rat and human liver. In all incubations the final concentration of DMSO, in which myristicin was dissolved, was kept at 1% (v/v). The formation of different microsomal metabolites was linear with time and microsomal protein concentration under the conditions described. Blank incubations were performed in the absence of the cofactor NADPH. All incubations were performed in triplicate.

Glucuronidation of 1-hydroxymyristicin to 1-hydroxymyristicin glucuronide.

The kinetic constants for the metabolic conversion of 1-hydroxymyristicin to 1-hydroxymyristicin glucuronide (HMG) by both male rat and human liver fractions were determined as described previously for the related 1-hydroxyalkenylbenzenes (Punt et al., 2008,

van den Berg et al., 2012, Punt et al., 2009, Martati et al., 2011, Martati et al., 2012, Al-Subeihi et al., 2011, Al-Subeihi et al., 2012). Briefly, incubations contained (final concentrations) 10 mM UDPGA and 0.5 mg/ml male Sprague–Dawley or pooled gender human S9 protein in 0.2 M Tris-HCl (pH 7.4) containing 10 mM MgCl₂. To overcome enzyme latency and to obtain maximal glucuronidation activity, incubations containing S9 were pretreated on ice with 0.025 mg/ml alamethicin added from a 200 times concentrated stock dissolved in methanol (Fisher et al. 2000, Lin and win 2002). After 15 minutes of alamethicin treatment, samples were pre-incubated at 37°C for 1 minutes, and reactions were subsequently started by adding 1-hydroxymyristicin at final concentrations of 10 to 1200 µM. 1-Hydroxymyristicin was added from 100 times concentrated stock solutions in DMSO. The reaction mixtures were incubated for 30 and 180 minutes for rat and human, respectively, and terminated by adding 25 µl (0.25 times the incubation volume) of ice-cold ACN. Blank incubations were carried out in the absence of the cofactor UDPGA. Experiments were performed in triplicate. The longer incubation time in human samples was required due to the lower rate of glucuronidation. The formation of 1-hydroxymyristicin glucuronide was linear with time and the S9 protein concentration under the experimental conditions described. All samples were centrifuged for 5 minutes at 16000g, and the supernatant was stored at –20°C until UPLC analysis.

Oxidation of 1-hydroxymyristicin to 1-oxomyristicin.

The kinetic constants for the enzymatic conversion of 1-hydroxymyristicin to 1-oxomyristicin were determined using incubation mixtures containing (final concentrations) 3 mM NAD⁺, 2mM GSH, and 1mg/ml rat or human liver microsomes in 0.2 M Tris-HCl (pH 7.4). GSH was added to the incubation mixtures to trap the reactive 1-oxo metabolite formed after oxidation of 1-hydroxymyristicin. The level of GSH in the incubations was optimized in a previous study to obtain maximum scavenging of 1-oxoestragole (Punt et al., 2009). To this end, incubations were

performed in the presence of increasing concentrations of GSH, ranging from 2 to 10 mM. At a concentration of 2 mM GSH maximum formation of GS-1 -oxoestragle was reached in the incubations, pointing at maximum scavenging of 1 -oxoestragle at this concentration (Punt et al., 2009). Kinetic constants for this reaction in rat and human liver were derived by performing incubations with NAD^+ as a cofactor, given that in rat and human liver, NAD^+ is mainly present in an oxidized form with levels of NAD^+ being much higher than those of NADH. In a previous study, it was shown that the highest level of 1 -hydroxy alkenylbenzene oxidation occurs in incubations with microsomes in the presence of NAD^+ as cofactor. In incubations with pooled human liver cytosol in the presence NAD^+ or NADP^+ , lower levels of oxidation were observed indicating that the reaction is not primarily catalyzed by alcohol dehydrogenases (ADH) or other enzymes present in the cytosol (Punt et al., 2010). The enzyme responsible for the oxidation may be 17 -hydroxysteroid dehydrogenase type 2 (17 -HSD2) (Punt et al., 2010). Prior to the addition of 1 -hydroxymyristicin at final concentrations ranging between 10 and 4000 μM to the incubation mixture from 100 times concentrated stock solutions in DMSO, samples were pre-incubated for 1 minutes at 37°C. Reactions were terminated after 10 minutes of incubation at 37°C by adding 25 μl (0.25 times the incubation volume) ice-cold ACN. The formation of the GSH conjugate of 1 -oxomyristicin (GS-1 -oxomyristicin) was linear with time and microsomal protein concentration under the experimental conditions used. Blank incubations were performed without the cofactor NAD^+ . Incubations were performed in triplicate. All samples were centrifuged for 5 minutes at 13000g, and the supernatant was stored at -20°C until UPLC analysis.

Sulfonation of 1-hydroxymyristicin to 1-sulfoxymyristicin.

The formation of 1-sulfoxymyristicin was determined using incubations containing male rat liver Sprague-Dawley or pooled gender human liver S9 proteins, PAPS as a cofactor, and GSH, which acts as a scavenger of the reactive carbocation formed due to the unstable nature of the 1-sulfoxy metabolite in an aqueous environment (van den Berg et al., 2012, Martati et al., 2011, Al-Subeihi et al., 2011). Incubation mixtures containing (final concentrations) 10 mM GSH, 0.2 mM PAPS, and 3 mg/ml S9 proteins in 0.1 M potassium phosphate (pH 8.2) were pre-incubated for 1 minutes at 37°C. After the pre-incubation 1-hydroxymyristicin dissolved in DMSO was added in final concentrations ranging between 10 and 6000 µM while keeping the final content of DMSO at 1% (v/v). The reaction was terminated after 360 minutes of incubation by adding 25µl (0.25 times the incubation volume) ice-cold ACN. The formation of the GSH conjugate of 1-sulfoxymyristicin was linear with time and S9 protein concentrations under the experimental conditions used. Blank incubations were performed in the absence of PAPS. Incubations were performed in triplicate. All samples were centrifuged for 5 minutes at 16000g, and the supernatant was stored at -20°C until UPLC analysis.

Identification and quantification of metabolism of myristicin and 1-hydroxymyristicin by UPLC.

Microsomal incubations with myristicin only detected primary metabolites, all incubations conditions were chosen such that substrate conversion did not exceed 10% of the initial substrate concentration, a condition that is also essential to ascertain adequate determination of the kinetic constants. Secondary metabolism of the relevant 1-hydroxy metabolite of myristicin was taken into account by determining the kinetic constants for its conversion in a) glucuronidation, b) sulfation and c) oxidation, again under conditions that allowed adequate definition of kinetic constants and with less than 10% substrate conversion. Incubation samples were subjected to

UPLC analysis that was performed as described previously (Punt et al., 2008). Identification was achieved by comparing the UV spectra of the formed metabolites to the spectra of the synthesized 1-hydroxymyristicin and 1-oxomyristicin reference standards. Quantification of all formed metabolites was done by comparing the peak areas to those of calibration curves of the corresponding reference compounds, determined using UPLC with photodiode array detection (UPLC-PDA). The UPLC system was composed of a Waters (Waters, Milford, MA) Acquity solvent manager, sample manager, and photodiode array detector, equipped with Water Acquity UPLC BEH C18 column.

For 2,3-dihydroxymyristicin, 5-allyl-2,3-dihydroxyanisole, that were found to have the same UV spectrum as 1-hydroxymyristicin, and for 1-hydroxymyristicin, estimation was based on comparison of the peak area of the formed metabolites to the calibration curve of the synthesized 1-hydroxymyristicin at a wavelength of 210nm. For 3-hydroxymyristicin, estimation was based on comparison of the peak area to the calibration curve GSH adduct of the synthesized 1-oxomyristicin at a wavelength of 212 nm, because 3-hydroxymyristicin was found to have the same UV spectrum as the GSH adduct of synthesized 1-oxomyristicin. The gradient for analysis of microsomal metabolites was performed with 100% ACN and ultrapure water containing 0.1% (v/v) TFA. The flow rate was 0.6 ml/min. The gradient started at 10% ACN, increased to 50 % ACN over 4 minutes, increased to 80% over 0.5 minutes, followed by decrease to 10 % ACN over 0.5 minutes, and finally kept at 10% for 1 minutes.

1-Hydroxymyristicin glucuronide was estimated based on comparison of the peak area of the formed metabolite to the calibration curve of 1-hydroxymyristicin at a wavelength of 210 nm. The flow rate was 0.6 ml/min. the gradient was made using a mixture of ACN and ultrapure water containing 0.1% (v/v) TFA. The gradient started at 10% ACN, increased to 60% over 3.5 minutes, after which ACN was increased to 80% over 0.5 min, and kept at 80% for 0.5 min, and finally decreased to 10 % over 0.5 min.

Quantification of GS-1 -oxomyristicin was based on a calibration curve of the GSH adduct of the synthesized 1 -oxomyristicin made as previously described (van den Berg et al., 2012, Punt et al., 2009, Martati et al., 2011, Al-Subeihi et al., 2011). In short, a 60 μ M concentration of the synthetic standard of 1 -oxomyristicin, dissolved in ACN, was incubated with different concentrations of GSH (i.e., 0-20 μ M) in 0.2 M Tris-HCl (pH 7.4) for 6 h at 37°C, resulting in full conversion of the GSH to GS-1 -oxomyristicin. Quantification was done by comparing the peak areas of the formed GS-1 -oxo metabolite in the incubation mixtures with peak areas of the GS-1 -oxomyristicin calibration curve thus obtained at a wavelength of 212 nm. The gradient for analysis of the metabolite consisted of a mixture of ACN and ultrapure water containing 0.1% (v/v) TFA. The flow rate was 0.6 ml/min, The running protocol started at 10% ACN, increased to 30% ACN over 2.5 minutes, after which ACN was increased to 80% over 0.5 min, kept at 80% for 0.5 min, followed by a decrease to 10% over 0.5 min, and finally kept at 10% for 0.5 min.

Quantification of 1 -sulfoxymyristicin was done using UPLC analysis as described for the estimation of 1 -sulfoxysafrole (Martati et al., 2011). The UV spectrum of the GSH adduct of 1 -sulfoxymyristicin was found to be similar to the UV spectrum of the GSH conjugate of 1 -oxomyristicin, and estimation of the GSH adduct of 1 -sulfoxymyristicin was thus accomplished by comparing the peak area of this metabolite to the calibration curve of GS-1 -oxomyristicin at a wavelength 305 nm. The gradient for analysis of the metabolite consisted a mixture of ACN and ultrapure water containing 0.1% (v/v) TFA. The flow rate was 0.6 ml/min, starting at 0% ACN and increasing the percentage of ACN to 20% over 0.2 minutes, followed by an increase to 30% ACN over 4.3 min, then increasing to 100% over 0.3 min, and keeping at 100% for 0.2 min, and finally decreasing to 0% over 0.2 minutes and keeping at 0% for 0.8 min. Separation and purification of the GSH adduct of 1 -sulfoxymyristicin was performed by collecting the peak of the metabolite from the UPLC column. Then LC-MS analysis of the metabolite was

conducted using a micro-TOF MS (Bruker) coupled to an Agilent LC (1200 Series) equipped with Altima C18 column (150 x 4.6 mm, 3 μ m). The mobile phase used consisted of (A) nanopure water with 0.1 % formic acid and (B) HPLC-grade ACN with 0.1 % formic acid. Elution was at a flow rate of 0.8 ml/min, starting at 22 % B with a linear increase to 100 % B in 30 min. Subsequently, the gradient returned linearly to the initial conditions in 2 minutes and remained 13 minutes at this condition prior to the next injection. Mass spectrometric analysis was in the negative electrospray mode using a spray capillary voltage of 4500 V, a capillary temperature of 200°C and nitrogen as nebulizer gas at 8.0 L/min.

Determination of kinetic constants

Kinetic constants for the metabolic conversions of myristicin and 1 -hydroxymyristicin were derived by fitting the data to the standard Michaelis–Menten equation,

$$v = V_{\text{m}} \times [S]/K_{\text{m}} + [S]$$

For conversion of 1 -hydroxymyristicin to 1 -sulfoxymyristicin, a first rate order linear equation was used;

$$v = k_{\text{H}} \times [S]$$

in which [S] represents the substrate concentration, V_{max} the maximum velocity, and K_{m} the Michaelis–Menten constant for the formation of the different metabolites of myristicin or 1 -hydroxymyristicin, k_{HMS} the first order rate constant for sulfonation of 1 -hydroxymyristicin.

Data analysis was accomplished using GraphPad Prism, version 5.04 (GraphPad Software, San Diego, CA).

Physiologically based kinetic (PBK) models.

Two PBK models were developed describing the relative importance of bioactivation and detoxification of myristicin in rat and human at different oral dose levels. The models developed

in this study were essentially based on the PBK models previously defined for the metabolism of estragole (Punt et al., 2008, Punt et al., 2009), methyleugenol (Al-Subeihi et al., 2011, Al-Subeihi et al., 2012), elemicin (van den Berg et al., 2012), and safrole (Martati et al., 2011, Martati et al., 2012) in rat and human. A schematic overview of the developed PBK models for myristicin metabolism in rat and human is shown in (Figure. 3).

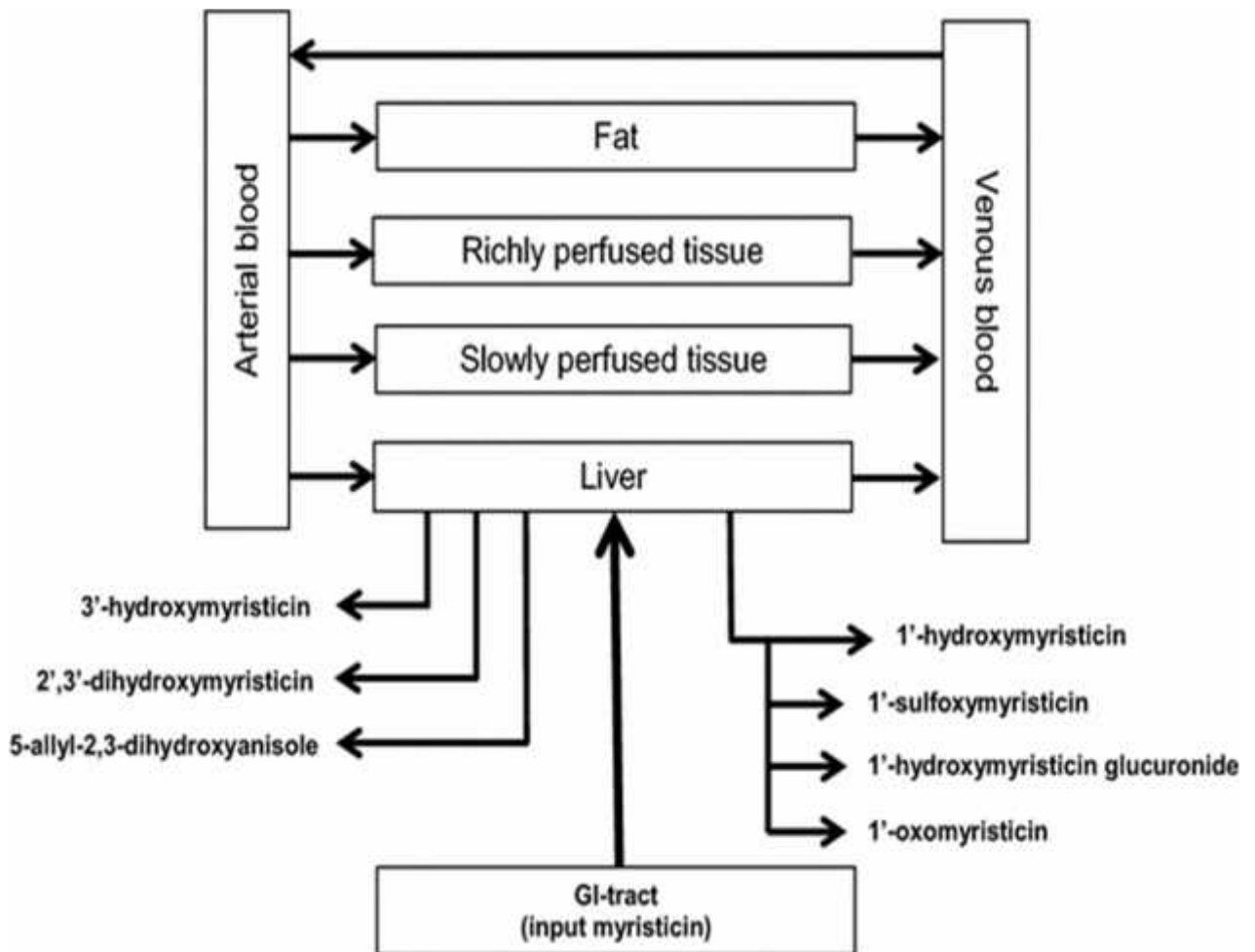


Figure 3: Schematic overview of the PBK model for myristicin in rat and human.

The models consist of several compartments representing different organs and tissues (i.e., liver, fat tissue, richly perfused tissues, and slowly perfused tissues) that are mutually connected through the systemic circulation. First-order kinetics was used to describe the uptake of myristicin from the gastrointestinal (GI) tract assuming a direct uptake by the liver with an

absorption rate constant (k_a) of 1.0 h^{-1} , which is based on the fast and complete absorption of the structurally related alkenylbenzene safrole from the GI tract (Punt et al., 2008). For rat and human, the liver was the only organ able to convert myristicin to different microsomal metabolites. 2,3-Dihydroxymyristicin (DHM), 3-hydroxymyristicin (3HM), 1-hydroxymyristicin (HM), 5-allyl-2,3-dihydroxyanisole (DHA) were formed in incubations with both rat and human liver.

Accordingly, mass balance equations for Myristicin in rat liver and human were as follows:

$$\begin{aligned} \partial AL_M / \partial t &= \partial Uptake_M / \partial t + QL \times (CA_M - CL_M / PL_M) \\ &\quad - V_{max_{HM}} \times CL_M / PL_M / (K_m_{HM} + CL_M / PL_M) \\ &\quad - V_{max_{3HM}} \times CL_M / PL_M / (K_m_{3HM} + CL_M / PL_M) \\ &\quad - V_{max_{DHA}} \times CL_M / PL_M / (K_m_{DHA} + CL_M / PL_M) \\ &\quad - V_{max_{DHM}} \times CL_M / PL_M / (K_m_{DHM} + CL_M / PL_M) \\ \partial Uptake / \partial t &= -\partial AGI_M / \partial t = K_a \times AGI_M, AGI_M(0) \\ &= \text{oral dose} \\ CL_M &= AL_M / VL \end{aligned}$$

Where $Uptake_M$ (μmol) is the amount of myristicin taken up from the GI tract, AGI_M (μmol) is the amount of myristicin remaining in the GI tract, and AL_M (μmol) is the amount of myristicin in the liver or CL_M is the myristicin concentration in the liver ($\mu\text{mol/L}$). CA_M and CV_M are the myristicin concentrations in the arterial and venous blood (both in $\mu\text{mol/L}$), QL is the blood flow rate to a tissue (L/h), QC is the cardiac output (L/h), VL is the volume of liver, PL_M is the tissue/blood partition coefficient of myristicin, and V_{max} and K_m are the values representing the maximum rate of formation and Michaelis–Menten constant, respectively, for the formation of 2,3-dihydroxymyristicin (DHM), 3-hydroxymyristicin (3HM), 1-hydroxymyristicin (HM), and 5-allyl-2,3-dihydroxyanisole (DHA).

The mass balance equation for the metabolic conversion of 1-hydroxymyristicin by glucuronidation, oxidation, and sulfonation in the liver in rat and human liver is as follows:

$$\begin{aligned} \frac{\partial AL_{HM}}{\partial t} = & V_{\max_{HM}} \times CL_M / PL_M / (K_{m_{HM}} + CL_M / PL_M) \\ & - V_{\max_{LHMG}} \times CL_{HM} / PL_{HM} / (K_{m_{LHMG}} + CL_{HM} / PL_{HM}) \\ & - V_{\max_{HMO}} \times CL_{HM} / PL_{HM} / (K_{m_{HMO}} + CL_{HM} / PL_{HM}) \\ & - k_{HMS} \times CL_{HM} / PL_{HM} \\ & CL_M = AL_M / VL \end{aligned}$$

where AL_{HM} is the amount of 1-hydroxymyristicin in the liver (μmol), CL_{HM} is the 1-hydroxymyristicin concentration in the liver ($\mu\text{mol/L}$), PL_{HM} is the liver/blood partition coefficient of 1-hydroxymyristicin, and V_{\max} and K_m are the maximum rate of formation and Michaelis–Menten constant, respectively, for the formation of the different 1-hydroxymyristicin metabolites in the liver, including 1-hydroxymyristicin glucuronide, 1-oxomyristicin, and k_{HMS} is the first order rate constant for sulfonation of 1-hydroxymyristicin that was used instead of K_m and V_{\max} as sulfonation showed no saturation. V_{\max} and K_m values and first order rate constants k in case of absence of saturation (for sulfonation of 1-hydroxymyristicin in rat and human) for the different metabolic pathways of myristicin and 1-hydroxymyristicin were derived from results from in vitro experiments in the present study. V_{\max} values that were derived in vitro expressed as $\text{nmol min}^{-1} (\text{mg liver microsomal or S9 protein})^{-1}$ were scaled to values representing the V_{\max} per $\mu\text{mol h}^{-1} (\text{g liver})^{-1}$ using microsomal protein yields of 35 mg/g for rat and 32 mg/g for human liver and S9 protein yields of 143 mg/g liver, as defined previously (Punt et al., 2008, Punt et al., 2009), based on Medinsky et al. (Medinsky, 1994). First order rate constant k expressed in $\text{ml min}^{-1} (\text{mg liver S9 protein})^{-1}$ was scaled to values expressed in ml h^{-1} per g liver using the same conversion factor for S9 protein yield. (Table 2) and (Table 3) summarize the physiological parameters (i.e., tissue volumes, cardiac output, and tissue blood flows) for rat and human, respectively, which were derived from the literature (Brown et al. 1997).

Table 2: parameters used in the PBK model for myristicin in male rat

physiological parameters (Brown, 1997)		tissue: blood partition coefficients	
body weight (kg)	0.25	myristicin	
percentage of body weight		liver	
Liver	3.4	fat	1.68
Fat	7.0	rapidly perfused	37.73
rapidly perfused	5.1	slowly perfused	1.68
slowly perfused	60.2		0.67
blood	7.4	1 -hydroxymyristicin	
		liver	0.94
cardiac output (l/h)	5.4		
percentage of cardiac output			
liver	25		
fat	7.0		
rapidly perfused	51.0		
slowly perfused	17.0		

Table 3: parameters used in the PBK model for myristicin in human

physiological parameters (Brown, 1997)		tissue: blood partition coefficients	
body weight (kg)	60	myristicin	
percentage of body weight		liver	4.22
liver	2.6	fat	83.45
fat	21.4	rapidly perfused	4.22
rapidly perfused	5.0	slowly perfused	2.81
slowly perfused	51.7		
blood	7.9	1-hydroxymyristicin	
		liver	0.93
cardiac output (l/h)	310		
percentage of cardiac output			
liver	22.7		
fat	5.2		
rapidly perfused	47.3		

Partition coefficients were derived *in silico* based on a method described by DeJongh et al. (DeJongh, 1997) using the log K_{ow} . Log K_{ow} values for myristicin (Clog P 3.1721) and 1-hydroxymyristicin (Clog P 1.6151) were estimated using Chemdraw professional 15 (ChemOffice® Professional 15.0 by perkin elmer). Mass balance equations were coded and numerically integrated in Berkely Madonna 8.3.18 (Macey and Oster, UC Berkeley, CA) using Rosenbrock's algorithm for stiff systems. PBK models in rat and human liver were run for 720 h, because that would be the time for total clearance of myristicin in human tissues after one dose.

Sensitivity Analysis.

To determine which parameters have the greatest influence on model predictions, a sensitivity analysis was performed as described previously (Punt et al., 2008, van den Berg et al., 2012, Punt et al., 2009, Martati et al., 2011, Martati et al., 2012, Al-Subeihi et al., 2011, Al-Subeihi et al., 2012). For this purpose, normalized sensitivity coefficients (SCs) were determined using the following equation:

$$SC = (C' - C)/(P' - P) \times (P/C)$$

Where C is the initial value of the model output, C' is the modified value of the model output resulting from an increase in parameter value, P is the initial parameter value, and P' represents the modified parameter value. An increase of 5% in parameter values was used to analyze the effect of a change in parameter on the formation of 1-hydroxymyristicin and 1-sulfoxymyristicin (expressed as a percentage of the dose). Each parameter was analyzed individually, while the other parameters were kept at their initial value.

Comparison of the PBK model-based prediction of bioactivation of myristicin to the PBK model based predictions for bioactivation of the structurally related compound safrole.

The predicted model outcomes for the formation of 1-hydroxymyristicin and 1-sulfoxymyristicin in the liver of rat and human were compared with the predicted dose-dependent formation of the 1-hydroxy- and 1-sulfoxy metabolite of the structurally related alkenylbenzene safrole. For this purpose, the previously defined PBK models for safrole described by Martati et al. (Martati et al., 2011, Martati et al., 2012) for rat and human were used. For the comparison the models describing the metabolism of myristicin and safrole were run for a period of 720 h.

Results

Microsomal conversion of myristicin.

To identify which organs are involved in the metabolism of myristicin in both male rat and human, incubations were performed using microsomal protein preparations from liver, kidney, lung, and small intestine of both species. Chromatographic analysis of these incubations revealed that for rat and human no detectable metabolism of myristicin occurred in small intestine, lung or kidney microsomes and metabolism was only observed for liver microsomes. An example of a chromatogram of an incubation of myristicin with male rat liver microsomes and NADPH as a cofactor is shown in (Figure. 4).

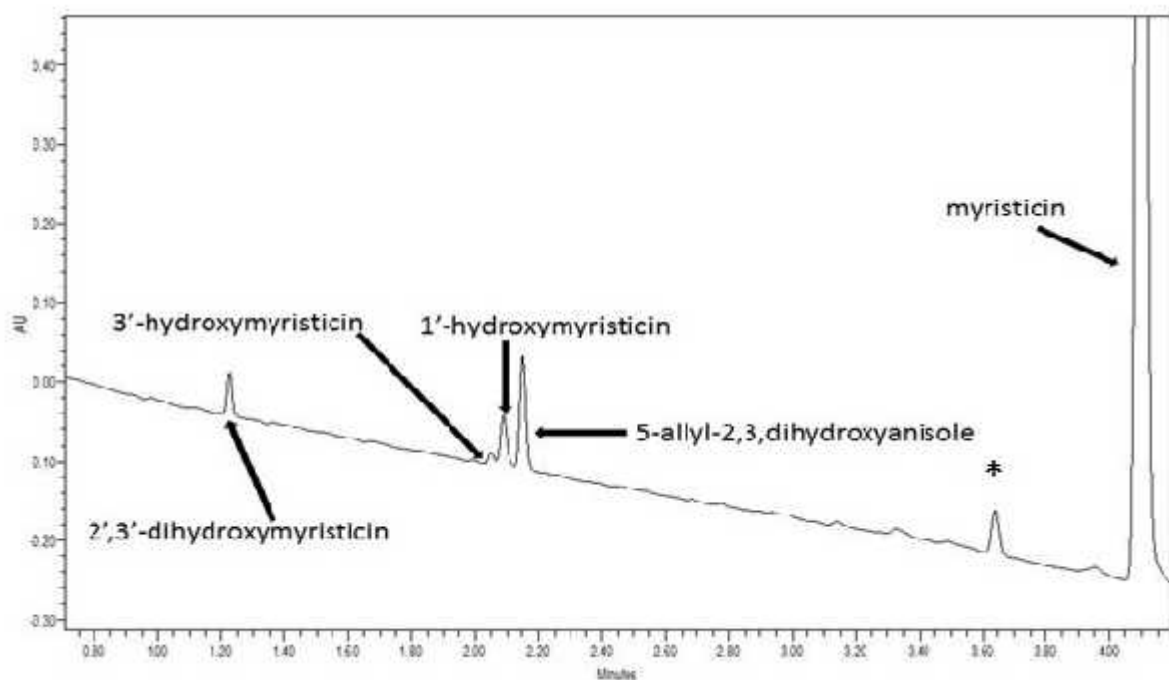


Figure 4: UPLC chromatogram of an incubation of myristicin (1000 μ M) with male rat liver microsomes. The peak marked with an asterisk (*) was also found in the blank incubation without NADPH.

In incubations with rat liver microsomes 2,3-dihydroxymyristicin ($R_t = 1.19$ min), 3-hydroxymyristicin ($R_t = 2.01$ min), 1-hydroxymyristicin ($R_t = 2.04$ min), and 5-allyl-2,3-dihydroxyanisole ($R_t = 2.11$ min) were formed. In incubations with human liver microsomes, the same four metabolites were found. Identification was done based on comparison of the UV spectra and retention times of the formed metabolites with those of the specific synthesized or

commercially available reference compounds. However, tentative identification of 2,3-dihydroxymyristicin was based on the fact that the epoxidation of the double bond in the allyl side-chain of estragole, methyleugenol, and safrole yields the 2,3-epoxide, found to be hydrolyzed by epoxide hydrolase to 2,3-dihydroxy metabolite (Luo et al., 1992, Luo and Guenther, 1996, Guenther, 2001). The hydrolysis product of the epoxide, 2,3-dihydroxy metabolite of myristicin, safrole or elemicin was detected in the urine of rats administered high doses (100 mg/kg bw) of each substance individually or a high dose of nutmeg (500 mg/kg bw) (Beyer et al., 2006). Data revealed that 3-hydroxymyristicin was formed directly from myristicin rather than from isomerization of 1-hydroxymyristicin since the formation of 3-hydroxymyristicin was not observed in incubations of 1-hydroxymyristicin with liver microsomes and NADPH (data not shown). The kinetic constants (i.e., V_{\max} and K_m) were derived from plots of the rates of formation of different microsomal metabolites in incubations with male rat liver microsomes, and human liver microsomes from myristicin at concentrations ranging from 25 to 1000 μM (for details, see Figure. S1 in the supplementary materials). The values obtained are shown in (Table 4), together with the catalytic efficiencies, calculated as V_{\max}/K_m . Analysis of incubations that were performed with male rat liver microsomal preparations revealed that the metabolite arising from *O*-demethylation of myristicin, namely, 5-allyl-2,3-dihydroxyanisole, was formed with the highest V_{\max} value.

Table 4: kinetic constants for metabolism of myristicin and 1'-hydroxymyristicin as derived from data obtained in incubations with Sprague-Dawley male rat liver microsomes and mixed gender pooled human liver microsomes and respective cofactors.

metabolite	abbreviation	rat				human			
		$K_m^{a,c}$	$V_{max}^{a,b}$	<i>in vitro</i> catalytic efficiency ^d	$k_{\pm sd}$	$K_m^{a,c}$	$V_{max}^{a,b}$	<i>in vitro</i> catalytic efficiency ^d	$k_{\pm sd}$
conversion of myristicin									
2',3'-dihydroxymyristicin	DHM	16±7	0.44±0.08	27.5		33±12	0.08±0.01	2.424	
3'-hydroxymyristicin	3HM	83±31	0.47±0.09	5.663		1629±154 ₅	0.29±0.14	0.178	
1'-hydroxymyristicin	HM	102±32	0.86±0.18	8.431		234±132	0.17±0.03	0.726	
5-allyl-2,3-dihydroxyanisole	DHA	33±11	1.3±0.23	39.394		118±36	0.93±0.13	7.881	
conversion of 1'-hydroxymyristicin									
1'-hydroxymyristicin glucuronide ^e	HMG	836±336	8.6±2.0	10.287		3140±243 ₄	0.08±0.03	0.025	
1'-oxomyristicin	HMO	5922±34 ₇₇	43.64±20.9	7.369		3244±264 ₆	32±14	9.864	
1'-Sulfoxymyristicin ^f	HSM								16.3×10 ⁻⁶

a: mean values of three independent measurements±SD.

b: nmol min⁻¹ (mg microsomal or S9 protein)⁻¹.

c: μM.

d: μl min⁻¹ (mg microsomal or S9 protein)⁻¹ (V_{max}/K_m × 1000 μl/ml).

e: experiments performed with S9 tissue fractions.

f: first order rate constant for product formation(ml/min/mg protien).

Moreover, 2,3-dihydroxymyristicin and 5-allyl-2,3-dihydroxyanisole were abundantly formed in incubations with male rat microsomal liver preparations with a high affinity. In incubations performed with male rat liver microsomes, 1-hydroxymyristicin and 3-hydroxymyristicin were the least important metabolites formed upon conversion of myristicin. In general, the catalytic efficiency for the formation of 5-allyl-2,3-dihydroxyanisole by male rat liver microsomes had the highest value, followed by the catalytic efficiency for the formation of 2,3-dihydroxymyristicin, 1-hydroxymyristicin and 3-hydroxymyristicin, respectively. The catalytic efficiency for the formation of 5-allyl-2,3-dihydroxyanisole was found to be approximately 7-fold higher than that for the formation of 3-hydroxymyristicin. In incubations with human liver fractions, 5-allyl-2,3-dihydroxyanisole was found to be the most abundant metabolite formed followed by 2,3-dihydroxymyristicin, 1-hydroxymyristicin and 3-hydroxymyristicin, respectively. Analysis of the catalytic efficiencies for the formation of the different microsomal metabolites of myristicin, obtained with pooled human liver microsomes, showed that the formations of 2,3-dihydroxymyristicin, 1-hydroxymyristicin and 3-hydroxymyristicin were the least important routes of myristicin metabolism, whereas the formation of 5-allyl-2,3-dihydroxyanisole represents the major pathway for the human liver microsomal conversion of myristicin.

Glucuronidation of 1-hydroxymyristicin.

Chromatographic analysis of incubations with male rat and mixed gender pooled human liver S9, UDPGA as cofactor and 1-hydroxymyristicin as substrate, revealed a peak at 1.36 minutes (chromatogram not shown). Moreover, chromatographic analysis of incubations performed in the absence of the cofactor UDPGA did not show a peak at a retention time of 1.36 min. Together, these data indicate that the compound eluting at 1.36 minutes can be assumed to be 1-hydroxymyristicin glucuronide. The rate of the metabolic conversion of 1-hydroxymyristicin

to 1-hydroxymyristicin glucuronide in incubations with both male rat and human liver fractions with increasing concentrations of 1-hydroxymyristicin are presented in (Figure. 5A and 5D), respectively. The kinetic constants derived from these plots are presented in (Table 4).

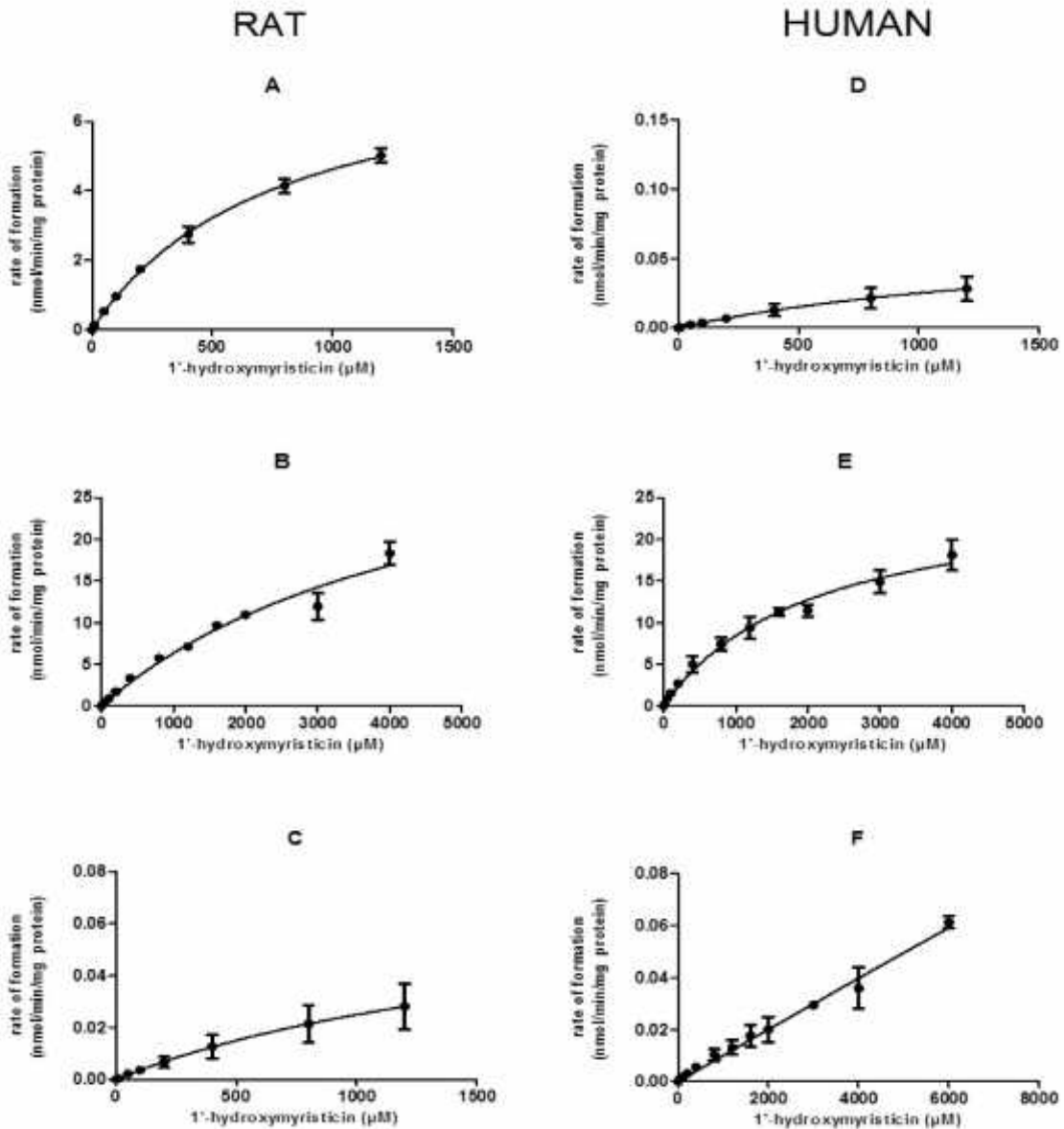


Figure 5: Concentration-dependent rate of (A) glucuronidation of 1-hydroxymyristicin in incubations with male rat liver S9 or (D) pooled human mixed gender liver S9, (B) oxidation of 1-hydroxymyristicin in incubations with pooled male rat liver microsomes or (E) pooled human mixed gender liver S9, and (C) sulfonation of 1-hydroxymyristicin in pooled male rat liver S9 or (F) pooled human mixed gender liver S9. Data points represent mean values \pm SD of three or four individual experiments.

Oxidation of 1-hydroxymyristicin.

The rate of oxidation of 1-hydroxymyristicin with increasing concentrations of 1-hydroxymyristicin in incubations with male rat and pooled human liver microsomes, are shown in (Figure. 5B and 5E) respectively, the kinetic constants derived from these data are presented in (Table 4).

Sulfonation of 1-hydroxymyristicin.

In the present study, GSH was used to trap the reactive 1-sulfoxymyristicin formed upon sulfonation of the proximate carcinogenic metabolite of myristicin, 1-hydroxymyristicin. The scavenging is based on a chemical reaction but can also be catalyzed by the GST present in the S9 incubations in which the sulfonation of 1-hydroxymyristicin was measured. Chromatographic analysis of incubations with male rat or mixed gender pooled human liver S9, increasing concentration of 1-hydroxymyristicin, PAPS, and GSH revealed a peak at 1.05 min, which was identified as the GSH adduct of the carbocation of 1-sulfoxymyristicin. Identification was achieved based on the chromatographic analysis of incubations performed in the absence of GSH and the presence of PAPS and liver S9 proteins since in these incubations no peak was found at 1.05 min. The identity was verified by LC-MS analysis, which revealed a deprotonated molecule at m/z 496, that corresponds to the expected $[M-H]^-$ mass of a GSH adduct of 1-sulfoxymyristicin. The rate of formation of 1-sulfoxymyristicin in incubations with male rat and mixed gender pooled human liver S9 are presented in (Figure. 5C and 5F), respectively. The kinetic constants for the conversion of 1-hydroxymyristicin to 1-sulfoxymyristicin in rat and human liver are presented in (Table 4).

Comparison of the kinetic constants for conversion of myristicin and 1-hydroxymyristicin by male rat and mixed gender pooled human tissue fractions.

To allow a comparison between the kinetic constants for metabolism of myristicin and 1-hydroxymyristicin by male rat and mixed gender pooled human tissue fractions, V_{\max} values that were derived in vitro expressed in $\text{nmol min}^{-1} (\text{mg microsomal or S9 protein})^{-1}$ were scaled to values representing the V_{\max} per $\mu\text{mol h}^{-1} (\text{g tissue})^{-1}$ using microsomal and S9 protein yields as described in literature (Medinsky, 1994) and previously used (Martati et al., 2012, van den Berg et al., 2012, Punt et al., 2009, Martati et al., 2011, Al-Subeihi et al., 2011, Al-Subeihi et al., 2012). Making use of the in vivo V_{\max} values derived accordingly, a scaled catalytic efficiency (scaled V_m in vivo/ K_m) for the formation of myristicin metabolites could be calculated (Table 5).

Table 5: scaled kinetic constants for metabolic conversion of myristicin and 1'-hydroxymyristicin by male rat and human tissue fractions

species		rat ^a				human ^a			
metabolite	abbreviation	scaled V _{max} , in vivo (μmol/h/g tissue) ^b	K _m (uM)	in vivo catalytic efficiency (ml/h/g tissue) ^c	k scaled (ml/hr/g tissue) ^d	scaled V _{max} , in vivo (μmol/h/g tissue) ^b	K _m (uM)	in vivo catalytic efficiency (ml/h/g tissue) ^c	k scaled (ml/hr/g tissue) ^d
conversion of myristicin									
2',3'-dihydroxymyristicin	DHM	0.924	16±7	0.0578		0.154	33±12	0.0047	
3'-hydroxymyristicin	3HM	0.987	83±31	0.0119		0.557	1629±1545	0.0003	
1'-hydroxymyristicin	HM	1.806	102±32	0.0177		0.326	234±132	0.0014	
5-allyl-2,3-dihydroxyanisole	DHA	2.73	33±11	0.0827		1.786	118±36	0.0151	
conversion of 1'-hydroxymyristicin									
1'-hydroxymyristicin glucuronide	HMG	73.788	836±336	0.0883		0.6864	3140±2434	0.0002	
1'-oxomyristicin	HMO	91.644	5922±3477	0.0155		61.44	3244±2646	0.0189	
1'-sulfoxymyristicin	HMS				0.15				0.14

a: mean values of three independent measurements.

b: Scaled V_{max} values were converted from in vitro V_{max} values based on microsomal protein yields of 35 and 32 mg/g tissue liver for rat and human, respectively, and a S9 protein yield of 143 mg/g liver.

c: catalytic efficiency (scaled V_{max} (app)/ K_m).

d: k scaled based on S9 protein yield of 143 mg/g liver.

For sulfonation, the rate constants for product formation (ml/min/mg protein) were scaled based on S9 protein yield of 143 mg/g liver. These values show that the catalytic efficiency for the formation of the proximate carcinogenic metabolite of myristicin, 1-hydroxymyristicin, was found to be 13-fold higher in male rat liver as compared to human liver. This difference in catalytic efficiency for the formation of 1-hydroxymyristicin is predominantly caused by the high affinity (expressed as K_m) and high activity (expressed as V_{max}) for its formation from myristicin in male rat liver, since the K_m value in rat liver incubations was 2-fold lower than that in human liver incubations and V_{max} in rat liver incubations was 5-fold higher than that in human liver incubations. The detoxification of 1-hydroxymyristicin by formation of 1-hydroxymyristicin glucuronide was found to be the main metabolic reaction with 1-hydroxymyristicin in rat. Glucuronidation of 1-hydroxymyristicin occurs in male rat with higher affinity than in human (i.e., K_m 836 μ M, whereas in human the K_m was 3140 μ M), analysis of the data revealed a high V_{max} value for 1-hydroxymyristicin glucuronidation resulting in a catalytic efficiency that was 400-fold higher in male rats as compared to human. Oxidation of 1-hydroxymyristicin was found to be 1.2 times more efficient in human liver as compared to male rat liver resulting from a 1.8-fold lower affinity in rat. Sulfonation was found to be the least efficient metabolic pathway for 1-hydroxymyristicin in both rats and human. For rat, the *in vivo* scaled k was 0.15 ml h⁻¹ (g tissue)⁻¹, and for human, it was 0.14 ml h⁻¹ (g tissue)⁻¹, indicating that sulfonation of 1-hydroxymyristicin is equally efficient in male rat liver and human liver. Altogether, it can be concluded that glucuronidation of 1-hydroxymyristicin, representing a detoxification pathway, is the most important pathway in rat and the oxidation is the most important pathway for conversion of 1-hydroxymyristicin in human. Moreover, on the basis of the kinetic data obtained, bioactivation of 1-hydroxymyristicin following sulfonation was found to represent only a minor pathway in both rat and human.

Evaluation of PBK model performance.

The performance of the newly developed PBK models for myristicin could not be evaluated against *in vivo* data because quantitative data on the formation or excretion of the different metabolites in rat or humans exposed to myristicin are not available. However, Beyer et al. (Beyer et al., 2006) reported that in rats and humans myristicin and safrole were *O*-demethylated. In the urine of the human nutmeg abuser, who had taken 5 nutmegs, the acetylated metabolites of 5-allyl-2,3-dihydroxyanisole, and 2,3-dihydroxymyristicin, could be identified. In the same study, *O*-demethylation of myristicin to generate 5-allyl-2,3-dihydroxyanisole seems to result in the main metabolite of myristicin detected in rat urine samples collected over a 24 h period after administration of a single oral dose of 100 mg/kg bw myristicin, with a percentage of 67% of the total dose (Beyer et al., 2006). In line with these results, the developed PBK model predicted 5-allyl-2,3-dihydroxyanisole to be the major metabolite formed at a dose of 100 mg/kg bw myristicin in rat after 24 h, with a percentage of 73% of the total dose. This predicted value of 73% of the dose matches well with the 67% observed in the *in vivo* rat study.

Important to note is that the PBK models for myristicin were based on the proposed biotransformation in (Figure. 2) and comparable with the PBK models for estragole, methyleugenol, and safrole, for which more data allowing evaluation of the models were available. The performance of the rat PBK models developed for estragole, methyleugenol, and safrole, was reported before (Punt et al., 2008, Martati et al., 2011, Al-Subeihi et al., 2011). Evaluation was done by comparing the predicted levels of a variety of metabolites in plasma or excreted in the urine of rats. Data revealed that the predicted PBK model values and the levels of these metabolites derived from *in vivo* studies adequately matched (Punt et al., 2008, Martati et al., 2011, Al-Subeihi et al., 2011). Furthermore, also for the developed human PBK models for estragole (Punt et al., 2009), methyleugenol (Al-Subeihi et al., 2012) and safrole (Martati et

al., 2012), a comparison could be made between the model predictions and the reported in vivo data for blood concentrations or the urinary excretion of some of the metabolites, thereby further supporting the validity of the models. Considering these data, it was concluded that the developed PBK models for myristicin will also adequately describe the in vivo levels of metabolites formed in rat and human after conversion of myristicin and 1-hydroxymyristicin at different oral dose levels of myristicin.

PBK model predictions.

PBK modelling was performed at dose levels of 0.05 and 300 mg/kg bw to allow comparison with the PBK model outcomes previously reported for safrole (Martati et al., 2011, Martati et al., 2012). Following an exposure to 0.05 mg/kg bw myristicin, both myristicin and its proximate carcinogenic metabolite 1-hydroxymyristicin were predicted and observed to be almost completely metabolized within a 720 h period in rat and human. At a higher oral dose level of 300mg/kg bw myristicin, both myristicin and 1-hydroxymyristicin were also predicted to be fully metabolized within 720 h. Therefore, for all further modelling, values were calculated at 720 h after dosing. (Figure. 6A) shows the PBK model-based predictions for the dose-dependent formation of the different microsomal metabolites of myristicin in rat. The percentage of the dose converted to 1-hydroxymyristicin is predicted to increase in a dose-dependent manner. Concurrent with the increased percentage of the dose that undergoes 1-hydroxylation of the alkene side chain, a 1.6-fold dose-dependent decrease in the percentage of the dose that underwent epoxidation to give 2,3-dihydroxymyristicin was observed comparing the levels at 0.05 and 300mg/kg bw. At the same time a less than 1.6-fold increase in the formation of 3-hydroxymyristicin was observed. The formation of 5-allyl-2,3-dihydroxyanisole did not change with increasing dose levels and was equal to 48% of the administered dose. (Figure. 6B) shows the dose-dependent increase in the formation of the

metabolites of 1-hydroxymyristicin in rat. This reveals a 1.8-fold increase in the percentage of the dose ultimately converted into 1-hydroxymyristicin glucuronide, 1-oxomyristicin, and 1-sulfoxymyristicin, going from a dose of 0.05 to 300 mg/kg bw. This dose-dependent increase in the formation of the different 1-hydroxymyristicin metabolites can be explained by the 1.8-fold increase of the formation of 1-hydroxymyristicin with increasing dose levels.

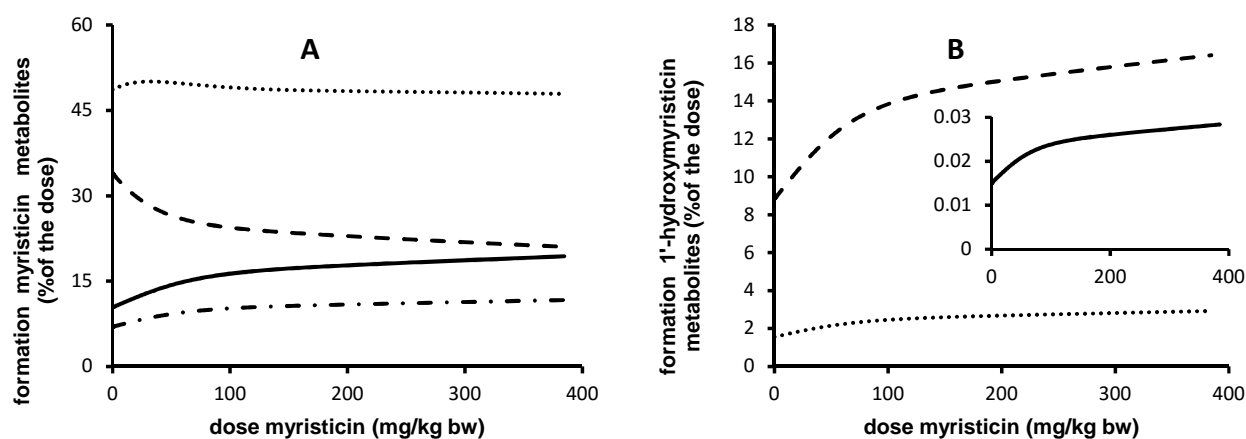


Figure 6: PBK-predicted dose-dependent changes in overall formation of (A) microsomal metabolites of myristicin in rat liver and (B) metabolites of 1-hydroxymyristicin in rat liver. The lines correspond to (A) 5-allyl-2,3-dihydroxyanisole (), 3-hydroxymyristicin (), 1-hydroxymyristicin (), and 2,3-dihydroxymyristicin (), and (B) 1-hydroxymyristicin glucuronide (), 1-sulfoxymyristicin (), and 1-oxomyristicin ().

Figure. 7A reveals that in human the percentage of the dose converted to 1-hydroxymyristicin equaled 6.5% at a dose of 0.05 mg/kg bw and increased to 8.0% at a dose of 300 mg/kg bw. Accompanying the increase in the formation of 1-hydroxymyristicin, were a 1.4-fold decrease in the formation of 2,3-dihydroxymyristicin and a steady formation of 5-allyl-2,3-dihydroxyanisole. Formation of 3-hydroxymyristicin was predicted to increase 1.8-fold with increasing dose from 0.05 to 300 mg/kg bw. (Figure. 7B) shows a 1.25-fold dose dependent increase in the percentage formation of 1-hydroxymyristicin glucuronide, 1-sulfoxymyristicin, and 1-oxomyristicin, in human liver with increasing dose from 0.05 to 300 mg/kg bw.

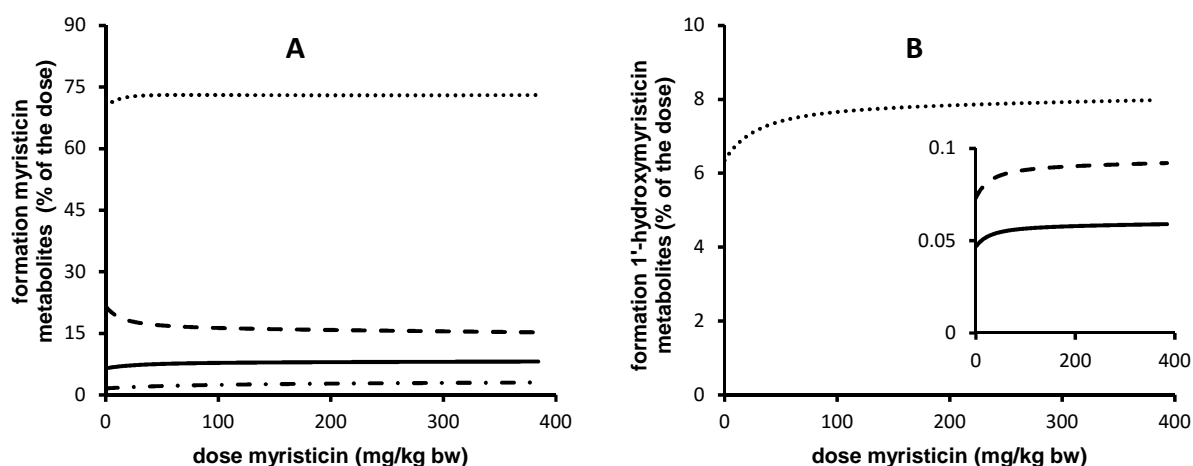


Figure 7: PBK model-based prediction of dose-dependent changes in overall formation of (A) microsomal metabolites of myristicin in human liver and (B) metabolites of 1-hydroxymyristicin in human liver. The lines correspond to (A) 5-allyl-2,3-dihydroxyanisole (—), 3-hydroxymyristicin (---), 1-hydroxymyristicin (· · ·), and 2,3-dihydroxymyristicin (— · —), and (B) 1-hydroxymyristicin glucuronide (—), 1-sulfoxymyristicin (---), and 1-oxomyristicin (· · ·).

Comparison of the relative extent of bioactivation of myristicin by rat and human liver revealed that formation of 1-hydroxymyristicin (expressed as nmol/g liver) is comparable in rat and human liver at the low dose of 0.05 mg/kg bw and 1.8-fold higher in rat liver than in human liver at a dose of 300 mg/kg bw (Figure. 8A). Formation of 1-sulfoxymyristicin (expressed as nmol/g liver) is 4-fold higher in human liver than in rat liver at a low dose of 0.05 mg/kg bw and 2.8-fold lower in rat liver than in human liver at a dose of 300 mg/kg bw (Figure. 8B).

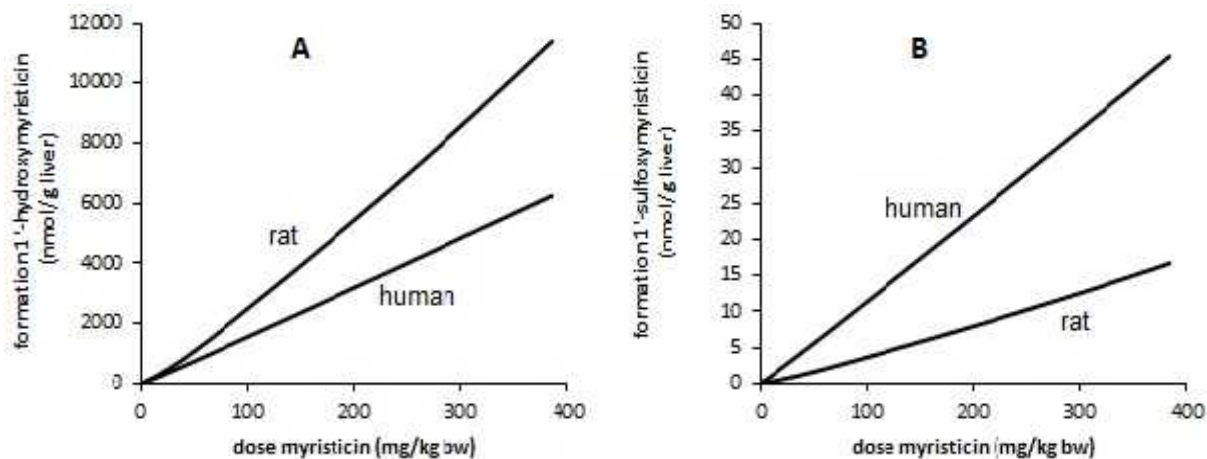


Figure 8: PBK model-based prediction of dose-dependent formation (mg/kg bw) of (A) 1-hydroxymyristicin and (B) 1-sulfoxymyristicin in rat and human liver.

Sensitivity Analysis.

A sensitivity analysis was performed to define model parameters that are capable of influencing the formation of 1-hydroxymyristicin and 1-sulfoxymyristicin in rat and human liver. For this purpose, normalized sensitivity coefficients (SCs) were calculated for all parameters at a dose of 0.05 mg/kg bw myristicin. This sensitivity analysis reveals to what extent small variation in the respective parameters influences the results. The sensitivity analysis also reveals to which parameters the predicted outcomes are most sensitive. The results of this analysis are presented in Figure 9.

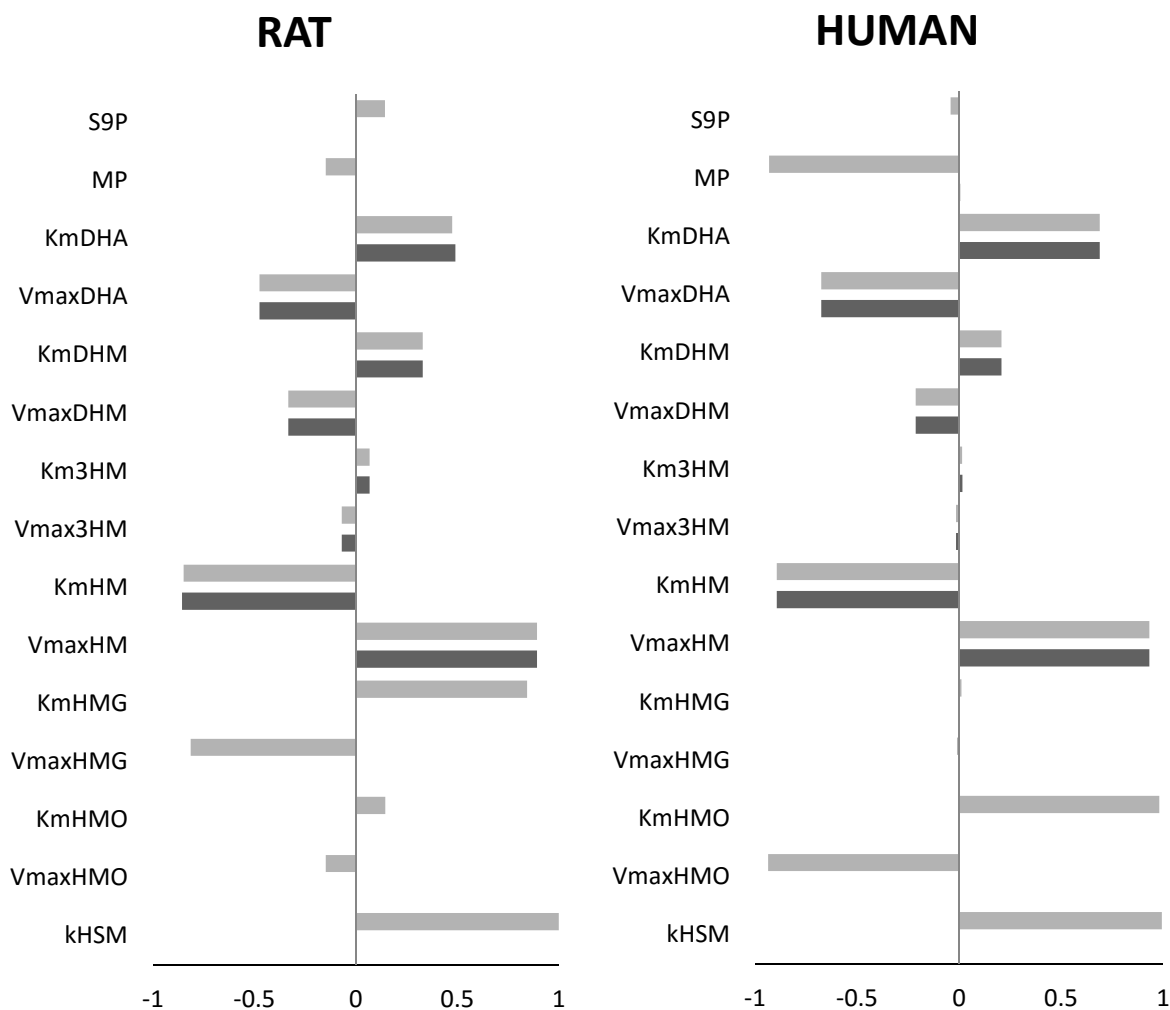


Figure 9: Normalized sensitivity coefficients for the formation from 1 -hydroxymyristicin (black) and 1 sulfoxymyristicin (grey) in the liver of rat or human.

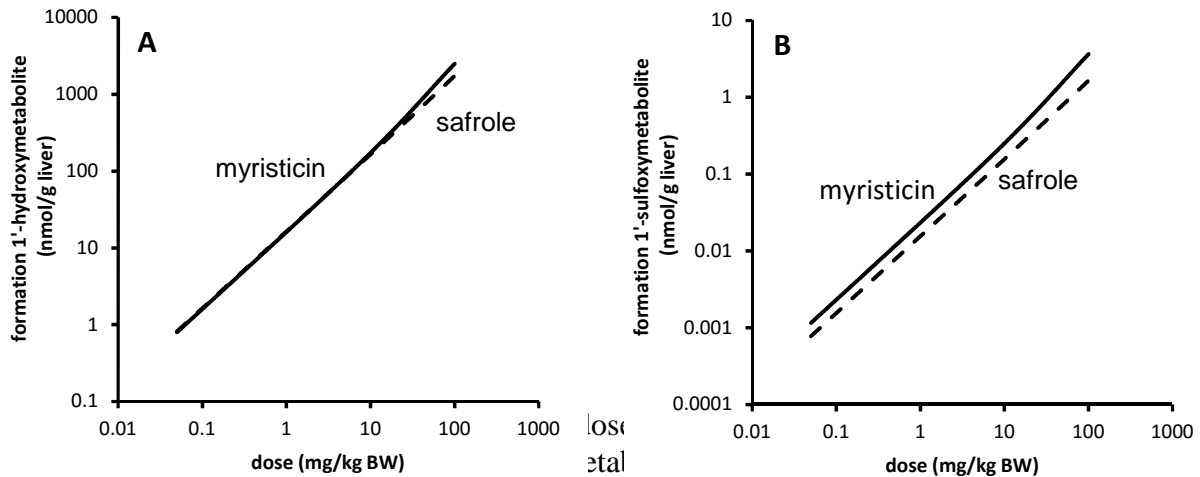
Figure 9 especially presents the parameters affecting the formation of 1 -hydroxymyristicin (black) and 1 -sulfoxymyristicin (grey) that have a normalized SC higher than $|0.1|$. In rat liver, the formation of ultimate carcinogen metabolite 1 -sulfoxymyristicin is primarily influenced by the kinetic constants of 1 -hydroxymyristicin formation from myristicin ($V_{\max HM}$, $K_{m HM}$). The kinetic constants for the formation of 5-allyl-2,3-dihydroxyanisole and 2,3-dihydroxymyristicin ($V_{\max DHA}$, $K_{m DHA}$, $V_{\max DHM}$, $K_{m DHM}$) were also found to highly influence the formation of 1 -hydroxymyristicin in rat and human liver. In rat liver, the formation of the ultimate carcinogenic metabolite 1 -sulfoxymyristicin is primarily influenced by the kinetic

constants of 1-hydroxymyristicin formation from myristicin ($V_{\max HM}$, $K_{m HM}$), the kinetic constants for the formation of 1-hydroxymyristicin glucuronide ($V_{\max HMG}$, $K_{m HMG}$), k , the first order rate constant for the sulfonation of 1-hydroxymyristicin (k_{HMS}), the kinetic constants for the formation of 5-allyl-2,3-dihydroxyanisole and 2,3-dihydroxymyristicin ($V_{\max DHA}$, $K_{m DHA}$, $V_{\max DHM}$, $K_{m DHM}$) were also found to highly influence the formation of 1-sulfoxymyristicin in rat liver. In human liver, the formation of the ultimate carcinogenic metabolite 1-sulfoxymyristicin is primarily influenced by the kinetic constants of 1-hydroxymyristicin formation from myristicin ($V_{\max HM}$, $K_{m HM}$), the kinetic constants for the formation of 1-oxomyristicin ($V_{\max HMO}$, $K_{m HMO}$), k , the first order rate constant for the sulfonation of 1-hydroxymyristicin (k_{HMS}), and liver microsomal protein yield (MP), the kinetic constants for the formation of 5-allyl-2,3-dihydroxyanisole and 2,3-dihydroxymyristicin ($V_{\max DHA}$, $K_{m DHA}$) were also found to highly influence the formation of 1-sulfoxymyristicin in human liver. The kinetic constants for the formation of 1-hydroxymyristicin glucuronide were found to highly influence the formation of 1-sulfoxymyristicin in rat liver and the kinetic constants for formation of 1-oxomyristicin were predicted to affect the formation of 1-sulfoxymyristicin in human liver to a high extent. These results reflect the fact that glucuronidation of 1-hydroxymyristicin in rat and oxidation of 1-hydroxymyristicin in human are considered as the most important competitive metabolic pathways to sulfonation.

Comparison of the PBK model-based prediction of bioactivation of myristicin by rat and human to that of its structurally related compound safrole.

In a next step the mode of action-based PBK models for myristicin metabolism in rat and human were used to facilitate a read-across from data on safrole (Martati et al., 2011, Martati et al., 2012). On the basis of the PBK models, a comparison was made for the dose-dependent formation of the proximate carcinogenic 1-hydroxy metabolite and of the ultimate carcinogenic

1-sulfoxy metabolite of myristicin and safrole in the liver of rats. (Figure 10) shows the dose-dependent formation of these metabolites in rat liver as predicted by the respective PBK models.



The PBK model-based predicted formation of the proximate carcinogenic 1-hydroxy metabolites shows that the formation of the 1-hydroxy metabolite of myristicin and safrole were predicted to be the same at low dose 0.05 mg/kg bw and 1.4-fold higher for myristicin than that of safrole at dose level 100mg/kg bw (Figure 10A). The predicted model outcomes for the formation of the ultimate carcinogenic 1-sulfoxy metabolites of safrole and myristicin is in (Figure 10B). The PBK models for rat predict the formation of 1-sulfoxymyristicin to be 1.5-fold higher for myristicin than safrole at low dose 0.05 mg/kg bw and 2.2-fold higher for myristicin than for safrole at dose level 100 mg/kg bw (Figure 11) shows the predicted dose-dependent formation of the 1-hydroxy metabolites and 1-sulfoxy metabolites of safrole and myristicin in human liver.

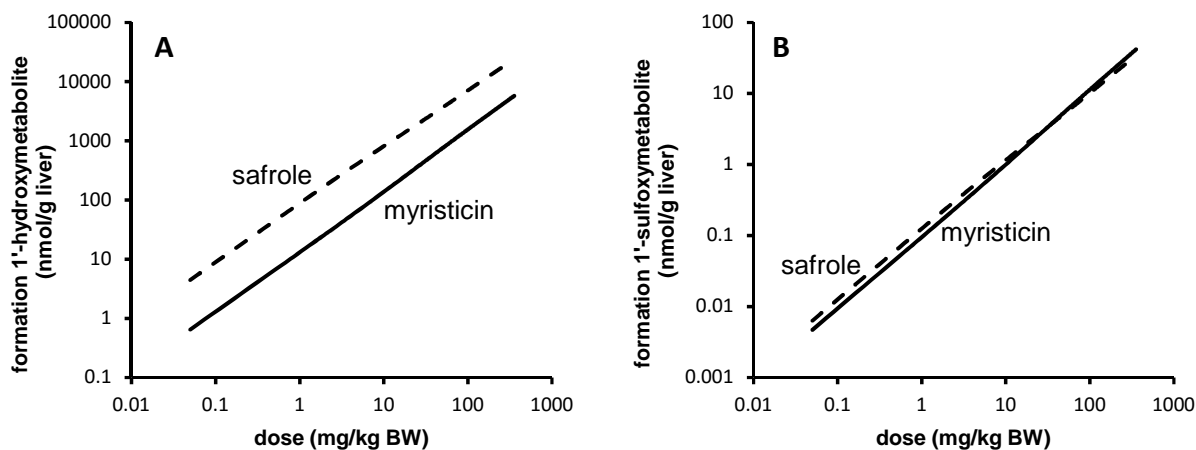


Figure 11: PBK model-based prediction of dose-dependent formation (nmol/g liver) of (A) 1-hydroxy metabolites and (B) 1-sulfoxy metabolites of myristicin (), and safrole () in human liver.

In human liver, the predicted formation of 1-hydroxymyristicin is 7-fold lower than the formation of 1-hydroxysafrole at a dose level 0.05 mg/kg bw and 4.5-fold lower for myristicin than for safrole at high dose 100 mg/kg bw (Figure 11A). The data also reveal that in human liver the formation of the DNA reactive 1-sulfoxy metabolite is comparable, 1.35 higher in safrole at low dose level 0.05 mg/kg bw, and 1.1-fold higher for myristicin at high dose level 100 mg/kg bw (Figure 11B).

Implications for risk assessment

The margin of exposure (MOE) concept was applied to assess the possible risks for human health resulting from the daily exposure to myristicin (JECFA, 2005, EFSA, 2005, Barlow, 2006, O'Brien, 2006). The MOE is a dimensionless ratio based on a reference point representing a dose causing a low but measurable cancer incidence in experimental animals (e.g., a BMDL₁₀), which is divided by the estimated daily intake in humans (EFSA, 2005). When the MOE is lower than 10000, the compound of interest is considered to be a priority for risk management actions and a concern for human health (EFSA, 2005). To date, tumor data for myristicin, from which a BMDL₁₀ can be derived, are absent in the available literature,

hampering the application of the MOE approach in the risk assessment of myristicin. Nevertheless, the results of the PBK model predictions presented above indicate that at dose levels in the range of the BMDL₁₀ values, the formation of 1-sulfoxy metabolites of myristicin in human liver is comparable (1.1-fold higher) to that of the structurally related safrole. On the basis of these considerations, and the limited difference in 1-sulfoxy metabolite formation for myristicin and safrole in rat and human liver, it was concluded that the BMDL₁₀ values of safrole could be used to perform an initial MOE based risk assessment for myristicin. Using the BMDL₁₀ for safrole of 1.9-5.1 mg/kg bw per day (van den Berg, 2011) and an estimated daily intake of myristicin of 0.0019 mg/kg bw per day (WHO, 2009) from use of herbs and spices, the MOE for myristicin would amount to 1000-2684. The estimated daily intake of safrole from spice and spice oil in USA that amounts to 0.001 mg/kg bw per day (WHO, 2009). These data result in an MOE for safrole of 1900-5100 indicating a priority for risk management that is somewhat lower than for myristicin.

Discussion

In the presented paper, the recently developed mode of action based PBK models for detoxification and bioactivation of the alkenylbenzene safrole (Martati et al., 2011, Martati et al., 2012) in male rat and human were extended to the structurally related alkenylbenzene myristicin. The newly developed PBK models combine biochemical and physico-chemical information on myristicin and on the physiology of the organism of interest (i.e., rat and human), enabling the quantification of detoxification and bioactivation in rat and human at realistic low exposure levels. The development of these models facilitates a risk assessment based on read-across from data on safrole, for which *in vivo* chronic toxicity studies are available, to myristicin, a compound for which toxicity data are limited.

The PBK models for myristicin defined in the present paper were able to predict the overall formation of the reactive 1-sulfoxymyristicin metabolite in the liver of rat and human thus enabling comparison to the overall formation of the 1-sulfoxy metabolite of the corresponding alkenylbenzene safrole. Comparison of the rat and human PBK model predictions indicated an only limited species dependent difference in the overall metabolic activation of myristicin. The difference observed were within the default factor of 4, which is generally used to describe kinetic differences between species (IPCS, 2010). The newly developed PBK model for myristicin was also used to compare the levels of metabolic activation of myristicin to those predicted previously for safrole in male rat and human liver (Martati et al., 2011, Martati et al., 2012). Results reveal that the formation of the proximate and ultimate carcinogenic metabolites of myristicin and safrole in rat liver appear to be comparable varying about 1.4-fold and 2.2-fold, respectively, with rat liver bioactivation of myristicin predicted to be somewhat higher than that of safrole for both metabolites. In humans, the formation of especially the 1-sulfoxy metabolites of the two alkenylbenzenes is predicted to be comparable (1.1-fold difference). The PBK model outcomes obtained for the formation of reactive 1-sulfoxy metabolites of myristicin and safrole, can be compared to the relative bioactivation of these two alkenylbenzenes observed in other studies. In an in vitro study with cultured human cells the ability of myristicin to form DNA adducts upon exposure of the cells to myristicin appeared to be almost the same as upon exposure to safrole (Zhou et al., 2007b) which is in line with the relative differences predicted by the PBK models. Data derived from another study in which mice were exposed to the alkenylbenzenes via intraperitoneal (i.p) injection (Table 1) suggest that the DNA adduct formation of safrole and myristicin is also not much different with DNA adduct formation in the liver of safrole being 2.7 times higher than that of myristicin (Randerath et al., 1984). In a parallel study, Phillips et al. (Table 1) reported that in neonatal mice both safrole and myristicin were able to form DNA adducts in liver, the DNA binding levels of

safrole and myristicin were 17.5 and 7.8 pmol/mg DNA, respectively (Phillips et al., 1984). It is important to note that in these mice studies DNA adduct levels were quantified by ³²P post labeling which is known to be less accurate than for example LC-MS in quantification of DNA adduct levels (Randerath et al., 1984). On the basis of the results now available, it can be concluded that using data on safrol for a read-across to myristicin is a reasonable approach for an initial risk assessment on myristicin. Such a risk assessment for myristicin can be based on the MOE approach. Because data on tumor formation are currently not available for myristicin, risk assessment for myristicin was performed using the BMDL₁₀ values for tumor formation by safrole, given the comparable bioactivation in human liver predicted by the newly developed PBK models, where the difference in the bioactivation of myristicin and safrole was predicted to be only 1.1-fold.

Using the BMDL₁₀ for safrole of 1.9-5.1 mg/kg bw per day (van den Berg, 2011) and an estimated daily intake of myristicin of 0.0019 mg/kg bw per day (WHO, 2009) from use of herbs and spices, the MOE for myristicin would amount to 1000 -2684. For comparison, the MOE values of safrole can be given, obtained at the estimated daily intake of safrole from spice and spice oil in USA that amounts to 0.001 mg/kg bw per day (WHO, 2009), and a BMDL₁₀ of safrole of 1.9-5.1 mg/kg bw per day (van den Berg, 2011). These data result in an MOE for safrole of 1900-5100 indicating a priority for risk management that is lower than for myristicin.

Altogether, the results obtained indicate that PBK modelling provides an important insight in the limited species differences between male rat and human in the metabolic activation of myristicin, and that in human liver formation of the ultimate carcinogenic 1-sulfoxy metabolites is almost the same for myristicin and safrole supporting a possibility for risk assessment for myristicin based on the MOE approach using the BMDL₁₀ for tumor formation of safrole as a reasonable but careful approximation. The present study provides an example of how PBK modelling can facilitate a read-across in risk assessment from compounds for which

in vivo toxicity studies are available to a compound for which only limited toxicity data have been described, thus contributing to development of alternatives for animal testing.

Acknowledgements

The authors would like to thank Dr. Yiannis Fiamegos for the synthesis of 1 -hydroxyapiol and Mr. Bert Spenkelink for the synthesis of 1 -oxoapiol. AMA and AJAM acknowledge financial support from the SOIT foundation (the Foundation for Stimulation Of Innovation in Toxicology). Part of this work has been supported by financial assistance of the European Union under the ENPI CBC Mediterranean Sea Basin Programme under project I.B/4.1/257, BRAMA (Botanicals Risk Assessment Training in the Mediterranean Area).

References

1. Al-Subeihi, A. A., Spengelink, B., Punt, A., Boersma, M. G., van Bladeren, P. J. & Rietjens, I. M. 2012. Physiologically based kinetic modeling of bioactivation and detoxification of the alkenylbenzene methyleugenol in human as compared with rat. *Toxicol Appl Pharmacol*, 260, 271-84.
2. Al-Subeihi, A. A., Spengelink, B., Rachmawati, N., Boersma, M. G., Punt, A., Vervoort, J., van Bladeren, P. J. & Rietjens, I. M. C. M. 2011. Physiologically based biokinetic model of bioactivation and detoxification of the alkenylbenzene methyleugenol in rat. *Toxicology in vitro : an international journal published in association with BIBRA*, 25, 267-85.
3. Barceloux, D. G. 2009. Nutmeg (*Myristica fragrans* Houtt.). *Disease-a-month : DM*, 55, 373-9.
4. Barlow, S., Renwick, A. G., Kleiner, J., Bridges, J. W., Busk, L., Dybing, E., Edler, L., Eisenbrand, G., Fink-Gremmels, J., Knaap, A., Kroes, R., Liem, D., Muller, D. J., Page, S., Rolland, V., Schlatter, J., Tritscher, A., Tueting, W., and Wurtzen, G. 2006. Risk assessment of substances that are both genotoxic and carcinogenic report of an International Conference organized by EFSA and WHO with support of ILSI Europe. *Food Chem. Toxicol*, 44, 1636-1650.
5. Benedetti, M. S., Malnoe, A. & Broillet, A. L. 1977. Absorption, metabolism and excretion of safrole in the rat and man. *Toxicology*, 7, 69-83.
6. Beyer, J., Ehlers, D. & Maurer, H. H. 2006. Abuse of nutmeg (*Myristica fragrans* Houtt.): studies on the metabolism and the toxicologic detection of its ingredients elemicin, myristicin, and safrole in rat and human urine using gas chromatography/mass spectrometry. *Therapeutic drug monitoring*, 28, 568-75.
7. Borchert, P., Miller, J. A., Miller, E. C. & Shires, T. K. 1973. 1'-Hydroxysafrole, a proximate carcinogenic metabolite of safrole in the rat and mouse. *Cancer research*, 33, 590-600.
8. Brown, R. P., Delp, M. D., Lindstedt, S. L., Rhomberg, L. R., and Beliles, R. P. 1997. Physiological parameter values for physiologically based pharmacokinetic models. *Toxicol. Ind. Health*, 13, 407-484.
9. DeJongh, J., Verhaar, H. J., and Hermens, J. L. 1997. A quantitative property-property relationship (QPPR) approach to estimate in vitro tissue-blood partition coefficients of organic chemicals in rats and humans. *Arch. Toxicol*, 72, 17-25.
10. Drinkwater, N. R., Miller, E. C., Miller, J. A. & Pitot, H. C. 1976. Hepatocarcinogenicity of estragole (1-allyl-4-methoxybenzene) and 1'-hydroxyestragole in the mouse and mutagenicity of 1'-acetoxyestragole in bacteria. *J Natl Cancer Inst*, 57, 1323-31.
11. EFSA 2005. Opinion of the Scientific Committee on a request from EFSA related to A Harmonised Approach for Risk Assessment of Substances Which are both Genotoxic and Carcinogenic.
12. EFSA 2009. Compendium of botanicals reported to contain naturally occurring substances of possible concern for human health when used in food and food supplements. *EFSA* 7, 100.
13. Fennell, T. R., Miller, J. A., and Miller, E. C. 1984. Characterization of the biliary and urinary glutathione and N-acetylcysteine metabolites of the hepatic carcinogen 1'-hydroxysafrole and its 1'-oxo metabolite in rats and mice. *Cancer research*, 44, 3231-3240.
14. Fisher, M. B., Campanale, K., Ackermann, B. L., VandenBranden, M., and Wrighton, S. A. 2000. In vitro glucuronidation using human liver microsomes and the pore-forming peptide alamethicin. *Drug Metab. Dispos.*, 28, 560-566.
15. Forrest, J. E. & Heacock, R. A. 1972. Nutmeg and mace, the psychotropic spices from *Myristica fragrans*. *Lloydia*, 35, 440-9.
16. Guenther, T. M., and Luo, G. 2001. Investigation of the role of the 2',3'-epoxidation pathway in the bioactivation and genotoxicity of dietary allylbenzene analogs. *Toxicology* 160, 47-58.
17. Hallstrom, H. & Thuvander, A. 1997. Toxicological evaluation of myristicin. *Natural toxins*, 5, 186-92.

18. Howes, A. J., Chan, V. S. & Caldwell, J. 1990. Structure-specificity of the genotoxicity of some naturally occurring alkenylbenzenes determined by the unscheduled DNA synthesis assay in rat hepatocytes. *Food Chem Toxicol*, 28, 537-42.
19. Innes 1969. J. Bioassay of pesticides and industrial chemicals for tumorigenicity in mice. *Nati. Cancer Inst*, 42, 1101- 1114.
20. Ioannides, C., Delaforge, M. & Parke, D. V. 1981. Safrole: its metabolism, carcinogenicity and interactions with cytochrome P-450. *Food and cosmetics toxicology*, 19, 657-66.
21. IPCS 2010. Characterization and application of physiologically based pharmacokinetic models in risk assessment.
22. Ishii, Y., Suzuki, Y., Hibi, D., Jin, M., Fukuhara, K., Umemura, T. & Nishikawa, A. 2011. Detection and quantification of specific DNA adducts by liquid chromatography-tandem mass spectrometry in the livers of rats given estragole at the carcinogenic dose. *Chemical research in toxicology*, 24, 532-41.
23. JECFA 2005. Sixty-fourth meeting. *FAO/WHO publication under WHO Food Additives*
24. 55 paper 83.
25. Jeurissen, S. M., Bogaards, J. J., Awad, H. M., Boersma, M. G., Brand, W., Fiamegos, Y. C., van Beek, T. A., Alink, G. M., Sudholter, E. J., Cnubben, N. H. & Rietjens, I. M. 2004. Human cytochrome p450 enzyme specificity for bioactivation of safrole to the proximate carcinogen 1'-hydroxysafrole. *Chem Res Toxicol*, 17, 1245-50.
26. Kobets, T., Duan, J. D., Brunnemann, K. D., Etter, S., Smith, B. & Williams, G. M. 2016. Structure-Activity Relationships for DNA Damage by Alkenylbenzenes in Turkey Egg Fetal Liver. *Toxicological sciences : an official journal of the Society of Toxicology*, 150, 301-11.
27. Lin, J. H., and Wong, B. K. 2002. Complexities of glucuronidation affecting in vitro in vivo extrapolation. *Curr. Drug Metab.*, 3, 623-646.
28. Luo, G. & Guenther, T. M. 1996. Covalent binding to DNA in vitro of 2',3'-oxides derived from allylbenzene analogs. *Drug metabolism and disposition: the biological fate of chemicals*, 24, 1020-7.
29. Luo, G., Qato, M. K. & Guenther, T. M. 1992. Hydrolysis of the 2',3'-allylic epoxides of allylbenzene, estragole, eugenol, and safrole by both microsomal and cytosolic epoxide hydrolases. *Drug metabolism and disposition: the biological fate of chemicals*, 20, 440-5.
30. Martati, E., Boersma, M. G., Spenkelink, A., Khadka, D. B., Punt, A., Vervoort, J., van Bladeren, P. J. & Rietjens, I. M. 2011. Physiologically based biokinetic (PBBK) model for safrole bioactivation and detoxification in rats. *Chem Res Toxicol*, 24, 818-34.
31. Martati, E., Boersma, M. G., Spenkelink, A., Khadka, D. B., van Bladeren, P. J., Rietjens, I. M. & Punt, A. 2012. Physiologically based biokinetic (PBBK) modeling of safrole bioactivation and detoxification in humans as compared with rats. *Toxicol Sci*, 128, 301-16.
32. Matthews, W. S. A. & Pickering, G. R. R., F.U. 1974. The distillation and composition of nutmed oils. *Proc. Int. Congr. Essential Oils*
33. Medinsky, M. A., Leavens, T. L., Csanady, G. A., Gargas, M. L., and Bond, J. A. 1994. In vivo metabolism of butadiene by mice and rats: A comparison of physiological model predictions and experimental data. *Carcinogenesis*, 15, 1329-40.
34. Miller, E. C., Swanson, A. B., Phillips, D. H., Fletcher, T. L., Liem, A. & Miller, J. A. 1983. Structure-activity studies of the carcinogenicities in the mouse and rat of some naturally occurring and synthetic alkenylbenzene derivatives related to safrole and estragole. *Cancer Res*, 43, 1124-34.
35. National Toxicology, P. 2000. NTP Toxicology and Carcinogenesis Studies of Methyleugenol (CAS NO. 93-15-2) in F344/N Rats and B6C3F1 Mice (Gavage Studies). *Natl Toxicol Program Tech Rep Ser*, 491, 1-412.
36. O'Brien, J., Renwick, A. G., Constable, A., Dybing, E., Muller, D. J., Schlatter, J., Slob, W., Tueting, W., van Benthem, J., Williams, G. M., and Wolfreys, A. 2006. Approaches to the risk assessment of genotoxic carcinogens in food: A critical appraisal. *Food Chem. Toxicol.*, 44, 1613-1635.

37. Phillips, D. H., Reddy, M. V. & Randerath, K. 1984. 32P-post-labelling analysis of DNA adducts formed in the livers of animals treated with safrole, estragole and other naturally-occurring alkenylbenzenes. II. Newborn male B6C3F1 mice. *Carcinogenesis*, 5, 1623-8.
38. Punt, A., Freidig, A. P., Delatour, T., Scholz, G., Boersma, M. G., Schilter, B., van Bladeren, P. J. & Rietjens, I. M. 2008. A physiologically based biokinetic (PBBK) model for estragole bioactivation and detoxification in rat. *Toxicology and applied pharmacology*, 231, 248-59.
39. Punt, A., Paini, A., Boersma, M. G., Freidig, A. P., Delatour, T., Scholz, G., Schilter, B., van Bladeren, P. J. & Rietjens, I. M. 2009. Use of physiologically based biokinetic (PBBK) modeling to study estragole bioactivation and detoxification in humans as compared with male rats. *Toxicol Sci*, 110, 255-69.
40. Randerath, K., Haglund, R. E., Phillips, D. H. & Reddy, M. V. 1984. 32P-post-labelling analysis of DNA adducts formed in the livers of animals treated with safrole, estragole and other naturally-occurring alkenylbenzenes. I. Adult female CD-1 mice. *Carcinogenesis*, 5, 1613-22.
41. Randerath K, P. K., Randerath E. 1993. Flavor constituents in cola drinks induce hepatic DNA adducts in adult and fetal mice. *Biochem Biophys Res Commun*, 192, 61-8.
42. Rietjens, I. M., Cohen, S. M., Fukushima, S., Gooderham, N. J., Hecht, S., Marnett, L. J., Smith, R. L., Adams, T. B., Bastaki, M., Harman, C. G. & Taylor, S. V. 2014. Impact of structural and metabolic variations on the toxicity and carcinogenicity of hydroxy- and alkoxy-substituted allyl- and propenylbenzenes. *Chem Res Toxicol*, 27, 1092-103.
43. Sammy, G. M. & W.W., N. 1968. Identification of the major components of nutmeg oil by gas chromatography and mass spectrometry. *Chem. Ind.*, 38, 1279-1280.
44. Swanson, A. B., Chambliss, D. D., Blomquist, J. C., Miller, E. C. & Miller, J. A. 1979. The mutagenicities of safrole, estragole, eugenol, trans-anethole, and some of their known or possible metabolites for *Salmonella typhimurium* mutants. *Mutation research*, 60, 143-53.
45. van den Berg, S. J., Patrizia Restani, Marelle G. Boersma, Luc Delmulle, Ivonne M. C. M. Rietjens 2011 Levels of Genotoxic and Carcinogenic Compounds in Plant Food Supplements and Associated Risk Assessment *Food and Nutrition Sciences*, 2, 989-1010.
46. van den Berg, S. J., Punt, A., Soffers, A. E., Vervoort, J., Ngeleja, S., Spenkelink, B. & Rietjens, I. M. 2012. Physiologically based kinetic models for the alkenylbenzene elemicin in rat and human and possible implications for risk assessment. *Chem Res Toxicol*, 25, 2352-67.
47. van den Berg SJPL, R. P., Boersma M, Delmulle L, Rietjens I 2011. Levels of Genotoxic and Carcinogenic Compounds in Plant Food Supplements and Associated Risk Assessment. *Food and Nutrition Sciences*, 2, 989-1010.
48. WHO 2009. Safety evaluation of certain additives, prepared by the Sixty-ninth meeting of the Joint FAO/WHO Expert Committee on Food Additives.
49. Wiseman, R. W., Fennell, T. R., Miller, J. A. & Miller, E. C. 1985. Further characterization of the DNA adducts formed by electrophilic esters of the hepatocarcinogens 1'-hydroxysafrole and 1'-hydroxyestragole in vitro and in mouse liver in vivo, including new adducts at C-8 and N-7 of guanine residues. *Cancer Res*, 45, 3096-105.
50. Wiseman, R. W., Miller, E. C., Miller, J. A. & Liem, A. 1987. Structure-activity studies of the hepatocarcinogenicities of alkenylbenzene derivatives related to estragole and safrole on administration to preweanling male C57BL/6J x C3H/HeJ F1 mice. *Cancer Res*, 47, 2275-83.
51. Wislocki, P. G., Borchert, P., Miller, J. A. & Miller, E. C. 1976. The metabolic activation of the carcinogen 1'-hydroxysafrole in vivo and in vitro and the electrophilic reactivities of possible ultimate carcinogens. *Cancer Res*, 36, 1686-95.
52. Wislocki, P. G., Miller, E. C., Miller, J. A., McCoy, E. C. & Rosenkranz, H. S. 1977. Carcinogenic and mutagenic activities of safrole, 1'-hydroxysafrole, and some known or possible metabolites. *Cancer research*, 37, 1883-91.
53. Zangouras, A., Caldwell, J., Hutt, A. J. & Smith, R. L. 1981. Dose dependent conversion of estragole in the rat and mouse to the carcinogenic metabolite, 1'-hydroxyestragole. *Biochemical pharmacology*, 30, 1383-6.

54. Zhou, G. D., Moorthy, B., Bi, J., Donnelly, K. C. & Randerath, K. 2007a. DNA adducts from alkoxyallylbenzene herb and spice constituents in cultured human (HepG2) cells. *Environmental and molecular mutagenesis*, 48, 715-21.
55. Zhou, S. F., Xue, C. C., Yu, X. Q. & Wang, G. 2007b. Metabolic activation of herbal and dietary constituents and its clinical and toxicological implications: an update. *Curr Drug Metab*, 8, 526-53.

Supplementary materials chapter 3

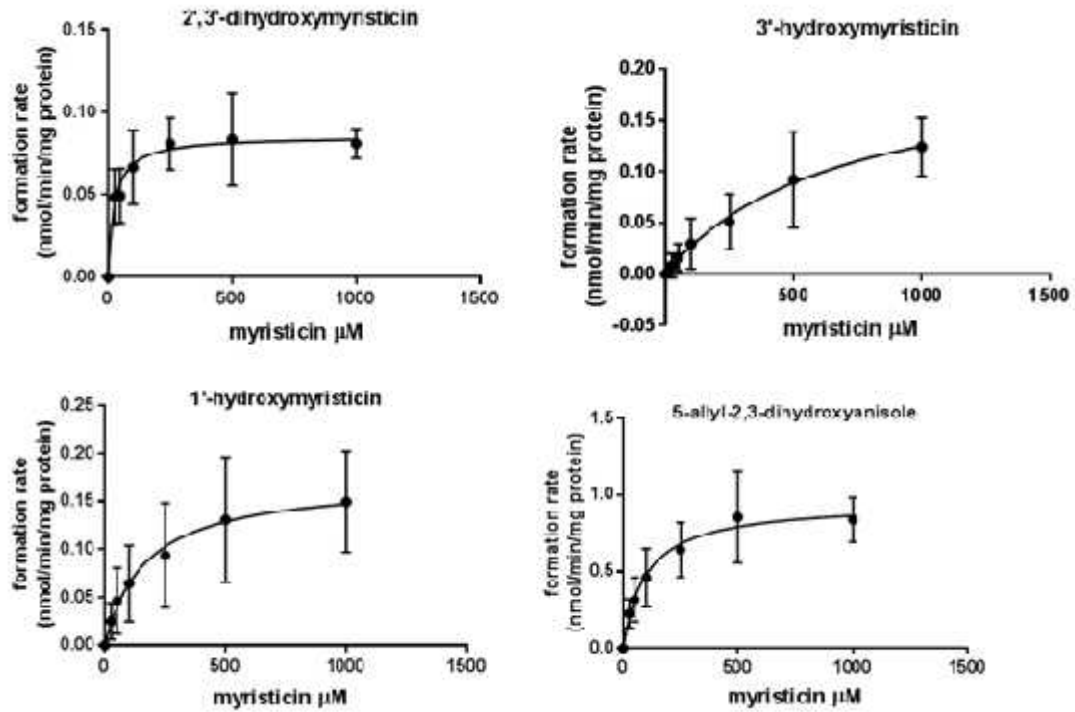


Figure S1 Concentration-dependent rate of myristicin metabolite formation in incubations with pooled human mixed gender liver microsomes. Curves for formation of four different phase I metabolites (2,3 -dihydroxymyristicin, 3 -hydroxymyristicin, 1 -hydroxymyristicin and 5-allyl-2,3-dihydroxyanisole) are presented.

Chapter 4

Level of alkenylbenzenes in parsley and dill based teas and associated risk assessment using the Margin of Exposure approach

Abdalmajeed M. Alajlouni , Amer J. Al_Malahmeh, Farida Insonia, Sebastiaan Wesseling, Jacques Vervoort, and Ivonne M.C.M. Rietjens.

Based on: Journal of Agricultural and Food Chemistry (2016) 64: 8640–8646

Abstract

Risk assessment of parsley and dill based teas that contain alkenylbenzenes was performed. To this end the estimated daily intake (EDI) of alkenylbenzenes resulting from use of the teas was quantified. Since most teas appeared to contain more than one alkenylbenzene, a combined risk assessment was performed based on equal potency of all alkenylbenzenes or using a so-called toxic equivalency (TEQ) approach through defining toxic equivalency factors (TEFs) for the different alkenylbenzenes. The EDI values resulting from consuming one cup of tea a day were 0.2–10.1 $\mu\text{g}/\text{kg}$ bw for the individual alkenylbenzenes, 0.6–13.1 $\mu\text{g}/\text{kg}$ bw for the sum of the alkenylbenzenes, and 0.3–10.7 μg safrole equiv/kg bw for the sum of alkenylbenzenes when expressed in safrole equivalents. The margin of exposure (MOE) values obtained were generally <10000, indicating a concern if the teas would be consumed on a daily basis over longer periods of time.

Introduction

At present there seems to be a growing interest for use of botanicals and botanical preparations in medicines, as food flavors and spices, drugs, food supplements and/or teas (Rietjens et al., 2008). This development is in part related to the fact that consumers consider natural products to be safe (Rietjens et al., 2008, EFSA, 2009a). However, botanicals and botanical products are well known to possibly contain a variety of natural toxins including chemicals like alkenylbenzenes, aristolochic acids, or pyrrolizidine alkaloids that are known to be genotoxic carcinogens (EFSA, 2009b, WHO, 2009, Van den Berg et al., 2011a). The present paper focuses on exposure to alkenylbenzenes as a result of use of parsley (*Petroselinum crispum*) and dill (*Anethum graveolens*) in teas. Parsley is available almost worldwide and is presently cultivated as an annual for its aromatic and attractive leaves (Simon and Quinn, 1988). Parsley has been used globally for many years as a diuretic and a medicine for treatment of kidney health problems (Kreydiyyeh and Usta, 2002, Bisset, 1994). In addition, many other medicinal claims have been associated with this botanical and its preparations, including stomach, carminative, and abortifacient effects (Farzaei et al., 2013, Kreydiyyeh and Usta, 2002). Dill is used as a medicinal herb for many purposes. For example, for treatment of gastrointestinal colic, for antispasmodic effects on the smooth muscle of the gastrointestinal tract, for treatment of disturbed nights, and for strengthening the brain (Heamalatha et al., 2011). Given all these possible effects the use of parsley and dill in food supplements and as teas becomes of increasing interest.

Parsley and dill based teas are available over the counter although they are known to contain the alkenylbenzenes apiol and myristicin (WHO, 2009, EFSA, 2009b).

Apiol and myristicin are structurally related to other alkenylbenzenes like safrole, methyleugenol, elemicin, and estragole reported to be of concern because of their potential to induce liver cancer in experimental rodents at high levels of exposure (Miller et al., 1983, Phillips et al., 1984). The alkenylbenzenes are rapidly absorbed after ingestion and transferred to the liver. In the liver one of

the metabolic pathways of these compounds leads to formation of a reactive 1-sulfoxy metabolite that can form adducts with cellular macromolecules including proteins and DNA, the latter contributing to the mode of action underlying the carcinogenicity (Borchert et al., 1973, Wiseman et al., 1985, Alajlouni et al., 2016). Thus, alkenylbenzenes are considered to be genotoxic and carcinogenic, and the risks associated with the levels of these alkenylbenzenes in a variety of botanicals and botanical preparations remains to be evaluated. To evaluate the risk of genotoxic and carcinogenic compounds, the so-called Margin of Exposure (MOE) approach was recommended by expert groups of EFSA, the Joint FAO/WHO expert committee on Food Additives (JECFA) and the International Life Sciences Institute (ILSI) (Barlow et al., 2006, EFSA, 2005, WHO, 2009, O'Brien et al., 2006). The MOE is a dimensionless ratio based on a reference point obtained from epidemiologic or experimental data on tumor incidence which is divided by the estimated daily intake in humans. The preferred reference point used in MOE calculations is the Benchmark Dose Lower confidence limit for 10% tumor incidence (BMDL₁₀). An MOE > 10000 is considered as a low priority for risk management actions (EFSA, 2005). The value of 10000 was defined based on considering various factors that cause uncertainties in the MOE including 1) a factor 100 for species differences and human variability in toxicokinetics and toxicodynamics, 2) a factor 10 for interindividual human variability in cell cycle control and DNA repair, and 3) a factor 10 for the reason that the BMDL₁₀ when used as a reference point is not identical to a NOAEL (EFSA, 2005). The aim of the present study was to assess the risk of exposure to alkenylbenzenes as a result of drinking parsley and dill based teas. This was done for parsley and dill based tea samples available on the local Dutch market and via the internet, using the MOE approach (EFSA, 2005). Given that chemical analysis of the collected samples revealed the presence of more than one alkenylbenzene in several of the parsley and dill based teas, combined exposure to different alkenylbenzenes was also taken into account.

Materials and Methods:

Chemicals and materials:

Nineteen parsley or dill containing tea samples were purchased from the Dutch market and online. The products were provided as tea bags, seeds or leaves. Some products were present as a mixture with other herbs. Product characteristics are summarized in Table S1. Estragole (purity 98% w/w (as indicated by the manufacturer)), methyleugenol (purity 99% w/w), safrole (purity >97% w/w), and myristicin (purity >97% w/w) were obtained from Sigma Aldrich (Zwijdrecht, Netherland). Apiol (purity >99%) and dill apiol (purity >99%) were obtained from Extrasynthese (Genay Cedex, France). Elemicin was obtained from Synchem OHG (Felsberg, Germany). Acetonitrile (ACN) (ULC/MS gradient), trifluoroacetic acid (TFA) and methanol (HPLC supra gradient) were acquired from Sigma Aldrich. Nanopure water was obtained from an Arium pro UF/VF water purification system (Sartorius Weighting Technology GmbH, Goettingen, Germany). Dimethyl sulfoxide (DMSO) was acquired from Acros Organics (Geel, Belgium).

Methanolic extraction:

Methanolic extraction was applied to completely extract and quantify the amount of different alkenylbenzenes present in the tea samples. The extraction was performed by adding 50 ml methanol to 0.5 g of tea followed by sonication for 15 minutes. Upon sonication the extract was filtered using a 0.45 μm syringe filter and the filtrate was stored at -20 °C until Ultra Performance Liquid Chromatography (UPLC) analysis. The method was based on the method described by Gursale et al. (Gursale et al., 2010). A recovery analysis for the different alkenylbenzenes was performed to account for possible losses during the extraction process if needed. To this end tea sample number nine (Table S1) was spiked with all alkenylbenzenes under study providing two spiked samples, one containing methyleugenol, myristicin, and apiol while the other contained

safrole, estragole, and elemicin. These spiked samples were analyzed by the same procedure as described above. The average percentage recoveries were found to equal $85.3\% \pm 2.9\%$ for estragole, $96.2\% \pm 6.0\%$ for methyleugenol, $101.1\% \pm 5.4\%$ for myristicin, and for apiol this was $94.5\% \pm 7.6\%$. Based on these outcomes the levels of the alkenylbenzenes detected in the different teas were corrected for sample recovery. The limit of detection values were $8.6 \mu\text{g/g}$ for myristicin, $9.3 \mu\text{g/g}$ for estragole, $6.4 \mu\text{g/g}$ for apiol and $7.9 \mu\text{g/g}$ for methyleugenol and limit of quantification values were $28.8 \mu\text{g/g}$ for myristicin, $30.9 \mu\text{g/g}$ for estragole, $21.5 \mu\text{g/g}$ for apiol and $26.4 \mu\text{g/g}$ for methyleugenol. The extraction procedure was shown to be linear with the amount of dry tea sample and water used up to 2% weight of tea/volume of water (data not shown).

Hot water extraction:

In order to mimic the way of preparation of homemade tea, hot water extraction was performed for the tea samples essentially as described before (Raffo et al., 2011, Van den Berg et al., 2014). As a first approximation, the weight of a parsley tea bag was taken to contain 2g of dry tea material (Table S1) and a cup of tea was assumed to contain 200 ml hot boiling water. To mimic this preparation method for the hot water extraction, 50 ml of boiling water were added to 0.5 g of each tea sample in a covered beaker and the mixture was incubated for 7 minutes. During this period the incubation was stirred three times. Subsequently the extract was centrifuged at 16,000 g for 5 minutes and the supernatant obtained was stored at $-20 \text{ }^\circ\text{C}$ until UPLC analysis.

UPLC analysis:

For analysis of the methanolic tea extracts the samples were analysed both in undiluted form and also diluted 10 times with methanol because the amount of the alkenylbenzenes was expected to be high, while hot water extracts were analyzed undiluted. UPLC analysis was performed using a

Waters (Waters, Milford, MA) Acquity solvent manager, sample manager, and diode array detector, equipped with a Water Acquity C18 1.7 μm column, 2.1 x 50 mm. The gradient was made with a mixture of ACN and ultrapure water containing 0.1% (v/v) TFA. The flow rate was 0.6 ml/min. After equilibrating the column at starting conditions of 31% ACN, the % ACN was kept at this level for 5 minutes and then increased to 80% over 4 minutes and kept at 80% for 1 minute, then decreased to 0% over 1.5 minutes and kept at 0% for 1 minute after which the % of ACN was returned to the starting conditions. Identification and quantification of the different alkenylbenzenes was done by comparison of the retention time, UV spectrum and peak areas obtained at 209 nm for apiol and myristicin and at 201 nm for methyleugenol and estragole to the retention time, UV spectrum and calibration curve of commercially available standards. In the present study no difference was made between parsley apiol and dill apiol since they co-eluted on the UPLC column. It appeared that due to the limited difference in their chemical structure, reflected by a different position of one of the methoxy substituents, parsley and dill apiol elute at the same retention time and could not be separated under the conditions applied. Their identification was based on the nature of the botanical ingredients listed to be part of the respective tea sample (Table S1).

Estimation of daily intakes of alkenylbenzenes resulting from the use of teas.

For estimation of the alkenylbenzene exposure resulting from use of the teas, the concentration of the alkenylbenzene quantified in the hot water extract was corrected by a factor that accounted for the amount of tea likely to be used to make a cup of tea. If possible this amount was derived from the amount present in the tea bags, or specified on the label. For those samples where this information was not available it was assumed that 2 grams of dry tea is used to prepare a cup (200 ml) of tea following the assumptions made by the ESCO working group, that 1.5 – 2.5 g of tea

material will be used to prepare a cup of tea of bitter fennel (EFSA, 2009a) and also based on the fact that most of the parsley tea bags appeared to contain 2g of dry tea material (Table S1).

Intake estimates for combined exposure to different alkenylbenzenes.

Since several of the tea samples appeared to contain more than one alkenylbenzene (see Result section), a combined exposure assessment and subsequent risk assessment were also performed. A first issue to solve for such a combined risk assessment is how to combine the levels of the different alkenylbenzenes when defining an estimated daily intakes (EDI). To this end it is of importance to take into account that there is high similarity between the different alkenylbenzenes; in structure, target organ, type of adverse effects, and mode of action through formation of a DNA reactive 1-sulfoxy metabolite contributing to formation of liver tumors. Based on this similar mode of action and similar target organ and end point the effect of combined exposure to different alkenylbenzenes present in the teas is assumed to be adequately described by dose addition. Based on these considerations two approaches were applied for the combined risk assessment. The first one was based on adding the levels of the different alkenylbenzenes as such, and the second approach was based on the use of a so-called Toxic Equivalency (TEQ) approach. For the latter approach, Toxic Equivalency Factors (TEFs) for the different alkenylbenzenes need to be defined, in order to allow expression of the EDIs of the combined exposure to the alkenylbenzenes in toxic equivalents. In the present study TEF values for the different alkenylbenzenes were defined taking safrole as the reference (TEF safrole = 1.00) enabling expression of the overall alkenylbenzene concentration and EDI in safrole equivalents. The TEF values for the different alkenylbenzenes were defined by taking the average of three approaches. In the first approach TEF values were defined based on data for DNA adduct formation by the different alkenylbenzenes in CD-1 mice as reported by Randerath et al. (Randerath et al., 1984). Based on these data the TEF values could be derived from the slopes of dose-response curves for DNA adduct formation in the liver for the

different alkenylbenzenes. The second approach for definition of TEF values was based on data obtained from human physiologically-based kinetic (PBK) models that allow prediction of the dose-dependent relative formation of the ultimate carcinogenic 1-sulfoxy metabolite representing the relative importance of the bioactivation route. This approach was feasible since for all alkenylbenzenes of interest PBK models to predict their relative bioactivation have been developed (Al-Subeihi et al., 2011, Martati et al., 2011, Punt et al., 2008, Van den Berg et al., 2012, Alajlouni et al., 2016). The third approach was based on the benchmark dose lower confidence limit for 10% tumor incidence above background (BMDL₁₀) values of alkenylbenzenes calculated based on carcinogenicity data reported by Miller et al. (Miller et al., 1983). For safrole, methyleugenol, and estragole such BMDL₁₀ values have been derived previously based on available in vivo tumor data (Van den Berg et al., 2011b). For apiol, elemicin and myristicin in vivo animal tumor data are not available and as a result BMDL₁₀ values cannot be defined from available tumor data but only estimated based on read-across from the structurally related alkenylbenzenes estragole and methyleugenol for elemicin (Van den Berg et al., 2012) or from safrole for myristicin (Al-Malahmeh et al., 2016) and apiol (Alajlouni et al., 2016). The average TEF of the three approaches above were used to calculate the EDI of the alkenylbenzenes extracted from the tea samples expressed in μg safrole equivalents/kg bw.

Calculation of the MOE

The MOE values were calculated in three ways; first the MOE values were calculated for the individual alkenylbenzenes using their respective BMDL₁₀ values, then the MOE values were calculated using a combined exposure assessment assuming equal potency of all alkenylbenzenes and the BMDL₁₀ for the major alkenylbenzene in each mixture, and finally MOE values were calculated based on the TEQ approach calculating the combined exposure in safrole equivalents

and using the BMDL₁₀ of safrole. BMDL₁₀ values were obtained from literature (Alajlouni et al., 2016, Van den Berg et al., 2011b, Al-Malahmeh et al., 2016).

Results:

Chemical analysis of samples:

Table 1 presents the level of different alkenylbenzenes found in the dry tea samples when using the methanol extraction method as well as the concentrations determined in the hot water extracts. The amounts of alkenylbenzenes extracted using hot water were significantly lower than the amounts extracted by methanol, the latter assumed to result in optimal extraction efficiency. The amount of alkenylbenzenes extracted into the hot water samples amounted to 10 to 62 % of the amount extracted using methanol. This indicates that there was wide variation in the hot water extraction efficiency which might be related to the actual form in which the dry sample was provided; whole fruits or fine cut (Table S1). Samples containing fine cut material resulted in extraction efficiencies of 15-62 % while samples containing whole fruits gave rise to extraction efficiencies of 10-18 %. The results obtained also revealed that 15 out of the 19 samples appeared to contain alkenylbenzenes with 7 out of the 15 samples containing alkenylbenzenes actually containing more than one alkenylbenzene. It was of interest to note that 10 samples appeared to contain apiol. Given the co-elution of apiol from parsley and dill, the nature of the apiol present can best be derived from the plant species present in the tea samples. Given the nature of the plant species present in the different tea samples (Table S1), it was likely that several apiol containing teas (3, 10, 11, 12, 16, 18 and 19) contained parsley apiol while 3 out of the apiol containing teas (4, 6 and 14) would contain dill apiol. Other alkenylbenzenes detected were myristicin, estragole, and methyleugenol.

EDI of individual alkenylbenzenes resulting from tea consumption.

Daily intake of different alkenylbenzenes was estimated based on the concentration of the alkenylbenzenes in the hot water extracts assuming a body weight of 70 kg (Table 1).

Table 1: Level of alkenylbenzenes found in the methanol and hot water extracts of different tea samples and the calculated extraction efficiency into hot water extracts^a.

tea sample	alkenylbenzenes detected	alkenylbenzene level in the dry tea sample Average \pm SD (in $\mu\text{g/g}$ dry tea preparation)	alkenylbenzene in the hot water extract ($\mu\text{g}/50$ ml infusion extracted from 1 g sample material \pm SD)	extraction efficiency into hot water infusion (%)	EDI based on consumption of one cup of tea ($\mu\text{g}/\text{kg}$ bw)
01	ND ^b	ND	ND	ND	-
02	methyleugenol	575.4 \pm 19.5	354.9 \pm 60.2	62	10.1
	estragole	302.6 \pm 20.3	66.3 \pm 7.2	22	1.9
03	apiol	51.2 \pm 5.0	31.3 \pm 3.0	61	0.9
04	apiol	18.5 \pm 2.1	ND	ND	-
05	methyleugenol	288.6 \pm 13.6	155.8 \pm 29.9	54	4.5
06	apiol	392.7 \pm 13.8	228.6 \pm 8.9	58	6.5
07	ND	ND	ND	ND	-
08	methyleugenol	235.3 \pm 30.7	131.6 \pm 26.6	56	3.8
09	myristicin	1269.8 \pm 68.3	125.7 \pm 17.8	10	3.6
10	myristicin	726.3 \pm 30.4	103.2 \pm 8.2	14	3.0
	apiol	226.4 \pm 9.0	75.6 \pm 5.9	33	2.2
11	myristicin	992.8 \pm 75.5	98.2 \pm 13.1	10	2.8
	apiol	381.8 \pm 24.8	124.4 \pm 10.6	33	3.6
12	myristicin	980.0 \pm 81.3	148.0 \pm 21.4	15	4.2
	apiol	576.4 \pm 44.7	290.9 \pm 39.8	50	8.3
13	methyleugenol	33.2 \pm 1.4	19.4 \pm 1.8	58	0.6
14	apiol	356.6 \pm 26.9	64.3 \pm 7.1	18	1.8
15	ND	ND	ND	ND	-
16	myristicin	64.6 \pm 11.3	21.4 \pm 1.8	33	0.6
	apiol	195.4 \pm 15.1	93.6 \pm 6.1	48	2.7
17	ND	ND	ND	ND	-
18	myristicin	1171.5 \pm 160.0	180.9 \pm 21.5	15	5.2
	apiol	667.9 \pm 33.5	276.3 \pm 24.8	41	7.9
19	myristicin	1055.6 \pm 34.5	150.1 \pm 13.1	14	4.3
	apiol	19.9 \pm 1.5	6.5 \pm 0.2	33	0.2

^aLevels presented were calculated back to original dry weight for the dry tea sample and presented as the amount per ml hot water extract. From these values the EDI's were calculated assuming intake of one cup of tea and a body weight of 70kg.

^bND: Not Detected.

EDI for combined exposure to alkenylbenzenes resulting from tea consumption:

Combined exposure was determined by adding up the individual levels and by using TEQ approach (table 2). TEF values for the different alkenylbenzenes were determined by three different approaches as explained in the Materials and method section. The detailed outcomes for the three methods are presented in Tables S2, S3 and S4 while Table 2 presents an overview of the TEF values thus obtained calculating the average of the TEF values obtained by the three methods.

Table 2: Overview and average of the TEF estimates obtained using the different protocols as presented in Table S2-S4.

compound	TEF derived from in vivo DNA adduct formation (Table S2)	TEF derived from human PBK model based prediction of 1 - sulfoxy metabolites formation (Table S3)	TEF derived from the BMDL ₁₀ for liver tumor formation (Table S4)	average TEF value \pm SD
safrole	1.00	1.00	1.00	1.00
myristicin	0.23	0.74	1.00	0.66 \pm 0.39
apiol	0.07	0.49	0.33	0.30 \pm 0.21
estragole	1.48	4.28	0.72	2.16 \pm 1.87
methyleugenol	0.95	0.92	0.14	0.67 \pm 0.46
elemicin	0.08	0.36	0.07	0.17 \pm 0.16

These average TEF values were used to determine the EDI of the combined exposure to alkenylbenzenes extracted from the tea samples expressed in safrole equivalents. The EDI values thus obtained are presented in Table 3.

Table 3: EDIs resulting from combined intake assessment of alkenylbenzenes assuming use of one cup of tea a day and 70 kg bw.

tea sample	alkenylbenzenes detected	EDI of the individual alkenylbenzenes based on consumption of one cup of tea ($\mu\text{g}/\text{kg}$ bw) as taken from Table 1	combined EDI of the individual alkenylbenzenes based on consumption of one cup of tea ($\mu\text{g}/\text{kg}$ bw) assuming similar potency	EDI for the individual alkenylbenzenes expressed in μg safrole equivalents/kg bw using the average TEF values resulting from 1 cup of tea	combined EDI in μg safrole equivalents per kg bw resulting from 1 cup of tea ^a
2	methyleugenol	10.1	12	6.7	10.7
	estragole	1.9		4	
3	apiol	0.9	0.9	0.3	0.3
5	methyleugenol	4.5	4.5	2.7	2.7
6	apiol	6.5	6.5	2	2
8	methyleugenol	3.8	3.8	2.2	2.2
9	myristicin	3.6	3.6	2.4	2.4
10	myristicin	2.9	5.1	2	2.7
	apiol	2.2		0.7	
11	myristicin	2.8	6.4	1.9	3
	apiol	3.6		1.1	
12	myristicin	4.2	12.5	2.8	5.3
	apiol	8.3		2.5	
13	methyleugenol	0.6	0.6	0.3	0.3
14	apiol	1.8	1.8	0.6	0.6
16	myristicin	0.6	3.3	0.4	1.2
	apiol	2.7		0.8	
18	myristicin	5.2	13.1	3.4	5.8
	apiol	7.9		2.4	
19	myristicin	4.3	4.5	2.8	2.9
	apiol	0.2		0.1	

^acalculated as (EDI of each alkenylbenzenes \times TEF (safrole equivalent))

Combined risk assessment of tea consumption using the Margin of Exposure (MOE).

Figure 1A presents the MOE values calculated for individual alkenylbenzenes using BMDL₁₀ values taken from literature (Alajlouni et al., 2016, Al-Malahmeh et al., 2016, Van den Berg et al., 2011b). The results obtained reveal MOE values generally below 10000 except for 2 values (samples T13 and T19) for which the MOE value was > 10000 for a minor alkenylbenzene in the mixture (Figure 1A).

Based on combined risk assessment, the MOE values for consumption of one cup of tea first were calculated by dividing the $BMDL_{10}$ of the major alkenylbenzene in the hot water extract by the EDI for the respective tea sample expressed as total alkenylbenzenes assuming equal potency. Second, the MOE values obtained by dividing the $BMDL_{10}$ of 1.9 mg/kg bw per day for safrole (Van den Berg et al., 2011b) by the EDI for the respective tea samples expressed in safrole equivalents (Figure 1B and 1C). The results obtained reveal MOE values that are all lower than 10000 for both approaches for the combined risk assessment except for sample number 13 calculated by the first approach for which the MOE is higher than 10000 (Figure 1B and 1C). The results also revealed that the MOE values obtained using the two methods for combined risk assessment do not vary substantially, with the final conclusion on the need for risk management for samples with $MOE < 10000$ being similar for both methods except for sample 13.

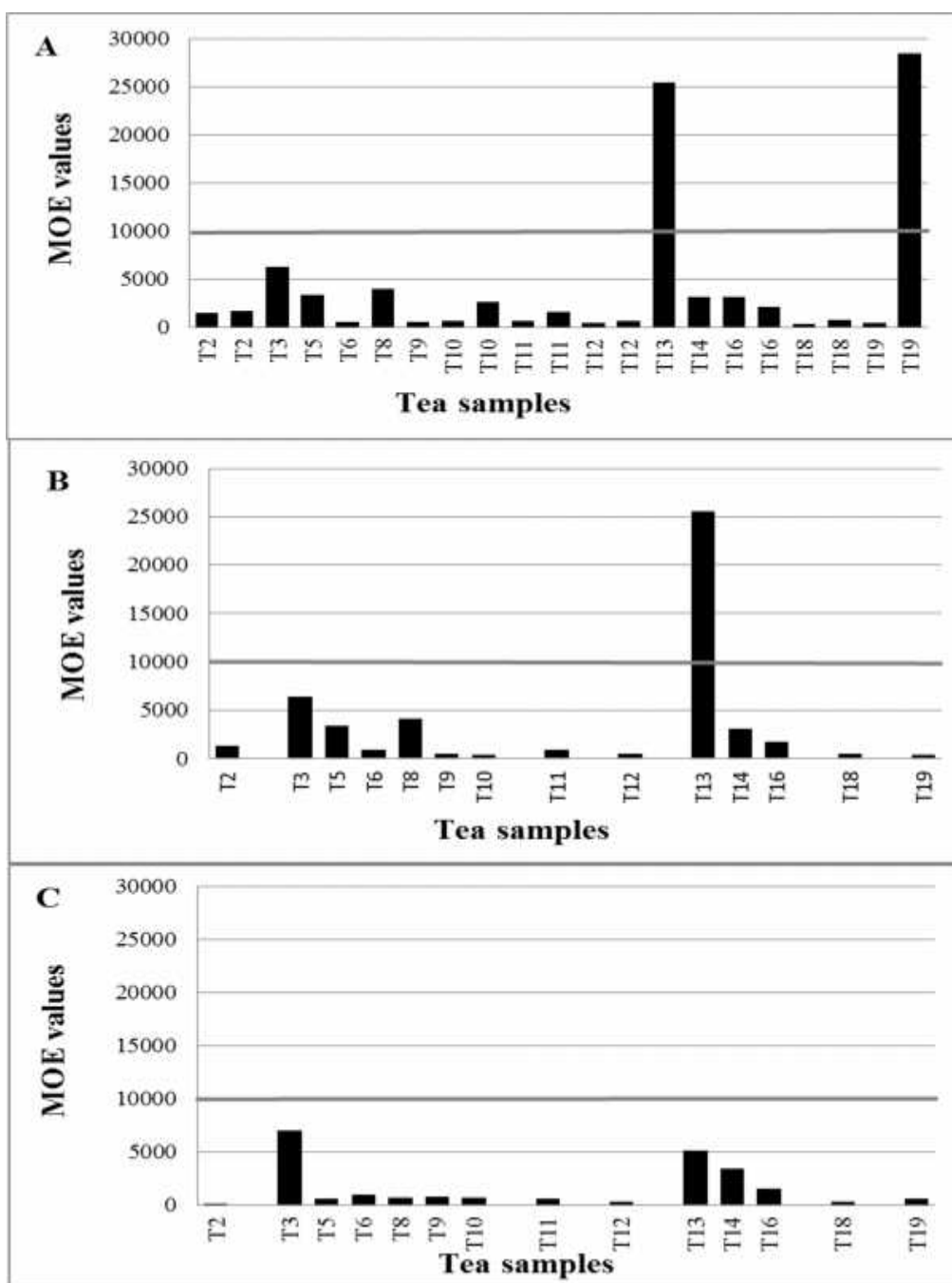


Figure 1: MOE values based on the three approaches used: A) MOE values for the individual alkenylbenzenes using their BMDL₁₀ values (apiol (5.7 mg/kg bw/day) (Alajlouni et al., 2016), myristicin (1.9 mg/kg bw/day) (Al-Malahmeh et al., 2016), methyleugenol (15.3 mg/kgbw/day) (Van den Berg et al., 2011b) and estragole (3.3 mg/kg bw/day) (Van den Berg et al., 2011b): B) MOE values for the combined exposure assuming equal potency of all alkenylbenzenes and using the BMDL₁₀ value of the major alkenylbenzenes in the mixture. MOE values for combined exposure using the TEQ approach based on safrole equivalents and using the BMDL₁₀ value of safrole (1.9 mg/kg bw/day) (Van den Berg et al., 2011b). The grey line represents the limit of MOE of 10000 with MOE values <10000 pointing at a priority for risk management.

Discussion:

The aim of the present study was to assess the risk of exposure to alkenylbenzenes as a result of drinking parsley and dill based teas. Chemical analysis of the overall levels of alkenylbenzenes in the different teas as derived from the methanol extractions revealed that 15 out of 19 tea samples analysed contained alkenylbenzenes, with 7 out of these 15 samples containing more than one alkenylbenzene. When making the hot water extracts it turned out that 14 out of 19 tea samples contained alkenylbenzenes at quantifiable levels while 7 out of these 14 contained more than one alkenylbenzene. This result points at the need for a combined risk assessment given the similar critical effect and target organ for the different alkenylbenzenes, being hepatocarcinogenicity induced via a genotoxic mode of action (Borchert et al., 1973, Wiseman et al., 1985, Kobets et al., 2016). The tea samples that contained more than one alkenylbenzenes were generally teas that did not contain only parsley or dill but were made of a combination of a wide variety of herbs including also parsley and/or dill. Apiol was detected in 10 out of 15 alkenylbenzene containing teas which is in line with the fact that the teas were selected based on having parsley or dill as a basic material, and parsley and dill are known to generally contain high levels of apiol (Semenov et al., 2007).

The total content of alkenylbenzenes in the dry tea samples ranged from 18-1269 $\mu\text{g/g}$ dry preparation. Different factors may cause this high variation of alkenylbenzene levels in the tea samples including genetic factors, geographical influences in cultivation, harvesting time, processing and manufacturing conditions, and the method of drying, which can all influence the concentrations of alkenylbenzenes (Smith et al., 2002).

To mimic the way of preparing of a cup of tea at home, and estimate the expected exposure to alkenylbenzenes when drinking tea made from the different samples, hot water extraction of the teas was performed. The hot water extraction efficiency for the alkenylbenzenes appeared to vary from 10-62%, reflecting that upon hot water extraction not all alkenylbenzenes present in the dry tea sample and detected in the methanolic extract will eventually end up in the tea as consumed.

This lower bioaccessability of the alkenylbenzenes from the tea samples upon extraction with hot water than with methanol can be explained by the fact that alkenylbenzenes have higher ability to dissolve in methanol than in water and may also be related to the ability of methanol to break down the cell walls thereby increasing the extraction efficiency. In addition the methanolic extraction method included ultrasonification that facilitates degradation of cell walls and release of cellular contents (Ebringerová and Hromádková, 1997). Finally also the form of tea sample may play role in extraction efficiency with extraction from fine cut material showing higher efficiency than that from whole fruit samples. Our results are comparable to those reported by Zeller and Rychlik reporting that hot water extraction of alkenylbenzenes from fennel is 45% (Zeller et al., 2009). On the other hand our results showed high hot water extraction efficiency compared to results reported by Van den Berg et al. (Van den Berg et al., 2014) for extraction of alkenylbenzenes from fennel teas, which was much lower, amounting to 0.1-2.3% perhaps related to the different herbal species involved.

Based on the chemical analysis of the hot water extracts, the EDI of alkenylbenzenes when actually consuming tea prepared from the different tea samples was determined. Based on consumption of one cup of tea the EDI values of the individual alkenylbenzenes ranged from 0.2-10.1 $\mu\text{g}/\text{kg}$ bw assuming a body weight of 70 kg. These EDI values resulted in MOE values that were generally below 10000, except for sample 13 and 19. Previously Van den Berg et al. (2014) evaluated the hazards and risk of the presence of the alkenylbenzene estragole in fennel based teas and found a similar result for especially children for which the MOE values for estragole exposure upon intake of one cup of fennel tea were generally < 10000 . For adults, however, especially upon intake of only one cup of tea, MOEs pointed at a low priority for risk assessment, being > 10000 (Van den Berg et al., 2014). MOEs for exposure to methyleugenol from other sources than tea were also provided. Grosch et al. (2013) reported a study in which levels of methyleugenol were quantified in various food items including samples of basil, estragon, pimento, nutmeg, several

teas, alcoholic beverages, and pesto. Based on the levels detected the authors estimated the exposure to methyleugenol to be below 1 $\mu\text{g}/\text{kg}$ bw/day for the average German population. As a worst case example they calculated an MOE of 3084 resulting from intake of 29 g of sauces and flavour ingredients per day using the methyleugenol level detected in pesto sauce of 5.3 mg/kg and a 60 kg bw (Grosch et al., 2013). And Smith et al. (2010) reported MOEs for exposure to methyleugenol from all food sources that ranged from 100-800 depending on the assumptions used in the exposure estimate (Smith et al., 2010).

By using the additive effect of alkenylbenzenes the combined EDI values obtained ranged from 0.6-13.1 $\mu\text{g}/\text{kg}$ bw. Based on this and using the BMDL_{10} of the major alkenylbenzene present in the sample, MOE values below 10000 were obtained for all samples except sample 13 (Figure 1B).

Use of the average TEF values resulted in combined EDI values that ranged from 0.3-10.7 $\mu\text{g}/\text{kg}$ bw. These values were generally 35-84 % of the combined EDI values obtained by just summing up the levels, which is mainly due to the fact that the TEF values for the different alkenylbenzenes are generally lower than 1.00 the value for the reference compound safrole (Table. 2). The MOE values obtained using these EDI values expressed in safrole equivalents and the BMDL_{10} of safrole of 1.9 mg/kg bw by were <10000 for all samples (Figure 1C).

Thus, all approaches chosen for estimating the EDI result in MOE values below 10000 for consumption of one cup of tea for 14 out of the 19 tea samples. The results also reveal that the MOE values obtained using the two methods for combined risk assessment do not vary substantially, with the final conclusion on the need for risk management for samples with MOE < 10000 being similar for both methods except for sample 13.

The overall conclusion did not change with the method used to estimate the MOE: in all three cases MOE values resulting from consumption of already one cup of tea per day were below 10000.

It is important however that these MOE values assume daily use of the herbal teas over longer periods of time and even lifelong while in reality some of these teas may be consumed for relatively shorter time periods especially when they would be used for medicinal purposes. Assuming use of the teas for periods of only a few weeks instead of during a whole life (70 years 52 weeks a year), would increase MOE values by two to three orders of magnitude indicating a far lower priority for risk management. Taking into account this consideration it is concluded that the present study shows that use of parsley and dill based teas is a concern especially for people who frequently drink large quantities of these herbal teas.

References:

1. Al-Malahmeh, A. J., Al-Ajlouni, A. M., Wesseling, S., Soffers, A. E., Al-Subeihi, A., Kiwamoto, R., Vervoort, J. & Rietjens, I. M. C. M. 2016. Physiologically based kinetic modeling of the bioactivation of myristicin. *Archives of toxicology*.
2. Al-Subeihi, A. A., Spenkeliink, B., Punt, A., Boersma, M. G., van Bladeren, P. J. & Rietjens, I. M. C. M. 2012. Physiologically based kinetic modeling of bioactivation and detoxification of the alkenylbenzene methyleugenol in human as compared with rat. *Toxicology and applied pharmacology*, 260, 271-84.
3. Al-Subeihi, A. A., Spenkeliink, B., Rachmawati, N., Boersma, M. G., Punt, A., Vervoort, J., van Bladeren, P. J. & Rietjens, I. M. C. M. 2011. Physiologically based biokinetic model of bioactivation and detoxification of the alkenylbenzene methyleugenol in rat. *Toxicology in vitro : an international journal published in association with BIBRA*, 25, 267-85.
4. Alajlouni, A. M., Al Malahmeh, A. J., Kiwamoto, R., Wesseling, S., Soffers, A. E., Al-Subeihi, A. A., Vervoort, J. & Rietjens, I. M. C. M. 2016. Mode of action based risk assessment of the botanical food-borne alkenylbenzene apiol from parsley using physiologically based kinetic (PBK) modelling and read-across from safrole. *Food Chem Toxicol*, 89, 138-50.
5. Barlow, S., Renwick, A. G., Kleiner, J., Bridges, J. W., Busk, L., Dybing, E., Edler, L., Eisenbrand, G., Fink-Gremmels, J., Knaap, A., Kroes, R., Liem, D., Muller, D. J., Page, S., Rolland, V., Schlatter, J., Tritscher, A., Tueting, W. & Wurtzen, G. 2006. Risk assessment of substances that are both genotoxic and carcinogenic report of an International Conference organized by EFSA and WHO with support of ILSI Europe. *Food and chemical toxicology : an international journal published for the British Industrial Biological Research Association*, 44, 1636-50.
6. Bisset, N. G. 1994. *Herbal Drugs and Phytotherapeutics*, Medpharm Scientific Publishers.
7. Borchert, P., Miller, J. A., Miller, E. C. & Shires, T. K. 1973. 1'-Hydroxysafrole, a proximate carcinogenic metabolite of safrole in the rat and mouse. *Cancer research*, 33, 590-600.
8. Ebringerová, A. & Hromádková, Z. 1997. The effect of ultrasound on the structure and properties of the water-soluble corn hull heteroxytan. *Ultrasonics Sonochemistry*, 4, 305-309.
9. EFSA 2005. European Food Safety Authority. Opinion of the scientific committee on a request from EFSA related to a harmonised approach for risk assessment of substances which are both genotoxic and carcinogenic. *The EFSA Journal*, 282, 1-31.
10. EFSA 2009a. Advice on the EFSA guidance Document for the Safety Assessment of Botanicals and Botanical Preparations Intended for Use as Food Supplement, based on Real Case Study. *EFSA Journal*, 7, 280.
11. EFSA 2009b. Compendium of Botanicals That Have Been Reported to Contain Toxic, Addictive, Psychotropic or Other Substances of Concern on Request of EFSA. *EFSA Journal*, 9, 1-100.
12. Farzaei, M. H., Abbasabadi, Z., Ardekani, M. R., Rahimi, R. & Farzaei, F. 2013. Parsley: a review of ethnopharmacology, phytochemistry and biological activities. *Journal of traditional Chinese medicine = Chung i tsa chih ying wen pan / sponsored by All-China Association of Traditional Chinese Medicine, Academy of Traditional Chinese Medicine*, 33, 815-26.
13. Grosch, S., Monakhova, Y., Kuballa, T., Ruge, W., Kimmich, R. & Lachenmeier, D. 2013. Comparison of GC/MS and NMR for quantification of methyleugenol in food. *European Food Research and Technology*, 236, 267-275.
14. Gursale, A., Dighe, V. & Parekh, G. 2010. Simultaneous quantitative determination of cinnamaldehyde and methyl eugenol from stem bark of *Cinnamomum zeylanicum* Blume using RP-HPLC. *Journal of Chromatographic Science*, 48, 59-62.
15. Heamalatha, S., Swarnalatha, S., Divya, M., Gandhi Lakshmi, R., Ganga Devi, A. & Gomathi, E. 2011. Pharmacognostical, Pharmacological, Investigation on *Anethum Graveolens*. *Research Journal of Pharmaceutical, Biological and Chemical Sciences*, 2, 564-574.

16. Kobets, T., Duan, J. D., Brunnemann, K. D., Etter, S., Smith, B. & Williams, G. M. 2016. Structure-Activity Relationships for DNA Damage by Alkenylbenzenes in Turkey Egg Fetal Liver. *Toxicological sciences : an official journal of the Society of Toxicology*, 150, 301-11.
17. Kreydiyyeh, S. I. & Usta, J. 2002. Diuretic effect and mechanism of action of parsley. *Journal of Ethnopharmacology*, 79, 353-7.
18. Martati, E., Boersma, M. G., Spenkeliink, A., Khadka, D. B., Punt, A., Vervoort, J., van Bladeren, P. J. & Rietjens, I. M. C. M. 2011. Physiologically based biokinetic (PBBK) model for safrole bioactivation and detoxification in rats. *Chemical research in toxicology*, 24, 818-34.
19. Martati, E., Boersma, M. G., Spenkeliink, A., Khadka, D. B., van Bladeren, P. J., Rietjens, I. M. C. M. & Punt, A. 2012. Physiologically based biokinetic (PBBK) modeling of safrole bioactivation and detoxification in humans as compared with rats. *Toxicological Sciences*
20. Miller, E. C., Swanson, A. B., Phillips, D. H., Fletcher, T. L., Liem, A. & Miller, J. A. 1983. Structure-activity studies of the carcinogenicities in the mouse and rat of some naturally occurring and synthetic alkenylbenzene derivatives related to safrole and estragole. *Cancer research*, 43, 1124-34.
21. O'Brien, J., Renwick, A. G., Constable, A., Dybing, E., Muller, D. J., Schlatter, J., Slob, W., Tueting, W., van Benthem, J., Williams, G. M. & Wolfreys, A. 2006. Approaches to the risk assessment of genotoxic carcinogens in food: a critical appraisal. *Food and chemical toxicology : an international journal published for the British Industrial Biological Research Association*, 44, 1613-35.
22. Phillips, D. H., Reddy, M. V. & Randerath, K. 1984. 32P-post-labelling analysis of DNA adducts formed in the livers of animals treated with safrole, estragole and other naturally-occurring alkenylbenzenes. II. Newborn male B6C3F1 mice. *Carcinogenesis*, 5, 1623-8.
23. Punt, A., Freidig, A. P., Delatour, T., Scholz, G., Boersma, M. G., Schilter, B., van Bladeren, P. J. & Rietjens, I. M. C. M. 2008. A physiologically based biokinetic (PBBK) model for estragole bioactivation and detoxification in rat. *Toxicology and applied pharmacology*, 231, 248-59.
24. Punt, A., Paini, A., Boersma, M. G., Freidig, A. P., Delatour, T., Scholz, G., Schilter, B., van Bladeren, P. J. & Rietjens, I. M. C. M. 2009. Use of physiologically based biokinetic (PBBK) modeling to study estragole bioactivation and detoxification in humans as compared with male rats. *Toxicological sciences : an official journal of the Society of Toxicology*, 110, 255-69.
25. Raffo, A., Nicoli, S. & Leclercq, C. 2011. Quantification of estragole in fennel herbal teas: implications on the assessment of dietary exposure to estragole. *Food Chem Toxicol*, 49, 370-5.
26. Randerath, K., Haglund, R. E., Phillips, D. H. & Reddy, M. V. 1984. 32P-post-labelling analysis of DNA adducts formed in the livers of animals treated with safrole, estragole and other naturally-occurring alkenylbenzenes. I. Adult female CD-1 mice. *Carcinogenesis*, 5, 1613-22.
27. Rietjens, I. M. C. M., Slob, W., Galli, C. & Silano, V. 2008. Risk assessment of botanicals and botanical preparations intended for use in food and food supplements: emerging issues. *Toxicology letters*, 180, 131-6.
28. Semenov, V. V., Rusak, V. V., Chartov, E. M., Zaretskii, M. I., Konyushkin, L. D., Firgang, S. I., Chizhov, A. O., Elkin, V. V., Latin, N. N., Bonashek, V. M. & Stas'eva, O. N. 2007. Polyalkoxybenzenes from plant raw materials 1. Isolation of polyalkoxybenzenes from CO₂ extracts of Umbelliferae plant seeds. *Russian Chemical Bulletin*, 56, 2448-2455.
29. Simon, J. E. & Quinn, J. 1988. Characterization of essential oil of parsley. *Journal of Agricultural and Food Chemistry*, 36, 467-472.
30. Smith, B., Cadby, P., Leblanc, J. C. & Setzer, R. W. 2010. Application of the margin of exposure (MoE) approach to substances in food that are genotoxic and carcinogenic: example: methyleugenol, CASRN: 93-15-2. *Food and chemical toxicology : an international journal published for the British Industrial Biological Research Association*, 48 Suppl 1, S89-97.
31. Smith, R. L., Adams, T. B., Doull, J., Feron, V. J., Goodman, J. I., Marnett, L. J., Portoghese, P. S., Waddell, W. J., Wagner, B. M., Rogers, A. E., Caldwell, J. & Sipes, I. G. 2002. Safety assessment of allylalkoxybenzene derivatives used as flavouring substances - methyl eugenol and estragole. *Food Chem Toxicol*, 40, 851-70.

32. Van den Berg, S. J., Punt, A., Soffers, A. E., Vervoort, J., Ngeleja, S., Spenklink, B. & Rietjens, I. M. C. M. 2012. Physiologically based kinetic models for the alkenylbenzene elemicin in rat and human and possible implications for risk assessment. *Chemical research in toxicology*, 25, 2352-67.
33. Van den Berg, S. J., Serra-Majem, L., Coppens, P. & Rietjens, I. M. C. M. 2011a. Safety assessment of plant food supplements (PFS). *Food & function*, 2, 760-8.
34. Van den Berg, S. J. P. L., Alhusainy, W., Restani, P. & Rietjens, I. M. C. M. 2014. Chemical analysis of estragole in fennel based teas and associated safety assessment using the Margin of Exposure (MOE) approach. *Food and Chemical Toxicology*, 65, 147-154.
35. Van den Berg, S. J. P. L., Restani, P., Boersma, M. G., Delmulle, L. & Rietjens, I. M. C. M. 2011b. Levels of Genotoxic and Carcinogenic Compounds in Plant Food Supplements and Associated Risk Assessment. *Food and Nutrition Sciences*, 989-1010.
36. WHO 2009. Safety evaluation of certain additives, prepared by the Sixty-ninth meeting of the Joint FAO/WHO Expert Committee on Food Additives. *World Health Organization* http://whqlibdoc.who.int/publications/2009/9789241660600_eng.pdf.
37. Wiseman, R. W., Fennell, T. R., Miller, J. A. & Miller, E. C. 1985. Further characterization of the DNA adducts formed by electrophilic esters of the hepatocarcinogens 1'-hydroxysafrole and 1'-hydroxyestragole in vitro and in mouse liver in vivo, including new adducts at C-8 and N-7 of guanine residues. *Cancer research*, 45, 3096-105.
38. Zeller, A., Horst, K. & Rychlik, M. 2009. Study of the metabolism of estragole in humans consuming fennel tea. *Chemical Research in Toxicology*, 22, 1929-37.

Supplementary materials chapter 4**Table S1:** Parsley and dill tea products used in the present study and their major characteristics. Information provided was derived from the label of the preparation unless stated otherwise.

tea sample	origin	form	how to use	ingredients
01	Canada	fine cut	one tea bag in boiling water for 3-5 or 7-12 minutes	parsley leaf
02	USA	fine cut	one tea bag in boiling water for 5-10 minutes and 1 to 3 cups a day	fennel seed, ginger root, cinnamon bark, chamomile flower, raspberry leaf, anise seed, dong quai root extract, chaste tree berry extract, Juniper berry extract, parsley leaf
03	Canada	fine cut	one tea bag in boiling water for 2-4 minutes	parsley
04	Canada	fine cut	One tea bag in boiling water for 2-4 minutes	dill seed
05	Hamburg, Germany	fine cut	one tea bag in boiling water for 5-10 minutes	<u>liquorice, cinnamon, burdock root, ginger, dandelion, fennel, anise, Juniper berries, coriander, cardamom, black pepper, parsley, sage, cloves, turmeric root</u>
06	The Netherlands	fine cut	no information provided	Aniseed, fennel, dill, caraway, fenugreek, liquorice, mustard seed
07	The Netherlands	fine cut	one tea bag (2 g) in boiling water for 5-10 minutes	aniseed, dill seed, caraway seed, mustard seeds, fennel seeds, fenugreek seeds, liquorice
08	The Netherlands	fine cut	one tea bag (2 g) in boiling water for 5-10 minutes	liquorice, cinnamon, burdock, dandelion, fennel, anise, coriander, Juniper, cardamom, black pepper, sage, parsley , cloves
09	The Netherlands	whole fruits	2 tablespoons of herbs on a pint of boiling water. 10 minutes infusion	parsley seed, stable herbs, liquorice, lovage, Juniper, aniseed

10	The Netherlands	powder	no information provided	chopped parsley leaf
11	The Netherlands	fine cut	no information provided	chopped parsley
12	The Netherlands	fine cut	no information provided	chopped parsley
13	The Netherlands	fine cut	no information provided	nettle, liquorice, yarrow, lungwort, malva leaf, knotgrass, elderflower, lady's mantle, bedstraw, plantain, basil, savory, dill, tarragon leaf, caraway seed, chervil, coriander, lovage, marjoram, lemon balm, parsley, rosemary, celery, thyme, fennel, strawberry leaves, blood root, blackberry leaves, rupturewort, pansy, speedwell, raspberry leaf, marigold, grass root, goldenrod, oat straw, clover honey, lime blossom, eyebright, pelargonium, rose, rosehip, verbena
14	The Netherlands	whole fruits	2 tablespoons of herbs on a pint of boiling water. 10 minutes infusion (indicated on internet)	dill, caraway, anise and cumin
15	The Netherlands	whole fruits	1 tablespoon in 500 ml boiling water for 10 min	fennel seed, dill seed, fenugreek, liquorice and anise
16	Canada	fine cut	one tea bag (1 g) in boiling water for 3-6 minutes	parsley leaf
17	Lithuania	fine cut	one tea bag (1.5 g) in boiling water for 5-7 minutes	chokeberry fruits, lavender flowers, parsley leaves, lemon-balm leaves, oregano herb, Java tea leaves
18	USA	fine cut	one tea bag (2 g) in boiling water for 10 minutes; 3 times daily	parsley leaves
19	USA	fine cut	one tea bag (1.5 g) in boiling water for 3 minutes and press the bag before removing	parsley leaves

Table S2: TEF values for the different alkenylbenzenes as derived from data reported for the dose-dependent level of DNA adduct formation in the liver of alkenylbenzene exposed CD-1 mice (Randerath et al., 1984).

compound	dose of alkenylbenzene (mg/kg.bw)	total Relative Adduct Labelling (RAL) (1 adduct in 10^7 nucleotides) $\times 10^7 \pm$ SD	slope of the curve for formation of DNA adduct in 10^7 nucleotides versus dose (mg / kg.bw)	TEF
safrole	0	0	1.68	1.00
	80	153 ± 27		
	400	678 ± 151		
myristicin	0	0	0.39	0.23
	80	56 ± 6.4		
	400	165 ± 30		
apiol	0	0	0.11	0.07
	80	12 ± 3.5		
	400	46 ± 9.5		
estragole	0	0	2.48	1.48
	80	109 ± 8.2		
	400	963 ± 51		
methyleugenol	0	0	1.6	0.95
	80	150 ± 15		
	400	646 ± 88		
elemicin	0	0	0.14	0.08
	80	6.2 ± 0.7		
	400	54 ± 5.3		

Table S3: TEF values for the different alkenylbenzenes as derived from the formation of the proximate carcinogenic 1-sulfoxy metabolites in liver in $\mu\text{mol/kg bw}$ as predicted by the available PBK models at a dose level of 0.01 mg/kg bw.

compound	1-sulfoxy metabolite concentration $\mu\text{mol/kg bw}$	reference for the PBK model	TEF (safrole equivalent)
safrole	3.28E-05	(Martati et al., 2012)	1.00
myristicin	2.44E-05	(Al-Malahmeh et al., 2016)	0.74
apiol	1.62E-05	(Alajlouni et al., 2016)	0.49
estragole	1.41E-04	(Punt et al., 2009)	4.28
methyleugenol	3.05E-05	(Al-Subeihi et al., 2012)	0.92
elemicin	1.20E-05	(Van den Berg et al., 2012)	0.36

Table S4: TEF values for the different alkenylbenzenes as derived from BMDL_{10} values reported in the literature.

compound	BMDL_{10} (mg/kg bw.day)	reference	TEF (safrole equivalent) ^a
safrole	1.9-5.1	(Van den Berg et al., 2011b)	1.00
myristicin	1.9-5.1	(Al-Malahmeh et al., 2016)	1.00
apiol	5.7-15.3	(Alajlouni et al., 2016)	0.33
estragole	3.3-6.5	(Van den Berg et al., 2011b)	0.72
methyleugenol	15.3-34	(Van den Berg et al., 2011b)	0.14
elemicin	30.6-68	(Van den Berg et al., 2012)	0.07

^a calculated using average BMDL_{10} value.

Chapter 5

Risk assessment of combined exposure to alkenylbenzenes through consumption of plant food supplements containing parsley and dill.

Abdalmajeed M. Alajlouni , Amer J. Al_Malahmeh, Marina Kalli, Sebastiaan Wesseling, Jacques Vervoort, and Iyonne M.C.M. Rietjens.

Journal of Food Additives and Contaminant: part A, 2017 (Accepted for publication)

Abstract

A risk assessment of parsley and dill based plant food supplements (PFS) containing apiol and related alkenylbenzenes was performed. First the levels of the alkenylbenzenes in the PFS and the resulting estimated daily intake (EDI) resulting from use of the PFS were quantified. Since most PFS appeared to contain more than one alkenylbenzene a combined risk assessment was performed based on equal potency or using a so-called Toxic Equivalency (TEQ) approach based on Toxic Equivalency Factors (TEFs) for the different alkenylbenzenes. The EDI values resulting from daily PFS consumption amount to 0.74 to 125 $\mu\text{g}/\text{kg}$ bw for the individual alkenylbenzenes, 0.74 to 160 $\mu\text{g}/\text{kg}$ bw for the sum of the alkenylbenzenes and 0.40 to 60 $\mu\text{g}/\text{kg}$ bw for the sum of alkenylbenzenes when expressed in safrole equivalents. The Margin of Exposure (MOE) values obtained were generally below 10000 indicating a priority for risk management if the PFS would be consumed on daily basis. Considering short term use of the PFS, MOE values would increase above 10000 indicating low priority for risk management. It is concluded that alkenylbenzene intake through consumption of parsley and dill based PFS is only of concern when these PFS are used for long periods of time.

Introduction

Parsley (*Petroselinum crispum*) and dill (*Anethum graveolens*) just like many other botanical and botanical preparations have been used for medicinal and edible purposes around the world because of their many active ingredients (Popovic et al., 2007, Heamalatha et al., 2011). Because people tend to assume that natural products are safe, use of botanicals and botanical preparations as plant food supplements (PFS) is increasing rapidly all over the world (Rietjens et al., 2008, EFSA, 2009a). Parsley and dill are widely used as flavoring agents in food or as medicinal drugs since many health claims suggest that use of these botanicals may promote health or cure a disease (Leung and Foster, 1996). Parsley is for example used as a curing agent in kidney health issues (Bisset, 1994, Blumenthal, 1999) and as a diuretic agent for treatment of some gastrointestinal tract problems (Kreydiyyeh and Usta, 2002). Dill is used for the treatment of gastrointestinal problems such as flatulence, indigestion, stomachache and colic, because of its antispasmodic effect on the smooth muscle of the gastrointestinal tract. In addition, dill has been used to stimulate and strengthen the brain and alleviate tiredness from disturbed nights (Heamalatha et al., 2011, Kaur and Arora, 2010). However, botanicals and PFS derived from parsley and dill may also contain harmful compounds such as the alkenylbenzenes apiol and myristicin (EFSA, 2009b, FAO/WHO, 2009). These two compounds are structurally related to alkenylbenzenes like safrole, estragole, methyleugenol, and elemicin (Figure 1) (FAO/WHO, 2009, EFSA, 2009b).

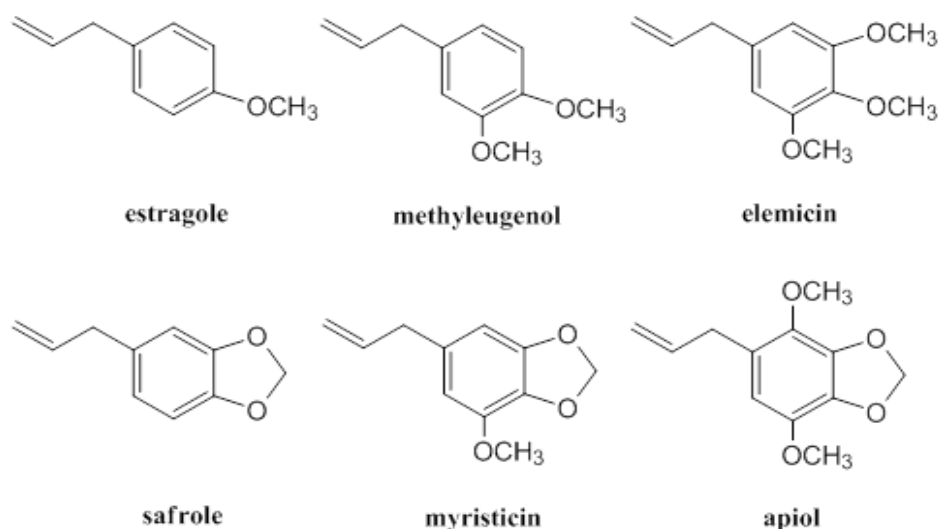


Figure 1: Structures of myristicin and apiol and related alkenylbenzenes

These alkenylbenzenes are of concern because they have been shown to be carcinogenic and genotoxic (Borchert et al., 1973, Miller et al., 1983, Wiseman et al., 1985, Randerath et al., 1984, FAO/WHO, 2009). Miller et al., for example, found that injection of high doses of safrole, methyleugenol, or estragole to mice over a 12 months period led to significant formation of hepatic tumors (Miller et al., 1983). Other alkenylbenzenes such as apiol and myristicin may be less potent carcinogens but still have the ability to induce hepatic tumors by a similar mode of action (Phillips et al., 1984, Randerath et al., 1984, Zhou et al., 2007). The mode of action underlying the ability of these compounds to induce cancer is considered to be the formation of DNA adducts upon formation of 1-sulfoxy metabolites (Figure 2) (Alajlouni et al., 2016b, Al-Malahmeh et al., 2016, Al-Subeihi et al., 2012, Van den Berg et al., 2012, Martati et al., 2012, Punt et al., 2009). The 1-sulfoxy metabolites of alkenylbenzenes have the ability to bind to cellular macromolecules including DNA.

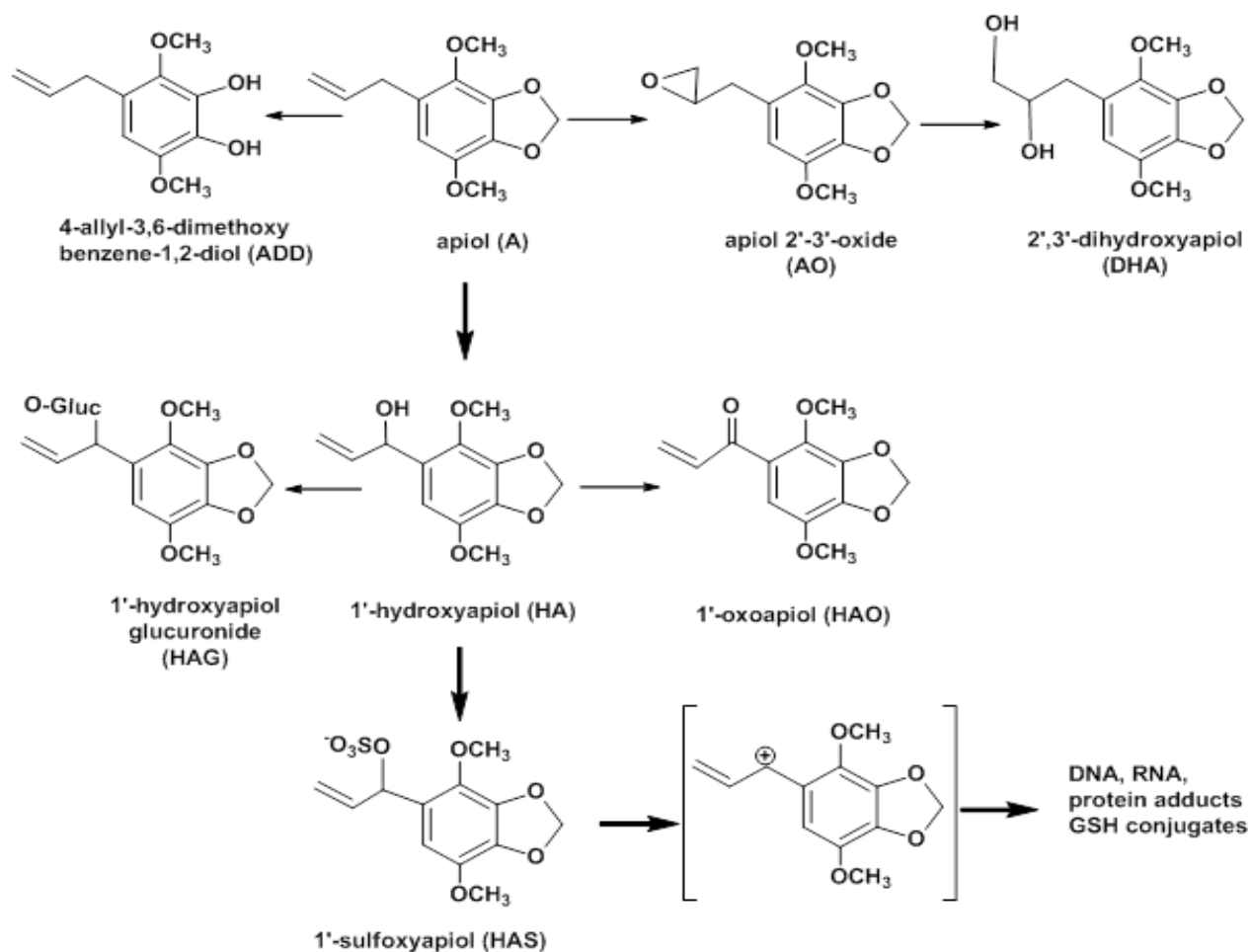


Figure 2: Metabolic pathways of apiol.

Because of their genotoxic and carcinogenic properties, the European Commission has prohibited the use of safrole, methyleugenol and estragole as pure substances in foodstuffs since September 2008 with exceptions for some specific products (European Commission (EC), 2008). Given that, there is currently no EU legislation specifically for botanicals other than the general food law Regulation 178/2002 (EFSA, 2009a) and the general food law provides the general basis for the assurance of a high level of protection of human health (European Commission (EC), 2002) and botanical based PFS do not fall under these regulations, it is of interest to characterize the

levels and accompanying hazards and risks of alkenylbenzene containing PFS. Some studies recently focused on PFS containing estragole, myristicin and safrole (Van den Berg et al., 2011) but so far parsley and dill based PFS potentially containing apiol and/or myristicin were not studied. A study on parsley and dill based teas showed that most of the examined samples contained alkenylbenzenes at levels that result in estimated intakes that would pose a priority for risk management assuming daily use of those teas (Alajlouni et al., 2016a). Therefore, the aim of the present study was to assess the risk of exposure to alkenylbenzenes as a result of consumption of PFS containing parsley and dill. To this end levels of alkenylbenzenes in parsley and dill containing PFS obtained on the market were quantified to facilitate a combined exposure assessment and a subsequent risk assessment by the so-called Margin of Exposure (MOE) approach which is the preferred method for risk assessment of compounds that are both carcinogenic and genotoxic (EFSA, 2005).

Materials and Methods

PFS and Chemicals

PFS based parsley and dill products were purchased from the local Dutch market and online. The products were in the form of capsules and pills. According to the information on the respective labels some products contained more than parsley or dill. Product information is summarized in Table 1. Estragole (purity 98% w/w (as indicated by the manufacturer)), methyleugenol (purity 99% w/w), safrole (purity >97% w/w), and myristicin (purity >97% w/w) were obtained from Sigma Aldrich (Zwijndrecht, Netherland). Apiol (purity >99%) and dill apiol (purity >99%) were obtained from Extrasynthese (Genay Cedex, France). Elemicin was obtained from Synchem OHG (Felsberg, Germany). Acetonitrile (ACN) (UPLC/MS gradient), trifluoroacetic acid (TFA) and

methanol (HPLC supra gradient) were acquired from Sigma Aldrich. Nano pure water was obtained from an Arium pro UF/VF water purification system (Sartorius Weighting Technology GmbH, Goettingen, Germany). Dimethyl sulfoxide (DMSO) was acquired from Acros Organics (Geel, Belgium).

Table 1: Parsley and dill based PFS used in the present study and their major characteristics.

PFS	Product name and type of supplement	Origin	PFS characteristics and recommended daily dose	Health claim
1	Vocht Support. Parsley containing dietary supplement capsules for a balanced diet.	Netherlands	Supplement consisting of 80 mg parsley , 80 mg ponytail (<i>Beaucarnea recurvate</i>), 80 mg bearberry (<i>Arctostaphylos uva-ursi</i>), 80 mg juniper (<i>Juniperus</i>), 80 mg goldenrod (<i>Solidago</i>), 30 mg calcium chloride / capsule. Recommended daily dose: 3 capsules per day.	Proper moisture balance.
2	Parsley Leaf. Parsley containing dietary supplement capsules.	USA	Supplement consisting of 450 mg parsley / capsule. Recommended daily dose: 6 capsules daily.	Treatment of anemia, high content in vitamin C. Protects breath from smelling.
3	Parsley Leaves Herbal dietary supplement capsules.	USA	Supplement consisting of 335 mg parsley / capsule. Recommended daily dose: 2 capsules per day.	Herbalists use the leaves to nutritionally support the kidneys and urinary system, but the whole plant can be used for general nutritional needs.

4	Liver Complex powder-Red beet, Horseradish, Dandelion and more. Dietary supplement powder.	Canada	<p>Supplement consisting of a mixture of powdered plant material.</p> <p>Supplement consisting of 450 mg parsley, 450 mg barberry (<i>Berberis vulgaris</i>), 450 mg dandelion (<i>Taraxacum</i>), 450 mg fennel (<i>Foeniculum vulgare</i>), 450 mg horse radish (<i>A Armoracia rusticana</i>), 450 mg rosehip (<i>Rosa canina</i>), and 450 mg beet root (<i>Beta vulgaris</i>) / ¼ teaspoon.</p> <p>Recommended daily dose: ¼ (1 g) teaspoon 3 times a day.</p>	Diuretic and has been shown to have bacteria-killing and fungicide effects in vitro.
5	Dill seed containing dietary supplement capsules.	Canada	<p>Supplement consisting of 450 mg dill seed / capsule.</p> <p>Recommended daily dose: 3 capsules per day.</p>	(-)
6	Dr.Clark Purity. Parsley containing dietary supplement capsules.	USA	<p>Supplement consisting of 385 mg freeze dried parsley / capsule.</p> <p>Recommended daily dose: 2 capsules daily.</p>	Supports kidney function, aids in detoxification, anti-inflammatory properties.
7	Interfresh. Parsley containing food supplement oil capsules.	UK	<p>Supplement consisting of 15 mg parsley seed oil / capsule.</p> <p>Recommended daily dose: 2 capsules up to 3 times a day.</p>	Bad breath remedy.
8	New care Parsley containing	Netherlands	<p>Supplement consisting of 80 mg parsley, 80 mg ponytail, 80 mg bearberry, 80 mg juniper, 80 mg</p>	Proper moisture balance.

	dietary supplement capsules.		goldenrod, 30 mg calcium chloride / capsule. Recommended daily dose: 3 capsules per day.	
9	B-50 Vitamin complex tablets containing parsley .	Netherlands	Supplement consists of a mixture of 2.5 mg powdered plant material. Recommended daily dose: 1 tablet per day	Supports central nervous system.
10	Mountain fresh Dill weed containing dietary supplement capsules.	UK	Supplement consisting of 500 mg dill / capsule. Recommended daily dose : 2-3 capsules daily	(-)
11	Mountain fresh Parsley Root containing dietary supplement capsules.	UK	Supplement consisting of 1000 mg parsley / capsule. Recommended daily dose : 1 capsule daily	(-)
12	Godon natural Garlic and Parsley	USA	Supplement consisting of 150 mg garlic (<i>Allium sativum</i>) and parsley / capsule. Recommended daily dose : 2 capsules daily	Cholesterol support, promotes cardiovascular health.
13	Nature's plus Garlic and Parsley oil	USA	Supplement consisting of 550 mg garlic and parsley / capsule Recommended daily dose : 2 capsules daily	(-)
14	SOLARAY	USA	Supplement consisting of	(-)

	Parsley leaves		430 mg parsley / capsule. Recommended daily dose : 4-8 capsules daily	
15	Pure healthland Garlic and Parsley	USA	Supplement consisting of 150 mg garlic and parsley / capsule. Recommended daily dose : 1-3 capsules daily	Support heart health Breathe freshening.
16	GI Nutrition Garlic and Parsley	Canada	Supplement consisting of 150 mg garlic and parsley / capsule. One Capsule daily	Immune and cholesterol support, powerful antioxidant.
17	Kroeger Herb Black Radish and Parsley	USA	Supplement consisting of 450 mg black radish (<i>Raphanus sativus</i>) and parsley / capsule. Recommended daily dose : 6 Capsule daily	Support the immune system and throat health.
18	Natures design Garlic complex including parsley	USA	Supplement consisting of 150 mg garlic and parsley / capsule. Recommended daily dose : 1-3 capsule daily	Lower cholesterol level, promotes health blood circulation and cardiovascular health.
19	Solgar Garlic Parsley	USA	Supplement consisting of 670 mg garlic and parsley / tablet. Recommended daily dose : 6 tablets daily	(-)

Quantification of alkenylbenzenes levels:

Methanolic extraction was applied to extract and quantify the amount of different alkenylbenzenes presents in the PFS samples. The method was based on the method described by Gursale et al. (Gursale et al., 2010). The extraction was performed by adding 50 ml methanol to 0.5 g of PFS

material followed by sonication for 15 minutes. Upon sonication, the extract was filtered using a 0.45 μm syringe filter and the filtrate was stored at $-20\text{ }^{\circ}\text{C}$ until Ultra Performance Liquid Chromatography (UPLC) analysis. To determine the accuracy of the method a recovery analysis for apiol, myristicin and estragole was performed to account for possible losses during the extraction process if needed. To this end, PFS sample number four (Table 1) was spiked with apiol, myristicin and estragole. The spiked sample was analysed by the same procedure as described above. The average percentages for recovery were found to equal $85.3\% \pm 2.9\%$ for estragole, $101.1\% \pm 5.4\%$ for myristicin, and $94.5\% \pm 7.6\%$ for apiol. Based on these outcomes the levels of the alkenylbenzenes detected in the different PFS were corrected for sample recovery. To determine the linearity of the extraction method, solutions of sample number four were prepared as follows: 0.5 g/200 ml, 0.5 g/100 ml, 0.5 g/50 ml, 0.5 g/25 ml, and 1 g/25ml. The results were shown to be linear up to the amount of 0.5 g PFS in 25 ml methanol.

UPLC analysis.

For analysis of the methanolic PFS extracts, the samples were analysed both in undiluted form and also diluted 10 times with ACN because the amount of the alkenylbenzenes was expected to be high. UPLC analysis was performed using a Waters (Waters, Milford, MA) Acquity solvent manager, sample manager, and diode array detector, equipped with a Water Acquity C18 $1.7\text{ }\mu\text{m}$ column, $2.1 \times 50\text{ mm}$. The gradient was made with a mixture of ACN and ultrapure water containing 0.1% (v/v) TFA. The flow rate was 0.6 ml/min. After equilibrating the column at the starting conditions of 31% ACN, the % ACN was kept at this level for 5 minutes and then increased to 80% over 4 minutes and kept at 80% for 1 min, then decreased to 0% over 1.5 minutes and kept at 0% for 1 minute after which the % ACN was returned to the starting conditions.

Identification and quantification of the different alkenylbenzenes were done by comparison of the retention time, UV spectra and peak areas obtained at 209 nm for apiol and myristicin and at 201 nm for estragole to the retention time, UV spectra and calibration curve of commercially available standards. It appeared that due to the limited difference in their chemical structure, reflected by a different position of one of the methoxy substituents, parsley and dill apiol elute at the same retention time and could not be separated under the conditions applied. Their identification was based on the nature of the botanical ingredients listed to be part of the respective PFS sample (Table 1).

Estimation of daily intakes of alkenylbenzenes resulting from the consumption of PFS.

For estimation of the alkenylbenzene exposure resulting from consumption of the PFS, the concentration of the alkenylbenzene quantified in the methanolic extract was multiplied by a factor taking the daily use of the PFS as recommended by the supplier (Table 1) into account.

Intake estimates for combined exposure to different alkenylbenzenes.

Based on the results (see results section), most of the PFS samples contained two alkenylbenzenes. Because of that a combined exposure assessment was applied. The effect of combined exposure to different alkenylbenzenes present in the PFS is assumed to be adequately described by dose addition, because all alkenylbenzenes share high similarity in structure, target organ, type of adverse effects and mode of action through formation of a DNA reactive 1-sulfoxy metabolite contributing to the formation of liver tumors. Based on these considerations two approaches were applied for the combined risk assessment. The first one was based on adding the levels of the different alkenylbenzenes as such assuming equal potency of each one. The second approach was

based on the use of a so-called Toxic Equivalency (TEQ) approach through defining Toxic Equivalency Factors (TEFs) for apiol, myristicin and estragole. The TEF values used for apiol, myristicin and estragole amounted to 0.30, 0.66 and 2.16 as compared to safrole as the reference (TEF=1.00) respectively, and were derived previously (Alajlouni et al., 2016a) based on i) data for DNA adduct formation by the different alkenylbenzenes in CD-1 mice as reported by Randerath et al. (Randerath et al., 1984), ii) data obtained from human physiologically-based kinetic (PBK) models that allow prediction of the dose-dependent relative formation of the ultimate carcinogenic 1-sulfoxy metabolite representing the relative importance of the bioactivation route, and iii) the benchmark dose lower confidence limit for 10% tumor incidence above background (BMDL₁₀) values of the alkenylbenzenes calculated based on carcinogenicity data reported by Miller et al. (Van den Berg et al., 2011) or by read-across (Alajlouni et al., 2016b, Al-Malahmeh et al., 2016, Van den Berg et al., 2012). The average TEF of the three approaches provided the TEF values mentioned above and these were used to calculate the estimated daily intake (EDI) of the alkenylbenzenes extracted from the PFS samples expressed in µg safrole equivalents/kg bw.

Calculation of the MOE

Risk assessment was performed using the MOE approach. The MOE values were obtained using EDI values and calculated in three ways; first the MOE values were calculated for the individual alkenylbenzenes using their respective BMDL₁₀ values amounting to respectively 5.7 mg/kg bw for apiol (Alajlouni et al., 2016b), 1.9 mg/kg bw for myristicin (Al-Malahmeh et al., 2016) and 3.3 mg/kg bw for estragole (Van den Berg et al., 2011). Second, the MOE values were calculated using a combined exposure assessment assuming equal potency of all alkenylbenzenes and the BMDL₁₀ for the major alkenylbenzene in the mixture. Finally MOE values were calculated based on the

TEQ approach calculating the combined exposure in safrole equivalents and using the BMDL₁₀ of safrole 1.9 mg/kg bw (Van den Berg et al., 2011) .

Results

Concentrations of alkenylbenzenes in the PFS

Table 2 presents the concentrations of the different alkenylbenzenes found in the PFS samples varying from 17 to 6487 µg/g. The results obtained revealed that 16 out of the 19 samples contained alkenylbenzenes with 11 out of these 16 samples containing both apiol and myristicin. One sample contained only estragole, two samples contained only apiol and two samples contained only myristicin.

Table 2: The concentrations and EDI of different alkenylbenzenes found in the PFS samples.

PFS sample	alkenylbenzenes detected	alkenylbenzene level in the PFS sample (ug/g)	EDI of the individual alkenylbenzenes ($\mu\text{g}/\text{kg bw}$) based on consumption of the PFS as recommended by the supplier (Table 1)	combined EDI of the alkenylbenzenes ($\mu\text{g}/\text{kg bw}$) based on consumption of the PFS as recommended by the supplier (Table 1) assuming similar potency	combined EDI in μg safrole equivalents per kg bw^a resulting from consumption of the PFS as recommended by the supplier (Table 1)
S2	myristicin	284.45	6.10	8.12	4.63
	apiol	94.54	2.03		
S3	myristicin	171.27	1.63	9.26	3.37
	apiol	800.99	7.63		
S4	estragole	17.17	0.74	0.74	1.59
S5	myristicin	1804.48	34.80	159.90	60.05
	apiol	6486.63	125.10		
S6	apiol	184.58	2.03	2.03	0.61
S7	myristicin	745.8	0.96	0.96	0.63
S10	apiol	93.04	1.33	1.33	0.40
S11	myristicin	331.83	4.74	4.74	3.13
S12	myristicin	375.70	1.61	2.86	1.44
	apiol	290.94	1.25		
S13	myristicin	716.20	11.25	14.66	8.45
	apiol	216.42	3.40		
S14	myristicin	127.80	4.71	16.01	6.50
	apiol	306.46	11.30		
S15	myristicin	329.70	1.41	2.32	1.21
	apiol	212.79	0.91		
S16	myristicin	323.40	1.39	2.24	1.16
	apiol	199.82	0.86		
S17	myristicin	71.20	2.75	9.52	3.85
	apiol	175.73	6.78		
S18	myristicin	323.60	1.39	2.20	1.16
	apiol	190.15	0.81		
S19	myristicin	26.00	1.49	9.02	3.24
	apiol	131.04	7.53		

^a calculated as (EDI of each alkenylbenzenes \times TEF (safrole equivalents))

EDI of the individual alkenylbenzenes.

The EDI of the individual alkenylbenzenes resulting from consumption of the PFS as recommended by the supplier (Table 1) was estimated based on the concentration of the different alkenylbenzenes in the PFS, the supplier recommendations for daily use and assuming a body weight of 70 kg. Table 2 presents the EDI values thus obtained. For individual alkenylbenzenes the EDI values amounted to 0.74 to 125 $\mu\text{g}/\text{kg}$ bw day. The combined EDI values calculated assuming equal potency or based on TEF values expressed in safrole equivalents, are also presented in Table 2. The EDI values obtained when assuming equal potency amounted to 0.74 to 159 $\mu\text{g}/\text{kg}$ bw day and those obtained using the TEQ approach amounted to 0.40 to 60 $\mu\text{g}/\text{kg}$ bw day. The TEQ approach generally results in lower values than the approach assuming equal potency because the major alkenylbenzenes present in the PFS have TEF values lower than 1.00.

Combined risk assessment of PFS consumption using the MOE.

Figure 3A presents the MOE values for the individual alkenylbenzenes obtained using the EDI values presented in table 2 and their BMDL_{10} values taken from literature (Alajlouni et al., 2016b, Al-Malahmeh et al., 2016, Van den Berg et al., 2011). MOE values for the combined risk assessment, obtained by dividing the BMDL_{10} of the major alkenylbenzene present in the PFS by the EDI for the respective PFS sample expressed as total alkenylbenzenes assuming equal potency, are presented in Figure 3B. MOE values obtained by dividing the BMDL_{10} of 1.9 mg/kg bw per day for safrole (Van den Berg et al., 2011) by the EDI for the respective PFS samples expressed in safrole equivalents are presented in Figure 3C. The results obtained reveal MOE values that are all lower than 10000 by using any method to calculate the MOE. Based on the combined risk assessment more than half of the samples are even below 1000 (Figure 3).

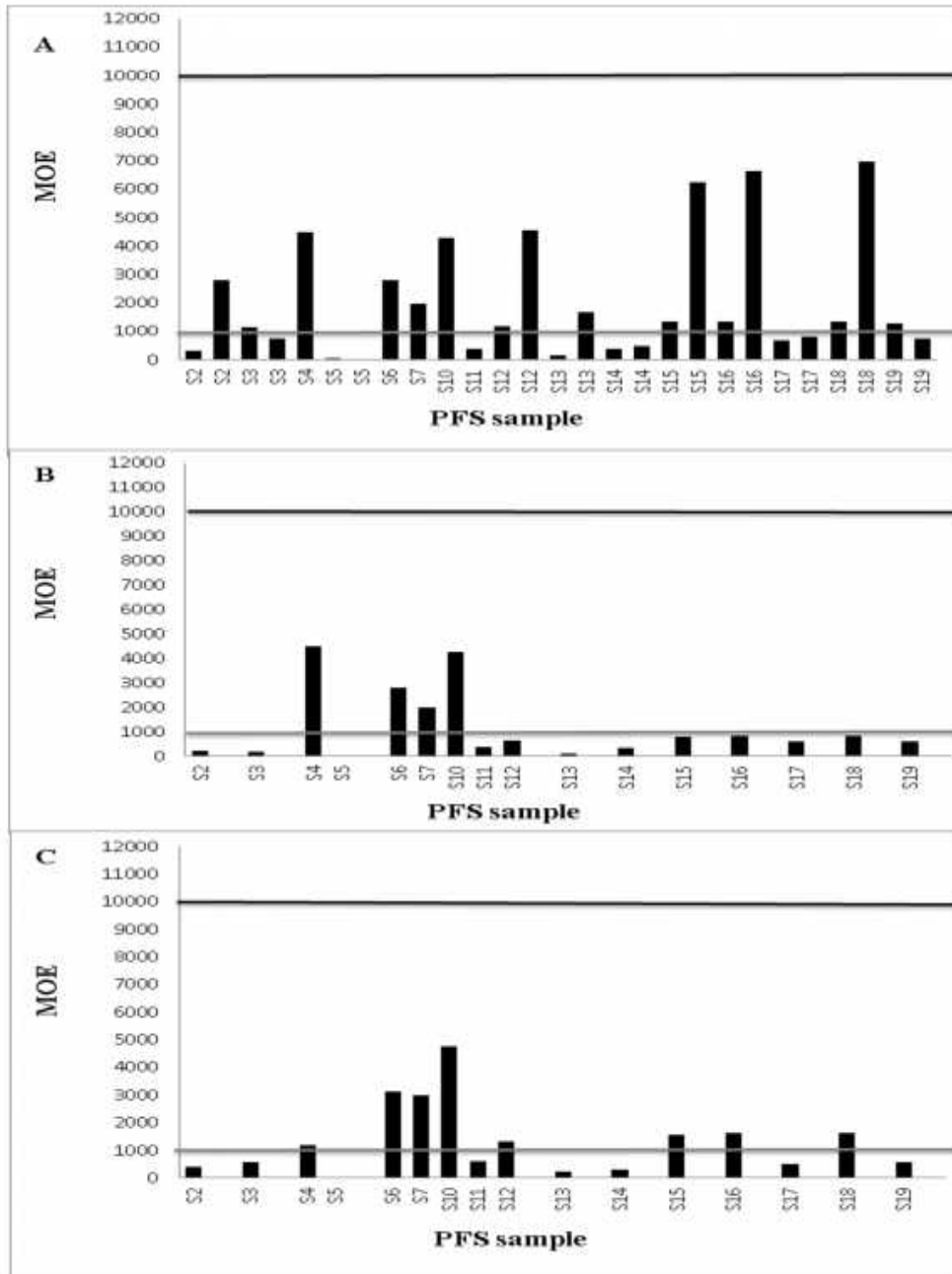


Figure 3: MOE values based on the three approaches used: A) MOE values for the individual alkenylbenzenes using their BMDL₁₀ values, B) MOE values for the combined exposure assuming equal potency of all alkenylbenzenes and using the BMDL₁₀ value of the major alkenylbenzene in the mixture, and C) MOE values for combined exposure using the TEQ approach based on safrole equivalents and using the BMDL₁₀ value of safrole. The black and grey horizontal lines represent an MOE value of 10000 and 1000 respectively.

It is important to note that this risk assessment based on the MOE as presented in figure 3, assumes long term exposure during a whole lifetime while the consumption of PFS may occur just for a short period of time of one or only a few weeks. The consequences of such a different exposure regimen may be estimated based on Haber's rule $k=C \times T$ where (k) is the toxic outcome, (C) is the concentration (or dose) of the toxic chemical and T is the time of exposure (Felter et al., 2011). This implies that the response upon lifetime exposure (75 years) to a certain dose level may be equivalent to an exposure during shorter than lifetime to a higher dose level according to the equation $(C_1 \times T_1 = C_2 \times T_2)$ (Felter et al., 2011, Van den Berg et al., 2014). Based on this assumption the relation between the total level of alkenylbenzenes detected in the PFS samples assuming equal potency and the amount of PFS consumed that would result in MOE values of 10000 was calculated for different frequencies of intake including lifetime, 4, 2 and 1 week. To present a worst case approach the $BMDL_{10}$ of myristicin was used to calculate the MOE values. The results thus obtained are presented in Figure 4. From the results presented it can be derived that a daily PFS consumption during lifetime of a PFS containing 8000 μg alkenylbenzenes/g PFS, would be of low concern only if the PFS would contain only 1.7 mg of the respective preparation. This is far less than the amount generally found in PFS samples (Table 1).

Figure 4 also reveals that the levels of alkenylbenzenes detected in the PFS samples within the present study, which vary between 100 and 8000 $\mu\text{g}/\text{g}$, would allow consumption of 1.7 to 133, 1600 to 119700, 3200 to 256500 and 6400 to 513000 mg of PFS upon lifetime, 4 weeks, two weeks and one week intake, respectively, to achieve MOE values above the 10000 safety limit for low priority for risk management.

To further illustrate how short term exposure would affect the MOE values the data presented in Figure 3 for lifetime exposure are presented in Figure 5 assuming four week exposure. From these

results it follows that assuming four week exposure the MOE values of all PFS are higher than 10000 indicating they would be of low priority for risk management.

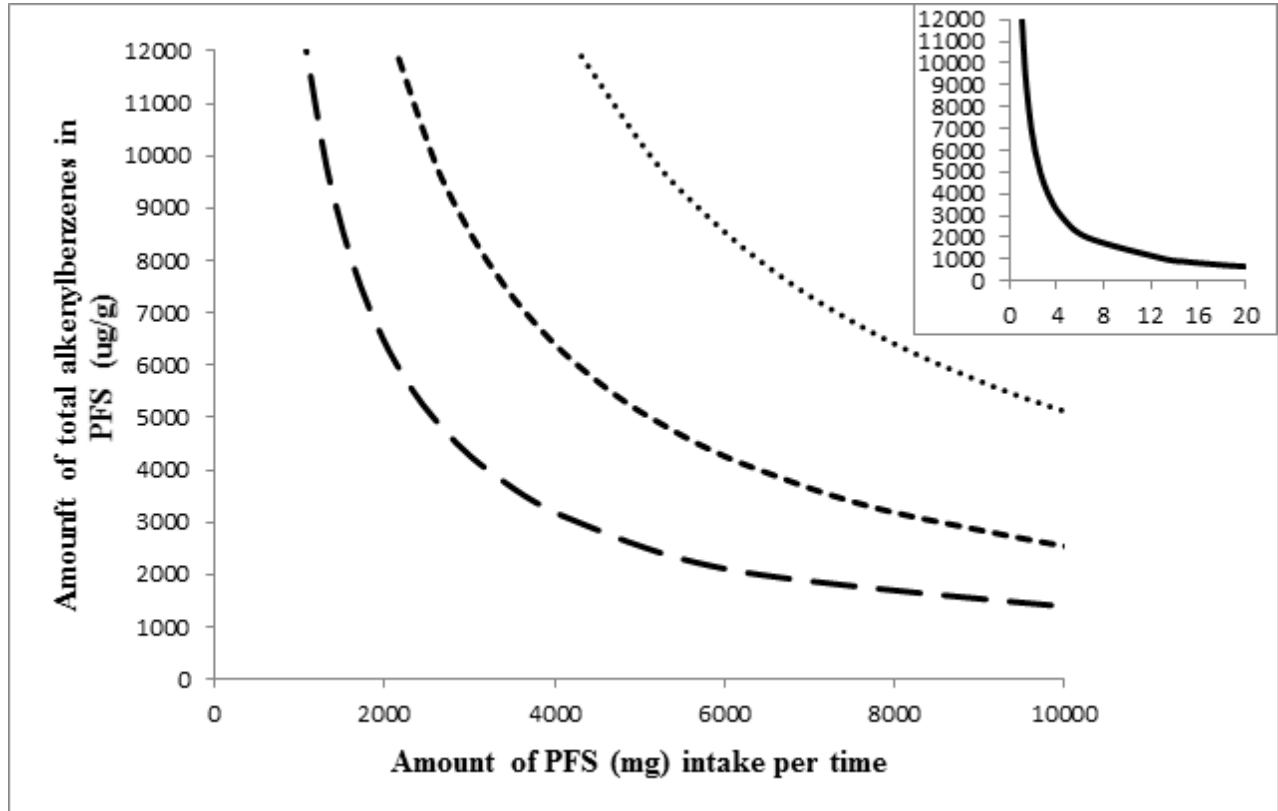


Figure 4: Relation between the total alkenylbenzenes level in a PFS, calculated based on equal potency ($\mu\text{g/g}$), and the amount of PFS consumption (mg) that would result in an MOE of 10000 upon lifetime intake (insert), one week intake (\cdots), two weeks intake ($----$), and four weeks intake ($— —$). Combinations of alkenylbenzenes levels and PFS intake that result in values below the respective curves result in MOE values above 10000 and would be of low priority for risk management.

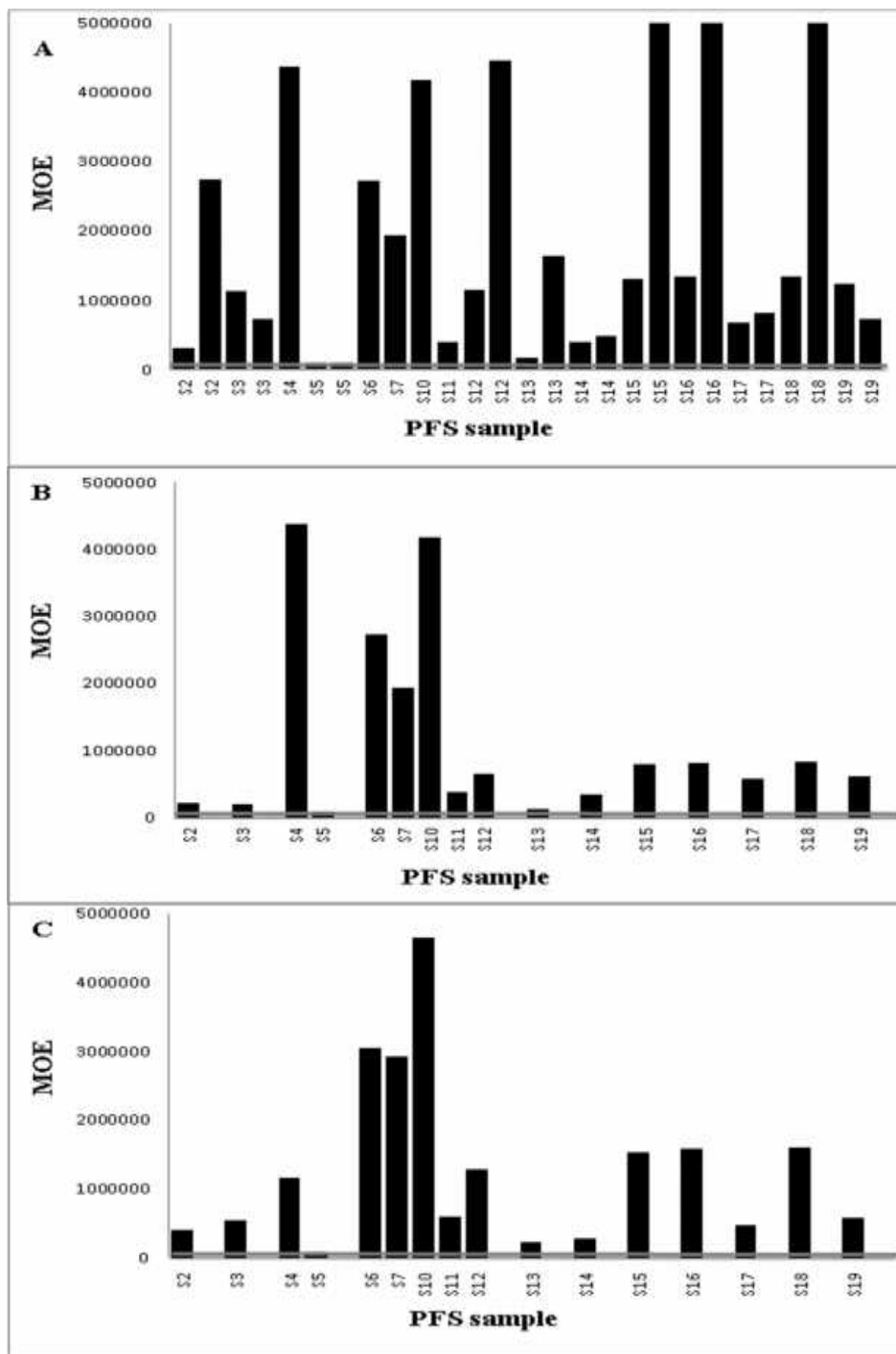


Figure 5: MOE values assuming 4 weeks intake and based on the three approaches used: A) MOE values for the individual alkenylbenzenes using their BMDL₁₀ values, B) MOE values for the combined exposure assuming equal potency of all alkenylbenzenes and using the BMDL₁₀ value of the major alkenylbenzenes in the mixture, and C) MOE values for combined exposure using the TEQ approach based on safrole equivalents and using the BMDL₁₀ value of safrole. The grey horizontal lines represent an MOE value of 10000 and all samples MOE values are above it.

Discussion

The objective of the current paper was to assess the risk of exposure to alkenylbenzenes as a result of consumption of parsley and dill based PFS. Based on chemical analysis of 19 PFS samples containing parsley or dill, 16 samples appeared to contain one or more alkenylbenzenes. One sample contained mainly estragole and this is probably because this PFS contained fennel in addition to parsley, and estragole is known to be the major alkenylbenzene in fennel (*Foeniculum vulgare*) (Van den Berg et al., 2014, Van den Berg et al., 2011). Two samples contained only myristicin. Two samples contained only apiol and 11 samples contained both apiol and myristicin. The results obtained also revealed wide variation in the level of the alkenylbenzenes present in the PFS which may be ascribed to various reasons including the type and amount of each herb within the PFS, genetic factors of these herbs, geographical influences during cultivation, harvesting time, processing and manufacturing conditions of the herbs, and the method of drying which can all influence the amount of alkenylbenzenes within the botanical and thus the PFS (Smith et al., 2002, Van den Berg et al., 2011, Rainer and L., 1983). In line with this variation, Vokk *et al.* (Vokk et al., 2011), for example, showed that myristicin within dill from Estonia makes up 1.67 % of the essential oil in summer while this level increased up to 28.15% of the essential oil during winter, while in parsley, myristicin appeared to be higher in summer amounting to 42.65% of the essential oil and lower in winter amounting to 30.67% of the essential oil. Apiol levels in dill were reported to vary from 0.05% of the essential oil in summer increasing up to 0.62 % of the essential oil in winter (Vokk et al., 2011). While in parsley apiol levels amounted to 0.11% of the essential oil in summer and increase up to 1.76 % of the essential oil in winter (Vokk et al., 2011). In addition to that the oil content in the dill seeds is around 7 times more than that of leaves (Vokk et al., 2011). Furthermore, depending on the stage of maturity of dill the apiol content was reported to range

from 0.7 to 4.35% of the essential oil while the myristicin content was reported to range from 0.0 to 7.63% (Huopalahti and Linko, 1983). In another study the effects of parsley source, type, size and color were studied for 104 different parsley plants, showing that apiol levels ranged from 0.1 to 22 % of the essential oil and myristicin levels from 0.1 to 68% (Simon and Quinn, 1988). These observations can explain the wide range of alkenylbenzene levels detected in the parsley and dill containing PFS of the present study.

Based on the chemical analysis of the PFS samples, the EDI of the alkenylbenzenes resulting from consuming these PFS could be determined. Based on consumption of the PFS as recommended by the suppliers, the EDI values of the individual alkenylbenzenes ranged from 0.74 to 125 $\mu\text{g}/\text{kg}$ bw assuming a body weight of 70 kg. These EDI values resulted in MOE values that were generally below 10000. Previously Van den Berg et al. (Van den Berg et al., 2011) evaluated the hazards and risks of the presence of the alkenylbenzenes estragole, methyleugenol, -asaron and safrol in basil (*Occimum basilicum*), nutmeg (*Myristica fragrans*), fennel, sassafras (*Sassafras albidum*), calamus (*Acorus calamus*) and cinnamon (*Cinnamomum zeylanicum*) based PFS and found a similar result with MOE values for exposure to these related alkenylbenzenes as a result of intake of these PFS also often < 10000 , also some PFS gave rise to MOE values far above this limit.

Since most of the PFS samples included in the present study contained two alkenylbenzenes, apiol and myristicin, a combined exposure and risk assessment was performed. The combined EDI values obtained assuming equal potency of the different alkenylbenzenes ranged from 0.74 to 160 $\mu\text{g}/\text{kg}$ bw. Based on this and using the BMDL_{10} of the major alkenylbenzene present in the sample MOE values below 10000 were obtained for all samples. Use of the average TEF values to express the EDI in safrole equivalents resulted in combined EDI values that ranged from 0.40 to 60 μg safrole equivalents/kg bw. These values were generally 40 to 64 % of the combined EDI values

obtained by summing up the levels, which is mainly due to the fact that the TEF values for the major alkenylbenzenes in the mixtures are lower than 1.00, the value for the reference compound safrole. In spite of this the MOE values obtained using these EDI values expressed in safrole equivalents and the BMDL₁₀ of safrole of 1.9 mg/kg bw were still <10000 for all samples.

Thus, it can be concluded that the overall conclusion did not change with the method used to estimate the MOE: in all three approaches MOE values resulting from consumption of the PFS as recommended by the provider per day were below 10000, and for many of the PFS even below 1000.

It is of interest to note that these MOE values refer to regular daily and lifetime consumption of the PFS which may be an overestimation of realistic human consumption. Based on Haber's rule, levels of alkenylbenzenes in PFS samples and consumption frequency of PFS directly impact the EDI and the resulting possible toxic effect presented by their MOE values.

Considering short term use of the PFS MOE values would increase above 10000 indicating low priority for risk management. It is concluded that intake of alkenylbenzenes through consumption of parsley and dill based PFS is only of concern when these PFS are used for longer periods of time.

Taking into account this consideration it is concluded that the present study shows that use of parsley and dill based PFS is a concern especially for people who use those PFS for a long period of time.

Finally, it is important to acknowledge that the targeted sampling strategy applied to collect the parsley and dill based food supplements, was focused on preparations available on the Dutch market and available via internet. Given the results of the present study it would be of interest to

extent the risk assessment to include samples all over Europe. In addition, one might consider the sample types to be extended to include other parsley and dill based food products such as smoothies, detox, breath refreshers or any other sources of exposure. In a previous study, we already investigated dill and parsley based teas obtained on the Dutch market and online and showed that the MOE values obtained were generally < 10000 indicating a concern if the teas would be consumed on a daily basis over longer periods of time (Alajlouni et al., 2016a).

References

1. Al-Malahmeh, A. J., Al-Ajlouni, A. M., Wesseling, S., Soffers, A. E., Al-Subeihi, A., Kiwamoto, R., Vervoort, J. & Rietjens, I. M. C. M. 2016. Physiologically based kinetic modeling of the bioactivation of myristicin. *Archives of toxicology*.
2. Al-Subeihi, A. A., Spenklink, B., Punt, A., Boersma, M. G., van Bladeren, P. J. & Rietjens, I. M. C. M. 2012. Physiologically based kinetic modeling of bioactivation and detoxification of the alkenylbenzene methyleugenol in human as compared with rat. *Toxicology and applied pharmacology*, 260, 271-84.
3. Alajlouni, A. M., Al-Malahmeh, A. J., Isnaeni, F. N., Wesseling, S., Vervoort, J. & Rietjens, I. M. 2016a. Level of Alkenylbenzenes in Parsley and Dill Based Teas and Associated Risk Assessment Using the Margin of Exposure Approach. *Journal of agricultural and food chemistry*.
4. Alajlouni, A. M., Al Malahmeh, A. J., Kiwamoto, R., Wesseling, S., Soffers, A. E., Al-Subeihi, A. A., Vervoort, J. & Rietjens, I. M. C. M. 2016b. Mode of action based risk assessment of the botanical food-borne alkenylbenzene apiol from parsley using physiologically based kinetic (PBK) modelling and read-across from safrole. *Food Chem Toxicol*, 89, 138-50.
5. Bisset, N. G. 1994. *Herbal Drugs and Phytotherapeutics*, Medpharm Scientific Publishers.
6. Blumenthal, M. 1999. *The Complete German Commission E Monographs*. , American Botanical Council: Austin.
7. Borchert, P., Miller, J. A., Miller, E. C. & Shires, T. K. 1973. 1'-Hydroxysafrole, a proximate carcinogenic metabolite of safrole in the rat and mouse. *Cancer research*, 33, 590-600.
8. Cousyn, G., Dalfrà, S., Scarpa, B., Geelen, J., Anton, R., Serafini, M. & Delmulle, L. 2013. Project BELFRIT: Harmonizing the Use of Plants in Food Supplements in the European Union: Belgium, France and Italy - A first Step. *European Food and Feed Law Review*, 8, 187-196.
9. EFSA 2005. European Food Safety Authority. Opinion of the scientific committee on a request from EFSA related to a harmonised approach for risk assessment of substances which are both genotoxic and carcinogenic. *The EFSA Journal*, 282, 1-31.
10. EFSA 2009a. Advice on the EFSA guidance Document for the Safety Assessment of Botanicals and Botanical Preparations Intended for Use as Food Supplement, based on Real Case Study. *EFSA Journal*, 7, 280.
11. EFSA 2009b. Compendium of Botanicals That Have Been Reported to Contain Toxic, Ad-dictive, Psychotropic or Other Substances of Concern on Request of EFSA. *EFSA Journal*, 9, 1-100.
12. EFSA 2012. Compendium of botanicals reported to contain naturally occurring substances of possible concern for human health when used in food and food supplements. *EFSA Journal*, 10.
13. European Commission (EC) 2002. Regulation (EC) No 178/2002 of the European Parliament and of the Council of 26 January 2002 laying down the general principles and requirements of food law, establishing the European food safety authority and laying down procedures in matters of food safety.
14. European Commission (EC) 2008. Regulation (EC) No 1334/2008 of the European Parliament and of the Council of 16 December 2008 on flavourings and certain food ingredients with flavouring properties for use in and on foods and amending Council Regulation (EEC) No 1601/91, Regulations (EC) No 2232/96 and (EC) No 110/2008 and Directive 2000/13/EC.
15. FAO/WHO 2009. Safety evaluation of certain food additives. *Sixty-ninth meeting of the Joint FAO/WHO Expert Committee on Food Additives (JECFA)*, 642.
16. Felter, S. P., Conolly, R. B., Bercu, J. P., Bolger, P. M., Boobis, A. R., Bos, P. M., Carthew, P., Doerr, N. G., Goodman, J. I., Harrouk, W. A., Kirkland, D. J., Lau, S. S., Llewellyn, G. C., Preston, R. J., Schoeny, R., Schnatter, A. R., Tritscher, A., van Velsen, F. & Williams, G. M. 2011. A proposed

- framework for assessing risk from less-than-lifetime exposures to carcinogens. *Critical Reviews in Toxicology*, 41, 507-44.
17. Gursale, A., Dighe, V. & Parekh, G. 2010. Simultaneous quantitative determination of cinnamaldehyde and methyl eugenol from stem bark of *Cinnamomum zeylanicum* Blume using RP-HPLC. *Journal of Chromatographic Science*, 48, 59-62.
 18. Heamalatha, S., Swarnalatha, S., Divya, M., Gandhi Lakshmi, R., Ganga Devi, A. & Gomathi, E. 2011. Pharmacognostical, Pharmacological, Investigation on *Anethum Graveolens*. *Research Journal of Pharmaceutical, Biological and Chemical Sciences*, 2, 564-574.
 19. Huopalahti, R. & Linko, R. R. 1983. Composition and Content of Aroma Compounds in Dill, *Anethum-Graveolens* L, at 3 Different Growth-Stages. *Journal of Agricultural and Food Chemistry*, 31, 331-333.
 20. Kaur, G. J. & Arora, D. S. 2010. Bioactivation potential of *Anethum graveolens*. *Foeniculum* and *trachyspermum ammi* belonging to the family umbelliferar-current status. *medicinal plants research*, 4, 087-094.
 21. Kreydiyyeh, S. I. & Usta, J. 2002. Diuretic effect and mechanism of action of parsley. *Journal of Ethnopharmacology*, 79, 353-7.
 22. Leung, A. & Foster, S. 1996. *Encyclopedia of Common Natural Ingredients Used in Food, Drugs and Cosmetics*, New York, John Wiley & Sons.
 23. Martati, E., Boersma, M. G., Spenkeliink, A., Khadka, D. B., van Bladeren, P. J., Rietjens, I. M. C. M. & Punt, A. 2012. Physiologically based biokinetic (PBBK) modeling of safrole bioactivation and detoxification in humans as compared with rats. *Toxicological Sciences*
 24. Miller, E. C., Swanson, A. B., Phillips, D. H., Fletcher, T. L., Liem, A. & Miller, J. A. 1983. Structure-activity studies of the carcinogenicities in the mouse and rat of some naturally occurring and synthetic alkenylbenzene derivatives related to safrole and estragole. *Cancer research*, 43, 1124-34.
 25. Phillips, D. H., Reddy, M. V. & Randerath, K. 1984. 32P-post-labelling analysis of DNA adducts formed in the livers of animals treated with safrole, estragole and other naturally-occurring alkenylbenzenes. II. Newborn male B6C3F1 mice. *Carcinogenesis*, 5, 1623-8.
 26. Popovic, M., Kaurinovic, B., Jakovljevic, V., Mimica-Dukic, N. & Bursac, M. 2007. Effect of parsley (*Petroselinum crispum* (Mill.) Nym. ex A.W. Hill, Apiaceae) extracts on some biochemical parameters of oxidative stress in mice treated with CCl₄. *Phytother Res*, 21, 717-23.
 27. Punt, A., Paini, A., Boersma, M. G., Freidig, A. P., Delatour, T., Scholz, G., Schilter, B., van Bladeren, P. J. & Rietjens, I. M. C. M. 2009. Use of physiologically based biokinetic (PBBK) modeling to study estragole bioactivation and detoxification in humans as compared with male rats. *Toxicological sciences : an official journal of the Society of Toxicology*, 110, 255-69.
 28. Rainer, H. & L., R. R. 1983. Composition and Content of Aroma Compounds in Dill, *Anethum graveolens* L., at Three Different Growth Stages. *Journal of agricultural and food chemistry*, 31, 331-333.
 29. Randerath, K., Haglund, R. E., Phillips, D. H. & Reddy, M. V. 1984. 32P-post-labelling analysis of DNA adducts formed in the livers of animals treated with safrole, estragole and other naturally-occurring alkenylbenzenes. I. Adult female CD-1 mice. *Carcinogenesis*, 5, 1613-22.
 30. Rietjens, I. M. C. M., Slob, W., Galli, C. & Silano, V. 2008. Risk assessment of botanicals and botanical preparations intended for use in food and food supplements: emerging issues. *Toxicology letters*, 180, 131-6.
 31. Simon, J. E. & Quinn, J. 1988. Characterization of essential oil of parsley. *Journal of Agricultural and Food Chemistry*, 36, 467-472.

32. Smith, R. L., Adams, T. B., Doull, J., Feron, V. J., Goodman, J. I., Marnett, L. J., Portoghese, P. S., Waddell, W. J., Wagner, B. M., Rogers, A. E., Caldwell, J. & Sipes, I. G. 2002. Safety assessment of allylalkoxybenzene derivatives used as flavouring substances - methyl eugenol and estragole. *Food Chem Toxicol*, 40, 851-70.
33. Van den Berg, S. J., Punt, A., Soffers, A. E., Vervoort, J., Ngeleja, S., Spenkelink, B. & Rietjens, I. M. C. M. 2012. Physiologically based kinetic models for the alkenylbenzene elemicin in rat and human and possible implications for risk assessment. *Chemical research in toxicology*, 25, 2352-67.
34. van den Berg, S. J. P. L., Alhusainy, W., Restani, P. & Rietjens, I. M. C. M. 2014. Chemical analysis of estragole in fennel based teas and associated safety assessment using the Margin of Exposure (MOE) approach. *Food and Chemical Toxicology*, 65, 147-154.
35. Van den Berg, S. J. P. L., Restani, P., Boersma, M. G., Delmulle, L. & Rietjens, I. M. C. M. 2011. Levels of Genotoxic and Carcinogenic Compounds in Plant Food Supplements and Associated Risk Assessment. *Food and Nutrition Sciences*, 989-1010.
36. Vokk, R., Lougas, T., Mets, K. & Karvets, M. 2011. Dill (*Anethum graveolens* L.) and Parsley (*Petroselinum crispum* (Mill.) Fuss) from Estonia: Seasonal Differences in Essential Oil Composition. *Agronomy research*, 9, 515-520.
37. Wiseman, R. W., Fennell, T. R., Miller, J. A. & Miller, E. C. 1985. Further characterization of the DNA adducts formed by electrophilic esters of the hepatocarcinogens 1'-hydroxysafrole and 1'-hydroxyestragole in vitro and in mouse liver in vivo, including new adducts at C-8 and N-7 of guanine residues. *Cancer research*, 45, 3096-105.
38. Zhou, G. D., Moorthy, B., Bi, J., Donnelly, K. C. & Randerath, K. 2007. DNA adducts from alkoxyallylbenzene herb and spice constituents in cultured human (HepG2) cells. *Environ Mol Mutagen*, 48, 715-21.

Chapter 6

General discussion, future perspectives and conclusion

General discussion

Apiol and myristicin belong to the group of alkenylbenzenes. Alkenylbenzenes are found in several herbs and spices including for example parsley, dill, basil, tarragon, fennel and nutmeg (Kreydiyyeh and Usta, 2002, Semenov et al., 2007, Smith et al., 2002). Alkenylbenzenes also occur in the essential oils of these herbs and spices (Smith et al., 2002). Human exposure to apiol and myristicin mainly occurs through the consumption of parsley and dill containing preparations including teas, spices and/or plant food supplements (PFS).

The Estimated Daily Intake (EDI) of myristicin due to daily consumption of spices has been estimated to be in the range of 684 ug/person per day (Gavin et al., 2007).

The EDI of apiol compared to other alkenylbenzenes is considered to be low. In the USA, the mean intake of apiol from spice and spice oils is estimated to be 2.84 ug/person per day while for other alkenylbenzenes like safrole, estragole, methyleugenol and myristicin, exposure may be at least 10 times higher (Gavin et al., 2007).

The alkenylbenzenes including apiol and myristicin have a similar molecular structure consisting of an allylbenzene nucleus containing one or more alkoxy ring substituents. Because of this structural similarity these compounds share similar metabolism, mode of action and biological effects (WHO, 2009, Van den Berg et al., 2012). Safrole, estragole and methyleugenol were shown to induce liver tumors at high dose levels in rodents via a metabolic pathway that includes formation of DNA adducts (Boberg et al., 1986, Boberg et al., 1983, Phillips et al., 1984, Randerath et al., 1984, Wiseman et al., 1985, Wislocki et al., 1976, Miller et al., 1983). For myristicin and apiol, long term carcinogenicity studies are not available (WHO, 2009), but in the present thesis, based on the similarities in the molecular structure and metabolic pathways between these two compounds and safrole, a mode of action based approach for their risk assessment was undertaken using

physiologically based kinetic (PBK) modelling and read-across from safrole for which adequate rodent tumor data are available.

PBK models are models established based on different parameters including physiological parameters, physico-chemical parameters, and metabolic parameters. The models describe the absorption, distribution, metabolism and excretion (ADME) of a chemical of interest (Krewski et al., 1994, Chiu et al., 2007, Rietjens et al., 2011). The use of PBK models allows the study of possible time and dose-dependent variations in metabolism, the prediction of the concentrations of the chemical and its metabolites within tissues and blood (Rietjens et al., 2011), and the study of interspecies differences through use of parameters of the species of interest (Andersen and Krishnan, 1994). In the present thesis PBK models were used to support a read-across from a compound for which adequate tumor data are available to compounds for which such data are absent.

The currently preferred risk assessment approach used to assess the risk of exposure to compounds that are both genotoxic and carcinogenic is the so-called margin of exposure (MOE) approach (EFSA, 2005). The MOE is calculated as the ratio between a dose level derived from human epidemiological data or from in vivo carcinogenicity data obtained in experimental animals, and the EDI. The preferred point of departure derived from the in vivo data to calculate the MOE is the lower confidence limit of the dose level that results in 10% extra cancer incidence above background levels, the so-called BMDL₁₀ (O'Brien et al., 2006, EFSA, 2005). BMDL₁₀ values can be defined for estragole, methyleugenol and safrole, since tumor data from rodent bioassays are available, while for the two related alkenylbenzenes, apiol and myristicin, such data do not exist so BMDL₁₀ values cannot be derived from experimental tumor data.

The present PhD project aimed to establish a mode of action based risk assessment of exposure to low doses of apiol and myristicin by using PBK modelling based read-across from safrole and to use

the results obtained to perform a risk assessment of consumption of PFS and teas containing parsley and dill.

In chapter 2 a PBK model for apiol was developed for rat and human in order to facilitate read-across from the related alkenylbenzene safrole. The models were developed based on *in vitro* metabolic parameters determined using relevant tissue fractions, *in silico* derived partition coefficients, and physiological parameters derived from the literature. The models were based on the models previously developed for the related alkenylbenzene safrole (Martati et al., 2012) and consisted of six compartments including liver as metabolizing compartment, and separate compartments for fat, arterial blood, venous blood, richly perfused and slowly perfused tissues. With the model obtained the relative extent of bioactivation and detoxification of apiol at different oral doses was examined. At low doses, formation of 4-allyl-3,6-dimethoxy benzene-1,2-diol (ADD) and 2,3-dihydroxyapiol (DHA) leading to detoxification appeared to be the major metabolic pathways, occurring in the liver. At high doses, the rat model revealed a relative increase in the formation percentage of the proximate carcinogenic metabolite 1-hydroxyapiol from 4% to about 7% of the dose at low and high dose levels respectively, occurring in the liver. This relative increase in formation of 1-hydroxyapiol leads to a relative increase in formation of 1-hydroxyapiol glucuronide, 1-oxoapiol, and 1-sulfooxyapiol with increasing dose levels, the latter metabolite being the ultimate carcinogenic metabolite of apiol. These results indicate that the relative importance of different metabolic pathways of apiol may vary in a dose-dependent way, leading to a relative increase in bioactivation of apiol at higher doses. In rat liver the percentage of the dose converted to the ultimate carcinogenic metabolite 1-sulfooxyapiol was predicted to increase from 0.003% of the dose at 0.05 mg/kg bw/day to 0.005% of the dose at a dose level of 300 mg/kg bw/day. This reflects a change of only 1.67-fold over the dose range of interest, which is expected to

only marginally influence the cancer risk estimate as compared to the effect of increasing the dose itself from 0.05 to 300 mg/kg bw/day. The human model revealed a slight decrease in the relative formation of the proximate carcinogenic metabolite 1 - hydroxyapiol from 6.7% to about 6.3% of the dose at low and high dose levels respectively, occurring in the liver. The formation of the ultimate carcinogen 1 -sulfoxyapiol amounted to 0.036% to 0.035% of the dose at low and high dose levels respectively. By comparing the PBK model based predicted 1 -sulfoxy metabolite formation of apiol with that for safrole, it appeared that at similar dose levels the formation of the 1 -sulfoxy metabolite for apiol is predicted to be about 3-fold lower than for safrole in rat liver and 2- fold lower in human liver. Based on these PBK modelling results, assuming the same mode of action for these two compounds, one could use the BMDL₁₀ for liver tumor formation in rat by safrole for risk assessment of the related compound apiol making a correction for the expected 3-fold lower formation of the ultimate carcinogenic 1 -sulfoxy metabolite at similar dose levels. Thus the BMDL₁₀ of safrole which amounts to 1.9-5.1 mg/kg bw per day (Van den Berg et al., 2011) was multiplied by factor of 3 resulting in a BMDL₁₀ of 5.7-15.3 mg/kg bw per day. Using the EDI of apiol resulting from intake from spice and spice oil in the USA that amounts to 4×10^{-5} mg/kg bw per day (Gavin et al., 2007), and a BMDL₁₀ of 5.7-15.3 mg/kg bw per day, the MOE would amount to 140000 -385000. This value is > 10000 indicating a low priority for risk management.

In chapter 3 a PBK model for myristicin was developed in rat and human in order to facilitate risk assessment based on read-across from the related alkenylbenzene safrole. The models were developed using the same parameters and compartments as for the apiol model in Chapter 2. In incubations of myristicin with rat and human liver microsomes the formed metabolites were 2,3 - dihydroxymyristicin (DHM), 3 -hydroxymyristicin (3HM), 1 -hydroxymyristicin (HM), and 5-allyl-2,3-dihydroxyanisole (DHA). At high doses, the rat and human model revealed a relative increase in

the formation of the proximate carcinogenic metabolite 1 - hydroxymyristicin. This relative increase in formation of 1-hydroxymyristicin leads to a relative increase in formation of 1 - hydroxymyristicin glucuronide, 1 -oxomyristicin, and 1 -sulfooxymyristicin with increasing dose levels, the latter metabolite being the ultimate carcinogenic metabolite of myristicin. As with apiol these results indicate that the relative importance of different metabolic pathways of myristicin may vary in a dose-dependent way, leading to a relative increase in bioactivation of myristicin at higher doses. In rat liver, the percentage of the dose converted to the ultimate carcinogenic metabolite 1 - sulfooxymyristicin increases from 0.015% of the dose at 0.05 mg/kg bw/day to 0.027% of the dose at a dose level of 300 mg/kg bw/day. This reflects a change of only 1.8-fold over the dose range of interest, which is a change that would be expected to only marginally influence the cancer risk estimate as compared to the effect of increasing the dose itself from 0.05 to 300 mg/kg bw/day. Also the human model revealed an increase in the formation percentage of the proximate carcinogenic metabolite 1 - hydroxymyristicin from 6.5% to about 8.0% of the dose at low and high dose levels respectively, occurring in the liver. The formation of the ultimate carcinogen 1 -sulfooxymyristicin amounted to 0.047% of the dose at 0.05 mg/kg bw/day and to 0.059% of the dose at a dose level of 300 mg/kg bw/day. By comparing the values predicted by the myristicin PBK models with values predicted for safrole by the safrole PBK models at similar dose levels, the formation of the 1 - sulfoxy metabolite is predicted to be about 2-fold lower for myristicin than for safrole in rat liver and almost the same in human liver. Based on this it can be concluded that at dose levels in the range of BMDL₁₀ values, the formation of the 1 -sulfoxy metabolites of myristicin in liver is comparable to that of the 1 -sulfoxy metabolites of the structurally related safrole. Based on that, and assuming the same mode of action for these two compounds, the PBK modelling results can support the use of the BMDL₁₀ values for tumor formation by safrole (1.9-5.1 mg/kg bw per day) for risk assessment of the

related compound myristicin. Based on the theoretical EDI of myristicin from spice and spice oil in USA that amounts to 0.0019 mg/kg bw per day, and a BMDL₁₀ of 1.9-5.1 mg/kg bw per day, the MOE would amount to 1000-2700, indicating a priority for risk management.

In chapter 4 a risk assessment of parsley and dill based teas that contain alkenylbenzenes was performed using the BMDL₁₀ values obtained in chapter 2 and 3 for apiol and myristicin. To this end, parsley and dill based tea samples were collected from the local Dutch market and via internet. To quantify the possible maximum concentrations of the alkenylbenzenes, the samples were extracted by applying a methanol extraction followed by alkenylbenzene quantification using UPLC. To obtain the EDI of the alkenylbenzenes resulting from use of the teas, the concentration of the alkenylbenzenes was also quantified in a hot water extract and the values thus obtained were corrected by a factor that accounted for the amount of tea likely to be used to make a cup of tea. Chemical analysis of the alkenylbenzenes present in the teas and their hot water extracts revealed the presence of more than one alkenylbenzene within most of the samples. Because of that a risk assessment for combined exposure to the alkenylbenzenes was also performed. Because the molecular structures and mode of action of these alkenylbenzenes are similar (JECFA, 2009), a dose addition approach can be used to calculate the combined exposure (van den Berg et al., 2006). For this combined risk assessment, the EDIs were calculated assuming equal potency of the alkenylbenzenes and also based on use of the so-called Toxic Equivalency (TEQ) approach. The Toxic Equivalency Factors (TEFs) for the different alkenylbenzenes were defined using safrole as the reference compound (TEF=1). The TEF values for the other compounds were defined using different sets of literature data, also including the PBK model based predictions for formation of the ultimate carcinogenic 1-sulfoxy metabolites and the BMDL₁₀ values obtained by read-across from safrole as defined for apiol and myristicin in Chapter 2 and Chapter 3 of the thesis. Risk assessment

for the exposure to the alkenylbenzenes via use of the selected teas was applied using the MOE approach. MOE values were calculated in three different ways; first the MOE values were calculated for the individual alkenylbenzenes using their respective BMDL₁₀ values amounting to respectively 5.7 mg/kg bw for apiol as obtained in Chapter 2 of the thesis (Alajlouni et al., 2016), 1.9 mg/kg bw for myristicin as obtained in Chapter 3 of the thesis (Al-Malahmeh et al., 2016), and 3.3 mg/kg bw for estragole and 15.3 mg/kg bw for methyleugenol (Van den Berg et al., 2011). Then the MOE values were calculated using a combined exposure assessment assuming equal potency of all alkenylbenzenes and using the BMDL₁₀ for the major alkenylbenzene in each mixture. Finally MOE values were calculated based on the TEQ approach calculating the combined exposure in safrole equivalents and using the BMDL₁₀ of safrole. MOE values obtained were generally < 10000, indicating a priority for risk management, especially for people who frequently drink large quantities of these herbal teas. Drinking of these herbal teas for shorter periods instead of during a whole lifetime will increase the MOE values above 10000 indicating a low priority for risk management.

Chapter 5 describes a risk assessment of consumption of parsley and dill based PFS. The PFS samples were collected from the local Dutch market and via internet. The PFS sample selection was based on the presence of dill or parsley within the PFS. The samples were extracted by methanol and analyzed using UPLC. The EDIs of the alkenylbenzenes were quantified and corrected based on the recommended dose of the PFS as indicated on the labels of the preparations. The results showed that most samples contain more than one alkenylbenzene, mainly apiol and myristicin. This is in line with the fact that a targeted sampling was applied collecting samples containing dill and/or parsley known to contain especially these alkenylbenzenes (Simon and Quinn, 1988, Vokk et al., 2011). As for the tea samples in Chapter 4 a combined exposure to alkenylbenzenes was included in the assessment. The EDI and MOE values were calculated based on the same approach used for tea

samples in Chapter 4. The results revealed that the MOE values of the PFS samples under study obtained using all three methods for risk assessment resulted in MOE values that were generally < 10000, indicating a need for risk management if the PFS would be consumed on a daily basis during a whole lifetime. However, since intake of PFS is not likely to occur daily during a whole lifetime, but rather for a short period of time, Haber's rule ($k=C \times T$ where (k) is the toxic outcome, (C) is the concentration (or dose) of the toxic chemical and T is the time of exposure), was applied to obtain insight in the consequences for the associated risks (Felter et al., 2011). Assuming shorter periods of exposure of for example one or two week or a month, using Haber's rule to correct for this shorter exposure, resulted in MOE values generally > 10000 indicating low priority for risk management. It was concluded that risks associated to use of these PFS would be negligible provided intake is limited to only a few weeks during a lifetime.

Future perspectives:

This thesis studied the risk assessment of parsley and dill based teas and PFS products that contain especially the alkenylbenzenes apiol and myristicin. To enable this risk assessment first read-across from tumor data on safrole was performed using PBK model based analysis. Previously, several studies focused on the adverse effects of safrole, estragole and methyleugenol, alkenylbenzenes that are known to be carcinogenic and genotoxic, but there are only a few studies focusing on adverse effects of apiol and myristicin. Therefore, this thesis focused on these two alkenylbenzenes. Future research on these food borne-compounds and their structural analogues may consider including some additional aspects that are discussed hereafter.

Improving PBK models for extrapolation in risk assessment of botanicals preparations.

The MOE approach needs carcinogenicity data to define the BMDL₁₀, whereas such data may be not present for many botanical ingredients. So, Chapter 2 and Chapter 3 present the development of a mode of action based PBK model approach to perform a read-across from a compound for which rodent tumor data are available (safrole) to compounds for which such data are missing (apiol and myristicin). Van den Berg et al. studied the risk assessment of the alkenylbenzene elemicin by using PBK model based read-across from estragole and methyleugenol (Van den Berg et al., 2012). The developed PBK models allow studying effects at low dose levels relevant for the human situation. This implies that the PBK models can study the (non-) linear effects at low doses that cannot be detected in animal experiments since they use high dose levels. A major advantage of the PBK models is that they allow quantification of the dose-dependent formation of the unstable reactive carcinogenic 1-sulfoxy metabolite thereby facilitating the read-across based on predictions of relative bioactivation. But still there are limitations for this PBK model based approach that may provide topics for future research. One disadvantage is the fact that PBK models need to be described for each single compound and that definition of these models is time consuming, because they require a large set of parameters. Although the time and costs of developing the PBK models for bioactivation and detoxification of genotoxic carcinogens is small compared to time and costs associated with performing a two year in vivo rodent carcinogenicity study, it may be of use to work on the development of generic PBK models. So, development of generic PBK models for a group of compounds will be more efficient for future risk assessment on genotoxic carcinogens for which rodent tumor data are not available and will save time and costs (Bessemers et al., 2014). The sensitivity analyses presented in this thesis could be of help to define the most influential parameters that should be included in such generic PBK models. A next step would be to take such models,

developed now for the alkenylbenzenes, to other botanical ingredients that are genotoxic and carcinogenic such as for example pyrrolizidine alkaloids for which rodent tumor data are also not widely available (Chen et al., 2017).

Extending of PBK models to Physiologically Based Dynamic (PBD) models

In Chapter 2 and Chapter 3 PBK models for apiol and myristicin were developed enabling prediction of bioactivation and detoxification of apiol and myristicin. However, the ultimate adverse effect, liver tumor induction, is a multistep process which depends not only on kinetic but also on dynamic processes that include in addition to bioactivation also DNA-adduct formation, DNA repair, mutation modulation, gene and protein expression and tumor formation. Therefore, for an even better read-across, these dynamic processes should be considered as well and might be describes in so-called physiologically based dynamic (PBD) models. Development of PBD models needs the description of dynamic characteristics in addition to the kinetic characteristics used in a PBK model. This can be achieved by extending the PBK models of apiol and myristicin to PBD models to predict the tumor incidences occurring at low realistic intake levels. A first step in this process would be extending of the PBK models to PBD models that describe the dose dependent formation of DNA adducts. Such PBD models have been described before for estragole and used to evaluate the interindividual human variation in bioactivation and DNA adduct formation resulting from estragole exposure (Paini et al., 2010, Punt et al., 2016). Another example is the use of physiologically based kinetic/dynamic (PBK/D) modelling to compare dose-dependent DNA adduct formation by cinnamaldehyde and 18 acyclic food-borne α , ω -unsaturated aldehydes showing that at doses relevant for human dietary exposure there was no concern for DNA adduct formation (Kiwamoto et al., 2016). So developing valid generic PBK models and extending these models to PBD models for

compounds of interest may help in developing even better approaches for read-across in risk assessment of genotoxic carcinogens. It is of interest to note that developing such PBD models, predicting in vivo DNA adduct formation by adding data on concentration dependent DNA adduct formation in primary hepatocytes to the PBK/D model, will at the same time take into account DNA adduct stability and DNA repair. DNA adduct stability and repair may turn out to be important factors in determining the ultimate mutagenic and carcinogenic potential of the alkenylbenzenes.

Cut off value for the MOE based risk assessment; Compound specific uncertainty factors.

Many approaches -qualitative and quantitative- can be used to assess the risk of genotoxic carcinogenic compounds. Data used in these approaches are mainly obtained from rodent bioassays performed at high dose levels. This implies that extrapolation to lower exposure levels is required in order to judge the risks at realistic human daily exposure levels. Several mathematical models have been proposed to perform this high to low dose extrapolation, with linear extrapolation being the simplest form. However, it is not known if and/or to what extent these mathematical models reflect the underlying biological processes. As a result the extrapolation from high dose to low dose exposure has been debated (Barlow et al., 2006, EFSA, 2005). In addition linear extrapolation of tumor data from animal studies to the human situation does not take into account species differences. Because of that, as an alternative to linear extrapolation, the MOE approach was developed to be used for risk assessment of compounds that are both carcinogenic and genotoxic (EFSA, 2005). In the present thesis, this MOE approach was the method of choice for the risk assessment of consumption of different herbal teas and PFS. The MOE approach uses a default cut-off value of 10000; above this value an exposure is considered as a low priority for risk management actions (EFSA, 2005). The value of 10000 was considered to include all possible uncertainties that may be involved and affect the risk assessment. The value of 10000 includes a factor of 100 for kinetic and

dynamic differences between species and within humans, a factor of 10 that presents the variability in cell cycle control and DNA repair within humans, and a factor of 10 that takes into account that the BMDL₁₀ represents a 10% Bench Mark Response (BMR) (EFSA, 2005, O'Brien et al., 2006).

The results of the present thesis show some insight into whether for apiol and myristicin the interspecies factor of 10, including a factor of 4 for differences in toxicokinetics and a factor 2.5 for differences in toxicodynamics (IPCS, 2010) would be adequate. The PBK model based predictions for the formation of the ultimate carcinogen for apiol in rat and human showed that at low dose in human the formation of the ultimate carcinogenic metabolite is 15 times higher than in rat, while for myristicin the difference was 4-fold. This suggests that a factor of 4 to take into account species differences in toxicokinetics may be sufficient for myristicin but not for apiol. There is no formal way to include this consideration in the MOE value used as the cut-off in making a risk management decision, but if the factor 4 for toxicokinetics would be increased to 15, the default cut-off value may increase accordingly and more samples could result in MOE values that might be of concern. This result also illustrates how these PBK model based results may assist the development of compound specific uncertainty factors and other default values in risk assessment.

Correction for less-than lifetime exposure.

The MOE is based on BMDL₁₀ data that are obtained in long term rodent carcinogenicity studies, and using EDI values also assuming lifetime exposure. However, exposure to the compounds under study as indicated in Chapters 4 and 5 may be for only a few weeks and not for a lifetime. In the present thesis, a framework was applied for assessing the risk to human health resulting from short time exposures that was proposed by Felter et al. for assessing the risk from less-than lifetime exposures to carcinogens (Felter et al., 2011). This was done by using the principle of Haber's Rule.

Haber's Rule states that $k=C \times T$ where (k) is the toxic outcome, (C) is the concentration (or dose) of the toxic chemical and T is the time of exposure. Chapter 5 of this thesis describes the application of Haber's Rule in the MOE approach to assess the potential risk for exposure to alkenylbenzenes from use of PFS for short periods of time instead of during a whole lifetime. Assuming a lifetime exposure to parsley and dill based PFS, MOE values for all samples were below 10000 indicating a priority for risk management, but when applying Haber's Rule and assuming consumption of these PFS for 4 weeks, all MOE values would be above 10000 suggesting a low priority for risk management. Use of Haber's Rule for products consumed for shorter periods of time may prevent overestimation of the actual risk to human health that may occur if MOE values are calculated assuming lifetime exposure. Applying Haber's Rule however is not a generally accepted approach when using the MOE for risk assessment of exposure to genotoxic carcinogens. Felter et al. (Felter et al., 2011) were the first to propose use of Haber's Rule for assessing the risk from less-than lifetime exposure to carcinogens. It is important to acknowledge the assumptions underlying this methodology, which include the fact that chemical-specific carcinogenicity data should be available and that the data support a linear dose-response relationship (Felter et al., 2011). Whether such a linear dose-response relationship would apply to the dose dependent induction of liver tumors by the alkenylbenzenes remains to be established and is actually a matter for considerable debate in the field of risk assessment of genotoxic carcinogens that is not yet resolved (EFSA, 2005). The linear dose-response relationship may depend on the mode of action underlying the carcinogenicity. The formation of the 1-sulfoxy metabolite and subsequently formed DNA adducts play an important role in the alkenylbenzene-induced carcinogenicity. In previous PBK based studies on detoxification and bioactivation of alkenylbenzenes it was shown that the bioactivation of alkenylbenzenes to their ultimate carcinogenic 1-sulfoxy metabolites is linear with the dose, from dose levels as low as levels

of realistic human dietary intake up to dose levels as high as the BMDL₁₀ inducing liver tumors in rodent bioassays (Rietjens et al., 2010, Punt et al., 2009, Al-Subeihi et al., 2012). Whether this linearity in alkenylbenzene bioactivation will also be reflected in linearity of mutagenicity remains to be established since the mutagenic potential of alkenylbenzene 1-sulfoxy metabolites has not been extensively quantified so far. Herrmann et al. (2012) investigated the mutagenic potential of sulfate conjugates of 1-hydroxymethyleugenol and showed that different isomeric hydroxylated metabolites of methyleugenol are mutagenic in an Ames test using *Salmonella typhimurium* TA100 strains expressing different sulfotransferase enzymes (Herrmann et al., 2012). This suggests that the formation of the 1-sulfoxy metabolite and subsequently formed DNA adducts play an important role in the alkenylbenzene-induced carcinogenicity, and that knowledge of the levels of DNA adduct formation in human livers at relevant dietary intake levels would be of use to facilitate risk assessment for low-dose alkenylbenzenes intake. In this respect it is of interest to note that Herrmann et al. 2013 reported formation of methyleugenol DNA adducts in 29 out of 30 human liver samples at levels that amounted for the maximal and median levels to 37 and 13 adducts per 10⁸ nucleosides respectively (Herrmann et al., 2013). The results of the present thesis imply that it would be of interest to look for also other alkenylbenzene DNA adducts in human liver samples. This possible formation of DNA adducts in human liver may also be investigated by combining the PBK models with data on alkenylbenzene concentration-dependent DNA adduct formation in isolated human hepatocytes to build PBD models as done for rat hepatocytes exposed to estragole previously (Paini et al., 2010). This study also revealed that not only bioactivation to the reactive 1-sulfoxy metabolite but also DNA adduct formation in rat liver was linear with the dose of estragole (Paini et al., 2012). Such studies in primary hepatocytes are likely to also account for possible repair and stability of the alkenylbenzene adducts and would thus provide insight in whether formation of

adducts even during a short period, could have irreversible effects and thus be deleterious, or whether they are likely to be repaired, thereby decreasing the risk. However, given that linear extrapolation from tumor data at high dose level to low dose level is generally considered the worst-case approach for this extrapolation (EFSA, 2005, COC, 2012, Edler et al., 2002) it may equally well be considered a conservative approach for extrapolation from high to low duration of exposure.

Banding of the MOE cut-off value

The results of the present thesis revealed that MOE values obtained for the different teas and PFS may vary orders of magnitude, and that MOE values lower than 10000 may vary from being close to 10000 to less than 1000 or even less than 100. At the current state-of-the-art there is no proposal on how to deal with an MOE of just below or just above 10000. So if use of a preparation results in an MOE value of 10500 its use would be a low priority for risk management while a sample with an MOE value of 9500 would be a high priority for risk management. In addition, there is no difference in the conclusion for a preparation with an MOE of just below 10000 and one that is close to 1 so for which exposure would be in the range of the doses that induce tumor formation in experimental animals. Discriminating between these situations to a further extent by banding the MOE cut-off value might help the risk managers in better defining risk management actions. The Committee of Carcinogenicity of chemicals in food, consumer products and the environment (COC) proposed a system of MOE banding as follow: MOE <10,000: May be a concern, MOE 10000-1000000: Unlikely to be a concern, MOE >1000000 Highly unlikely to be a concern (COC, 2012). But still this proposal groups all values below the 10000. One could consider further banding of MOE cut-off values that are < 10000 as follows: MOE < 1000: Very high concern, MOE = 1000-5000: High concern, MOE = 5000- 10000: Moderate concern.

All together it is concluded that an internationally scientific framework to assess and refine the MOE approach, taking into account shorter than life time exposures and banding of MOE cut-off values would be of use, and improve the potential of the MOE approach for risk assessment.

Combined exposure to alkenylbenzenes

In the present study chemical analysis revealed that the parsley and dill based products can contain more than one alkenylbenzene. Therefore combined exposure to these alkenylbenzenes was taken into account in the risk assessment (Meek et al., 2011, EFSA, 2013, Pose-Juan et al., 2016). In this combined risk assessment, equal potencies but also different potency of the different alkenylbenzenes was considered, the latter resulting in definition of so-called TEF values. In an ideal situation such TEF values should be based on the endpoint under consideration, i.e. tumor formation. The carcinogenic potency of alkenylbenzenes was shown in previous studies (Miller et al., 1983, Phillips et al., 1984, Randerath et al., 1984, Zhou et al., 2007), but these studies focused on only a few of the alkenylbenzenes under study and did not provide data for myristicin and apiol that could be compared to those of safrole, estragole and myristicin to set TEF values. Therefore in the present thesis TEF values were determined using an alternative approach using BMDL₁₀ values obtained via read-across from safrole but also surrogate endpoints including relative formation of the ultimate carcinogenic 1-sulfoxy metabolite and DNA adduct formation upon in vivo exposure. Use of such surrogate endpoints for definition of TEF values is in line with what has been done for definition of such relative potencies for other groups of chemicals including for example pyrrolizidine alkaloids (Merz and Schrenk, 2016) for which interim relative potency factors were defined based on available literature data on in vitro cytotoxicity, genotoxicity in *Drosophila*, and acute toxicity in rodents (LD50) (Merz and Schrenk, 2016). In another study, Botana et al. calculated the relative potency

factors for a group of marine biotoxins, the so-called diarrhetic shellfish toxins, indicating a priority for the type of data to be used when defining these potencies: 1) data from human intoxications, 2) acute toxicity data upon oral administration to animals, 3) acute toxicity data upon intraperitoneal administration to animals and 4) in vitro data, indicating that use of other data than the ultimate endpoint relevant for human risk assessment would be feasible (Botana et al., 2017). Another example can be found in the TEF values derived for dioxins. Van den berg et al. (van den Berg et al., 2006) defined TEF values for dioxin like compounds based primarily on in vivo experiments but indicated that if in vivo data were limited, data from the in vitro experiments can be used as long as there is a structural relationship between the compounds, and they have the same mode of action and adverse response.

In the present thesis we defined TEF values for the different alkenylbenzene compounds based on the average of three methods; DNA adduct formation in CD-1 mice (Randerath et al., 1984), formation of the ultimate carcinogenic 1-sulfoxy metabolite as predicted by the PBK models (Alajlouni et al., 2016, Al-Malahmeh et al., 2016, Van den Berg et al., 2012, Al-Subeihi et al., 2012, Punt et al., 2009, Martati et al., 2012) and BMDL₁₀ values for tumor formation in rodent bioassays (Alajlouni et al., 2016, Al-Malahmeh et al., 2016, Van den Berg et al., 2012). The first method represents the potency of the compounds to bind to DNA while the second one presents the formation of the ultimate carcinogenic metabolite at levels representing human intake, while the last method is based on rodent carcinogenicity data from long term exposure with high dose and/or read-across from these data. Thus, we used some surrogate endpoints in addition to an endpoint that really refers to potency for tumor formation, the BMDL₁₀. However, it should be acknowledged that by using read-across from tumor data on safrole, the BMDL₁₀ values for apiol and myristicin were actually also in part surrogate endpoints that were not based on experimental tumor data for the

compounds under consideration. On the other hand, the approach reveals a useful application of PBK modelling in defining differences in relative potencies for tumor formation without the need for further animal testing and thus contributing to the 3Rs in safety testing.

Matrix effects in risk assessment of botanicals products

In the present thesis, PBK models that were used to quantify the formation of the ultimate carcinogenic metabolites were defined for pure compounds. It is of interest to note that teas and PFS appeared to contain one or more botanicals and their extracts may represent a complex mixture of bioactive compounds that may interact and thereby increase or decrease the toxicity of the compound under study. Schilter et al. described that the use of single pure compounds might not represent a sufficient starting point for risk assessment of botanicals or botanical preparations, because other compounds found within the matrix may affect the kinetic or dynamic processes of the compound of interest (Schilter et al., 2003). For example, the bioavailability of β -carotene when consumed within a matrix of mixed vegetables is about 14% of the bioavailability observed when it is consumed as pure β -carotene (van het Hof et al., 1999). Jeurissen et al. 2008 studied the effect of the matrix from basil on estragole bioactivation and DNA adduct formation by using a methanolic basil extract and found that co-incubation with the extract reduced the level of estragole bioactivation and DNA adduct formation both in incubations with isolated DNA as well as in HepG2 human hepatoma cells (Jeurissen et al., 2008). Subsequently, Alhusainy et al. identified the responsible compound that caused the decrease of estragole bioactivation as the flavonoid nevadensin (Alhusainy et al., 2010). In similar studies it was shown that safrole bioactivation was inhibited by malabaricone C a compound present in mace together with safrole (Martati et al., 2014). The inhibition of bioactivation of estragole and safrole was shown to mainly occur through

inhibition of sulfotransferase mediated bioactivation of these compounds and could be even demonstrated to occur in an in vivo rodent bioassays using relatively high dose levels (Alhusainy et al., 2010, Martati et al., 2014). However, subsequent PBK modelling of the effect revealed that at low doses that represent realistic human intake, the inhibition of the bioactivation as described above may not occur and the matrix effect on the bioactivation of the compound of interest may be absent because at such low dose levels the concentrations of the inhibitors in the liver may not reach the K_i values required for SULT inhibition (Rietjens et al., 2015). Based on this example it appears that for some compounds use of a pure compound will give a better starting point for the risk assessment at low dose levels, than using the whole extract. So the study of matrix effects should be done on a case-by-case basis using approaches that take the mode of action and the dose dependency of the interaction into account (Rietjens et al., 2015). Obviously, many compounds present in the matrix of botanicals and botanical preparations may affect the absorption, distribution, metabolism and/or excretion of botanical ingredients of interest thereby causing deviations as compared to what would be observed when testing the pure compound. Given the complexity of such matrix effects the EFSA working group already has indicated that such matrix effects should be studied on a case by case basis (EFSA, 2013). Development of mode of action based PBK analysis of such possible matrix effects can help to investigate whether interactions observed in rodent bioassays at high dose levels may still be valid at realistic human exposure levels.

Botanical products quality control

A final issue to consider that may affect the risk assessment of the different herbal products are the data about the finished product and the quality of the botanical used to produce the product and how to document such information correctly on the product label (Walker, 2004). Since the herbal extracts contain many compounds that may not all have a biological activity it is not possible to name all these compounds on the product label. Instead it would be of use to at least list the active ingredients and their actual levels in the preparation of interest. This would be of use for both the beneficial ingredients as well as for the ingredients of concern, the first to not mislead the consumer and the latter to guarantee the safety of the proposed use and levels of intake. Levels of such marker ingredients would at the same time be of use for quality control of the respective preparation and at least reflect adequate quality during the whole production process, including the growing conditions, storage conditions, details of the extraction procedure, type of final products and any other herbs used during the production (Sanzini et al., 2011). Applying of such a quality control and labeling of levels of ingredients of concern will aid the risk assessors and facilitate the risk assessment of these products. This would also require validation of analytical methods and reference standards to identify the active compounds. Adequate chemical characterization of the botanicals and botanical preparations would also prevent botanical adulterants and contaminants (Swanson, 2002). Applying of a good quality control during botanical product preparation with establishment of validated analytical methods to identify the bioactive compound within these products will facilitate risk assessment and quality control of the final product. Based on that integrated monitoring plans should be applied from farming to marketing of botanical products to make sure that all will be performed under good quality measures and that labeling includes all the required information.

Conclusion

This thesis examined the risk assessment of parsley and dill based products that contain alkenylbenzenes using read-across through building of PBK models for two alkenylbenzenes (apiol and myristicin). This facilitated the estimation of a BMDL₁₀ for apiol and myristicin without the need for a rodent bioassay. These BMDL₁₀ values were subsequently of use in the risk assessment of exposure to these two alkenylbenzenes via use of parsley and dill based teas and PFS. The overall conclusion of the risk assessment of consumption of parsley and dill based teas and PFS revealed that daily lifetime consumption of most of these products would be a priority for risk management. On the other hand, exposure to those products for shorter periods of time will increase the MOE values to levels > 100000 indicating a low priority for risk management. Thus, it can be concluded that the risks associated with the use of these teas and PFS would be limited, provided intake is for only a few weeks during a lifetime. The thesis also provided new proofs of principle of how PBK model based approaches can facilitate novel non-animal based studies in risk assessment contributing to the development of alternatives for animal testing.

References

1. Al-Malahmeh, A. J., Al-Ajlouni, A. M., Wesseling, S., Soffers, A. E., Al-Subeihi, A., Kiwamoto, R., Vervoort, J. & Rietjens, I. M. C. M. 2016. Physiologically based kinetic modeling of the bioactivation of myristicin. *Archives of toxicology*, 91, 713-734.
2. Al-Subeihi, A. A., Spenkelink, B., Punt, A., Boersma, M. G., van Bladeren, P. J. & Rietjens, I. M. C. M. 2012. Physiologically based kinetic modeling of bioactivation and detoxification of the alkenylbenzene methyleugenol in human as compared with rat. *Toxicology and Applied Pharmacology*, 260, 271-84.
3. Alajlouni, A. M., Al Malahmeh, A. J., Kiwamoto, R., Wesseling, S., Soffers, A. E., Al-Subeihi, A. A., Vervoort, J. & Rietjens, I. M. C. M. 2016. Mode of action based risk assessment of the botanical food-borne alkenylbenzene apiol from parsley using physiologically based kinetic (PBK) modelling and read-across from safrole. *Food Chem Toxicol*, 89, 138-50.
4. Alhusainy, W., Paini, A., Punt, A., Louisse, J., Spenkelink, A., Vervoort, J., Delatour, T., Scholz, G., Schilter, B., Adams, T., van Bladeren, P. J. & Rietjens, I. M. C. M. 2010. Identification of nevadensin as an important herb-based constituent inhibiting estragole bioactivation and physiology-based biokinetic modeling of its possible in vivo effect. *Toxicology and Applied Pharmacology*, 245, 179-190.
5. Andersen, M. E. & Krishnan, K. 1994. Physiologically based pharmacokinetics and cancer risk assessment. *Environmental Health Perspectives*, 102 Suppl 1, 103-8.
6. Barlow, S., Renwick, A. G., Kleiner, J., Bridges, J. W., Busk, L., Dybing, E., Edler, L., Eisenbrand, G., Fink-Gremmels, J., Knaap, A., Kroes, R., Liem, D., Muller, D. J., Page, S., Rolland, V., Schlatter, J., Tritscher, A., Tueting, W. & Wurtzen, G. 2006. Risk assessment of substances that are both genotoxic and carcinogenic report of an International Conference organized by EFSA and WHO with support of ILSI Europe. *Food and chemical toxicology : an international journal published for the British Industrial Biological Research Association*, 44, 1636-50.
7. Bessems, J. G., Loizou, G., Krishnan, K., Clewell, H. J., 3rd, Bernasconi, C., Bois, F., Coecke, S., Collnot, E. M., Diembeck, W., Farcas, L. R., Geraets, L., Gundert-Remy, U., Kramer, N., Kusters, G., Leite, S. B., Pelkonen, O. R., Schroder, K., Testai, E., Wilk-Zasadna, I. & Zaldivar-Comenges, J. M. 2014. PBTK modelling platforms and parameter estimation tools to enable animal-free risk assessment: recommendations from a joint EPAA--EURL ECVAM ADME workshop. *Regul Toxicol Pharmacol*, 68, 119-39.
8. Boberg, E. W., Miller, E. C. & Miller, J. A. 1986. The metabolic sulfonation and side-chain oxidation of 3'-hydroxyisosafrrole in the mouse and its inactivity as a hepatocarcinogen relative to 1'-hydroxysafrrole. *Chemico-biological interactions*, 59, 73-97.
9. Boberg, E. W., Miller, E. C., Miller, J. A., Poland, A. & Liem, A. 1983. Strong evidence from studies with brachymorphic mice and pentachlorophenol that 1'-sulfoxysafrrole is the major ultimate electrophilic and carcinogenic metabolite of 1'-hydroxysafrrole in mouse liver. *Cancer research*, 43, 5163-73.
10. Botana, L. M., Hess, P., Munday, R., Nathalie, A., DeGrasse, S. L., Feeley, M., Suzuki, T., van den Berg, M., Fattori, V., Gamarro, E. G., Tritscher, A., Nakagawa, R. & Karunasagar, I. 2017. Derivation of toxicity equivalency factors for marine biotoxins associated with Bivalve Molluscs. *Trends in Food Science & Technology*, 59, 15-24.
11. Chen, L., Mulder, P. P. J., Louisse, J., Peijnenburg, A., Wesseling, S. & Rietjens, I. 2017. Risk assessment for pyrrolizidine alkaloids detected in (herbal) teas and plant food supplements. *Regul Toxicol Pharmacol*, 86, 292-302.

12. Chiu, W. A., Barton, H. A., DeWoskin, R. S., Schlosser, P., Thompson, C. M., Sonawane, B., Lipscomb, J. C. & Krishnan, K. 2007. Evaluation of physiologically based pharmacokinetic models for use in risk assessment. *Journal of applied toxicology : JAT*, 27, 218-37.
13. COC. 2012. *Risk Characterisation Methods* [Online]. Committee on carcinogenicity of chemicals in food consumer products and the environment. Available: https://www.gov.uk/government/uploads/system/uploads/attachment_data/file/315883/Risk_characterisation_methods.pdf.
14. Edler, L., Poirier, K., Dourson, M., Kleiner, J., Mileson, B., Nordmann, H., Renwick, A., Slob, W., Walton, K. & Wurtzen, G. 2002. Mathematical modelling and quantitative methods. *Food Chem Toxicol*, 40, 283-326.
15. EFSA 2005. Opinion of the Scientific Committee on a request from EFSA related to A Harmonised Approach for Risk Assessment of Substances Which are both Genotoxic and Carcinogenic. *The EFSA Journal*, 282, 1-31.
16. EFSA 2013. International frameworks dealing with human risk assessment of combined exposure to multiple chemicals. 3313-3382.
17. Felter, S. P., Conolly, R. B., Bercu, J. P., Bolger, P. M., Boobis, A. R., Bos, P. M., Carthew, P., Doerrer, N. G., Goodman, J. I., Harrouk, W. A., Kirkland, D. J., Lau, S. S., Llewellyn, G. C., Preston, R. J., Schoeny, R., Schnatter, A. R., Tritscher, A., van Velsen, F. & Williams, G. M. 2011. A proposed framework for assessing risk from less-than-lifetime exposures to carcinogens. *Critical Reviews in Toxicology*, 41, 507-44.
18. Gavin, C. L., Williams, M. C. & Hallagan, J. B. 2007. 2005 FEMA poundage and technical effects update survey. . Washington, DC, USA,: Flavor and Extract Manufacturers Association.
19. Herrmann, K., Engst, W., Appel, K. E., Monien, B. H. & Glatt, H. 2012. Identification of human and murine sulfotransferases able to activate hydroxylated metabolites of methyleugenol to mutagens in Salmonella typhimurium and detection of associated DNA adducts using UPLC-MS/MS methods. *Mutagenesis*, 27, 453-62.
20. Herrmann, K., Schumacher, F., Engst, W., Appel, K. E., Klein, K., Zanger, U. M. & Glatt, H. 2013. Abundance of DNA adducts of methyleugenol, a rodent hepatocarcinogen, in human liver samples. *Carcinogenesis*, 34, 1025-30.
21. IPCS 2010. Characterization and application of physiologically based pharmacokinetic models in risk assessment.
22. JECFA 2009. Safety evaluation of certain food additives. Geneva: WHO.
23. Jeurissen, S. M., Punt, A., Delatour, T. & Rietjens, I. M. 2008. Basil extract inhibits the sulfotransferase mediated formation of DNA adducts of the procarcinogen 1'-hydroxyestragole by rat and human liver S9 homogenates and in HepG2 human hepatoma cells. *Food and chemical toxicology : an international journal published for the British Industrial Biological Research Association*, 46, 2296-302.
24. Kiwamoto, R., Ploeg, D., Rietjens, I. M. & Punt, A. 2016. Dose-dependent DNA adduct formation by cinnamaldehyde and other food-borne alpha,beta-unsaturated aldehydes predicted by physiologically based in silico modelling. *Toxicol In Vitro*, 31, 114-25.
25. Krewski, D., Withey, J. R., Ku, L. F. & Andersen, M. E. 1994. Applications of physiologic pharmacokinetic modeling in carcinogenic risk assessment. *Environmental Health Perspectives*, 102 Suppl 11, 37-50.
26. Kreydiyyeh, S. I. & Usta, J. 2002. Diuretic effect and mechanism of action of parsley. *Journal of Ethnopharmacology*, 79, 353-7.
27. Martati, E., Boersma, M. G., Spenkeliink, A., Khadka, D. B., van Bladeren, P. J., Rietjens, I. M. C. M. & Punt, A. 2012. Physiologically based biokinetic (PBBK) modeling of safrole bioactivation and detoxification in humans as compared with rats. *Toxicological Sciences*

28. Martati, E., Boonpawa, R., van den Berg, J. H. J., Paini, A., Spengelink, A., Punt, A., Vervoort, J., van Bladeren, P. J. & Rietjens, I. M. C. M. 2014. Malabaricone C-containing mace extract inhibits safrole bioactivation and DNA adduct formation both in vitro and in vivo. *Food and Chemical Toxicology*, 66, 373-384.
29. Meek, M. E., Boobis, A. R., Crofton, K. M., Heinemeyer, G., Van Raaij, M. & Vickers, C. 2011. Risk assessment of combined exposure to multiple chemicals: A WHO/IPCS framework. *Regulatory Toxicology and Pharmacology*, 60, S1-S14.
30. Merz, K. H. & Schrenk, D. 2016. Interim relative potency factors for the toxicological risk assessment of pyrrolizidine alkaloids in food and herbal medicines. *Toxicology Letters*, 263, 44-57.
31. Miller, E. C., Swanson, A. B., Phillips, D. H., Fletcher, T. L., Liem, A. & Miller, J. A. 1983. Structure-activity studies of the carcinogenicities in the mouse and rat of some naturally occurring and synthetic alkenylbenzene derivatives related to safrole and estragole. *Cancer research*, 43, 1124-34.
32. O'Brien, J., Renwick, A. G., Constable, A., Dybing, E., Muller, D. J., Schlatter, J., Slob, W., Tueting, W., van Benthem, J., Williams, G. M. & Wolfreys, A. 2006. Approaches to the risk assessment of genotoxic carcinogens in food: a critical appraisal. *Food and chemical toxicology : an international journal published for the British Industrial Biological Research Association*, 44, 1613-35.
33. Paini, A., Punt, A., Scholz, G., Gremaud, E., Spengelink, B., Alink, G., Schilter, B., van Bladeren, P. J. & Rietjens, I. M. 2012. In vivo validation of DNA adduct formation by estragole in rats predicted by physiologically based biodynamic modelling. *Mutagenesis*, 27, 653-63.
34. Paini, A., Punt, A., Viton, F., Scholz, G., Delatour, T., Marin-Kuan, M., Schilter, B., van Bladeren, P. J. & Rietjens, I. M. C. M. 2010. A physiologically based biodynamic (PBBD) model for estragole DNA binding in rat liver based on in vitro kinetic data and estragole DNA adduct formation in primary hepatocytes. *Toxicology and Applied Pharmacology*, 245, 57-66.
35. Phillips, D. H., Reddy, M. V. & Randerath, K. 1984. 32P-post-labelling analysis of DNA adducts formed in the livers of animals treated with safrole, estragole and other naturally-occurring alkenylbenzenes. II. Newborn male B6C3F1 mice. *Carcinogenesis*, 5, 1623-8.
36. Pose-Juan, E., Fernandez-Cruz, T. & Simal-Gandara, J. 2016. State of the art on public risk assessment of combined human exposure to multiple chemical contaminants. *Trends in Food Science & Technology*, 55, 11-28.
37. Punt, A., Paini, A., Boersma, M. G., Freidig, A. P., Delatour, T., Scholz, G., Schilter, B., van Bladeren, P. J. & Rietjens, I. M. C. M. 2009. Use of physiologically based biokinetic (PBBK) modeling to study estragole bioactivation and detoxification in humans as compared with male rats. *Toxicol Sci*, 110, 255-69.
38. Punt, A., Paini, A., Spengelink, A., Scholz, G., Schilter, B., van Bladeren, P. J. & Rietjens, I. M. C. M. 2016. Evaluation of Interindividual Human Variation in Bioactivation and DNA Adduct Formation of Estragole in Liver Predicted by Physiologically Based Kinetic/Dynamic and Monte Carlo Modeling. *Chemical Research in Toxicology*, 29, 659-668.
39. Randerath, K., Haglund, R. E., Phillips, D. H. & Reddy, M. V. 1984. 32P-post-labelling analysis of DNA adducts formed in the livers of animals treated with safrole, estragole and other naturally-occurring alkenylbenzenes. I. Adult female CD-1 mice. *Carcinogenesis*, 5, 1613-22.
40. Rietjens, I. M., Lousse, J. & Punt, A. 2011. Tutorial on physiologically based kinetic modeling in molecular nutrition and food research. *Molecular nutrition & food research*, 55, 941-56.
41. Rietjens, I. M. C. M., Punt, A., Schilter, B., Scholz, G., Delatour, T. & van Bladeren, P. J. 2010. In silico methods for physiologically based biokinetic models describing bioactivation and detoxification of coumarin and estragole: Implications for risk assessment. *Molecular Nutrition & Food Research*, 54, 195-207.
42. Rietjens, I. M. C. M., Tyrakowska, B., van den Berg, S. J. P. L., Soffers, A. E. M. F. & Punt, A. 2015. Matrix-derived combination effects influencing absorption, distribution, metabolism and excretion

- (ADME) of food-borne toxic compounds: implications for risk assessment. *Toxicology Research*, 4, 23-35.
43. Sanzini, E., Badea, M., Santos, A. D., Restani, P. & Sievers, H. 2011. Quality control of plant food supplements. *Food Funct*, 2, 740-6.
 44. Schilter, B., Andersson, C., Anton, R., Constable, A., Kleiner, J., O'Brien, J., Renwick, A. G., Korver, O., Smit, F. & Walker, R. 2003. Guidance for the safety assessment of botanicals and botanical preparations for use in food and food supplements. *Food and chemical toxicology : an international journal published for the British Industrial Biological Research Association*, 41, 1625-49.
 45. Semenov, V. V., Rusak, V. V., Chartov, E. M., Zaretskii, M. I., Konyushkin, L. D., Firgang, S. I., Chizhov, A. O., Elkin, V. V., Latin, N. N., Bonashek, V. M. & Stas'eva, O. N. 2007. Polyalkoxybenzenes from plant raw materials 1. Isolation of polyalkoxybenzenes from CO₂ extracts of Umbelliferae plant seeds. *Russian Chemical Bulletin*, 56, 2448-2455.
 46. Simon, J. E. & Quinn, J. 1988. Characterization of essential oil of parsley. *Journal of Agricultural and Food Chemistry*, 36, 467-472.
 47. Smith, R. L., Adams, T. B., Doull, J., Feron, V. J., Goodman, J. I., Marnett, L. J., Portoghese, P. S., Waddell, W. J., Wagner, B. M., Rogers, A. E., Caldwell, J. & Sipes, I. G. 2002. Safety assessment of allylalkoxybenzene derivatives used as flavouring substances - methyl eugenol and estragole. *Food Chem Toxicol*, 40, 851-70.
 48. Swanson, C. A. 2002. Suggested guidelines for articles about botanical dietary supplements. *American Journal of Clinical Nutrition*, 75, 8-10.
 49. van den Berg, M., Birnbaum, L. S., Denison, M., Vito, M. D., Farland, W., Feeley, M., Fiedler, H., Hakansson, H., Hanberg, A., Haws, L., Rose, M., Safe, S., Schrenk, D., Tohyama, C., Tritscher, A., Tuomisto, J., Tysklind, M., Walker, N. & E., P. R. 2006. The 2005 World Health Organization Re-evaluation of Human and Mammalian Toxic Equivalency Factors for Dioxins and Dioxin-like Compounds. *Toxicological Sciences*, 93, 223-241.
 50. Van den Berg, S. J., Punt, A., Soffers, A. E., Vervoort, J., Ngeleja, S., Spenkeliink, B. & Rietjens, I. M. C. M. 2012. Physiologically based kinetic models for the alkenylbenzene elemicin in rat and human and possible implications for risk assessment. *Chemical research in toxicology*, 25, 2352-67.
 51. Van den Berg, S. J. P. L., Restani, P., Boersma, M. G., Delmulle, L. & Rietjens, I. M. C. M. 2011. Levels of Genotoxic and Carcinogenic Compounds in Plant Food Supplements and Associated Risk Assessment. *Food and Nutrition Sciences*, 989-1010.
 52. van het Hof, K. H., Brouwer, I. A., West, C. E., Haddeman, E., Steegers-Theunissen, R. P. M., van Dusseldorp, M., Weststrate, J. A., Eskes, T. K. A. B. & Hautvast, J. G. A. J. 1999. Bioavailability of lutein from vegetables is 5 times higher than that of beta-carotene. *American Journal of Clinical Nutrition*, 70, 261-268.
 53. Vokk, R., Lougas, T., Mets, K. & Karvets, M. 2011. Dill (*Anethum graveolens* L.) and Parsley (*Petroselinum crispum* (Mill.) Fuss) from Estonia: Seasonal Differences in Essential Oil Composition. *Agronomy research*, 9, 515-520.
 54. Walker, R. 2004. Criteria for risk assessment of botanical food supplements. *Toxicol Lett*, 149, 187-95.
 55. WHO 2009. Safety evaluation of certain additives, prepared by the Sixty-ninth meeting of the Joint FAO/WHO Expert Committee on Food Additives. *World Health Organization* http://whqlibdoc.who.int/publications/2009/9789241660600_eng.pdf.
 56. Wiseman, R. W., Fennell, T. R., Miller, J. A. & Miller, E. C. 1985. Further characterization of the DNA adducts formed by electrophilic esters of the hepatocarcinogens 1'-hydroxysafrole and 1'-hydroxyestragole in vitro and in mouse liver in vivo, including new adducts at C-8 and N-7 of guanine residues. *Cancer research*, 45, 3096-105.

57. Wislocki, P. G., Borchert, P., Miller, J. A. & Miller, E. C. 1976. The metabolic activation of the carcinogen 1'-hydroxysafrole in vivo and in vitro and the electrophilic reactivities of possible ultimate carcinogens. *Cancer research*, 36, 1686-95.
58. Zhou, G. D., Moorthy, B., Bi, J., Donnelly, K. C. & Randerath, K. 2007. DNA adducts from alkoxyallylbenzene herb and spice constituents in cultured human (HepG2) cells. *Environ Mol Mutagen*, 48, 715-21.

Chapter 7

Summary

Summary

Alkenylbenzenes including estragole, methyleugenol, safrole, elemicin, apiol, and myristicin are naturally occurring in many herbs such as parsley, dill, basil, tarragon, fennel and nutmeg (Kreydiyyeh and Usta, 2002, Smith et al., 2002, Semenov et al., 2007). Estragole, methyleugenol and safrole are genotoxic and carcinogenic in rodent bioassays inducing liver tumors (Boberg et al., 1986, Boberg et al., 1983, Drinkwater et al., 1976, Miller et al., 1983, Swanson et al., 1981, Wiseman et al., 1985, Wiseman et al., 1987, Wislocki et al., 1977). Because of that, the use of methyleugenol, safrole and estragole as pure substances in foodstuff has been prohibited in the EU from September 2008 onwards (European Commission (EC), 2008). For apiol and myristicin data for their risk assessment are limited and more research is needed to support the evaluation of the risk resulting from consumption of products containing these compounds (WHO, 2009). The aim of the current thesis was to perform a mode of action based risk assessment of exposure to low doses of apiol and myristicin by using physiologically based kinetic (PBK) modelling based read-across from other alkenylbenzenes and to use the results obtained for risk assessment of consumption of plant food supplements (PFS) and other botanical products containing parsley and dill.

Chapter 1 provides general background information to alkenylbenzenes especially apiol and myristicin, a description of the chemical, metabolic and toxicity characteristics of apiol and myristicin and other structurally related alkenylbenzenes, a brief outline of the method used for their risk assessment and a short introduction to PBK modelling. Besides that, Chapter 1 include the aim of the current thesis. In Chapter 2 and Chapter 3, PBK models for respectively apiol and myristicin in male rat and human were defined, enabling prediction of dose-dependent effects in bioactivation and detoxification of these alkenylbenzenes. The PBK model based predictions were

subsequently compared to those for safrole enabling estimation of a BMDL₁₀ for apiol and myristicin from read-across from the BMDL₁₀ available for safrole, thereby enabling risk assessment of current dietary exposure to apiol. In Chapter 4 and 5, the risk assessment of exposure to apiol and related alkenylbenzenes through drinking of parsley and dill based herbal teas and consumption of parsley and dill containing PFS was performed using the BMDL₁₀ values derived in Chapter 2 and 3. The results showed that consumption of parsley and dill based herbal teas and PFS would be a priority for risk management if consumed for longer periods of time. Chapter 6 includes a general discussion of the thesis results obtained and the future perspectives that describe the needs to further research, based on alternatives for animals testing, to improve the risk assessment approaches for different botanical preparations.

Altogether, the results obtained through different thesis chapters show that integration of different approaches provides the basis for a mode of action and PBK modelling based read-across from compounds for which tumor data are available to related compounds for which such data are lacking. This can contribute to the development of alternatives for animal testing and will facilitate the risk assessment of compounds for which in vivo toxicity studies on tumor formation data are unavailable.

References

1. Boberg, E. W., Miller, E. C. & Miller, J. A. 1986. The metabolic sulfonation and side-chain oxidation of 3'-hydroxyisosafrrole in the mouse and its inactivity as a hepatocarcinogen relative to 1'-hydroxysafrrole. *Chemico-biological interactions*, 59, 73-97.
2. Boberg, E. W., Miller, E. C., Miller, J. A., Poland, A. & Liem, A. 1983. Strong evidence from studies with brachymorphic mice and pentachlorophenol that 1'-sulfooxysafrrole is the major ultimate electrophilic and carcinogenic metabolite of 1'-hydroxysafrrole in mouse liver. *Cancer research*, 43, 5163-73.
3. Drinkwater, N. R., Miller, E. C., Miller, J. A. & Pitot, H. C. 1976. Hepatocarcinogenicity of estragole (1-allyl-4-methoxybenzene) and 1'-hydroxyestragole in the mouse and mutagenicity of 1'-acetoxyestragole in bacteria. *J Natl Cancer Inst*, 57, 1323-31.
4. European Commission (EC) 2008. Regulation (EC) No 1334/2008 of the European Parliament and of the Council of 16 December 2008 on flavourings and certain food ingredients with flavouring properties for use in and on foods and amending Council Regulation (EEC) No 1601/91, Regulations (EC) No 2232/96 and (EC) No 110/2008 and Directive 2000/13/EC.
5. Gavin, C. L., Williams, M. C. & Hallagan, J. B. 2007. 2005 FEMA poundage and technical effects update survey. .
6. Kreydiyyeh, S. I. & Usta, J. 2002. Diuretic effect and mechanism of action of parsley. *Journal of Ethnopharmacology*, 79, 353-7.
7. Miller, E. C., Swanson, A. B., Phillips, D. H., Fletcher, T. L., Liem, A. & Miller, J. A. 1983. Structure-activity studies of the carcinogenicities in the mouse and rat of some naturally occurring and synthetic alkenylbenzene derivatives related to safrrole and estragole. *Cancer Res*, 43, 1124-34.
8. Semenov, V. V., Rusak, V. V., Chartov, E. M., Zaretskii, M. I., Konyushkin, L. D., Firgang, S. I., Chizhov, A. O., Elkin, V. V., Latin, N. N., Bonashek, V. M. & Stas'eva, O. N. 2007. Polyalkoxybenzenes from plant raw materials 1. Isolation of polyalkoxybenzenes from CO₂ extracts of Umbelliferae plant seeds. *Russian Chemical Bulletin*, 56, 2448-2455.
9. Smith, R. L., Adams, T. B., Doull, J., Feron, V. J., Goodman, J. I., Marnett, L. J., Portoghese, P. S., Waddell, W. J., Wagner, B. M., Rogers, A. E., Caldwell, J. & Sipes, I. G. 2002. Safety assessment of allylalkoxybenzene derivatives used as flavouring substances - methyl eugenol and estragole. *Food and chemical toxicology : an international journal published for the British Industrial Biological Research Association*, 40, 851-70.
10. Swanson, A. B., Miller, E. C. & Miller, J. A. 1981. The side-chain epoxidation and hydroxylation of the hepatocarcinogens safrrole and estragole and some related compounds by rat and mouse liver microsomes. *Biochim Biophys Acta*, 673, 504-16.
11. Van den Berg, S. J. P. L., Restani, P., Boersma, M. G., Delmulle, L. & Rietjens, I. M. C. M. 2011. Levels of Genotoxic and Carcinogenic Compounds in Plant Food Supplements and Associated Risk Assessment. *Food and Nutrition Sciences*, 989-1010.
12. WHO 2009. Safety evaluation of certain additives, prepared by the Sixty-ninth meeting of the Joint FAO/WHO Expert Committee on Food Additives. *World Health Organization* http://whqlibdoc.who.int/publications/2009/9789241660600_eng.pdf.
13. Wiseman, R. W., Fennell, T. R., Miller, J. A. & Miller, E. C. 1985. Further characterization of the DNA adducts formed by electrophilic esters of the hepatocarcinogens 1'-hydroxysafrrole and 1'-hydroxyestragole in vitro and in mouse liver in vivo, including new adducts at C-8 and N-7 of guanine residues. *Cancer research*, 45, 3096-105.
14. Wiseman, R. W., Miller, E. C., Miller, J. A. & Liem, A. 1987. Structure-activity studies of the hepatocarcinogenicities of alkenylbenzene derivatives related to estragole and safrrole on administration to preweanling male C57BL/6J x C3H/HeJ F1 mice. *Cancer research*, 47, 2275-83.

15. Wislocki, P. G., Miller, E. C., Miller, J. A., McCoy, E. C. & Rosenkranz, H. S. 1977. Carcinogenic and mutagenic activities of safrole, 1'-hydroxysafrole, and some known or possible metabolites. *Cancer research*, 37, 1883-91.

Appendices

Acknowledgment

During my PhD life at Netherlands, I have met so many people who gave me good memories. I would like to take this opportunity to formally express my sincere appreciation to these people.

I would like to express my first and most sincere gratitude to my promotor Ivonne Rietjens for the continuous support of my PhD study and research, for her patience, motivation, enthusiasm, and immense knowledge. Her guidance helped me in all the time of research and writing of this thesis. I could not have imagined having a better advisor and mentor for my PhD study.

Besides my promotor, I would like to thank my co-promotors Jacques Vervoort and Sebas Wesselling for their encouragement and insightful comments.

I would like to express my special thanks to Ala' who introduced me to Ivonne and gave me the opportunity to be part of the toxicology team.

Special thanks for really I don't know what to call him; brother, friend, colleague, just AMER is enough for being with me all the way during my PhD, for the stimulating discussions, for the sleepless nights we were working together before deadlines, and for all the fun we have had in the last four years.

I would like sincerely to thank Bert, Hans, Laura, Marelle, Nico, Ans Punt, Jochem, Lidy, Irene, Gre and Ans Soffers for the support and great talks that we had together.

Thank you all my friends at Toxicology Arif, Arthem, Ashraf, Aziza, Barae, Diana, Deigo, Gerogia, Hequn, Jia, Jonathan, Justine, Karsten, Lenny, Lu, Marcia, Marta, Mebra, Mengying, Myrthe, Nacho, Rieko, Rozaini, Samantha, Shuo, Suparmi, Wasma. I will miss the good times we have spent together.

I would like to thank all my friends Ahmad in Netherlands and all my friends and Colleagues at my institute in Jordan.

Last but not the least, I would like to thank my family: my mother for giving birth to me at the first place and supporting me spiritually throughout my life, my brothers and sisters who always are supportive to me and of course I can't forget to thank my lovely wife and kids for being so patient and so helpful during the last four years.

At the end I would like to especially thank my father and my best friend Jaser who were both always encouraging and supportive but unfortunately passed away during my PhD.

Curriculum vitae

Abdalmajeed Alajlouni was Born in Assarih, Jordan on December 29th, 1979. After his secondary school in 1997, he started a Bachelor degree in Veterinary Medicine and Surgery from Veterinary Medicine School at Jordan University of Science and Technology following 5 years study period with honours and obtained his degree by June 2002. By August 2003 he started his work at Aqaba special economic zone authority as food inspector then he moved to work as food microbiologist at Aqaba International Laboratories. During His work period, he obtained his MS degree in microbiology in 2012 from Veterinary Medicine School at Jordan University of Science and Technology. In 2013, he was selected as a PhD student at a project implemented under the ENPI CBC Mediterranean Sea Basin programme funded by the European union entitled: Botanical Risk Assessment training in the Mediterranean Area (BRAMA), in collaboration with partners from Egypt, Greece, Italy, and the Netherlands. From Jan. 2014 to Jan 2018 he joined the toxicology team at toxicology department under supervision of Prof. Ivonne M.C.M Rietjens, on the study discussed in the present thesis. In parallel to his PhD project, he followed all the needed postgraduate training courses in Toxicology and was registered as European Toxicologist. After finishing his PhD study, he will return to his work at Aqaba International laboratories as a researcher to start new research opportunities at his institute in Jordan.

List of publications

- 1- **Alajlouni, A. M.**, Al Malahmeh, A. J., Kiwamoto, R., Wesseling, S., Soffers, A. E., Al-Subeihi, A. A., Vervoort, J. & Rietjens, I. M. 2016. Mode of action based risk assessment of the botanical food-borne alkenylbenzene apiol from parsley using physiologically based kinetic (PBK) modelling and read-across from safrole. *Food and chemical toxicology*. 89, 138-150.
- 2- **Alajlouni, A. M.**, Al-Malahmeh, A. J., Isnaeni, F. N., Wesseling, S., Vervoort, J. & Rietjens, I. M. 2016. Level of alkenylbenzenes in parsley and dill based teas and associated risk assessment using the margin of exposure approach. *Journal of agricultural and food chemistry*. 64(45): 8640-8646.
- 3- **Alajlouni, A. M.**, Al-Malahmeh, A. J., Kalli, M., Wesseling, S., Vervoort, J. & Rietjens, I. M. 2016. Risk assessment of combined exposure to alkenylbenzenes through consumption of plant food supplements containing parsley and dill. *Journal of food additives and contaminants: part A*. (in press).
- 4- Al-Malahmeh, A. J., **Al-Ajlouni, A.**, Wesseling, S., Soffers, A. E., Al-Subeihi, A., Kiwamoto, R., Vervoort, J. & Rietjens, I. M. 2017. Physiologically based kinetic modeling of the bioactivation of myristicin. *Archives of toxicology*. 91(2): 713-734.
- 5- Al-Malahmeh, A. J., **Al-Ajlouni, A.**, Wesseling, S., Vervoort, J. & Rietjens, I. M. 2017. Determination and risk assessment of naturally occurring genotoxic and carcinogenic alkenylbenzenes in basil-containing sauce of pesto. *Journal of Toxicology Reports*, 4, 1–8.
- 6- Al-Malahmeh, A. J., **Alajlouni, A. M.**, Wesseling, S., Ning, J., Vervoort, J. & Rietjens, I. M. 2017. Determination and risk assessment of naturally occurring genotoxic and carcinogenic alkenylbenzenes in nutmeg-based plant food supplements. *Journal of Applied Toxicology* (in press).

Overview of completed training activities

Discipline specific courses	
Molecular toxicology	2014
Cell toxicology	2014
Organ toxicology	2015
Epidemiology	2014
Ecotoxicology	2014
Lab animal science	2014
Pathobiology	2014
Risk assessment	2014
Immunotoxicology	2014
Medical and Forensic	2014
Meetings	
International symposium 3R, Denmark (poster presentation)	2015
International Conference on medicinal herbs, Jordan	2015
General courses	
VLAG PhD week	2014
Analytical chemistry skills	2014
Measurement science and statistics	2014
Optional	
Preparation of research proposal	2014
Attending scientific presentation at toxicology	2014-2017
PBK modelling	2014
General Toxicology	2014

Approved by the graduate school VLAG

Financial support from Wageningen University for printing this thesis is gratefully acknowledged.

Printing: Digiforce, Proefschriftmaken.nl, De Limiet 24c, 4131 NR Vianen.

Cover design: Isdar digital press, Jordan

AbdAlmajeed M. Alajlouni 2017